Shock metamorphism of potassic feldspars

P. B. Robertson

SHOCK METAMORPHISM OF POTASSIC FELDSPARS

A thesis submitted for the degree of Doctor of Philosophy in the University of Durham

P.B. Robertson

Graduate Society

October, 1973

ABSTRACT

Hypervelocity meteorite impact produces transient pressures as high as several megabars and temperatures in excess of 1500°C. Shock metamorphism describes the effects upon the target rocks, effects most distinctive in the range approximately 100-600kb. Shock deformation produced in potassic feldspars at three terrestrial craters and in experimentally shocked K-spar have been examined. Pressures in natural material were estimated from deformation of coexisting quartz and plagioclase, and in experiments pressures were calculated using impedance matching.

At Charlevoix crater, Quebec, pressures above 170kb have induced chemical remobilization partially converting film perthite to spindle microperthite in orthoclase and microcline. In orthoclase, shock produced cleavages form parallel to $(2\bar{1}0)$ and (120) at 170kb, and above 300kb parallel to $(11\bar{2})$, (031), $(01\bar{1})$ and (101). Planar deformation features resulting from lattice gliding, form initially at 200kb, and are well developed at 230-270kb. In orthoclase they are generally parallel to $(24\bar{1})$ and $(\bar{2}41)$, and $(13\bar{1})$, (110) and (120) in microcline. Above 300kb some sets become glide twins. Structural state of the feldspars is apparently not affected in the pressure range examined ($\leq$ 360kb).

In the breccias of Lac Couture crater, Quebec, strong deformation twins and planar features develop in microcline above 150kb, and some of the twins may obey a 'diagonal' twin law.

Single crystal microcline was experimentally shocked at pressures from 37 to 417kb. Three shock regions were recognized: Regime I (<100kb) normal elastic compression, Regime II (100-300kb) mixed phase region, Regime III (>300kb) high pressure phase region. Shock cleavages, $(11\bar{1})$, $(\bar{1}11)$ and (hk0), developed initially below 60kb, contain glass at highest pressures. Planar features, generally parallel to $(11\bar{1})$ and $(\bar{1}11)$ also, appear at 154kb becoming more pronounced with increasing pressure, with poorly defined deformation twins occurring above 175kb. X-ray patterns show that long range structural order diminishes above 150kb accompanied by formation of a low-birefringent, unidentified phase, possibly a high-pressure, disordered modification of K-feldspar.

Differences in the pressure required for formation of particular shock effects between craters, and between natural and experimental systems are due to differences in structural state of the feldspars.

At Brent crater, Ontario, partially recrystallized alkali feldspars in shocked basement gneisses show compositional variations due to incomplete homogenization. This is not a shock effect but results from thermal metamorphism by the overlying melt layer. A similar thermal effect has produced chemical variations in some highly shocked orthoclases at Charlevoix.

TABLE OF CONTENTS

TABLE OF CONTENTS (CONT'D)

LIST OF FIGURES

LIST OF TABLES

CHAPTER I

INTRODUCTION

I.1 Meteorite Impact Phenomena

I.1.1 Terrestrial Meteorite Craters

The study of phenomena associated with meteorite impacts on the Earth and Moon is a comparatively recent area of geological interest. Millman (1971) and Dence (1972) have provided summaries of the historical development of meteorite crater investigations, and presented lists of verified, probable, and possible impact sites throughout the world; these lists require almost constant revision as new sites are continually being reported. Barringer Meteor Crater, Arizona (also called Coon Butte, Meteor Crater, and Arizona Crater) was the first to be identified in 1905, followed by the discovery of about a dozen additional terrestrial craters during the next forty-five years. V.B. Meen's assertion in 1950 that the New Quebec (Chubb) Crater in Quebec was caused by meteorite impact encouraged C.S. Beals of the Dominion Observatory of Canada (now the Earth Physics Branch of the Department of Energy, Mines and Resources) to institute a systematic search for meteorite craters in Canada. The success of this programme can be measured by the fact that twenty fossil meteorite impact craters have been confirmed in Canada (Robertson and Grieve, 1973). Several other promising sites in remote areas of Canada await investigation before their genesis can be established.

The number of confirmed terrestrial meteorite craters varies according to the criteria used for their identification. Some scientists believe that the meteorite or its fragments must be discovered before an origin by impact can be proved. On this basis 63 craters (52 are from 4 sites) greater than 10m in diameter exist, the largest being

the 1200m Barringer Meteor Crater. Dence (1972) lists 42 additional sites ranging from 0.48km to 100km in diameter in which meteoritic material has not been discovered, but where the origin is best explained as due to hypervelocity impact of a large meteorite or comet. The absence of meteoritic fragments from these large near-circular structures is not surprising. The energy released by the impact of the bolide, estimated at 57×10^6kg, which formed the Barringer Meteor Crater, for example, was sufficient to produce partial fusion of the meteorite and of a large volume of country rock (Shoemaker, 1963). The more massive meteorites which have created the much larger craters would have released correspondingly higher energies resulting in a larger fraction of the meteorite being melted or even vapourized, and disseminated throughout the large volume of the crater. As Millman (1971) pointed out, even if the meteorite was not fused but only shattered it would represent only about a 10^{-4} fraction of the volume of the terrestrial rocks involved, and chances of recovery of the small fragments, readily broken down by weathering, are remote.

Many of the geological features associated with meteorite impact, such as brecciation and melting, are characteristic also of conventional styles of metamorphism and volcanism, and are therefore of little value as definitive criteria for establishing the origin of craters. In the early 1960's it was recognized that rocks from established and probable impact sites do, however, possess certain features characteristic of a unique style of deformation subsequently called shock metamorphism. The dependence on high pressures for the formation of shock metamorphism effects has been shown by their

duplication in nuclear and chemical explosion craters, and in laboratory shock experiments. In the absence of recognizable meteoritic material, the occurrence of shock metamorphic deformation in rocks from ancient circular structures is now the sufficient and definitive criterion for confirming their origin by meteorite impact.

I.1.2 Shock Metamorphism

I.1.2A Shock Environments

Although shock metamorphism results from the action of high pressures and temperatures, an important factor is strain rate. Strain rates are generally expressed in terms of deformation (per cent strain) per second, and typical tectonic rates are of the order of 10^{-14}%/sec, or approximately 1% in 3¼ million years (Carter, 1971). Turner (1968) stated that pressures involved in regional metamorphism are largely the result of lithostatic load of the overlying rocks (approximately 300bars/km depth), supplemented by tectonic overpressures. Ernst et al. (1970) have shown that the contribution of tectonic overpressure is minimal, even in the blueschist (glaucophane schist) facies where it attains a maximum level. Maximum stress in regional metamorphism of crustal rocks is less than 10kb (Stöffler, 1971a)

Experiments designed to duplicate metamorphic deformation must be carried out at strain rates which enable detectable strain to be produced during the lifetime, or interest-span, of the investigator. Therefore, rates between approximately 10^{-4}%/sec and 10^{-9}%/sec are practical limits for static compression in the laboratory, and pressures involved are generally less than 100kb. In striking contrast, strain

rates produced by the impact of a large meteorite travelling at approximately 15km/sec are of the order of 10^4%/sec to 10^6%/sec (1% strain per microsecond), or 20 orders of magnitude greater than tectonic rates, with maximum pressures ranging up to several megabars (Stöffler, 1971a). Peak pressures decay in fractions of a second, post-shock temperatures exceed 1500°C, and chemical and physical equilibrium is not usually achieved. It is therefore not surprising that deformations typical of shock metamorphism are unlike those produced by dynamic metamorphism.

I.1.2B Typical Shock Effects

Over the past decade many studies of shock metamorphism have been undertaken. Some describe shock effects in the suite of rocks and minerals from particular impact sites (for example Engelhardt and Stöffler, 1968), and others deal solely with shock deformation of specific minerals or mineral families based on observations gathered from many sites (Robertson et al., 1968, among others). In addition, summary articles have been compiled relating several aspects of shock metamorphism (Chao, 1967 and 1968; Stöffler, 1971a). Laboratory shock experiments achieving pressures of several hundred kilobars, with strain rates comparable to those in natural impacts, have also been carried out on various minerals and rocks to correlate features produced at known shock pressures with those observed in nature (see references in Chapter IV).

The following five numbered sections summarize typical shock effects which are developed in common rock-forming minerals. In some

instances the literature references given represent the only documentation of a particular feature, but in most cases they have been selected from several references in order to encompass a variety of environments and researchers.

1) Development of planar elements of a variety of types, either in anomalous abundance, with uncommon crystallographic orientations, or of unusual character. Included in this group are fractures, kink-bands, deformation twins, deformation lamellae, and planar deformation features. The first three deformations are common in tectonic environments and cannot be presented as uniquely characteristic of shock-loading. However, in impact or explosion craters there is an anomalous abundance and perfection in the development of cleavage fractures in quartz (Bunch and Cohen, 1964; Robertson et al., 1968), and in feldspars, amphiboles, pyroxenes and carbonates (Short, 1966); kink-bands in biotite are particularly well developed (Cummings, 1968; Hörz, 1969) and their orientation has been related to stress direction; shock-induced mechanical twinning is prominent in plagioclase and clinopyroxene (Chao et al., 1970), in ilmenite (Minkin and Chao, 1970; Sclar, 1971), and in sphene (Borg, 1970). A comprehensive review of the types of planar elements found both in shocked rocks, and in rocks deformed under low strain rates, in nature and experiment, is given by Carter (1971).

Deformation lamellae and planar deformation features are similar in that they are planar, optical discontinuities occurring in sets of fixed crystallographic orientation, but the former are of detectable width. They are apparently the locus of dislocations within

deformed crystal lattices and may be filled by glass, high-pressure polymorphs, or gas- or liquid-filled cavities. Engelhardt and Bertsch (1969) prepared a summary of the physical and optical characteristics of planar deformation features in quartz from the Ries Crater, Germany, and Robertson et al. (1968) showed that the preferred orientation of planar feature sets in quartz changes with pressure. Similar planar deformation features with corresponding orientations have been produced in quartz in shock experiments above 100kb (Hörz, 1968; Müller and Defourneaux, 1968). The identification of planar deformation features in quartz is now the most easily and widely applicable single criterion used for recognition of shock metamorphic effects. Planar deformation features of similar character occur in plagioclase (Stöffler, 1968; Robertson et al, 1968; Dworak, 1969), in amphibole, pyroxene and olivine (Chao et al., 1970; Engelhardt et al., 1970), in sillimanite (Stöffler, 1970) and in scapolite (Wolfe and Hörz, 1970).

2) Conversion of minerals to an isotropic, sometimes dense, glassy phase at temperatures well below their normal melting point. These phases are called "diaplectic" ("destroyed by striking", Engelhardt and Stöffler, 1968) or "thetomorphic" ("adopted-form", Chao, 1967) glasses which are produced by breakdown of long-range order of the crystal lattice without fusion. Such diaplectic glasses have densities lower than the crystalline form from which they are derived whereas, in the case of plagioclase at least, the density is higher than thermally melted glasses of equivalent composition (Bunch et al., 1967; Stöffler and Hornemann, 1972). Crystal outlines are often preserved and diaplectic glasses of different minerals can exist adjacent to one

another without mixing. Maskelynite, diaplectic plagioclase, is the most common example from terrestrial rocks (Stöffler, 1967; Dworak, 1969) and from shocked lunar material (Chao et al., 1970; Engelhardt et al., 1970). Diaplectic glasses of quartz (Chao, 1967; Dence et al., 1973) and of alkali feldspar (Bunch, 1968) are also reported from terrestrial rocks, but in lesser abundance. Although diaplectic forms may occur as the direct result of compression by the shock wave (Kieffer, 1971), they are probably more commonly produced by inversion from a high-pressure crystalline phase, which is unstable in the post-shock P-T environment (Stöffler, 1971a; Stöffler and Hornemann, 1972).

3) Oxidation or breakdown into chemical components. In shock-metamorphosed rocks in which the quartz and feldspars are transformed to diaplectic glass, mafic minerals appear largely unaffected, except for enhanced development of kink bands in biotite, and weak planar features in pyroxenes and amphiboles. In contrast to the less compact tectosilicates, the micas, amphiboles and pyroxenes apparently do not transform to an isotropic phase. However, at high shock pressures, temperature effects become prominent and are readily seen in the mafic minerals. Oxidation of biotite and amphibole is evidenced by faded absorption colours and concentrations of iron oxides as rims or along fractures. The breakdown may proceed completely to form a mixture of iron oxides and silicate glass (Chao, 1967a).

4) Solid state phase changes. The tectosilicates, and perhaps other mineral groups, may transform to dense polymorphs at high shock pressures. In general, when the shock load is released such phases invert to states of lower free energy, usually the appropriate diaplectic glass

(Stöffler, 1971a), but small amounts of these polymorphs can persist under favourable post-shock conditions. Stishovite, a tetragonal polymorph of SiO_2, forms in crystalline rocks at shock pressures between 120 and 450kb, but because of its instability at high post-shock temperatures it inverts to diaplectic glass, and has been recovered from only two impact craters (Stöffler, 1971b). Coesite, a monoclinic polymorph of SiO_2, is believed to nucleate from the diaplectic glass as post-shock temperature and pressure drop through its stability field. It has been discovered in three nuclear and chemical explosion craters, and eight meteorite impact sites (Stöffler, 1971b; Dence et al., 1973).

Jadeite, identified in diaplectic plagioclase glass from the Ries Crater (James, 1971), is believed to have formed from the compression and breakdown of oligoclase at approximately 250 to 300kb. Also from the Ries Crater, chaoite (hexagonal graphite) is found as lamellae in graphite from samples in which the tectosilicates have been converted to diaplectic glass (El Goresy and Donnay, 1968). Diamond and lonsdaleite (a hexagonal, wurtzite-like diamond) were formed from shocked graphite in the Popigai crater, Siberia (Masaitis et al., 1972). Lonsdaleite was also extracted from the Canyon Diablo iron meteorite (Frondel and Marvin, 1967) which created the Barringer Meteor Crater.

High-pressure crystalline phases of unknown or partially determined nature have been recovered from laboratory shock experiments on garnet (Ahrens and Graham, 1971; R.V. Gibbons, personal communication, 1972) and microcline (Sclar and Usselman, 1970). Hugoniot shock

experiments (see Chapter IV) revealed that high pressure transformations probably occur in several common minerals, but material was not recovered from the experiments and the development or identity of the phases was not confirmed.

5) Fusion. Temperatures accompanying the most intense shock pressures may exceed melting temperatures of all mineral phases (Stöffler, 1971a). The tectosilicates are the first to melt and many examples of shocked rocks are described in which apparently normal mafic minerals exist in practically homogeneous silicate glass. With increasing temperatures all phases are eventually fused resulting in mixed or homogeneous glasses, in which spherules of nickel-iron from fusion of the meteorite have been recognized (Chao, 1967a). Depending on the subsequent cooling history of the fused rocks they may remain as glasses, as in the suevite ejected from the Ries Crater, or crystallize as 'normal' igneous rocks such as the 400km^3 layered complex at Manicouagan (Dence, 1971).

The description of shock features in the five preceding sections was in a sequence from low- to high-grade levels of shock metamorphism, spanning the range from approximately 20 to 1000kb. The development of a particular type of shock feature can occur in two minerals at significantly different pressures, because of crystal lattice differences between the two. For example, planar deformation features initially develop in tectosilicates between 120 and 150kb, but a shock load of approximately 450kb is necessary for their formation in chain silicates (Stöffler, 1972). Similarly, crystalline biotite showing only a strong pattern of kink bands can occur with

diaplectic quartz and feldspar in an assemblage shocked to 300kb or greater. Thus, for a polymineralic assemblage the level of shock metamorphism (pressure and temperature) associated with its formation is determined by characterization of the typical shock effects in all mineral constituents. Most of the styles of deformation described in the literature occur in quartz and feldspar and over a relatively wide pressure range. Thus, the tectosilicates are well suited as the basis of a scheme of progressive shock metamorphism advanced by Stöffler (1971a), which incorporates subdivisions proposed by Robertson et al. (1968) for low pressure effects.

I.1.2C Shock Effects in K-feldspars

Quartz and plagioclase are terrestrially abundant, and plagioclase and pyroxenes are present in virtually all lunar rocks, and shock effects developed in these minerals are well known. In contrast, despite the abundance and widespread occurrence of potassic feldspars in terrestrial rocks, little detailed information is available regarding shock deformation, natural or experimental, of orthoclase and microcline. Most authors have found it sufficient to describe in detail shock effects in plagioclase, including the indexing of planar deformation features and measurement of refractive indices of diaplectic glasses, and then simply to add that potassic feldspars show similar styles of deformation. In several other instances the particular feldspar has not been identified, possibly because the level of shock deformation has obscured any definitive characteristics. However, the following observations on shock

metamorphism of potassic feldspars have been presented in the literature.

K-feldspar in granodiorite at the Hardhat nuclear explosion crater shows rudimentary to distinct sets of finely-spaced "microfractures" in a few grains (Short, 1966a). Extremely strong undulose extinction occurs in potassic feldspar from Ries breccias (Engelhardt et al., 1969). Bunch (1968) reported "kink bands" in potassic feldspar from four North American craters, and "deformation bands" subparallel to (010) in K-feldspar from a Lac Couture breccia.

Dence (1968) noted that "planar features" formed in a mesoperthitic microcline at a higher shock level than in the coexisting plagioclase in rocks from beneath the Brent crater. In a sample estimated to have been shocked to 120kb by the Hardhat event, a few K-feldspar grains contain weak "planar features", but too few for measurement (Short, 1968). "Planar features or deformation lamellae" form parallel or subparallel to (001) in alkali feldspar from a Lac Couture sample (Bunch, 1968). Robertson (1968) noted twin-like "planar features" in orthoclase from the Charlevoix (La Malbaie) structure, and Rondot (1968) noted that in hand specimen these feldspars are red or cream-coloured in contrast to the pink tones of the unshocked grains. Sclar and Usselman (1970) detected "several sets of shock-induced planar features" in intermediate microcline experimentally shocked to about 250kb. From a series of recovery shock experiments to 345kb on crushed orthoclase, Kleeman (1971) found that "planar features" were not common but where observed they were "quite fine, generally of submicron scale". His experiments showed that planar features are better developed if the duration of the shock pulse is

extended by the use of thicker striker plates.

Decrease of optic axial angle has been reported as evidence of changes in structural state of alkali feldspar to a less-ordered form. Stöffler (1966) noted "orthoclase with optical properties of sanidine" and Engelhardt et al. (1969) found alkali feldspars in the Ries Crater with 2V lowered to "sanidine values". Optic axial angles of alkali feldspar at Charlevoix decrease from 55° for samples near the margin of the crater, to 45° in rocks from the central uplift (Robertson, 1968). The microcline shocked by Sclar and Usselman (1970) showed a 2Vα decrease from 78° to 50-64°. In contrast, 2Vα in deformation bands within orthoclase from the Lac Couture breccia (Bunch, 1968) has increased from 60° to 70° and the material has changed from a monoclinic to triclinic feldspar. Aitken and Gold (1968) measured the triclinicity of alkali feldspars around the Lac Couture, New Quebec, Brent and Vredefort craters, and the Pretoria Salt Pan, but concluded that differences in structural state were related to normal crystallization factors and were not shock-induced. In a subsequent investigation, Aitken (1970) was similarly unable to ascribe changes in triclinicity of orthoclase and microcline from the Charlevoix crater to shock loading. He felt, however, that anomalous cell parameters for some of these feldspars might be attributed to structural distortion due to impact. Sclar and Usselman's (1970) shocked intermediate microcline showed a change to monoclinic symmetry (high sanidine they believed) by the decrease from 0.4 to 0.0 in its triclinicity.

The most commonly reported shock deformational effect in potassic feldspars is its conversion to a diaplectic glass. Engelhardt

et al. (1969) describe "irregular or lamellar isotropization" of alkali feldspar as the initiation of this transformation. Diaplectic glasses from breccias of the Ries Crater have been noted by Stöffler (1966), Chao (1967b, 1968a, 1968b), and Engelhardt et al. (1969). Chao (1967a) illustrates a "vitreous perthite" from the Ries Crater in which the host potassic feldspar is a glass with included stringers of higher refractive index plagioclase glass. Diaplectic glass of alkali feldspar composition occurs as small inclusions in a diaplectic calcic plagioclase glass within a fragment from a Mare Tranquillitatis lunar breccia (Engelhardt et al., 1970). Recovery shock experiments have yielded mixtures of original crystalline alkali feldspar and diaplectic glass with refractive indices of 1.506-1.514 (Kleeman, 1971) and 1.487 (Sclar and Usselman, 1970), the latter with a density of 2.360g cm^{-3} (refractive index and density of thermally fused glass of high Or composition are approximately 1.487 and 2.376g cm^{-3} respectively (Barth, 1969)).

The only crystalline, presumed high-pressure, polymorph of potassic feldspar reported occurs as minute grains with high refractive index and birefringence in the diaplectic glass recovered in Sclar and Usselman's (1970) experiment. These grains produced a Debije-Scherrer pattern of six reflections which did not agree with any known or predicted phases, and could not be indexed on the basis of cubic, hexagonal, tetragonal, orthorhombic or monoclinic symmetry (Usselman, personal communication, 1972).

Fused alkali feldspar glasses created by very high temperatures accompanying strong shock pulses are also known in the Ries Crater

(Engelhardt and Stöffler, 1968; Engelhardt et al., 1969). Kurat and Richter (1968, 1972) analysed portions of the fused matrix of "Bimsstein" from the Kofels crater, Austria, and reported an $Or_{67}Ab_{25}An_8$ composition.

From the above comparatively few, generalized observations it can be seen that shock deformation effects in alkali feldspar do follow the same trend as those in plagioclase. Strong fracturing develops at low pressures which leads to a variety of planar deformations, such as kink bands, deformation bands, deformation lamellae, and planar deformation features, all probably with crystallographically controlled orientations. Changes in structural state to forms with a degree of Si-Al ordering reduced from that in the original feldspar are shown by a decrease in optic axial angle to values usual for sanidine. Isotropization begins along the various deformation planes where, presumably, high-pressure modification commences, and conversion to diaplectic glass can occur. It is possible that under suitable conditions small amounts of a crystalline, dense polymorph may persist, or it may invert to a lower-free-energy, crystalline phase which can exist under normal P-T conditions. Temperatures accompanying the highest shock pressures exceed the melting point of K-feldspar and fused alkali feldspar glass results.

I.2 Research Objectives

The purpose of the present study is to outline in more detail the scheme of progressive shock metamorphism of potassic feldspars up to the point where fusion is complete, in a similar fashion to that described for the low to medium levels of shock

deformation of quartz (Robertson et al., 1968). The basic framework for this scheme will be the observations presented in the earlier paragraphs describing the shock effects in the common rock-forming minerals, particularly those on alkali feldspars. Details will be provided from observations on samples displaying as wide a range of shock effects as are available from Canadian meteorite craters, supplemented and complemented by examination of experimentally shocked microcline. It is hoped that information from these two sources, combined with Hugoniot data, will permit the correlation of particular styles of deformation with pressures of formation.

Samples investigated in this study are from the collection of the Rock Physics Laboratory, Gravity Division, Earth Physics Branch of the Department of Energy, Mines and Resources, Ottawa, Canada, and were collected by the author or other members of the Laboratory. Included in this collection are complete suites of rocks from eighteen of the twenty confirmed Canadian meteorite craters, plus representative samples from many important non-Canadian impact sites.

Almost all the Canadian craters are located in granitic terrain with potassic-feldspar-bearing rocks forming a portion of the pre-impact lithology. In most cases, however, available samples showing evidence of shock deformation are from the allochthonous, mixed-breccia units formed from fall-back and slumping into the crater following excavation. Thus, assessment of the degree of shock metamorphism of the samples as a function of their original position relative to the shock centre cannot be made. However, in two particular localities (the Brent Crater, Ontario, and the Charlevoix Crater, Quebec),

rocks spanning the range from unshocked to moderately highly shocked can be sampled in essentially their original position, relative to the crater centre. Hence, most of the observations have been made on specimens from these latter two sites. In addition, several fragments from allochthonous breccias at the Lac Couture crater, Quebec, were examined in detail because they contain coarsely-twinned maximum microcline, not present in the Brent or Charlevoix suites.

I.3 Acknowledgements

Sections of this study were carried out at three institutions and many people in addition to those mentioned below aided in its completion by deed or discussion. In the Department of Geological Sciences, University of Durham, Professor Malcolm Brown provided guidance and patience in supervising the research, and his critical reading of the manuscript is much valued. Mr. Michael Dence and Dr. Richard Grieve of the Rock Physics Laboratory, Ottawa, gave many hours in discussion and assessment of the manuscript. Much of the sample preparation for all phases of examination and experiment was done by Mr. Rene Wirthlin at the Rock Physics Laboratory. Professor Thomas Ahrens made available the shock experiment facilities of the Seismological Laboratory, California Institute of Technology, and his advice regarding this aspect of the research is appreciated. Dr. John Kleeman and Mr. Herrmann Spetzler assisted in carrying out the experiments which were supported in part by NASA grant NGL05-002-105. Thanks go to Dr. Friedrich Hörz, Lunar Science Institute, Houston for providing three samples of experimentally shocked microcline, and to Dr. George Plant, Geological Survey of Canada, for an electron micro-

probe analysis of highly shocked K-feldspars. The entire venture was made possible through the programme of leave for furthering education of the Public Service Commission, Canada, upon the recommendation of Dr. M.J.S. Innes, Chief (1952-1972), Gravity Division, Earth Physics Branch, Department of Energy, Mines and Resources.

CHAPTER II

STRUCTURAL DEFORMATION IN ORTHOCLASE AND MICROCLINE

The term "structural" deformation is used here to describe all shock effects governed by the degree of Si-Al ordering in the feldspar lattice, such as structural state and related optical parameters, plus all types of planar deformations including fractures, cleavage, twinning, deformation lamellae and planar deformation features. In contrast, Chapter III contains descriptions of changes in the chemical composition of the feldspars due to shock loading. The samples examined are from the Charlevoix and Lac Couture craters in Quebec Province.

II.1 Charlevoix Crater

II.1.1 Introduction

The Charlevoix crater, at one time known as the La Malbaie crater (Robertson, 1968), is a semicircular structure approximately 350km northeast of Montreal exposed on the north shore of the St. Lawrence River (Fig. II.1). It has the form of a complex crater (Dence, 1968) with an upraised central peak and a peripheral depression 35km in diameter (Fig. II.2), but approximately 40% of the circle has been removed in the south, southeast and east where it is truncated by the river. Despite its large size it remained undiscovered until comparatively recently (Robertson, 1967), because of the incomplete circularity. The peripheral valley is approximately 1½km wide with the hills of the outer margin rising gradually to 900 or 1000m. The inner wall rises steeply from sea level to 300m, levels to a plateau about 5km wide with several small hills, and rises again

Fig. II.1

Location of the Charlevoix, Lac Couture, and Brent craters on the Canadian Precambrian Shield (shaded area).

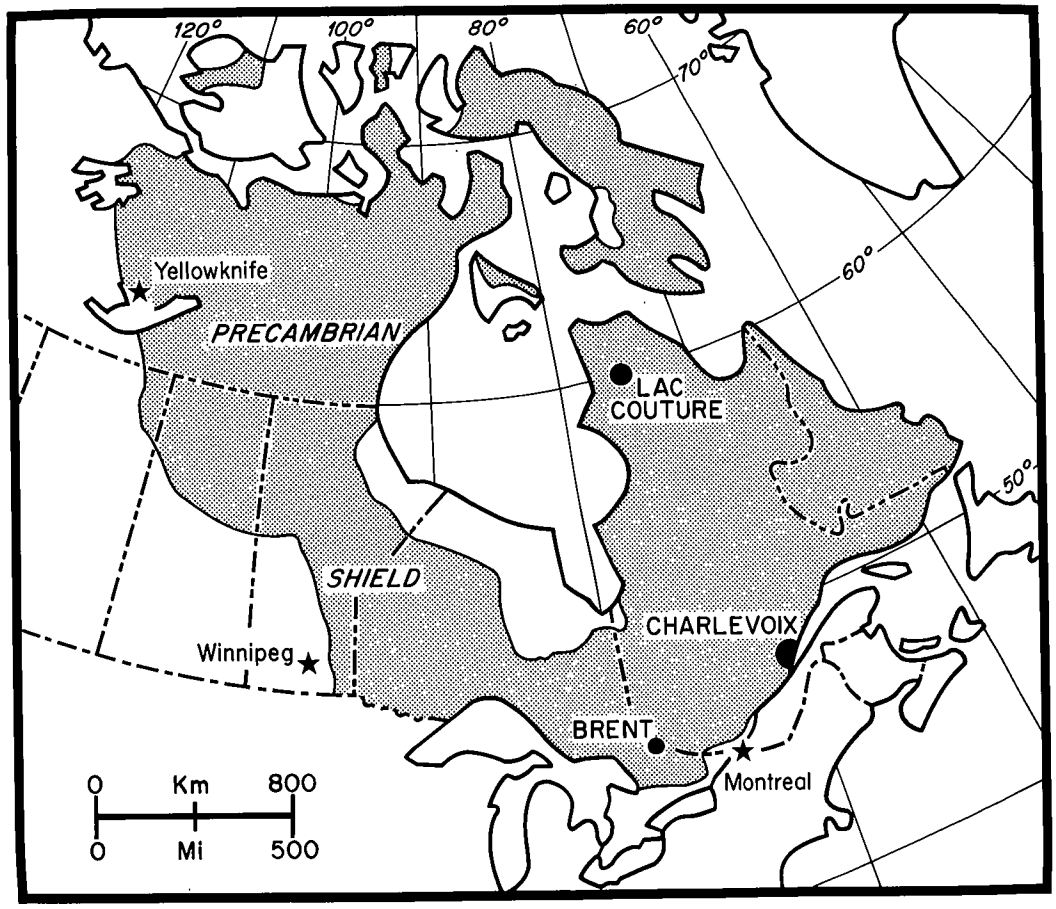
120°
100°
80°
60°
70°
60°
50°
Yellowknife
PRECAMBRIAN
LAC
COUTURE
SHIELD
CHARLEVOIX
Winnipeg
BRENT
Montreal
0 Km 800
0 Mi 500

Fig. II.2

Shaded contour map showing topographical expression of the Charlevoix crater. A peripheral, semicircular valley 35km in diameter extends inland from the St. Lawrence River (horizontal lines), enclosing a central plateau with a range of hills forming a crude semi-ring around the central peak of Mont des Éboulements (see Fig. II.4), 780m above the river. The hills outside the valley rise to an average of 900m. Contour interval 400 ft (122m), and shading lightens for each 800 ft (244m) rise in elevation. Reprinted from Robertson (1968).


2400
600
800
N
0 Mi 6
0 Km 10

to 780m on Mont des Éboulements, the highest of the group of hills forming the central peak. The plateau drops off sharply along the edge of the river.

Stratigraphic evidence reveals that the crater formed between late Middle Ordovician and late Devonian times (Robertson, 1968), confirmed by dates of 342m.y. and 372m.y. obtained from recrystallized "impactite" (Rondot, 1971a). The meteorite impacted on a probably thin, shelf-facies sequence of Middle Ordovician limestones overlying crystalline Grenville rocks on the margin of the Precambrian Shield. During the Acadian Orogeny in late Devonian time, thrusting from the southeast dumped an unknown thickness of early Palaeozoic sedimentary rocks on the edge of the Shield, obliterating the southeastern part of the crater. Remnants of these rocks form Isle aux Coudres lying in the St. Lawrence River within the perimeter of the original circular depression (Fig. II.3). Erosion has removed most of the Middle Ordovician limestone except for downfaulted outcrops along the St. Lawrence River and inland along the peripheral valleys. Grenville rocks exposed within the crater include (from presumed oldest to youngest) granitic gneisses and migmatites outcropping in the eastern quarter; charnockitic gneisses underlying most of the central, southwestern and northern regions; and an anorthosite body, with marginal dioritic and gabbroic rocks, intersected by the crater in the northwest. Several faults have been mapped (Rondot, 1968), the strongest being parallel to the river and between it and Mont des Éboulements. Evidence that the Charlevoix structure is a meteorite crater has been presented by Robertson (1968) and Rondot (1968, 1970,

Fig. II.3

Geological units intersected by the Charlevoix crater. The charnockitic gneisses, which have been subdivided into four main units by Rondot (1966, 1967, 1969, 1971b), are part of the Laurentide Park massif. Reprinted from Robertson (1968).

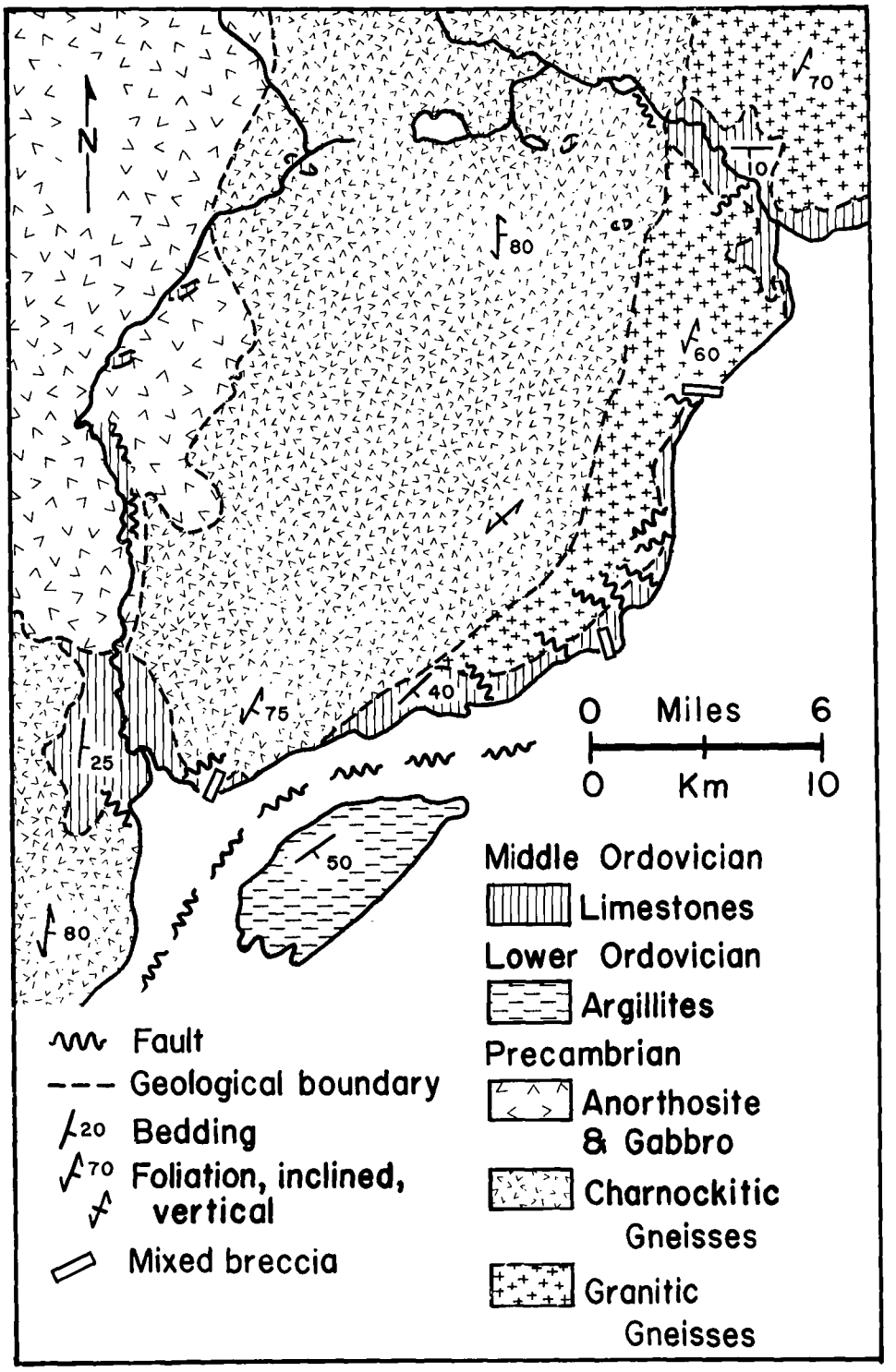
N
70
10
80
60
75
40
25
50
80
0 Miles 6
0 Km 10
Middle Ordovician
Limestones
Lower Ordovician
Argillites
Precambrian
Anorthosite & Gabbro
Charnockitic Gneisses
Granitic Gneisses
Fault
Geological boundary
20 Bedding
70 Foliation, inclined,
vertical
Mixed breccia

1971a) and includes brecciation, shatter cones and pseudotachylites on the macro-scale, and microscopic shock deformation features in the breccias and basement rocks. Two small outcrops of "impactite" are the remains of a presumed layer of rocks melted by the impact and later recrystallized. Robertson (1968) studied in detail the planar deformation features in quartz from basement rocks outcropping on the plateau and central peak regions. It was shown that on the basis of quartz deformation, degree of shock metamorphism decreases outward in zones concentric about Mont des Éboulements, and is not detected in quartz beyond approximately 10km from the central peak. Only a moderate level of shock metamorphism is found in the most highly deformed rocks on Mont des Éboulements, produced by shock pressures in the 250 to 350kb range as correlated with Hörz's (1968) shock experiments on quartz. Rocks displaying shock metamorphism typical of higher pressures have been eroded, although a few have been discovered in a glacial deposit near the foot of Mont des Éboulements.

Level of shock metamorphism is a function not only of pressure, but depends also on the pressure-time and temperature-time profiles, orientation with regard to stress direction, and grain size and mineralogy of the target rocks. Coesite, for example, has been produced only once in shock experiments (Deribas et al., 1966) where pulse duration is of the order of 10^{-7} to 10^{-5} sec, but has been reported from several terrestrial meteorite craters where peak pressure endures for 10^{-2} to 10^{-1} sec or longer (Stöffler, 1972), and has been produced in static deformation experiments at pressures as low as 10kb (Green, 1972) where peak pressures have been maintained for much longer periods.

Similar considerations apply in the development of coesite under conditions where high temperatures have persisted, allowing the sluggish quartz-coesite transition to occur. The dependence of degree of deformation on orientation relative to the shock direction has been shown in shock experiments (Hörz, 1968; Müller and Hornemann, 1969) where different crystallographic orientations relative to the shock wave resulted in different sets of planar deformation features. Most geologic materials are polymineralic, and therefore, pressure-time and temperature-time profiles existing in a particular grain will vary due to stress-wave interactions at grain boundaries, particularly where adjacent grains have different physical properties. In a natural impact event these parameters cannot be controlled, but by sampling in a single rock type, preferably one without strong mineral orientations, it can be assumed that all significant variables have a fairly constant effect. Thus comparison of shock effects in a particular mineral between rocks of the same suite can be accomplished whether or not the comparison holds for the same mineral in two different rock types.

II.1.2 Charnockitic Rocks

Charlevoix is the most suitable of the Canadian impact sites for a systematic study of shock deformation in potassic feldspars. It is accessible and intersected by roads, outcrops are numerous and well distributed and, except in the wooded hills of the central peak, the outcrops are easily visible in open farmland. At Charlevoix two potassic-feldspar-bearing units, the granitic gneisses and migmatites and the charnockitic gneisses, can be sampled from the central peak

outward to well beyond the peripheral valley where shock deformation has not occurred. The charnockitic gneiss unit was chosen for detailed study in preference to the granitic gneisses and migmatites for several reasons: a greater overall distribution, particularly in the central uplift where highest shock levels occur; a high K-feldspar content (30%-40%); examples of shock levels higher than preserved in outcrop are found in glacial debris; and the granitic gneisses and migmatites outcrop along the river where faulting and the effects of thrusting during the Acadian Orogeny may complicate the interpretation of shock deformation.

The Charlevoix crater region has been mapped by the Quebec Department of Natural Resources at a scale of one inch to one mile (Rondot, 1966, 1967, 1969, 1971b). The crater lies on the southeastern margin of the Grenville province, the youngest structural province of the Canadian Precambrian Shield and a stable platform during the last 900m.y. The charnockitic rocks underlying 75% of the preserved crater are part of the Laurentide Park massif, a body of pyroxene-bearing granitoid rocks covering approximately 285,000km^2 northeast of Quebec City. Within the crater region these rocks have been mapped mainly as "green feldspar migmatite", "green charnockite and quartz monzonite", "green syenite and monzonite" and "granulated garnet charnockite". The latter three are less abundant and occur as north- or northeast-trending zones, $\frac{1}{2}$ to $1\frac{1}{2}$km wide, within the green feldspar migmatites. All types possess a poorly-developed gneissosity.

"Charnockite" was first used by Holland (1900) to describe the acid member of acid to ultrabasic, granular textured rocks containing

highly pleochroic orthopyroxene in the province of Madras, India. Howie (1955) continued this usage and suggested that the term "charnockitic" best described rocks having affinities with this series. The type charnockite contains abundant microperthitic microcline, with associated quartz, andesine, hypersthene, ilmenite and magnetite, with minor biotite, hornblende, apatite and zircon. Holland believed it to be an igneous rock but Howie thought the series was the product of high-grade regional metamorphism of a series of calc-alkali plutonic rocks. Charnockites and charnockitic rocks have been described from widespread regions and, although proponents of a metamorphic genesis outnumber those favouring an igneous origin, there have been champions for each hypothesis. In general terminology, charnockites are granulite-facies rocks with orthopyroxene and abundant, generally perthitic, potassic feldspar. The series mapped in the Charlevoix region agrees with this description.

Rocks from eighty-one outcrops in the charnockitic rocks were examined (Fig. II.4) to delimit the outer margin of detectable shock deformation in the potassic feldspars. From these, twenty-five (primary) samples from the peak of Mont des Éboulements, and at intervals outward to approximately 25km, were studied in detail to characterize their level of shock metamorphism. Although the samples are from outcrops mapped as green feldspar migmatites, green syenite and monzonite, and green charnockite and quartz monzonite, they do not all agree with their respective map nomenclature. They are charnockitic due to the presence of orthopyroxene, but on the basis of quartz, K-feldspar, and plagioclase content, these rocks are granites, adamellites, syenites,

Fig. II.4

Sample distribution within the charnockitic rocks, Charlevoix crater. Larger, numbered circles locate samples studied in detail. Dashed lines are approximate geological contacts (cf. Fig. II.3).

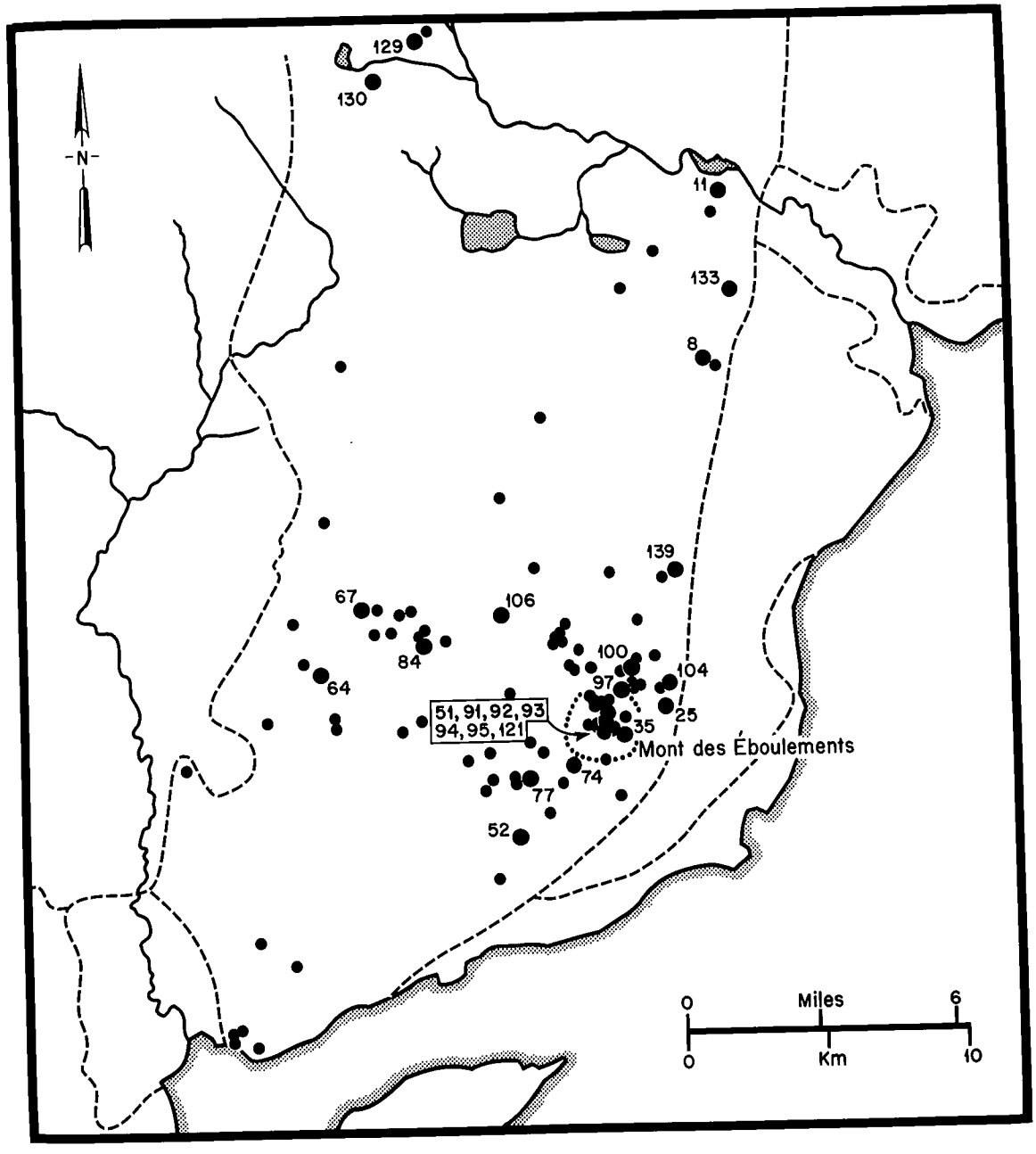
129
130
N
11
133
8
139
67
106
84
100
97
104
64
51, 91, 92, 93
94, 95, 121
25
35
Mont des Éboulements
74
77
52
0
Miles
6
0
Km
10

monzonites and syenodiorites. A classification, unrelated to field occurrence, was based on additional mineralogical characteristics obtained from modal analyses of the twenty-five primary samples (Table II.1). The rocks of the charnockitic series are thus grouped as charnockitic granites, charnockitic microcline granites, and charnockitic syenodiorites.

The charnockitic granites were studied in detail in 12 samples from the peak of Mont des Éboulements and at intervals outward to 24km (Table II.1, Fig. II.4). In hand specimen they are medium-grained rocks displaying poor to moderate gneissic banding, although a few are from massive outcrops. Fresh specimens farthest from the shock centre are olive-green to grayish-green, the colour being imparted by greenish feldspars and gray quartz. Nearer the central peak, samples are lighter coloured due to the milky appearance of shocked quartz, and gray to pink feldspars. Shatter cones occur to some degree in all rocks within 12km of Mont des Éboulements with the strongest development near 7km (Robertson, 1968), and thus surfaces of all samples collected within this region exhibit the linear fluting of partial cones.

The charnockitic granites are identified in thin section by a significant quartz content, and by perthitic, untwinned, potassic feldspar, generally well in excess of the amount of plagioclase. Grain-size of the quartzo-feldspathic minerals ranges from approximately 0.1mm to 1.0mm within samples and averages between 0.4 and 0.6mm. Modal analyses of the charnockitic granites are given in Table II.1. The generally well-twinned plagioclase is an oligoclase or andesine of An_{23} to An_{36}, averaging about An_{31} (determined by Michel-Lévy method),

Table II. 1 Modal analyses of charnockitic rocks of Charlevoix

	sample	quartz	k-spar	plagio-clase	ortho-pyroxene	clino-pyroxene	amphibole	biotite	opaques	garnet	apatite	others
	8	19.5%	34.4%	37.0%	6.7%	2.3%	0.5%	0%	0.9%	0%	0.3%	0 %
	11	13.3	45.5	22.0	2.6	0.2	10.0	0	5.4	0	0.6	0.5
	25	33.4	43.1	21.5	0	0	1.9	tr	0.1	0	0	0
	51	14.8	46.1	24.6	4.9	4.0	0	0	5.1	0	0.3	0.3
charnockitic	52	25.0	60.6	9.6	0.3	0	3.9	0	0.3	0	0.1	0.3
	67	24.0	22.9	44.3	4.4	0.1	2.9	0.3	3.3	0	0.1	0.4
granites	74	15.3	26.9	45.9	10.5	0	tr	0	1.1	0	0.3	0.1
	77	14.4	48.1	30.3	4.4	0	0	0	1.0	1.4	0	0.3
	84	34.1	25.6	30.5	3.3	tr	3.5	tr	2.6	0	0.3	0.1
	104	29.8	44.4	19.4	4.5	0.9	0	0	0.8	0	0.4	tr
	106	34.4	39.1	21.9	0.9	0	2.0	0	1.4	0	0.1	0.3
	130	24.3	46.7	18.2	9.1	0	0	tr	1.7	0	tr	tr
	35	21.5	44.3	23.5	6.1	0.3	0	0	3.9	0	0.1	0.4
charnockitic	64	31.6	43.7	21.6	1.2	0.9	0	0	0.9	0	0.1	0.1
	97	33.6	21.5	37.6	5.5	0.1	0.4	0	1.3	0	0	0
microcline	121	0	48.9	42.4	4.9	2.7	tr	0	0.8	0	0	0.2
	133	16.9	36.5	39.0	4.4	1.1	tr	0.6	1.5	0	tr	0
granites	139	24.5	34.8	36.2	4.0	0	0	0	1.1	0.2	0.1	0.1
	91	0	17.1	42.8	9.4	0	9.8	5.5	3.3	11.1	0.8	0.4
	92	0	11.6	53.8	14.6	5.3	6.8	2.4	4.1	0	1.3	0.3
charnockitic	93	0	16.9	52.5	4.8	0.4	14.3	0.8	6.3	0	4.1	0.1
	94	0	14.5	55.0	7.9	2.2	12.6	1.3	5.5	0	0.9	0.1
syenodiorites	95	0	26.0	64.3	5.8	1.0	0	0	2.3	0	0.5	0.3
	100	0	62.3	25.8	9.0	0	0	0	2.3	0	0	0.8
	129	0	24.3	48.3	13.1	7.6	tr	0	5.1	0	1.4	0.3

a composition in close agreement with plagioclase of the acid member of the Madras charnockites (Howie, 1955). Potassic feldspar is untwinned, perthitic orthoclase. The strongly pleochroic orthopyroxenes of the charnockitic granites lie in the iron-rich eulite and orthoferrosilite portion of the enstatite-ferrosilite series (electron probe analyses), compositions more typical of metamorphic than igneous rocks (Deer et al., 1963b). The coexisting clinopyroxene is a ferroaugite. Amphibole, biotite and garnet compositions were not determined.

The charnockitic microcline granites (6 samples) are similar to the charnockitic granites in most aspects and in hand specimen, rocks of the two groups cannot be distinguished. However, the main difference detected in thin section is that the K-feldspar shows grid twinning and on this basis has been identified as microcline. Modal analyses of the charnockitic microcline granites are presented in Table II.1. Plagioclase is an oligoclase or andesine (An_{23} to An_{38}, average An_{31}) and is well-twinned. The microcline in general shows poor grid-twinning commonly restricted to less than half the grain, whereas it is well-defined and evenly developed in others. Microcline from most samples is microperthitic. The orthopyroxene is an iron-rich variety, and the clinopyroxene is ferroaugite.

Rocks of the charnockitic syenodiorite group (7 samples) underlie a large part of the north slope of Mont des Éboulements (Fig. II.4) where shock deformation is strongest, and were sampled for this reason although they are not commonly encountered elsewhere in the crater. In hand specimen they are medium-grained rocks displaying a poor to moderate gneissic banding, or a poor foliation in biotite-rich

samples. Fresh specimens are pinkish-gray to dark olive-green. Samples 91 to 94 on the north slope of Mont des Éboulements and within 100m of the summit, are from a zone more basic than the other samples and show a slightly different character, being in hand specimen the darkest of this group. Although the overall grain size of the charnockitic syenodiorites is like that of the other two groups described, the range within samples is larger. Quartz in visible amounts is absent from these rocks and it is largely this characteristic which distinguishes the charnockitic syenodiorites from the other two groups. Modal analyses of the charnockitic syenodiorites are given in Table II.1. The high degree of shock metamorphism in the rocks on Mont des Éboulements and strong alteration of plagioclase and mafic minerals prevented accurate composition determinations in the charnockitic syenodiorites. Plagioclase of the more siliceous members is an andesine (An_{33}). Electron microprobe analyses on sample 129, 25km from Mont des Éboulements reveals that the composition of orthopyroxene is $En_{40}Fs_{52}Wo_8$ and the clinopyroxene is a salite, both pyroxenes having lower Fe contents than those in the two granitic groups. Potassic feldspar is an untwinned, perthitic orthoclase of the same general appearance as that found in the charnockitic granites.

It is evident from the modal analyses and petrography that although each of the three groups possesses characteristics which distinguish it from the other two, significant variation exists within a group, in particular between the siliceous and basic rocks of the charnockitic syenodiorites. This grouping, however, is not intended as an exhaustive and mutually exclusive petrographic classification. Since this is a study of shock metamorphism of potassic feldspar, the three-fold

division of the charnockitic rocks is designed to provide three suites with the K-feldspar in different mineralogical environments or assemblages. Thus the classification is, in effect: (a) charnockitic granites - rocks with orthoclase and quartz; (b) charnockitic microcline granites -- rocks with microcline and quartz; (c) charnockitic syenodiorites- rocks with orthoclase but no quartz, and a generally higher mafic content.

II.1.3 Levels of Shock Metamorphism Preserved

The relative degree of shock metamorphism in Charlevoix samples can be determined from shock effects in the common, rock-forming minerals, particularly quartz and plagioclase. Shock pressures can be assigned to the various levels by using data from recovery experiments in which typical shock features were produced in quartz and plagioclase.

From a study of planar deformation features in shocked quartz (Plate II.1a), Robertson et al. (1968) found that sets become more abundant with increasing degree of shock metamorphism, and that planes with particular crystallographic orientations are characteristic of successive shock levels. Proceeding from low to high degree, quartz with planar deformation features parallel {0001} was designated as type A, parallel $\{10\bar{1}3\}$ as type B, $\{22\bar{4}1\}$ as type C, and $\{10\bar{1}2\}$ as type D. Development of diaplectic quartz characterizes type E quartz. Type A has only one set of planar deformation features, whereas an average of five or six sets is typical of type D. Robertson (1968) showed that initial development of type A occurs at approximately 10km from the central peak at Charlevoix, and type D is restricted to the central peak zone, 2km in diameter. Type E quartz was not found.

Plate II.1

a) Two sets of decorated planar deformation features parallel to $\{10\bar{1}3\}$ in type B quartz from Charlevoix (sample MBP 25). Crossed polars.

b) Sinuous recrystallization of plagioclase originally converted to maskelynite by shock deformation (sample MBP 122). Crossed polars.

a)

125μ

b)

500μ

Shock experiments have been carried out on quartz to delimit the pressure ranges where particular cleavages and planar deformation features develop. Müller and Défourneaux (1968) shocked single quartz crystals, cut parallel {0001}, at pressures from 95 to 330kb. Hörz (1968) performed similar experiments at pressures from 52 to 270kb on quartz cut parallel {0001}, $\{10\bar{1}0\}$, and $\{10\bar{1}1\}$. Summarizing their results, planar features initially developed parallel $\{10\bar{1}3\}$ (type B quartz) between 105 and 119kb. Planes oriented parallel $\{10\bar{1}2\}$(type D quartz) formed above approximately 160kb and became as abundant as $\{10\bar{1}3\}$ sets at about 250kb. Both orientations persisted to the highest pressures achieved in the experiments. Planes with most of the other orientations measured in naturally shocked quartz were also produced, including $\{22\bar{4}1\}$ (type C quartz) at 170kb only. Basal features, {0001}, typifying type A quartz were not reported by Müller and Défourneaux, and did not develop below 162kb in Hörz's experiments. Hörz (and many others) believed that planar deformation features form only where shock pressures have surpassed the Hugoniot elastic limit (see Appendix D). He also showed that their development and orientation is dependent on orientation of the grain with respect to the shock front, due to differences in value of the Hugoniot elastic limit for different orientations. Deformation occurred at lower pressures, and was more intense, where the shock front was normal to{0001}, rather than normal to a prism or rhombohedron. This is an apparent contradiction of Fowles' (1967) data which indicated the Hugoniot elastic limit for Z-cut quartz, {0001}, lies between 100-150kb, but for X-cut, $\{2\bar{1}\bar{1}0\}$, is between 55 and 85kb.

It is possible that planar deformation features may develop

at pressures of approximately 85±15kb in grains suitably oriented with respect to the shock front, thus producing type A quartz deformation. The abundance and orientation of planar deformation features in quartz can serve to determine approximate shock pressures in the range from 85 to 250kb±10%.

Shock metamorphic effects in plagioclase have been less well correlated with pressure. Planar deformation features initially develop over approximately the same pressure range as those in quartz and are parallel to certain crystallographic planes of low indices (Robertson et al., 1968), but a breakdown similar to that for quartz has not been established. The formation of maskelynite, however, is a useful indicator of minimum shock pressures. Partial conversion begins in Stage I (Stöffler, 1971a) above 100kb. Complete transformation has been achieved in experiments at 330kb (Müller and Hornemann, 1967), at 340-375kb (Stöffler and Hornemann, 1972), and at 300kb (Gibbons, 1973). Thus, complete transformation of plagioclase to maskelynite at approximately 350kb± 10% is a valuable indication of minimum pressure. Stöffler and Hornemann cautioned that shock wave behaviour of plagioclase in multiphase polycrystalline rocks may differ from that observed in single-crystal experiments, but for crystalline, non-porous rocks with a low content of high-impedance mafic minerals, such as granitic rocks, the difference is not appreciable.

The degree of shock metamorphism in the charnockitic rocks at Charlevoix has been determined from measurement of planar deformation features in quartz (Robertson, 1968 and this study), and observation of maskelynite was not observed, but plagioclase in most samples from

Table II.2 Degree of shock metamorphism in charnockitic rocks of Charlevoix.

	sample	distance from centre (km)	planar deformation features in quartz: % with planes	average sets per grain	% A	% B	% C	% D	maskelynite (devitrified) development	shock pressure (kb)	shock temperature microcline (°C)	post-shock temperature feldspar (°C)
charnockitic granites	130	24.1	0						none	<50	<250	<100
	11	19.3	0						"	<50	<250	<100
	8	13.4	0						"	<50	<250	<100
	84	7.2	48	0.48	48	0	0	0	"	100± 10%	<250	<100
	52	5.0	62	0.67	58	4	0	0	"	110 "	<250	<100
	67	9.6	68	0.76	60	8	0	0	"	110 "	<250	<100
	77	3.3	96	2.24	36	52	4	4	"	160 "	<250	<100
	106	5.5	92	2.28	0	80	12	0	"	170 "	<250	<100
	104	2.7	100	2.72	4	88	8	0	"	175 "	<250	<100
	25	2.3	100	3.35	0	77	5	18	"	200 "	<250	<100
	74	1.7	100	3.76	0	44	8	48	"	230 "	300±50	100±30
	51	0.0	100	5.50	0	16	6	78	incipient	300 "	530 "	230"
charnockitic microcline granites	133	16.0	0						none	<50	<250	<100
	64	10.3	8	0.08	8	0	0	0	"	90±10%	<250	<100
	139	6.3	68	0.80	60	8	0	0	"	110 "	<250	<100
	97	1.5	100	4.80	0	28	36	36	incipient	270 "	375±50	130±30
	35	0.7	100	5.74	0	16	4	80	none	300 "	530 "	230 "
	121	0.3		no quartz					incipient	300 "	530 "	230 "
charnockitic syenodiorites	129	25.1		no quartz					none	<50	<250	<100
	100	2.4		"					"	190±10%	<250	<100
	91	0.1		"					incipient	270 "	375±50	130±30
	92	0.1		"					complete	330 "	630 "	245 "
	93	0.1		"					"	340 "	695 "	250 "
	95	0.1		"					"	350 "	760 "	255 "
	94	0.05		"					"	360 "	825 "	260 "

Mont des Éboulements is a microcrystalline mosaic devitrified from diaplectic glass (Plate II.1b). The charnockitic syenodiorites lack quartz and their level of deformation is based partly on the shock level of quartz-bearing rocks in nearby outcrops. Shock pressures have been assigned to each sample from these data (Table II.2); shock and post-shock temperatures for microcline were taken from Stöffler and Hornemann (1972, Fig. 10).

The most highly shocked rocks preserved in outcrop at Charlevoix represent pressures of approximately 360kb±10%. It is presumed that material of higher shock grades has been eroded. There is a strong correlation between degree of shock metamorphism and distance from Mont des Éboulements, but this relationship is not rigid.

II.1.4 Shock Metamorphism of Potassic Feldspars

II.1.4A Structural State

The fundamental structural unit of silica and the silicate minerals is a silicon atom tetrahedrally bonded to four oxygen atoms. By sharing corner oxygen atoms the SiO_4 tetrahedra are linked to form a continuous three-dimensional network. In many silicates some of the tetravalent silicon anions are replaced by trivalent aluminum anions, and electroneutrality is maintained by introduction of positive cations. Aluminum substitutes for one quarter of the silicon atoms in the alkali feldspars, $KAlSi_3O_8$ (Orthoclase) and $NaAlSi_3O_8$ (Albite), and one half the silicon atoms in the anorthite molecule, $CaAl_2Si_2O_8$. The degree of order-disorder, or structural state of the feldspars, is a measure of the rigidity of the Al-Si substitution in particular sites, which is

a function of conditions of formation.

The "orthoclase" unit cell comprises four $KAlSi_3O_8$ molecules, providing sixteen sites for the four Al and twelve Si atoms. In the varieties with monoclinic symmetry (sanidine, adularia, orthoclase) these sixteen sites occur as two equivalent sets, T_1 and T_2, of eight sites each. To permit monoclinic symmetry, Al must substitute randomly for Si in all sites of at least one set, that is the probability of finding an Al atom must be constant for each site of the set. Two extreme possibilities exist: (1) Two Al atoms occupy sites in each set and the probability of finding an aluminum atom in any site of set T_1=probability in T_2=$\frac{1}{4}$. This case represents complete disorder and typifies the sanidine structure. (2) All four Al atoms occupy sites in one set (T_1) so that the probability T_1=$\frac{1}{2}$ and probability T_2=0. This is the most highly ordered monoclinic feldspar structure and is known as hypo-orthoclase. Orthoclase is a monoclinic feldspar with degree of ordering transitional between sanidine and hypo-orthoclase.

Alkali feldspars with triclinic symmetry contain sixteen Al-Si sites in four equivalent sets, $T_1(0)$, $T_1(m)$, $T_2(0)$, and $T_2(m)$, each with four sites. The most highly ordered triclinic feldspar has all four aluminum atoms substituting in one of these sets to the exclusion of the other three. This structure typifies maximum microcline, and triclinic feldspars with less rigorous ordering are intermediate microclines.

Although the ordering extremes of high sanidine and maximum microcline are known in nature, hypo-orthoclase is not found. In a review of ordering in natural and theoretical K-feldspars, Barth (1969,

Fig. 3.10) noted that orthoclase with an order index between 33% and 67% (sanidine=0%, hypo-orthoclase=67%, maximum microcline=100%) is unstable and does not occur in nature.

The degree of ordering is inversely proportional to the temperature of crystallization. Sanidine is characteristic of high temperature environments. Orthoclase forms above approximately 500°C, below which the change to triclinic symmetry occurs, and maximum microcline becomes stable below approximately 300°C (Barth, 1969). Knowledge of the degree of order of a feldspar is therefore useful in interpreting its origin or history subsequent to primary crystallization, and several methods have been devised for such a determination. The most reliable, but certainly the least practical for routine petrologic studies, is to determine the average size of the $(SiAl)O_4$ tetrahedra and, from knowledge of the Si-O, Si-Si, Al-O and Al-Al bond lengths, to calculate the average Al content of each anion site. Other methods more commonly used are based on X-ray or optic studies and rely on the variation of optic and crystallographic parameters with degree of ordering. Several of these techniques are described below.

Recent studies have attempted to determine whether P-T conditions during and following hypervelocity impact are reflected in changes of structural state of the potassic feldspars from rocks within and in the immediate vicinity of meteorite craters. These studies have necessarily been restricted to feldspars subjected to shock metamorphism conditions lower than that required for conversion of feldspar to diaplectic glass. Aitken and Gold (1968) and Aitken (1970) measured triclinicity values of microcline from rocks surrounding four meteorite

craters, i.e. New Quebec Crater, Lac Couture, Brent, and the Vredefort Dome. Triclinicity determinations are useful only for determining the relative structural state of triclinic feldspars. In each instance the measured variations in triclinicity reflected lithologic and structural variations and could not be correlated with degree of shock metamorphism based on the distance of the sample from the crater's centre. The samples from the three Canadian sites were collected from outcrops on the crater rim and outward, in rocks which show no typical shock deformation features. Samples from the deeply eroded central region of the Vredefort Dome were examined, but Aitken and Gold (1968) do not provide a description of shock effects in these rocks to permit an estimate of level of shock metamorphism. It seems likely that shock pressures did not exceed 100kb, and quite probably less than about 60kb in the rim rocks; residual shock-temperatures were less than 100°C and thus the lack of evidence for changes in structural state of these microclines is not surprising.

Aitken (1970) separated K-feldspar from samples collected from the Charlevoix crater. Only one locality lies in the central peak region and all others are from zones now estimated to have experienced shock pressures of less than 150kb. From X-ray diffraction studies of these samples and of samples from the four craters of the earlier work (Aitken and Gold, 1968), unit cell parameters were determined and α^* vs γ^* was plotted. Theoretical values vary from 90° for both α^* and γ^* in all monoclinic feldspars to approximately 90.4° and 92.3°, respectively, in maximum microcline. Therefore, such a plot (Mackenzie and Smith, 1956) allows a partial calculation

of triclinic structural state but allows no insight into the degree of ordering of monoclinic varieties. Using this method, Aitken (1970) found that differences in structural states of K-feldspars could be detected in the rocks from each crater, including a few "anomalous" feldspars, but again, these variations could not be correlated with degree of shock metamorphism. Aitken recorded that most of the "anomalous" feldspars were from the larger craters, Charlevoix and Vredefort.

It has been shown in laboratory Recovery experiments that changes in degree of ordering are produced in feldspars by shock loading. Intermediate microcline shocked to approximately 250kb (Sclar and Usselman, 1970) yielded a mixture of diaplectic glass and residual crystalline feldspar. Triclinicity of the feldspar decreased from 0.4 (pre-shock) to 0.0, indicating a decrease in order to a monoclinic feldspar identified from X-ray patterns as high sanidine. Shock loading of albite to 250kb in the same series of experiments also induced disordering. Temperatures were neither measured nor calculated in these experiments but in a series of Recovery shock experiments of similar design and starting material, Kleeman (1970) calculated post-shock temperatures of 650°-700°C at 200kb and 900°-1000°C at 300kb. Thus, disordering is produced as a result of elevated temperatures accompanying moderate shock pressures, although the effects of the shock wave itself on the disordering process are not known.

The structural state or relative degree of ordering was determined for the potassic feldspars in the charnockitic rocks of the Charlevoix crater. Aitken's (1970) failure to detect shock-induced

structural state changes at Charlevoix may be due to his lack of samples from the central peak region where P-T conditions may have been at a level suitable for such changes. It was hoped that the samples from Mont des Éboulements used in the present study (Fig. II.4, Table II.2) would be sufficient to resolve this difficulty. Structural state was determined by the following five methods and the results compared:

(1) optic angle vs composition; (2) triclinicity; (3) three-peak method; (4) b vs c; (5) Barth's %-ordering.

Methods 2-5 are partly based on X-ray diffraction studies. For this purpose potassic feldspar was separated from crushed portions of each sample by standard heavy-liquid procedures. Standard thin sections and polished thin sections were used in the determinations of method 1.

II.1.4A (i) Optic angle vs composition

Four series of alkali feldspars were distinguished by Tuttle (1952) on the basis of optic angle and orientation of the optic plane. They are: high sanidine - high albite, sanidine - anorthoclase cryptoperthite, orthoclase cryptoperthite, and microcline cryptoperthite. The above sequence corresponds to a general increase in degree of order. An alkali feldspar can generally be placed in one of these series through knowledge of its composition, optic angle, and orientation of the optic plane. These parameters were determined for the 25 primary charnockite samples. Compositions were calculated from SiO_2, Al_2O_3, K_2O, Na_2O, and CaO determined by electron microprobe analysis. Iron and barium oxides are insignificant as determined in a few specimens. The average, and range of composition for each sample are presented in Table II.3

Table II.3 K-feldspar compositions and optic angles in charnockitic rocks of Charlevoix.

	sample	composition (Or)			optic angle (2Vα)		
		mean	range	std. dev'n	mean	range	std. dev'n
charnockitic granites	130	86.5	82.7-91.0	2.98	56°	60-64°	5.53
	11	79.7	71.8-85.8	5.06		n.d.	
	8	86.0	76.5-90.4	4.92	71	62-82	6.28
	84	85.2	71.5-89.2	7.11	55	52-58	3.26
	52	84.5	78.1-87.2	3.69	59	46-80	7.82
	67	80.6	64.4-87.8	7.17	53	36-67	6.09
	77	82.5	74.8-86.5	4.18	68	48-88	13.96
	106	87.4	85.4-89.9	2.06	55	44-64	5.29
	104	83.1	72.8-89.3	6.27	60	48-71	8.31
	25	81.0	70.7-90.3	5.44	68	47-94	10.19
	74	85.1	74.8-89.2	4.30	58	50-66	4.59
	51	71.2	59.7-81.2	5.26	54	37-77	10.72
charnockitic microcline granites	133	84.7	76.9-89.0	3.41	63	52-72	5.71
	64	88.3	75.3-91.9	4.81	84	74-95	5.95
	139	88.5	83.7-91.4	2.62	74	70-84	4.09
	97	86.8	82.7-90.2	3.49	63	58-72	4.49
	35	74.8	70.0-80.3	4.05	75	56.90	11.23
	121	82.8	70.7-91.2	6.40	77	64-86	5.89
charnockitic syenodiorites	129	92.5	91.1-94.0	1.23	65	46-76	8.53
	100	86.6	74.8-89.5	4.35	55	43-72	7.18
	91	82.4	79.2-84.3	2.08	64	54-75	5.54
	92	79.2	76.9-80.4	1.49	50	40-66	6.28
	93	77.0	75.6-78.4	1.18	50	40-64	6.76
	95	78.5	75.1-81.8	2.14	47	32-64	7.76
	94	50.0	17.6-77.4	13.23	57	32-69	4.36

and represent as few as five, to as many as fifty determinations, usually from two points on each of five grains. Optic angles (Table II.3) were measured using universal-stage techniques on five to forty grains per thin section. Optic angle vs composition is plotted in Fig. II.5, which delimits Tuttle's four series and includes data for reference feldspars of known structural state (Wright and Stewart, 1968).

A significant spread in composition and optic angle was found in virtually all samples, as shown by the values for range and standard deviation in Table II.3, and mean values of each were used in Fig. II.5. Composition and optic angle determinations on specific grains within samples enabled their structural states to be plotted. Although a small range exists within all samples, the individual structural states cluster about the values determined using mean values. The one exception occurs in sample 94. In this sample, optic angle is relatively consistent within grains but the wide range of composition (see Chapter III, Table III.6) results in a large spread in structural state. The mean value was thus deemed of little significance and sample 94 does not appear on Fig. II.5.

Potassic feldspars of the charnockitic rocks occur with a wide range of structural states from orthoclase to maximum microcline (Fig. II.5a). The occurrence of high and low structural states in both highly and weakly shocked rocks suggests that the differences in ordering are probably not due to relative degree of shock metamorphism. The variation appears, rather, to be controlled by initial mineralogy; feldspars of the charnockitic microcline granites (Fig. II.5c) are microclines, those of the charnockitic syenodiorites (Fig. II.5d) are

Fig. II.5

Optic axial angle ($2V\alpha$) *vs.* composition of potassic feldspars in charnockitic granites (b), charnockitic microcline granites (c), charnockitic syenodiorites (d), and all charnockitic rocks (a), Charlevoix. Heavy lines delimit Tuttle's (1952) four series of alkali feldspars. Dashed lines give positions of several standard feldspars and their alkali exchanged equivalents as determined by Wright and Stewart (1968). Approximate shock pressures of samples estimated from deformation in quartz and plagioclase (Table II.2).

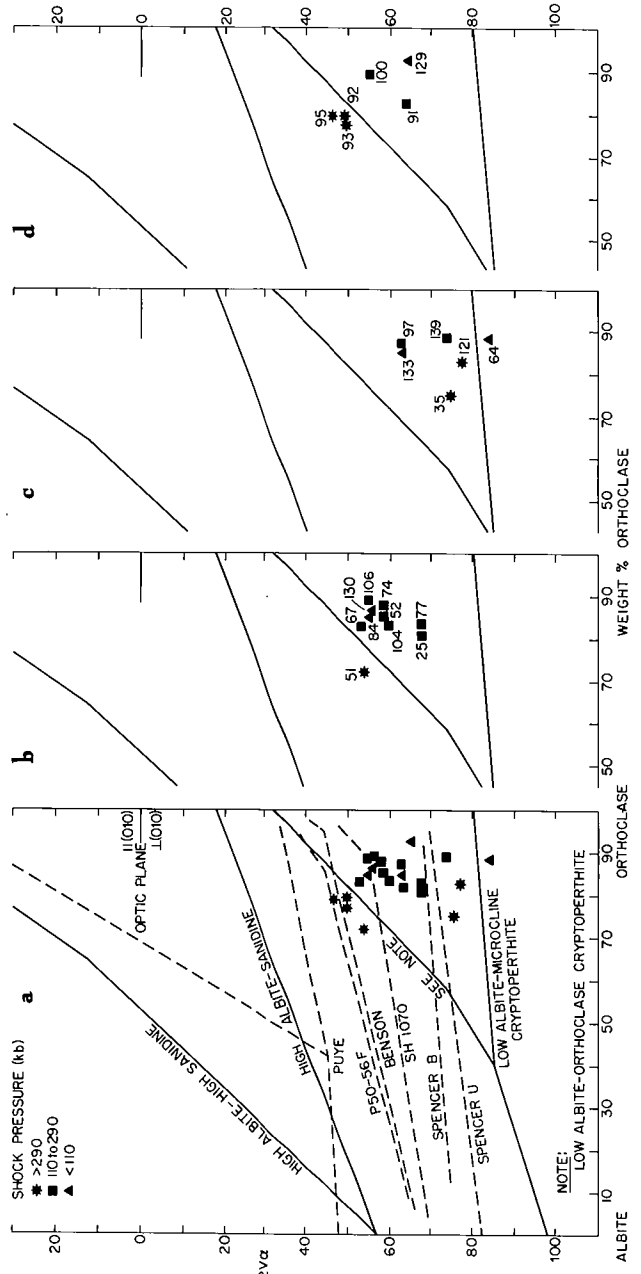
a
b
c
d
SHOCK PRESSURE (kb)
>290
110to290
<110
OPTIC PLANE
⊥(010)
II(010)
HIGH ALBITE-HIGH SANIDINE
HIGH ALBITE-SANIDINE
PUYE
P50-56 F
BENSON
SH 1070
SPENCER B
SPENCER U
LOW ALBITE-MICROCLINE CRYPTOPERTHITE
NOTE:
LOW ALBITE-ORTHOCLASE CRYPTOPERTHITE
2Vα
ALBITE
ORTHOCLASE
WEIGHT % ORTHOCLASE

generally orthoclase, and K-feldspars with structural states generally between the two characterize the charnockitic granites (Fig. II.5b). A possible correlation between low structural state and high shock level is provided by samples 51, 92, 93, and 95. However, the latter three are charnockitic syenodiorites, the unit with poorest sample distribution (5 of the 7 lie within 0.1km of the crater centre) so that it is not clear in this case whether the low structural states are initial or a shock characteristic.

Variation of optic angle within specimens occurs in rocks from "normal" geologic terrains. Barth (1969) reported that Ohta and Kizaki measured 2V from 40° to 70° within a single potassic feldspar crystal. Also, several of the Charlevoix samples lying outside the expected limits of shock metamorphism, particularly sample 129 at 25km, show a wide spread of $2V\alpha$ between grains. Thus a range of optic angle within a rock sample cannot necessarily be ascribed to shock deformation.

In order to determine whether the magnitude of the spread of $2V\alpha$ is related to shock, the standard deviation of optic angle values for each sample was plotted against the distance from the crater centre of the sample locality (Fig. II.6). Standard deviation beyond 9km is approximately uniform (5.5 to 6.5) whereas a large scatter of values, both higher and lower, occurs nearer the centre. There is a slight general increase in the standard deviation of optic angle as the crater centre is approached, particularly evident in the charnockitic granites.

Fig. II.6

Standard deviation of optic axial angle (2Vα) of potassic feldspars at Charlevoix *vs.* outcrop distance from crater centre.

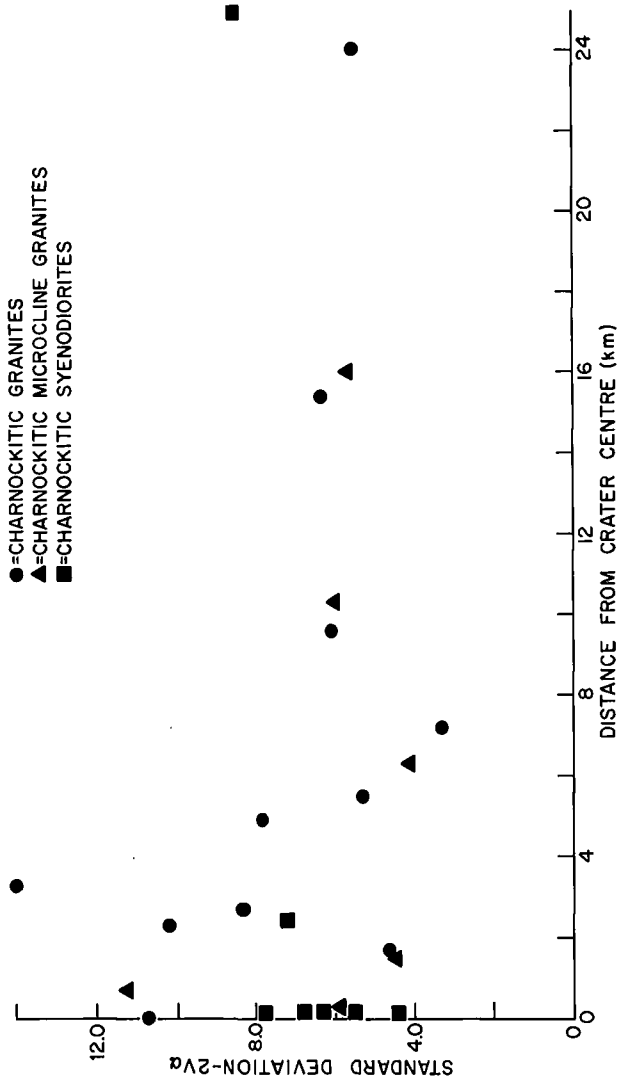
●=CHARNOCKITIC GRANITES
▲=CHARNOCKITIC MICROCLINE GRANITES
■=CHARNOCKITIC SYENODIORITES
STANDARD DEVIATION-2Vα
12.0
8.0
4.0
0
0
4
8
12
16
20
24
DISTANCE FROM CRATER CENTRE (km)

II.1.4A (ii) Triclinicity

Triclinicity of microclines from the charnockitic rocks was determined by multiplying by 12.5 the value d_{131}-$d_{1\bar{3}1}$ calculated from X-ray diffraction traces (Table II.4). Maximum microclines have the widest peak split and triclinicities near 1.0, intermediate microclines have a smaller (131)-($1\bar{3}1$) peak split, and in monoclinic feldspars $d_{131}=d_{1\bar{3}1}$ so that there is no peak split and triclinicity is zero (Goldsmith and Laves, 1954).

Potassic feldspars of the charnockitic microcline granites are intermediate microclines, generally with very low triclinicity (approximately 0.15). No variation in triclinicity related to shock pressure is evident.

II.1.4A (iii) Three-peak method

Wright (1968) and Wright and Stewart (1968) showed that the structural state and approximate composition of alkali feldspars can be determined from the CuKα_1 values of 2θ for $\bar{2}01$, 060, and $\bar{2}04$ reflections. Such determinations are made by plotting $2\theta_{060}$ vs $2\theta_{\bar{2}04}$ to obtain a $2\theta_{\bar{2}01}$ calculated value, and comparing with reference feldspars of known structural state (Wright, 1968, Fig. 3). If the difference between observed and calculated $2\theta_{\bar{2}01}$ is less than 0.1°, the approximate composition of the feldspar can be determined (Wright, 1968, Fig. 4). Differences exceeding 0.1° characterize anomalous alkali feldspars.

Mean 2θ values of $\bar{2}01$, 060 and $\bar{2}04$ were obtained for K-spars of the 25 primary charnockitic samples from X-ray diffraction traces

Table II.4 Triclinicity of K-feldspar in charnockitic rocks of Charlevoix

	Sample	Shock pressure (kb)	Triclinicity $(d_{131}-d_{1\bar{3}1}) \times 12.5$
charnockitic granites		<50 to 270±10%	0.0
charnockitic microcline granites	121	270±10%	0.11±0.01
	35	270±10%	0.16±0.01
	97	250±10%	0.16±0.01
	139	110±10%	0.04±0.01
	64	90±10%	0.16±0.01
	133	<50	0.13±0.01
charnockitic syenodiorites		<50 to 270±10%	0.0

using potassium bromate as an internal standard. Fig. II.7 is a 2θ plot of 060 vs $\bar{2}04$ and includes Wright's (1968) data for $\bar{2}01$ and positions of reference feldspars of known structural state.

The wide range of structural states shown by optic angle and composition measurements (Fig. II.5) is repeated in the three-peak determination (Fig. II.7). Initial mineralogy control is again evident. Structural states of potassic feldspar in the charnockitic granites (Fig. II.7b) show a rough cluster near the reference feldspars, SH-1070 and Benson, which are orthoclases with slightly less than maximum monoclinic ordering. K-feldspars of the charnockitic microcline granites (Fig. II.7c) have structural states close to that of Spencer B, which Wright and Stewart (1968) claim is "probably almost as highly ordered as any natural 'monoclinic' (to x-ray powder diffraction) potassic alkali feldspar". Thus, despite the grid twinning and slight triclinicity of these feldspars, some may have monoclinic symmetry. According to Fig. II.7d, potassic feldspars of the charnockitic syenodiorites are orthoclases generally of a lower degree of ordering than those in the charnockitic granites.

A range of structural states exists within each lithologic unit, particularly in the charnockitic granites, but a correlation between relative degree of order and shock level cannot be made. Although most of the samples with the lowest degree of ordering are from Mont des Éboulements (samples 92 to 95) this appears to be a mineralogic function rather than evidence for decrease of ordering with increasing shock level.

The 2θ difference between $\bar{2}01$ observed and $\bar{2}01$ taken from

Fig. II.7

Structural state of potassic feldspars determined from $2\theta_{\bar{2}04}$ *vs.* $2\theta_{060}$ (three-peak method). Reference feldspars (a), charnockitic granites (b), charnockitic microcline granites (c), and charnockitic syenodiorites (d) at Charlevoix. Lines of negative slope give $2\theta_{\bar{2}01}$ values for feldspar of various structural states and compositions.

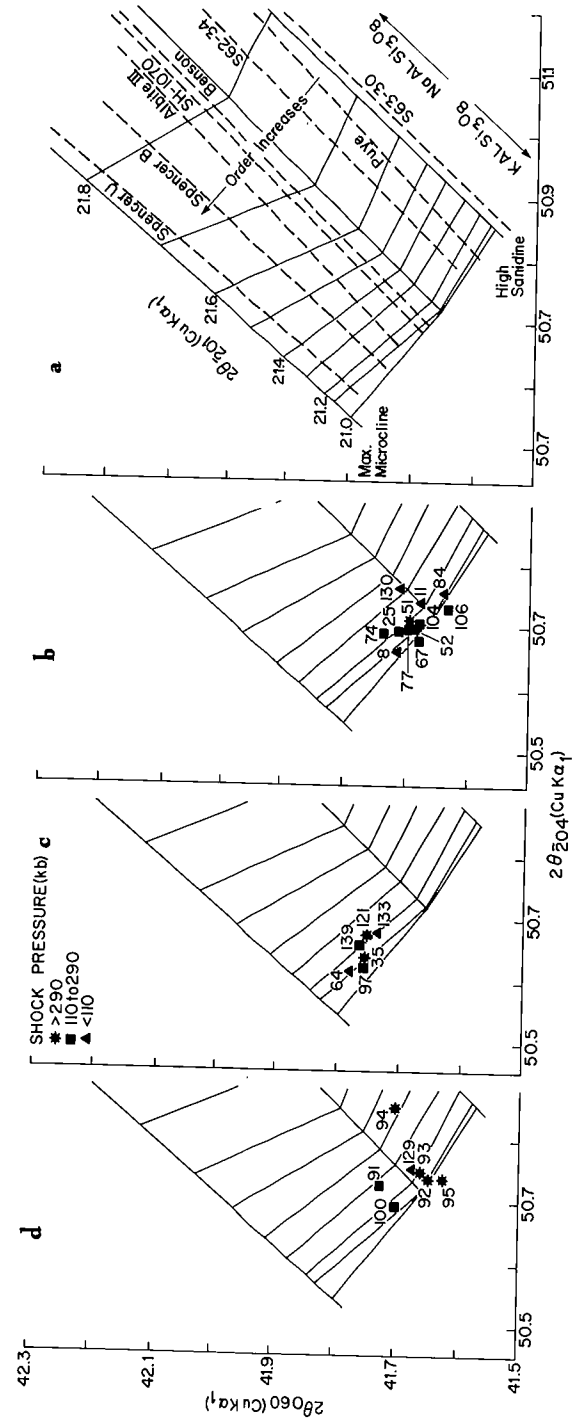
a
b
c
d
SHOCK PRESSURE(kb)
>290
110to290
<110
Max. Microcline
High Sanidine
Order Increases
Spencer U
Spencer B
Albite III
Benson
Pulse
KAlSi3O8
NaAlSi3O8
2θ060 (Cu Kα1)
2θ201 (Cu Kα1)
2θ204(Cu Kα1)

Table II.5 Normal and anomalous K-feldspars of the charnockitic rocks of Charlevoix (three-peak method)

	sample	$\lvert 2\theta_{\bar{2}01}$ obs. $- 2\theta_{\bar{2}01}$ calc. $\rvert$	
	130	0.31±.04°	anomalous*
	11	0.19 "	anomalous
	8	0.05 "	normal
	84	0.09 "	normal
charnockitic	52	0.08 "	normal
granites	67	0.05 "	normal
	77	0.12 "	anomalous
	106	0.10 "	normal
	104	0.09 "	normal
	25	0.13 "	anomalous
	74	0.17 "	anomalous
	51	0.15 "	anomalous
	133	0.17±.04	anomalous
	64	0.07 "	normal
charnockitic	139	0.19 "	anomalous
microcline	97	0.04 "	normal
granites	35	0.03 "	normal
	121	0.17 "	anomalous
	129	0.20±.04	anomalous
	100	0.13 "	anomalous
charnockitic	91	0.18 "	anomalous
syenodiorites	92	0.03 "	normal
	93	0.03 "	normal
	95	0.20 "	normal
	94	0.31 "	anomalous

*Feldspars are anomalous if $\lvert 2\theta_{\bar{2}01\ \text{observed}} - 2\theta_{\bar{2}01\ \text{calculated}} \rvert > 0.1^{\circ}$ (Wright, 1968).

Fig. II.7 was calculated for each sample (Table II.5). Fourteen samples are anomalous because this difference exceeds 0.1°. Wright (1968) does not explain the meaning of this term or the significance of feldspars which are anomalous. The degree of "anomalousness" of the Charlevoix K-feldspars cannot be correlated with shock level; in fact the two most anomalous samples, 94 and 130, are from outcrops among the nearest and farthest, respectively, from Mont des Éboulements.

II.1.4A (iv) b versus c

From b and c unit cell dimensions of several alkali feldspars of known composition and structural state Wright and Stewart (1968, Fig. 2b) constructed a diagram from which the relative structural state, composition, and a dimension can be read for any feldspar whose b and c values are known. In general, for feldspars of constant composition the degree of Si/Al ordering increases as b decreases and c increases.

The structural state of potassic feldspars in the charnockitic samples were obtained by this method. X-ray diffractometer traces were run with a spinel internal standard, and unit cell parameters were calculated using the revised version of a least-squares refinement program by Evans et al. (1963). Unit cell data for each sample are presented in Appendix A. Fig. II.8 is a plot of b versus c and incorporates Wright and Stewart's (1968) data for a values and positions of reference feldspars of known structural state.

The range of structural states and the correlation with initial mineralogy determined earlier are repeated using the b vs c

Fig. II.8

Structural state of reference alkali feldspars (a), potassic feldspars in charnockitic granites (b), in charnockitic microcline granites (c), and in charnockitic syenodiorites (d) at Charlevoix determined from b vs. c unit-cell dimensions. Lines of negative slope give a unit-cell dimensions for feldspars of various structural states and compositions.

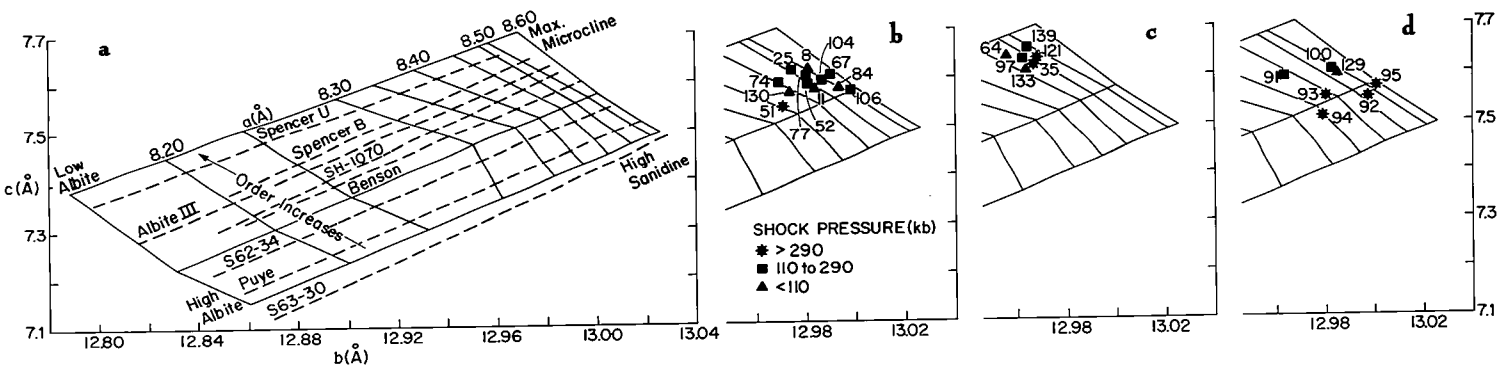
a
b
c
d
c(Å)
b(Å)
a(Å)
8.20
8.30
8.40
8.50
8.60
Max. Microcline
Low Albite
High Sanidine
High Albite
Albite III
Order Increases
Spencer U
Spencer B
SH-1970
Benson
S62-34
Puye
S63-30
7.7
7.5
7.3
7.1
12.80
12.84
12.88
12.92
12.96
13.00
13.04
12.98
13.02
SHOCK PRESSURE(kb)
> 290
110 to 290
< 110

method. Potassic feldspars in the charnockitic granites are orthoclases whose structural states lie between those of the reference feldspars, Spencer B and Benson (Fig. II.8b). These are orthoclases of maximum and intermediate Si/Al ordering, respectively (Wright and Stewart, 1968). Structural states of the K-feldspars in the charnockitic microcline granites (Fig. II.8c) are those of intermediate microclines. Although a large scatter of structural states exists for K-feldspars of the charnockitic syenodiorites (Fig. II.8d), most are orthoclases with a lower degree of ordering than in the potassic feldspars of the charnockitic granites.

A range of structural states exists for the potassic feldspars of the charnockitic granites and charnockitic syenodiorites and to a lesser extent within the charnockitic microcline granites, but the variation cannot be correlated with degree of shock metamorphism.

II.1.4A (v) Barth's per cent - ordering

As a graphical means of determining the structural state of potassic feldspars, Barth (1969, Fig. 3.10) constructed a triangular diagram with high sanidine, hypo-orthoclase, and maximum microcline at the apices, representing respectively 0%, 66.7% and 100% ordering of the Al and Si atoms. The diagram incorporates curves for ordering values transitional between the three reference structures, triclinicity curves for microclines, optic angle curves, and orientation of the optic plane. Sanidines and orthoclases lie along the left join from 0% to 33% ordering. Intermediate microclines occur along the horizontal join between 33% and 66.7%, and with increasing order to

maximum microcline in the lower right corner. Feldspars in the upper part of the triangle are believed not to exist in nature.

The relative structural states of the charnockitic samples from Charlevoix were determined from Barth's diagram (Fig. II.9) using the measured values for $2V\alpha$, triclinicity, and per cent-ordering. The latter was determined (Table II.6) from the inverse relationship between $\underline{c}^*/\underline{b}^*$ and per-cent ordering established by Jones (see Barth, 1969, Fig. 3.9 (C)). For most samples, plotting the three variables did not furnish a unique solution. Therefore, the feldspars in charnockitic granites and charnockitic syenodiorites on Fig. II.9 are the mean position of 2V versus triclinicity and per cent-ordering versus triclinicity. Positions of the feldspars of the charnockitic microcline granites were obtained by a similar process. For samples 35, 97, 121, and 139, however, the curves for 2V versus per cent-ordering, and 2V versus triclinicity either do not intersect, or do so outside the diagram, so their positions are based on per cent-ordering and triclinicity.

The alkali feldspars of the charnockitic rocks occur with a variety of structural states, controlled apparently by initial mineralogy. K-feldspars of the charnockitic granites are orthoclases with ordering generally between 24% and 35% (Fig. II.9b). Samples 8, 25, and 77 plot outside the field of stable feldspars primarily because of $2V\alpha$ values anomalously high for monoclinic symmetry. Potassic feldspars of the charnockitic syenodiorites are also orthoclases with 20% to 27% ordering, with 35% order in sample 35, and sample 91 lying outside the stability field. Intermediate microclines having approximately 42% to 46% order

Fig. II.9

Relationship between per cent order, $2V\alpha$ and triclinicity, for potassic feldspars (a). Potassic feldspars in charnockitic granites (b), charnockitic microcline granites (c), and charnockitic syenodiorites (d) at Charlevoix are plotted. Diagram reproduced after Barth (1969, Fig. 3.10).

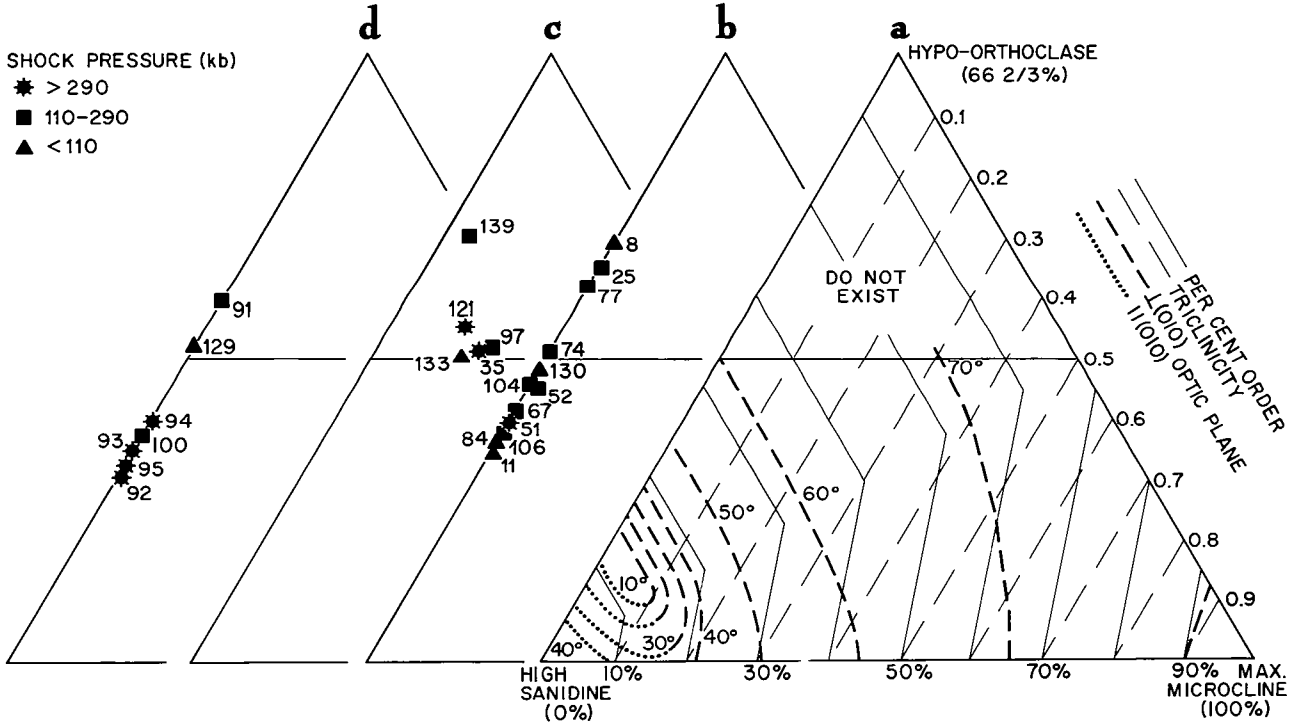
d
c
b
a
SHOCK PRESSURE (kb)
> 290
110–290
< 110
HYPO-ORTHOCLASE
(66 2/3%)
DO NOT
EXIST
PER CENT ORDER
TRICLINICITY
⊥(010) OPTIC PLANE
//(010) OPTIC PLANE
0.1
0.2
0.3
0.4
0.5
0.6
0.7
0.8
0.9
70°
60°
50°
40°
30°
10°
40°
HIGH
SANIDINE
(0%)
10%
30%
50%
70%
90% MAX.
MICROCLINE
(100%)
91
129
94
93
100
95
92
139
121
97
133
35
104
52
67
51
84
106
11
8
25
77
74
130

Table II.6 Per cent order of K-feldspars in charnockitic rocks of Charlevoix

	sample	c* (±.00005)	b* (±.00005)	c*/b* (±.002)	per cent ordering (±2%)
	130	.1546(4)	.0770(8)	2.006(2)	34
	11	.1546(8)	.0770(2)	2.008(3)	24
	8	.1545(4)	.0770(4)	2.006(2)	34
	84	.1546(9)	.0769(7)	2.009(9)	20
	52	.1546(2)	.0770(4)	2.007(1)	29
charnockitic	67	.1545(4)	.0769(8)	2.007(6)	27
granites	77	.1545(8)	.0770(4)	2.006(5)	33
	106	.1547(1)	.0769(3)	2.009(2)	23
	104	.1547(1)	.0769(3)	2.009(2)	23
	25	.1544(8)	.0770(8)	2.004(3)	38
	74	.1545(5)	.0771(1)	2.004(4)	38
	51	.1548(4)	.0771(0)	2.008(3)	24
	133	.1544(8)	.0771(4)	2.002(7)	44
	64	.1543(3)	.0772(0)	1.999(1)	60
charnockitic	139	.1543(6)	.0771(3)	2.001(2)	50
microcline	97	.1543(0)	.0771(4)	2.000(3)	52
granites	35	.1544(4)	.0771(2)	2.002(6)	45
	121	.1543(5)	.0770(3)	2.002(7)	44
	129	.1545(9)	.0770(2)	2.007(2)	29
	100	.1546(3)	.0770(2)	2.008(0)	25
	91	.1545(7)	.0771(4)	2.004(0)	39
charnockitic	92	.1548(0)	.0769(6)	2.072(0)	18
syenodiorites	93	.1548(5)	.0770(4)	2.070(0)	22
	95	.1547(0)	.0769(2)	2.011(3)	20
	94	.1549(8)	.0770(5)	2.011(5)	19

characterize the charnockitic microcline granites, with sample 139 anomalous inside the unstable K-feldspar region.

Samples 8, 25, 77, 91, and 139 are not as unusual as their occurrence within the field of unstable feldspars suggests. Many natural orthoclases of high 2V, including Spencer B and others commonly used as standards, plot on the upper half of the left join, and thus the significance of some parts of Barth's diagram may be questioned.

The range of K-feldspar ordering displayed in the charnockitic rocks cannot be correlated with relative levels of shock metamorphism.

II.1.4A (vi) Summary of data on structural states

A wide range of structural states, from partially ordered orthoclase to intermediate microcline, is shown by potassic feldspar of the charnockitic rocks. Each of the three lithologic subgroups is characterized by feldspars of a particular range of ordering. Orthoclases structurally between Spencer B, a highly-ordered orthoclase (approximately 50%), and Benson, a less-ordered form (approximately 21%) occur in the charnockitic granites. K-feldspar of the charnockitic syenodiorites is also orthoclase but generally in a lower-ordered state (20%-27%) than that in the charnockitic granites, although some overlap exists between these two groups. Intermediate microclines with triclinicity approximately 0.12, and 49% ordering are found in the charnockitic microcline granites. The main variation of structural state is apparently a lithologic function and not due to relative levels of shock metamorphism.

A smaller range of structural states occurs within each of the three lithologic units. This variation similarly cannot be correlated

with degree of shock metamorphism because both strongly and weakly shocked feldspars occur with high- and low-percentage ordering. Feldspars with a low structural state, however, are more common among the most highly shocked rocks than in weakly shocked or unshocked samples. This is a possible correlation which might be clarified by additional sampling, particularly from outcrops of the charnockitic syenodiorites.

II.1.4B Microscopic Evidence for Deformation

Potassic feldspars of the charnockitic rocks are anhedral, perthitic, untwinned or poorly twinned in the case of microclines, and average approximately 0.5 to 0.7mm in diameter with a range between 0.3 and 2mm.

II.1.4B (i) Perthite development

Potassic feldspars in the unshocked rocks from outside the crater or near its margin contain plagioclase in two forms of perthitic intergrowth. Film perthite occurs as thin lamellar planes which universal stage measurements have shown are parallel to a vicinal plane in the $[0\bar{1}0]$ zone, i.e. approximately $\{70\bar{1}\}$ (Plate II.2a). See Appendix B for methods used to determine Miller indices. Scanning by electron microprobe at 3μ/sec for sodium and potassium confirmed that the lamellae are Na-rich bands, although their exact composition was not determined. The lamellae are straight and uniformly about 1.5-2μ wide, spaced at approximately 6μ intervals. Each lamella comprises a series of linear segments, 150-200μ long, which pinch out at either end. The segments overlap slightly in an *en echelon* arrangement to produce what appears as a continuous lamella (except when viewed at highest magnification) which crosses the grain

Plate II.2

a) Film perthite and bleb perthite in weakly shocked orthoclase from Charlevoix (sample MBP 106). Narrow, discontinuous, film perthite lamellae are parallel the Murchisonite parting, $\{70\bar{1}\}$. Interference contrast illumination.

b) Perthitic intergrowths in shocked orthoclase (sample MBP 25). Discontinuous film perthite lamellae on margin (right) grade into spindle or string microperthite in interior. Interference contrast illumination.

a)

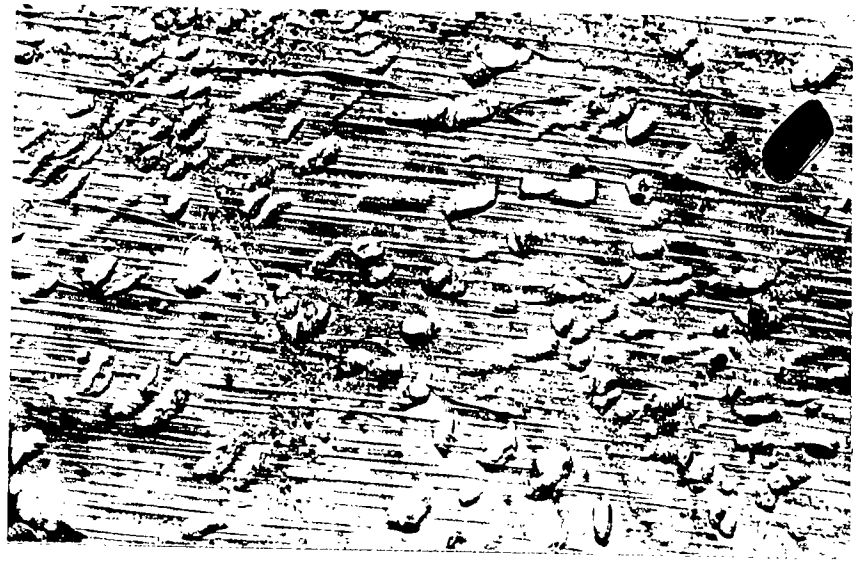

125 μ

b)

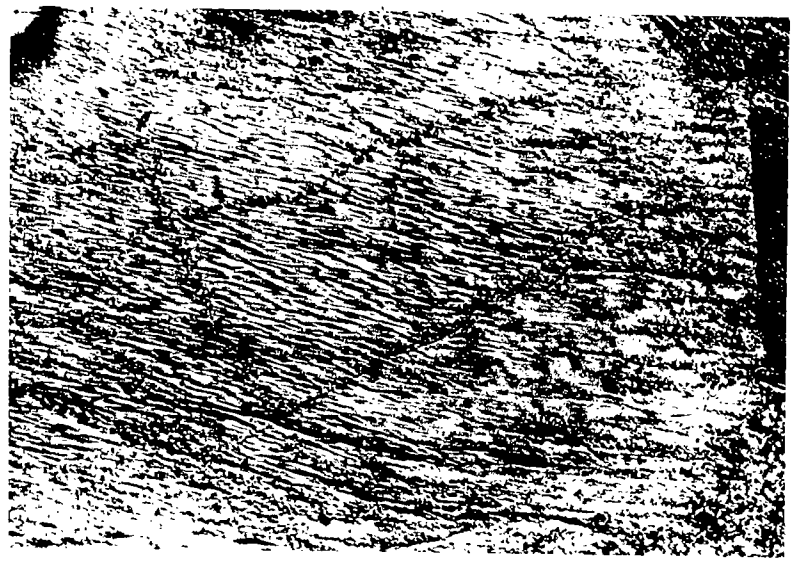

125 μ

from one margin to the other. The planes are generally altered near the grain margins to a highly birefringent mineral, probably a sheet silicate. In microclines the lamellae form subparallel to the pericline twin-composition plane, and the two are difficult to distinguish.

Plagioclase also occurs in the unshocked K-feldspars in coarser, irregular or elongate blebs, 10μ wide by 120μ, generally restricted to the central 80% of each grain (Plate II. 2a). Although crystallographic orientation of the coarser perthitic intergrowth was not determined, one set of blebs lies in the $\{70\bar{1}\}$ plane, and another set approximately normal to it. In contrast to the film perthite, the blebs are generally not altered.

The two forms of perthite are preserved throughout the weakly shocked potassic feldspars, but undergo a progressive change in the highly shocked samples. Beginning in the centre of grains, the film perthite is broken up, by narrowing and pinching out at intervals along the lamellae, into a series of narrow spindles. As breakdown proceeds over a larger portion of the grain, the spindles become broader and further separated; the $\{70\bar{1}\}$ lamellae are preserved on the grain margins. Continued breakdown produces a cluster of aligned spindles or blebs paralleling the film perthite but without the defined spacing of the lamellae (Plate II. 2b). Near the grain boundaries where the $\{70\bar{1}\}$ lamellae are retained the spindles are numerous, but become larger and fewer towards the centre of the grain (Plate II. 3a). In more highly shocked K-feldspars the centre comprises a braid microperthite, generally only sub-parallel to the preserved, marginal, film perthite lamellae (Plate II. 2a). Commonly there is a

Plate II.3

a) Perthitic intergrowths in shocked microcline (sample MBP 121). Discontinuous film perthite lamellae on margins grade into spindle or string microperthite in interior. Size and spacing of spindles increases towards centre. Plane-polars.

b) Perthitic intergrowths in shocked microcline (sample MBP 121). Altered film perthite lamellae near margins grade into string microperthite in interior. Crossed polars.

c) Perthitic intergrowths in shocked orthoclase (sample MBP 25). Film perthite lamellae near margins disappear in apparently homogeneous grain centre. Plane-polars.

a)

200μ

b)

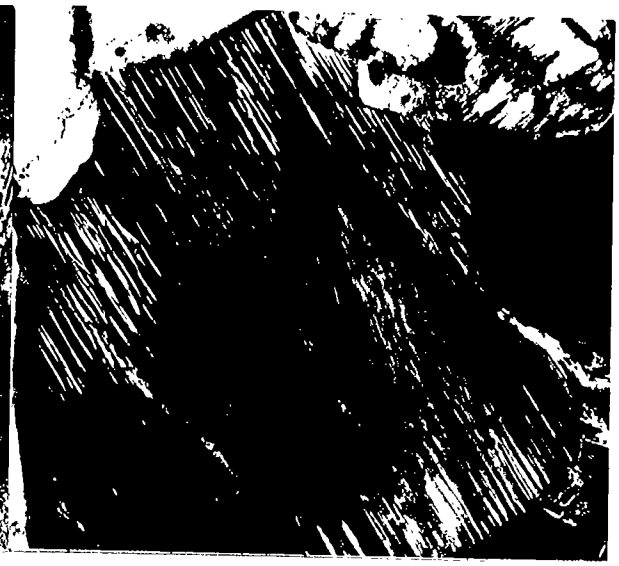

200μ

c)

125μ

slight difference in extinction position between the central and peripheral regions. In some grains there is an intermediate zone where neither lamellae nor braid microperthite are present. In rare cases the {70$\bar{1}$} lamellae persist near the grain boundaries but the central area is free from visible perthitic intergrowth (Plate II. 3c). In the most highly shocked samples, planar optical discontinuities approximately parallel to {70$\bar{1}$} are visible. Exsolution along these planes was not detected, and an electron microprobe scan for sodium and potassium did not reveal a compositional variation related to the planes.

The first signs of the transition from film perthite to braid perthite are visible in a few grains from samples shocked to approximately 110 to 170kb. Most grains in these samples (i.e. 52, 67, 139, 77 and 106) do, however, exhibit continuous film perthite lamellae. The remainder of the charnockitic samples shocked to greater than 170kb, show some evidence of the transition in most or all grains. Disappearance of {70$\bar{1}$} perthite lamellae (although weak planar discontinuities with this orientation exist) is evident above approximately 310kb.

Transformation of the bleb perthite is more abrupt than that of the film perthite. The blebs, in some cases larger or more abundant than others, are present in K-feldspars from all samples for which pressures less than 175kb have been estimated (with the exception of sample 139). They are absent in all samples suffering higher shock pressures.

Correlation between destruction of the original perthitic textures and increasing shock pressure is an indication that the breakdown

and transition to other forms of perthitic growth is related to the pressure-temperature environment produced by meteorite impact.

II.1.4B (ii) Deformation planes

K-feldspars in the charnockitic rocks were examined by universal-stage techniques to discover whether shock-produced planar deformations of the type reported in quartz and feldspars from other meteorite craters (e.g. Robertson et al., 1968) are present.

The orientation of optic directions, cleavages, twins, film perthite lamellae, and shock features were determined from generally thirty grains per sample. The optic and crystallographic data were plotted in stereographic projection on a Wulff net, from which the prominent $\{00\bar{1}\}$ and $\{010\}$ cleavages, and albite and pericline twin composition planes were readily identified. Measurement on the stereogram of the interplanar angles between the cleavages and the plane of the film perthite helped establish the Miller indices of the latter as $\{70\bar{1}\}$. A standard stereogram of each grain was prepared by a rotation centering the Z optic direction vertically, with X and Y in the horizontal plane. Preferably, the standard orientation should be based on three crystallographic directions, such as the poles to $\{001\}$ and $\{010\}$ cleavages and the $\{70\bar{1}\}$ lamellae. All three were often not measurable, either because they were not developed or due to restricted tilting of the U-stage. On the other hand, at least two optic directions are always accessible and therefore the third, being at right angles to them, can always be plotted.

The stereograms were superimposed providing a composite plot

of all planar elements for the K-feldspar of each charnockitic sample. The use of optic directions as reference axes for the stereograms does not always allow unambiguous correlation of planes between grains, and thus the "best fit" method, described in Appendix B, was used to prepare the composite stereograms. Planar elements were indexed by overlaying the composite plots on a standard stereographic projection of alkali feldspar. The standard projection was prepared from the average crystallographic parameters (Appendix A) obtained in X-ray determinations, in conjunction with optic versus crystallographic relationships compiled by Marfunin (1962, pp.60-64) for potassic feldspars with structural states similar to those at Charlevoix.

Cleavages in unshocked or weakly shocked potassic feldspar are common with {001} and {010} forms, and only these two, developed in most grains. Cleavages with other orientations are rare and occur in most orthoclases shocked to greater than approximately 170kb. Fig. II. 10 is a composite stereogram of all such fractures. Although a wide scatter is evident, the cleavages tend to form parallel to planes in four zones, with poorly defined concentrations within each zone. Cleavages in the [001] zone, {hk0} planes, approximately parallel to $(\bar{2}10)$ and (120), are the most common and are developed in samples shocked in the 170kb to 300kb range (Table II. 7).

In contrast to the nearly ubiquitous development of [001] fracturing in the moderately shocked rocks, fractures near $(11\bar{2})$ in the [111] zone, occur only in feldspars from 51 to 95, two of the most highly shocked samples. Similarly, cleavages parallel to (031) and $(01\bar{1})$, and others near (101) in a non-indexed zone, are restricted

Fig. II.10

Stereogram of shock-induced cleavages (solid circles) in potassic feldspar from charnockitic rocks at Charlevoix shocked to greater than 170kb. Reference axes of the stereogram are optic directions X, Y and Z. Cleavages tend to form in crude zones (dashed lines) identified by indices within square brackets. Open circles are indexed planes of the feldspar lattice.

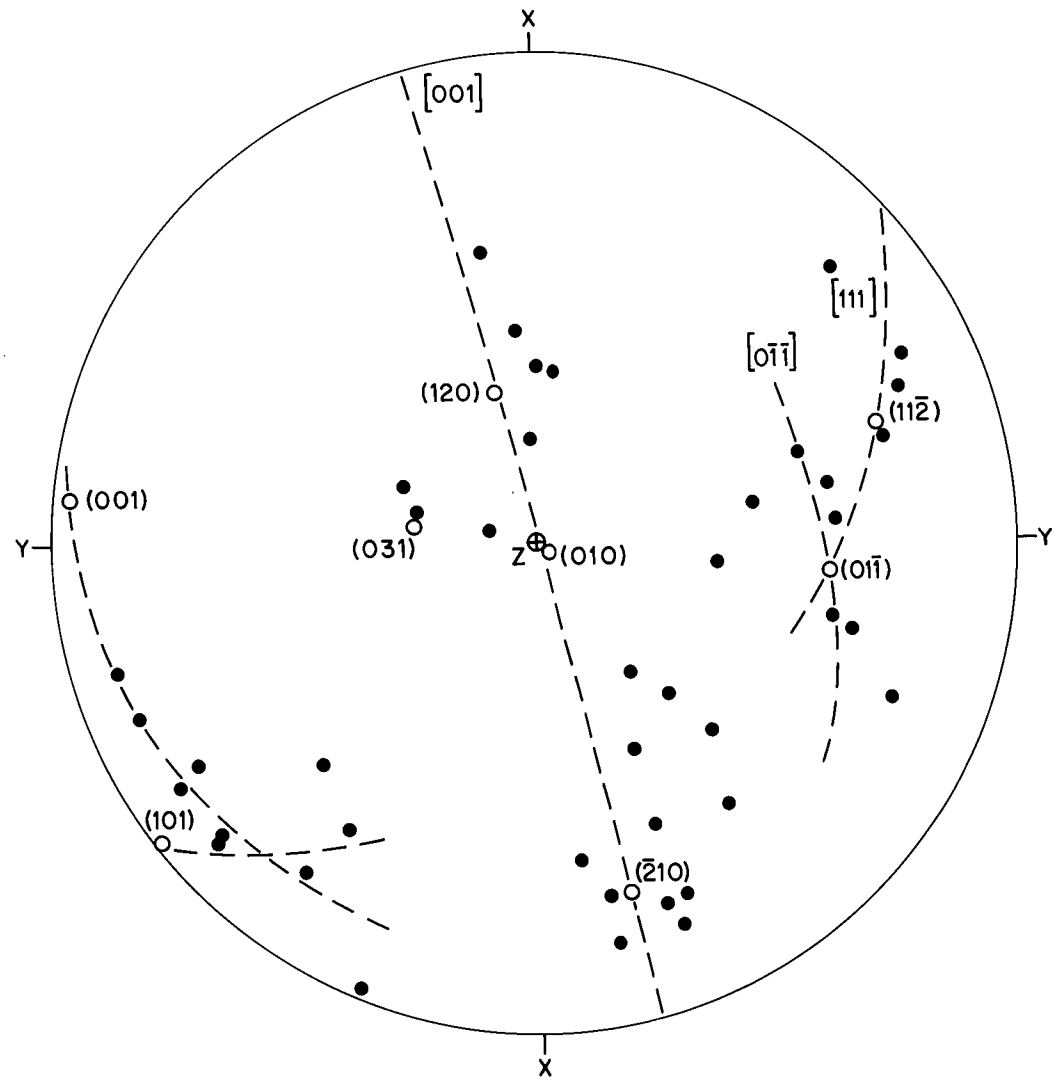
X
[001]
[111]
[01$\bar{1}\bar{1}$]
(120)
(11$\bar{2}$)
(001)
Y
(031)
Z
(010)
(01$\bar{1}$)
Y
(101)
($\bar{2}$10)
X

Table II.7 Shock-induced deformation planes, in orthoclase and microcline from charnockitic rocks of Charlevoix.

	sample	pressure (kb)	grains measured	per cent with planar features	average sets per grain	maximum sets per grain	shock induced cleavages
orthoclases	129	50	17	0	-	-	none
	130	"	10	0	-	-	none
	11	"	10	0	-	-	none
	8	"	10	0	-	-	none
	84	100	10	0	-	-	none
	52	110	35	0	-	-	none
	67	110	35	0	-	-	none
	77	160	35	0	-	-	$(\bar{2}10)$
	106	170	35	0	-	-	none
	104	175	17	0	-	-	none
	100	190	35	66	1.6	4	[001]
	25	200	50	2	1.0	1	none
	74	230	35	0	-	-	[001]
	91	270	35	57	1.6	3	$(\bar{2}10)$
	51	300	93	83	1.9	4	$(\bar{2}10)(11\bar{2})$ $(031)(011)$
	92	330	35	86	2.4	6	$(\bar{2}10)$
	93	340	35	83	1.8	5	none
	95	350	50	78	2.0	4	$(11\bar{2})(101)$
	94	360	35	91	1.5	4	none
microclines	133	<50	12	0	-	-	none
	64	90	10	0	-	-	none
	139	110	17	0	-	-	none
	97	270	15	56	1.7	3	none
	35	300	31	39	1.1	2	none
	121	300	27	44	1.8	4	none

to samples 51 and 95 respectively. Shock-produced fractures were not observed in samples 93 and 94, nor in the microclines, although the usual {001} and {010} cleavages are as common in these samples as in the K-feldspars showing lesser shock deformation.

Planar deformation features, similar to those characteristic of shocked quartz and plagioclase, occur in orthoclase and microcline in samples for which shock pressures greater than 200kb have been estimated (Table II.7). (The anomalously strong development in sample 100 may be due to an inaccurate pressure estimate). In general, as level of shock metamorphism increases, a greater percentage of the orthoclase grains exhibit planar features. At approximately 200kb, few grains contain planes of this type; at 270kb they occur in more than half the grains; and at 360kb, 90% of the potassic feldspars show this form of shock deformation. Based solely on the percentage of feldspars with observable planar features at a given pressure, microcline appears less susceptible than orthoclase to this style of deformation, at least over the pressure range displayed in the rocks in outcrop at Charlevoix.

In their initial development, planar deformation features appear as the traces of planar discontinuities without measurable width (Plates II.4a, 7a) occurring in one or more sets of straight, parallel planes, generally two or three sets per grain to a maximum of six. Although the planes of a set are uniformly spaced, sets with 2μ-intervals exist in the same grain as others spaced 5μ apart. The planes do not cross grain boundaries; they first form as a few planes of short extent

Plate II.4

a) Weak development of single set of narrow planar deformation features in shocked orthoclase (sample MBP 51). Interference contrast illumination.

b) Two strongly developed sets of shock-induced multiple twins in shocked orthoclase from Charlevoix (sample MBP 94). Margins not in focus due to tilting on universal stage. Crossed polars.

a)

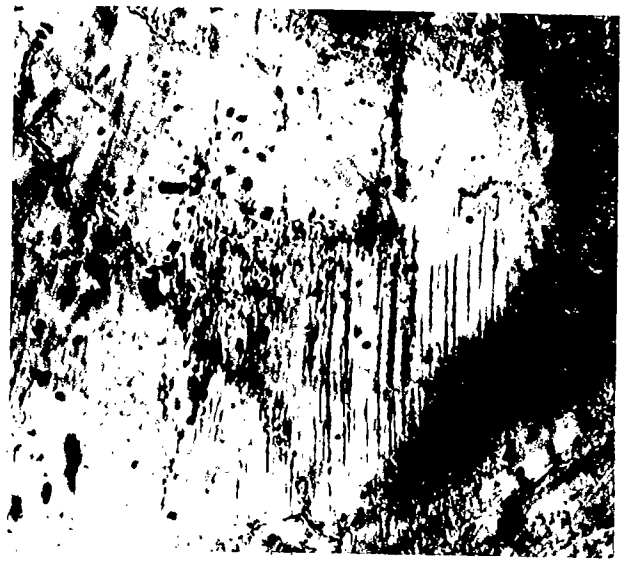

80 μ

b)

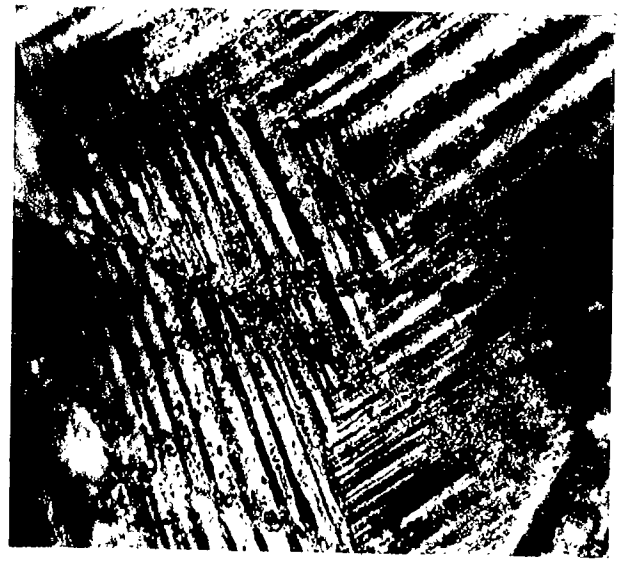

150 μ

restricted to domains near grain margins. With stronger development, intersecting sets appear throughout grains, and individual planes traverse the width of the feldspar. Some planes do not contain resolvable inclusions or material of different refractive index, and thus are only faintly visible. The observation of most planes, however, is enhanced by innumerable minute inclusions, or decorations.

Above approximately 300kb, some strong sets of planar deformation features are twin-like in appearance (Plates II.4b, 5, 6), whereas others retain the narrow, linear character shown in the less shocked feldspars. The twin-like planar features comprise two alternating sets of parallel lamellae differing from one another in extinction (Plates II.4b, 5a), relief (Plate II.6a), refractive index and alteration. In most cases the two sets are of approximately equal width, 4 to 8μ, and uniform along their length. The higher relief set usually contains abundant minute inclusions which, in some cases are contained in finely-spaced planes within the lamellae (Plate II.5b). The alternate lamellae are generally featureless, although they rarely contain planar features also. The inclusion-rich lamellae have a slightly higher refractive index than the featureless lamellae. The two sets show a difference in extinction angle of about 7-8° with a maximum of 15°. Optic orientations could not be measured within lamellae for the purpose of establishing a possible twin law. In cases where two sets of twin-like features with different orientations intersect, the narrow, decorated planes included in alternate lamellae of one set are the broad lamellae of the other set, and vice versa.

Portions of the higher relief lamellae contain a yellowish-

Plate II.5

a) Two strongly developed sets of shock-induced multiple twins in shocked orthoclase (sample MBP 94). Darker lamellae contain abundant inclusions. Crossed polars.

b) Planar shock features in orthoclase (sample MBP 93). Mechanical twin lamellae trend ENE, and alternate lamellae contain sets of narrow, closely-spaced, planar deformation features. Plane-polars.

a)

80 μ

b)

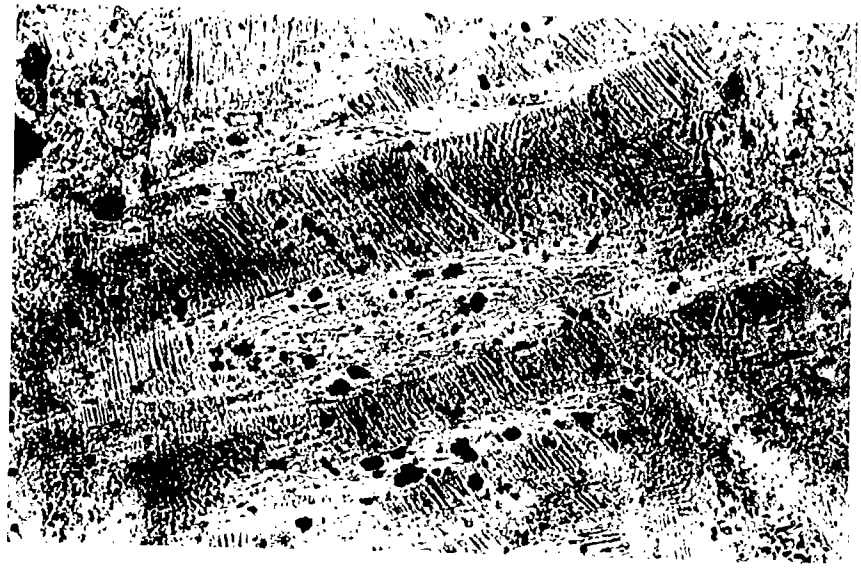

125 μ

Plate II.6

a) Two sets of shock-induced multiple twinning in orthoclase from Charlevoix (sample MBP 92). Differences in relief between dark and light lamellae are enhanced by interference contrast illumination.

b) Shock-induced multiple twinning in orthoclase (sample MBP 95). Dark lamellae contain unresolvable, high relief, low refractive index material due to partial conversion to low-ordered state, possibly diaplectic glass. Plane-polars.

a)

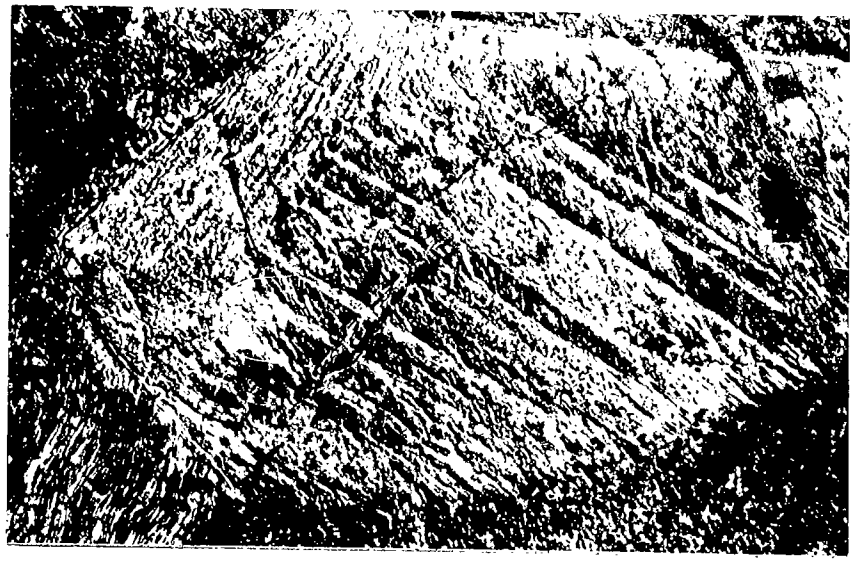

80μ

b)

30μ

Plate II.7

a) Weak development of planar deformation features (trending E) in shocked microcline from Charlevoix (sample MBP 97). Planar features are continuous across boundaries of grid twins running NE and NW. Crossed polars.

b) Shock-induced multiple twinning in microcline from float sample at Charlevoix. Set of shock twins trending NE are confined to one set of albite lamellae (trending E), and alternate albite lamellae contain sets trending NNE and NW. Pericline twins are not visible. Crossed polars.

a)

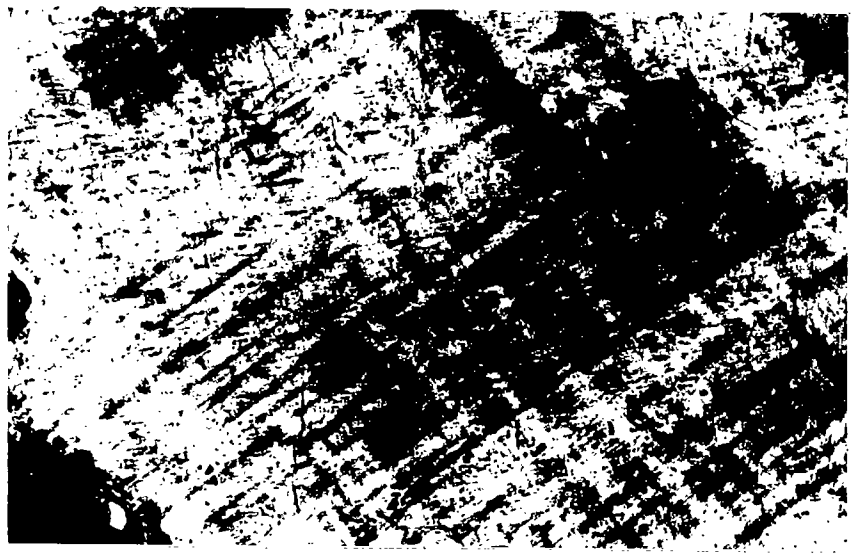

125 μ

b)

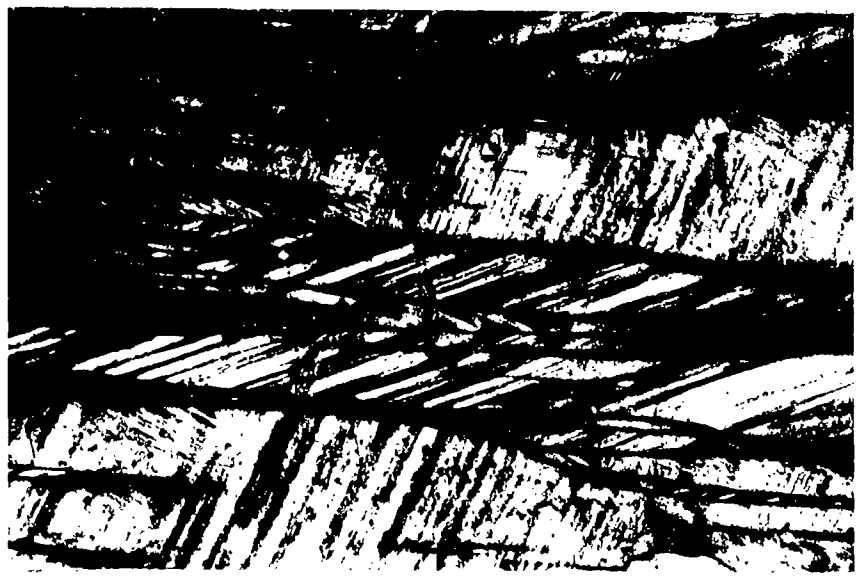

80 μ

green, low-birefringent, microcrystalline aggregate. In appearance and development it is similar to the alteration of maskelynite found in partially converted albite twin lamellae in coexisting plagioclase. The orthoclase planar features, however, do not appear isotropic, or even selectively reduced in birefringence as is typical of incipient maskelynite development.

Twin-like planar deformation features in microcline were not detected in outcrop samples but were observed (Plate II.7b) in float material from an erosional deposit near the periphery of Mont des Éboulements. Portions of some twin lamellae, both original M-twinning and the shock-induced features, are isotropic and of lower refractive index than microcline, indicating possible breakdown of the potassic feldspar to diaplectic glass. The approximate shock level of these samples, based on planar feature development in quartz, was not determined.

Orientation of planar deformation features in K-feldspar of the charnockitic rocks was determined from stereographic plots. Composite plots, contoured with the aid of a Mellis net, for such features in orthoclase and microcline are shown in Figs. II.11 and 12, respectively. In orthoclase the planar features exhibit a wide scatter, but three marked concentrations and a number of zonal trends exist. The greatest development of planes lies in the [102] zone at approximately 30° from (010), with $(24\bar{1})$ being the plane with low indices nearest the nucleus of the grouping. The second most abundant occurrence of planar features lies in the same zone but at approximately 37° from (010) in the opposite sense, near $(\bar{2}41)$. The third prominent development of

Fig. II.11

Contoured stereogram of planar deformation features in orthoclase from charnockitic rocks at Charlevoix shocked to greater than 170kb. Reference axes of the stereogram are optic directions, X, Y and Z. Shaded contours represent percentages of 464 measurements. Miller indices are given for planes of the feldspar lattice (open circles) near the contoured maxima. Contours extend along crude zones (dashed lines) identified by indices within square brackets.

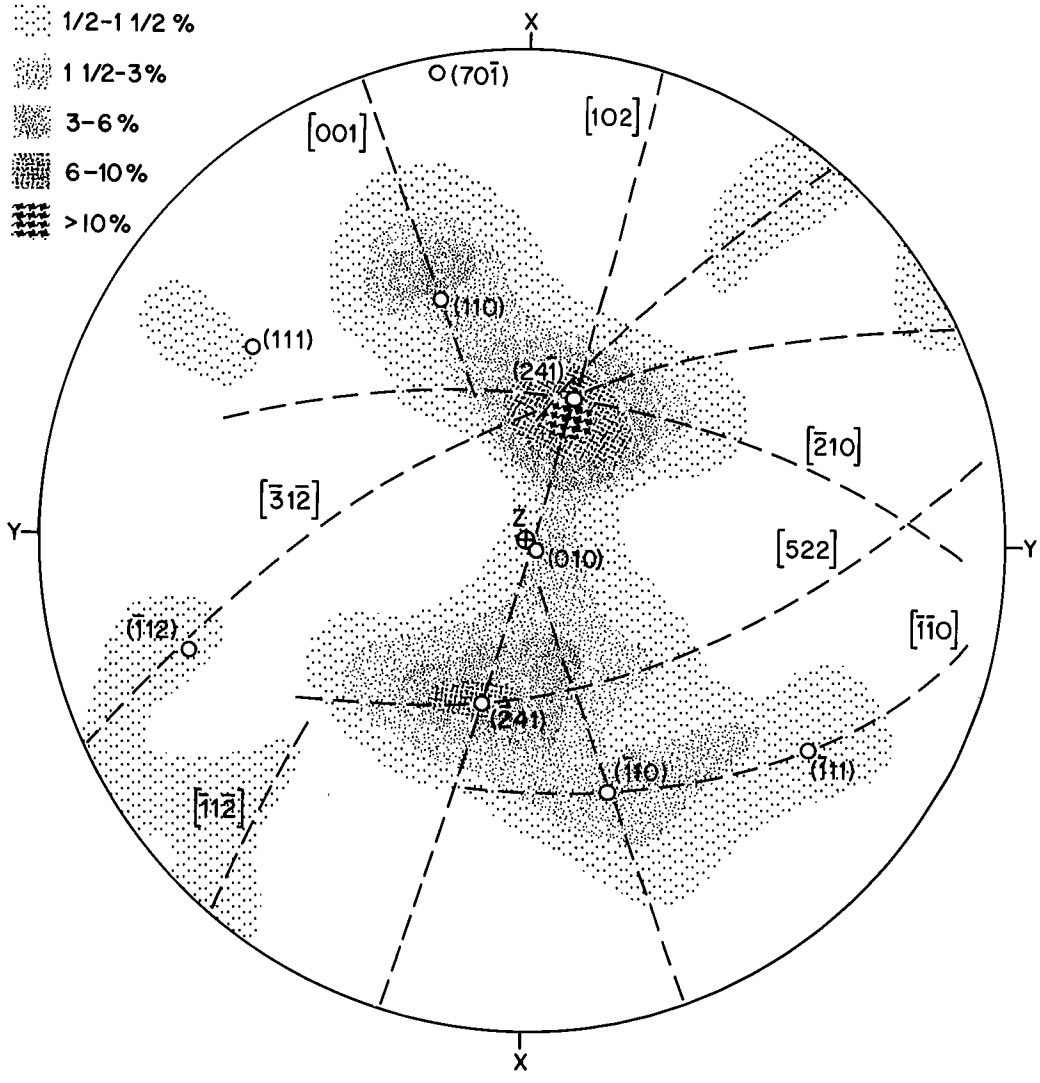
1/2-1 1/2 %
1 1/2-3%
3-6 %
6-10%
>10%
X
X
Y
Y
Z
(70$\bar{1}$)
[001]
[102]
(110)
(111)
(24$\bar{1}$)
[$\bar{2}$10]
[3$\bar{1}$2]
(010)
[522]
($\bar{1}$12)
[$\bar{1}\bar{1}$0]
($\bar{2}\bar{4}$1)
($\bar{1}$10)
($\bar{1}$11)
[$\bar{1}$1$\bar{2}$]

these shock-induced planes occurs in the [001] zone, 62° from (010) and near (110), although (430) is the low-index orientation nearest the focus of the planes.

Some data have been obscured by the use of contoured diagrams. In most grains, particularly those from the highly shocked samples, two, three or four intersecting sets of planar features are developed with orientations within 10 to 15° of one another, but each identifiable as a separate set. Thus most of the diffused pattern surrounding the three concentrations is not due to wide variation in orientation of a single, common set, but is caused primarily by these two or more sets per grain with similar orientations. The amoeba-like protuberances of the contour diagram reflect the development of these sets along poorly-defined zones. Thus the contoured summit near $(24\bar{1})$ does not necessarily represent planes with these specific indices, but is the statistical concentration of sets in zones such as [102] and $[\bar{2}10]$. Similarly, the contoured maximums near $(\bar{2}41)$ and (110) are created by sets of planar features formed in the [522] and [001] zones respectively.

Planar features with orientations other than those included in the three well-defined groups are less common in the shocked orthoclases. One such weaker grouping lies near $(\bar{1}10)$ at the intersection of the [001] and $[\bar{1}\bar{1}0]$ zones. Planar features also develop within the latter zone near $(\bar{1}1\bar{1})$. Although the formation of shock features in this zone is generally restricted to one set per grain, two sets separated by a small angular distance have been noted. Planar features parallel to (010) also form a minor distinct group. Even less commonly observed orientations plot in the vicinity of (111), and along zones

with axes approximately parallel to $[\bar{3}1\bar{2}]$ and $[\bar{1}1\bar{2}]$. Only one set for each of these orientations exists per grain.

The sets of planar deformation features with twin-like character belong to the groups near $(24\bar{1})$ and $(\bar{2}41)$. The decorated planes within these broader lamellae are generally planes in the same zone but from the opposite set. For example, broad lamellae near $(\bar{2}41)$ contain finely-spaced planes in the [102] zone near, but not the same as $(24\bar{1})$, and vice versa. Equally as common is the occurrence of $\{70\bar{1}\}$ planes within the $(24\bar{1})$ twin-like features. Whether these are the original film-perthite lamellae or shock-produced planar deformation features cannot be resolved, and thus they do not appear in the composite plot (Fig. II.11). Planar features parallel to the less common orientations do not exhibit twin-like character.

More than 90% of the sets of planar features measured in microcline plot in four prominent groups or along poorly-defined zones between the groups (Fig. II.12). The overall contoured pattern is similar to that for orthoclase, although the corresponding maxima are displaced by 5° to 17°, and zone axes are only roughly equivalent. The differences may mean that planar features are developed in microcline along planes with slightly different orientations than those in orthoclase. On the other hand, the orthoclase and microcline sets may have the equivalent indices but the use of the same standard stereogram for both feldspars may cause the disparity. A third possibility is that the microcline contoured diagram is based on only eleven per cent of the number of orthoclase measurements, and statistically the two diagrams should not be compared.

Fig. II.12

Contoured stereogram of planar deformation features in microcline from charnockitic rocks at Charlevoix shocked to greater than 170kb. References axes of the stereogram are optic directions X, Y, and Z. Shaded contours represent percentages of 51 measurements. Miller indices are given for planes of the feldspar lattice (open circles) near the contoured maxima. Contours extend along crude zones (dashed lines) identified by indices within square brackets.

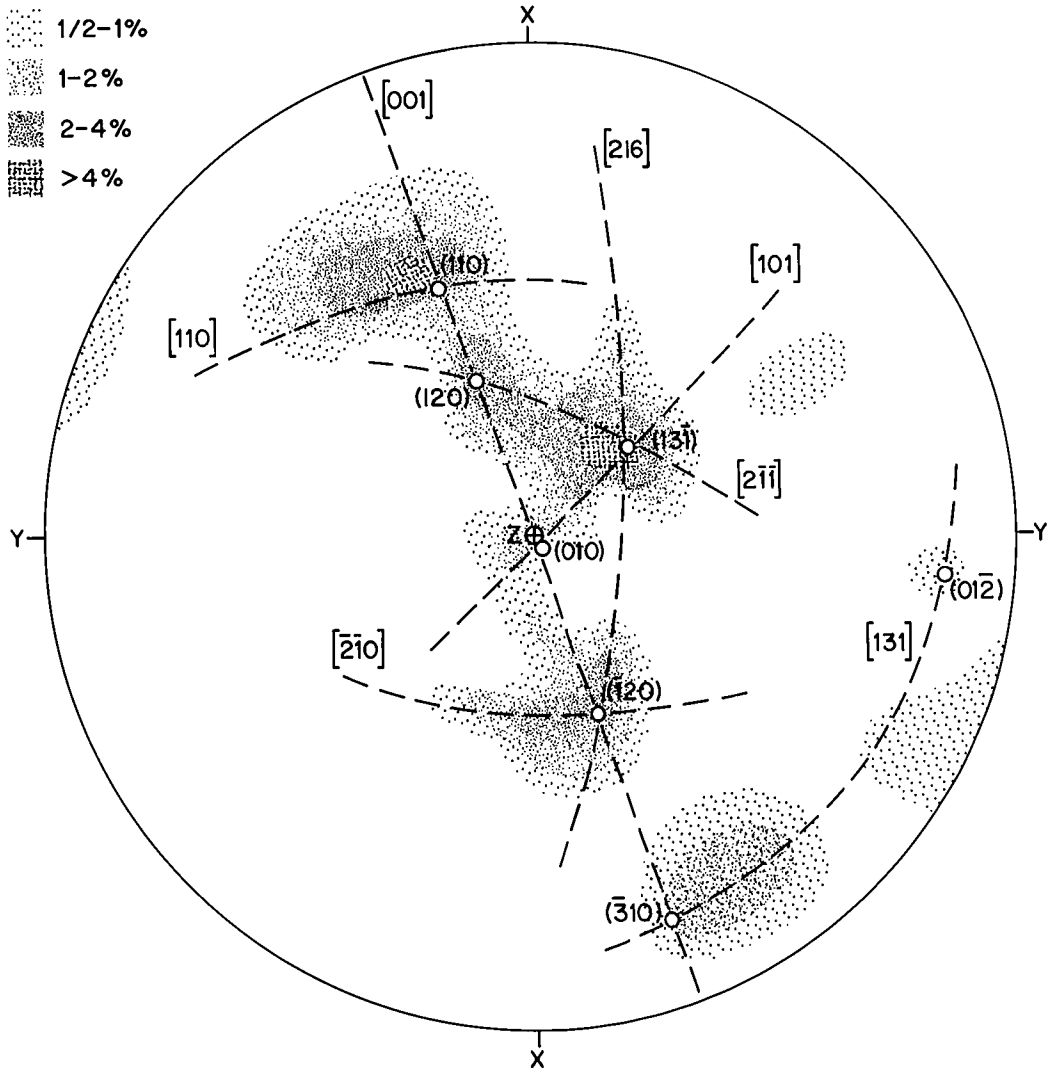
1/2-1%
1-2%
2-4%
>4%
X
Y
Z⊕
[001]
[216]
[101]
[110]
(110)
(120)
(131)
[2$\bar{1}\bar{1}$]
(010)
(01$\bar{2}$)
[$\bar{2}$10]
[131]
($\bar{1}$20)
($\bar{3}$10)

In microclines the most common sets lie in the [101] zone approximately 28° from (010), near (13$\bar{1}$). Almost as common are deformation features lying in the [001] zone at approximately 63° from (010), near (110). Their development is unusual in that these latter sets were observed only in sample 97. A third concentration of points occurs centred at 38° from (010) in the [001] zone near ($\bar{1}$20). This group is matched by planes parallel to (120) at 39° from (010) in the opposite portion of the [001] zone. Planes with other orientations, such as the few in the [131] zone, and (010), are rare.

As in orthoclase, two, or rarely three sets of planar features with similar but distinctly separate orientations may occur in the same grain. These sets generally form within 5° to 15° of one another along zones of low indices, as indicated in Fig. II.12 by the extension of contours roughly parallel to zones such as [110], [$\bar{2}$10], [101] and [2$\bar{1}\bar{1}$].

II.1.4B (iii) Summary of microscopic evidence for deformation

Unshocked and weakly deformed orthoclase and microcline at Charlevoix contain coarse bleb-perthite, and film perthite in narrow lamellae parallel to {70$\bar{1}$}, which traverse the complete grain. The bleb perthite is not present in samples which experienced shock pressures greater than approximately 175kb. The film perthite lamellae grade imperceptibly into string microperthite in the central portion of some K-feldspars shocked to more than 170kb. With increasing pressure the {70$\bar{1}$} lamellae are evident only on grain margins, or are entirely absent, and the string microperthite occupies most of the grain.

Cleavages in unshocked and weakly shocked potassic feldspars

are the common {001} and {010} forms. In addition to these fractures, cleavages in the [001] zone approximately parallel to $\{\bar{2}10\}$ and {120} occur in orthoclases which experienced shock pressures greater than 170kb. Weakly developed in orthoclase above 300kb are cleavages near $\{11\bar{2}\}$, {031}, {011} and {101}. Shock-induced cleavages with unusual orientations were not observed in deformed microclines.

Planar deformation features are weakly developed in potassic feldspar shocked at approximately 200kb, but become abundant somewhere in the pressure range between 230 and 270kb, and occur in 91% of orthoclase grains from sample 94 (360kb). In approximate order of decreasing abundance, sets in orthoclase are: in the [102] zone near $\{24\bar{1}\}$ and $\{\bar{2}41\}$, in the [001] zone near {110} and {010}, in the $[\bar{1}\bar{1}0]$ zone near $\{\bar{1}10\}$ and $\{\bar{1}11\}$, and in the $[\bar{1}1\bar{2}]$ and $[\bar{3}1\bar{2}]$ zones. Planar features parallel to $\{70\bar{1}\}$ may replace the film-perthite lamellae.

The orientation and relative abundance of planar deformation features in microcline and orthoclase is similar, although somewhat weaker in the former. Planar features in microcline are parallel to $\{13\bar{1}\}$, near {110}, {120}, $\{\bar{1}20\}$ and {010} in the [001] zones, and a weak development in the [131] zone. Particular orientations in orthoclase and microcline do not seem, by their appearance or absence, to be characteristic of a particular range of shock pressures.

Initially the planar deformation features are narrow planes without measurable width, generally filled with minute inclusions or decorations. There are usually two or three sets per grain, to a recorded maximum of six sets. Above approximately 300kb the $\{24\bar{1}\}$ and $\{\bar{2}41\}$ sets are broad (5-8μ), twin-like features in which alternate

lamellae show slight refractive index and extinction angle differences. Finely-spaced, decorated planar features are visible in alternate lamellae of a set, imparting a higher relief to these lamellae. Portions of some higher-relief lamellae contain a microcrystalline material, possibly an alteration product of diaplectic glass formed preferentially along lamellae. Low refractive index, isotropic material occurring along M-twins and planar features in some microclines may be the potassic feldspar equivalent of maskelynite.

II.2 Lac Couture Crater

II.2.1 Introduction

Lac Couture is an ancient, deeply eroded meteorite crater lying at 60°N latitude in the northern regions of Quebec Province (Fig. II.1). Impact occurred in the Paleozoic or Mesozoic eras (Dence, 1972) in Archean gneisses of the Superior Province of the Precambrian Shield. The lake is roughly 17km in diameter. A nearly circular island-free centre of 10km diameter defines the original crater.

Beals et al. (1967) visited the site in 1963, attracted by its anomalous shape in a region of elongate, glacially modified lakes. Breccia boulders and pebbles were found amongst the glacial debris lying on the islands and mainland on the western (down-glaciation) periphery of the lake only (Fig. II.13). Subsequent petrographic examinations confirmed evidence for shock metamorphism in the breccias, ranging from weak planar feature development in tectosilicates to partial melting, and Lac Couture was classed as a "probable" meteorite impact crater. Thirteen depth soundings from a single traverse of the lake

Fig. II.13

Lac Couture crater, Quebec. Breccia float has been found on islands and mainland on the western crater margin (blackened). East to west glaciation is shown by the trend of eskers (chevron pattern).

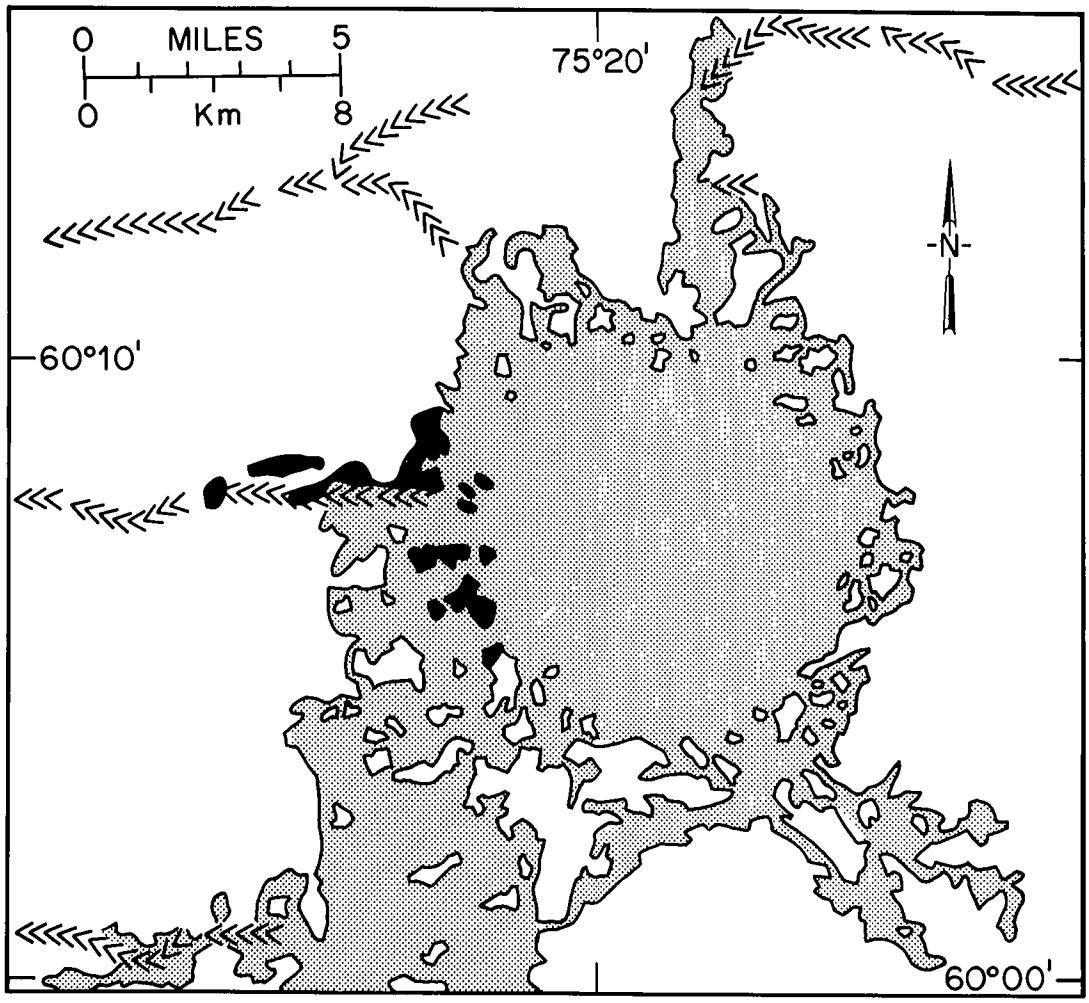
0 MILES 5
0 Km 8
75°20'
60°10'
60°00'
N

revealed water depths to a maximum of 118m, with a vague suggestion of central uplift.

In 1964 Gold, Robertson and Aitken (Tuttle et al., 1965) collected breccia samples from the glacial debris and carried out geologic mapping in selected areas on the islands and mainland around Lac Couture. Robertson (1965) reported that the region is underlain by granitic and granodioritic gneisses of the almandine-amphibolite facies of regional metamorphism. The rocks comprise oligoclase, microcline, quartz, epidote, chloritized biotite and minor hornblende, forming a weak gneissic banding. Rock fragments in the impact breccias have the same lithology as that of the country rocks.

Potassic feldspar of the gneisses in outcrop is maximum microcline with triclinicity values between 0.88 and 0.98 (Robertson, 1965; Aitken, 1970), and generally displays coarse grid-twinning. Structural state determinations on well-twinned microcline in weakly to moderately shocked breccia fragments revealed triclinicities between 0.92 and 0.96, i.e. maximum microclines also.

II.2.2 Shock Metamorphism of Microcline

To supplement the measurements of shock-induced planar elements in microclines from Charlevoix, microclines from Lac Couture breccias were examined microscopically, using the universal-stage techniques described earlier. K-feldspar from this crater was selected because the coarse M-twinning often allowed optical orientation to be determined within individual lamellae related by a known twin law, and thus the orientation of planar deformation features within twin lamallae

may be determined. One drawback is in establishing the approximate level of shock metamorphism from planar feature development in coexisting quartz grains. Some of the microclines examined occur in rock fragments containing shocked quartz, but many are found as single mineral fragments in the breccia matrix.

Of the four breccia samples used (Table II.8), three contained one suitable lithic fragment only, whereas four were found in the one remaining. Five of these seven fragments contained shocked quartz in which the abundance and orientation of planar deformation features was determined. From these data the gneissic fragments were estimated to have been shocked to pressures from 150 to 280kb±20-25kb (Table II.8). The relative positions of optic directions, twin-composition planes, cleavages and planar deformation features were measured in eighteen microcline grains. The measured parameters were plotted stereographically on a Schmidt net, and rotated to a standard position with (010), the albite twin-composition plane, vertical. A composite plot was obtained by superimposing each stereogram, using the best-fit method, on a standard maximum-microcline orientation diagram. This procedure produced less ambiguous results than encountered with the Charlevoix feldspars because three optic directions, two twin-composition planes, and occasional cleavages were available as reference points.

Unlike the majority of planar deformation features observed in Charlevoix microclines, most shock features in the Lac Couture feldspars are broad and twin-like (Plate II.8), and are often better developed than the grid-twinning. The lamellae vary in width along their length to a maximum of approximately 30μ, and members of alternate

Table II.8 Shock metamorphism of quartz from Lac Couture breccias

sample	rock fragment	No. grains	per cent with planar features	quartz deformation: avg. sets per grain	% type A	% type B	% type C	% type D	estimated pressure (kb)	microcline grains measured
DLC 6-63	1	15	100	2.23	7	54	39	0	170±20	63-1
DLC 6-63A	1	none								63A-1
"	2	4	100	2.0	0	100	0	0	150±20	63A-2
"	"									63A-3
"	3	3	100	4.0	0	0	0	100	280±25	63A-4
"	4	none								63A-5
DLC 6-63D	1	15	93	1.53	7	86	7	0	155±20	63D-1
"	"									63D-2
"	"									63D-3
"	"									63D-4
"	"									63D-5
"	"									63D-6
"	"									63D-7
"	"									63D-8
DLC 6-63H	1	15	93	2.2	0	53	40	0	170±20	63H-1
	"									63H-2
	"									63H-3

Plate II.8

a) Shock-induced multiple twinning (trending E) in microcline from Lac Couture (grain 63D-5). Albite and pericline twins trend N and E respectively. Set of shock twins visible are in A_2 quadrant (see caption below) and have $\{\bar{1}30\}$ composition plane. Crossed polars.

b) Shock-induced multiple twinning in microcline (grain 63A-4). Pericline twinning (E-W) separates quadrants A_2 (upper left and centre) and P_2 (lower). Albite twinning (N-S) forms a narrow, lamellar, A_1 quadrant (right centre) with another A_2 quadrant on its right. Quadrant P_1 is not visible in the photograph. Shock twins trending NE and NNW in A_2 have $\{\bar{1}30\}$ and $\{120\}$ composition planes respectively. Orientation of twins in A_1 are not known. Crossed polars.

a)

200μ

b)

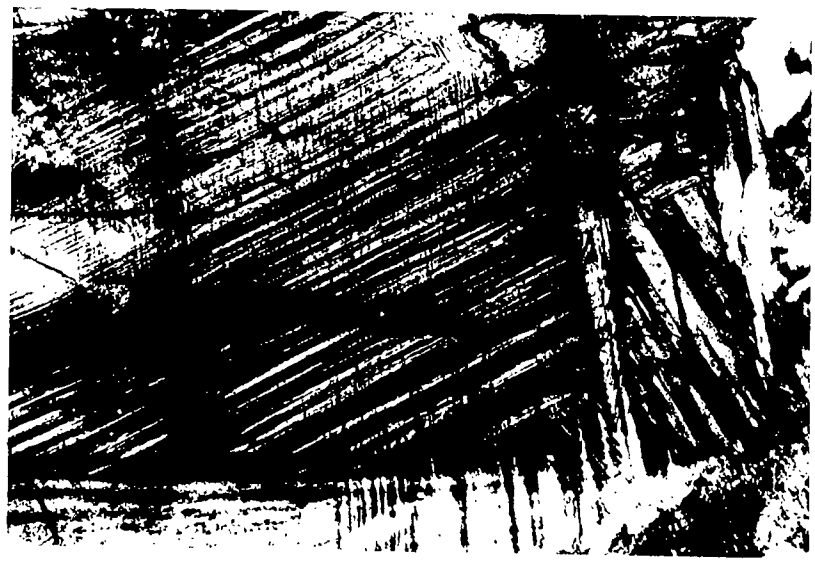

200μ

sets are not of equal width. Alternate lamellae are visible due to extinction angle differences up to 15°, and one set commonly contains abundant, minute inclusions resulting in higher relief than the other set. In some cases the minute inclusions are seen to lie along narrow, finely-spaced planes within these lamellae, but generally only a random scattering is apparent. The difference between narrow, decorated planes and broad, twin-like features appears to be one of scale rather than form. Within grains, twin-like lamellae become narrower and grade into planes with only a faintly detectable extinction difference, or without perceptible width. In addition, planar features of a given orientation tend, in general, to be narrow when confined by fine albite or pericline twins, but become broader in the same grain where the M-twins are coarser, or grid-twinning is absent. Planar features, both twin-like and narrow planes, are restricted to particular sets of the albite and pericline lamellae and do not generally cross twin-composition boundaries (Plate II.7b) except where the M-twinning is poorly developed. Similarly, finely spaced planar features are developed within the twin-like shock features and are restricted to individual lamellae.

The orientations of planar deformation features measured in the Lac Couture microclines are plotted in Fig. II.14. Virtually all planes fall into one of five rather tight groups, illustrating crystallographic control. Most abundant are planes parallel to (120) and (130), followed by ($\bar{1}$30), (110) and (210), (11$\bar{1}$) and (22$\bar{1}$), and in the [110] zone between ($\bar{1}$10) and (00$\bar{1}$). The planar feature data were analyzed to determine whether the orientation of planes developed within one set of twin lamellae differs systematically from that of planes in

Fig. II.14

Stereogram of planar deformation features (solid circles) in microcline from Lac Couture breccias. Positions within the microcline lattice of optic directions (crosses within circles), twin composition planes (asterisks), and reference planes (open circles) are plotted. Dashed line represents trace of the [110] zone.

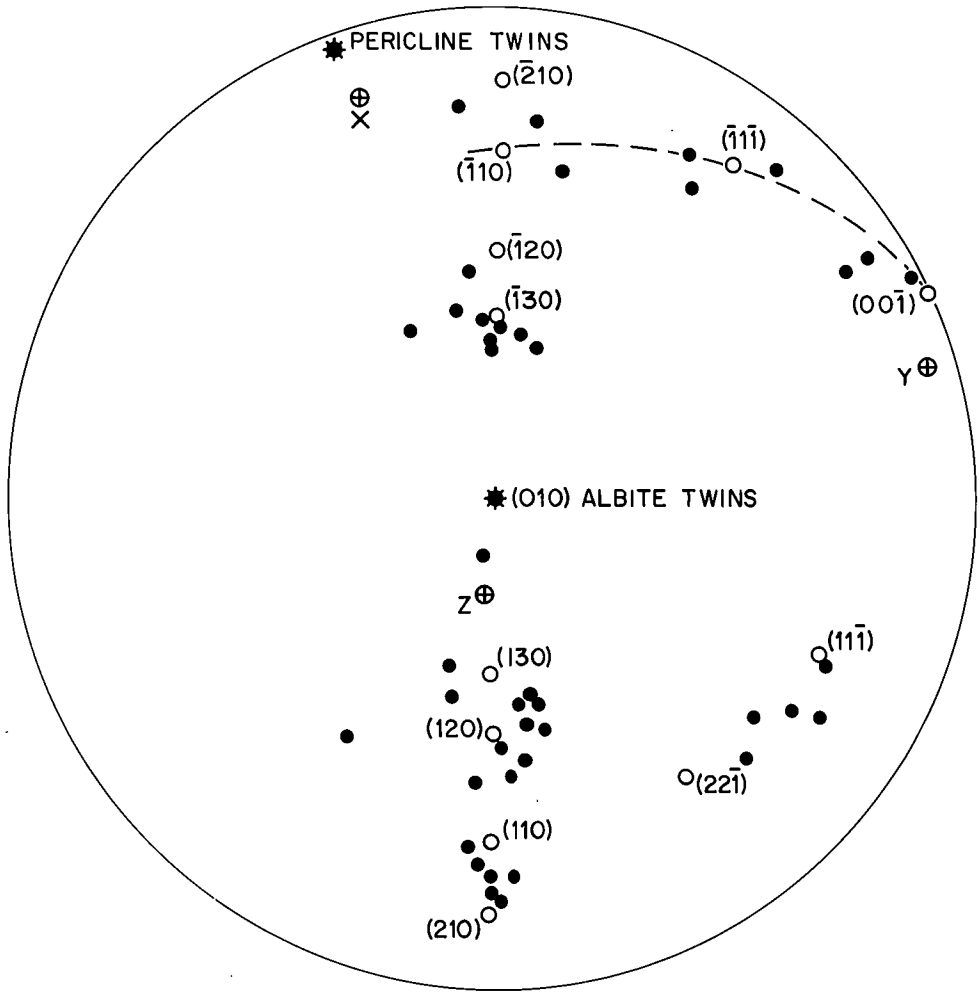
PERICLINE TWINS
(2̄10)
(1̄1̄1̄)
(1̄10)
(1̄20)
(1̄30)
(00 1̄)
Y
(010) ALBITE TWINS
Z
(130)
(11 1̄)
(120)
(22 1̄)
(110)
(210)

other lamellae. Coarse M-twinning, according to albite and pericline twin laws, produces a checkerboard grid on (001) with four quadrants of differing crystallographic orientation. One quadrant is arbitrarily designated as A_1; the adjacent quadrant separated by the albite twin-composition plane, (010), is A_2; the quadrant also adjacent to A_1 but separated by the pericline twin-composition plane, is P_1; the remaining quadrant is P_2 and is crystallographically related to A_1 by the M-twin law. Laves (1950) has shown that this is a simplistic view of the true crystallographic relationships between M-twin components, but it is adequate for this study. Table II.9 lists the orientations of planar features by quadrant for the twelve microcline grains in which optics can be measured in at least two quadrants. As the choice of the A_1 quadrant is arbitrary, it was identified by the development of shock features with orientations near (120) or (130). A distinct pattern becomes evident, although exceptions do occur. Orientations near (120) and (130) are characteristic of A_1; planes parallel to (110), (210) and $(\bar{1}30)$ are typically found in A_2; planar features lying in the [110] zone, and others near $(11\bar{1})$ and $(22\bar{1})$, generally form in P_1 and P_2, but not necessarily respectively.

Optic orientations were obtained from both sets of lamellae, in four instances where the twin-like features were broad enough to allow these measurements. These data were plotted stereographically to determine whether, if the features are truly twins, a twin law could be identified from the angle between the pole to the twin-composition plane and the twin axis. This angle is 0° for normal twins, and 90° for both parallel and complex twin laws. A measured angle of 17° in one

Table II. 9 Planar deformation features in microcline from Lac Couture breccias.

grain	planar features by quadrant* A_1	A_2	P_1	P_2	Comments
63-1	(120)	(010)			($\bar{1}$30) within one set of (010)
		($\bar{1}$30)			
63A-1	(120) to (130)	($\bar{1}$30)			
		(130)			
63A-2	(120)				
	(110)				
63A-3	(120)	(110)			
		($\bar{1}$30)			
63A-4		(110) to (210)	($\bar{2}$10)	($\bar{1}1\bar{1}$)	(131) within one set of ($\bar{1}1\bar{1}$)
		($\bar{1}$30)	($\bar{1}1\bar{3}$)	(131)	
				($11\bar{1}$) to ($22\bar{1}$)	
63A-5				(130)	
				(110)	
				($11\bar{1}$)	
63D-5	(130)	($\bar{1}$30)			(130) of A_2 and ($11\bar{1}$) both within one set of ($\bar{1}$30)
		(130)			
		($11\bar{1}$)			
63D-6	(120)			(130)	
				(110) to (210)	(110) and ($11\bar{1}$) both within one set of (130)
				($11\bar{1}$) to ($22\bar{1}$)	
63D-7	(120) to (130)	(110)			
		($\bar{1}$30)			
63H-1		($\bar{1}$30)		($\bar{1}$10)	
63H-2	(120) to (130)				
63H-3			($\bar{1}$10)	($11\bar{1}$)	
			($\bar{1}1\bar{1}$)		

* Quadrants produced by grid twinning. Crystallographic relationship between quadrants described in text.

set parallel to ($\bar{1}30$) indicates that these twin-like planes may be related by a normal twin law. On the other hand, angles of 42°, 46°, and 49° for sets parallel to ($\bar{1}30$), (110), and ($\bar{1}30$) respectively do not support the existence of any of the three common twin laws.

II.3 Discussion

The effects of shock metamorphism of potassic feldspar from Charlevoix and Lac Couture craters have been examined with regard to structural state, perthitic exsolution, and development of planar elements characteristic of shock deformation.

Structural state studies have proven inconclusive and thus are similar to the results of Aitken (1970). In general, degree of ordering does not change with increasing shock metamorphism over the pressure range characterized by the Charlevoix samples (up to 360kb). A variety of structural states can be found in potassic feldspars of the charnockitic rocks, a variation in thermal history which can be correlated largely with pre-impact mineralogy. Orthoclase with a low degree of ordering (average 24 per cent) typifies the charnockitic syenodiorites, an orthoclase of somewhat greater ordering (average 29 per cent) occurs in the charnockitic granites, and an intermediate microcline (average ordering 49 per cent) is the characteristic K-feldspar of the charnockitic microcline granites. These values are not unusual for natural feldspars. According to Barth (1969) the most common monoclinic feldspars are sanidines and orthoclases with 15 to 33 per cent order. Although microclines with high triclinicity (0.8 to 1.0) are generally more common than those with lower values, intermediate microclines

displaying little or no grid twinning have often been described from siliceous or intermediate charnockitic rocks (Wilson, 1950; Howie, 1955; Parras, 1958).

A lesser variation of structural state also occurs within each of the three rock units. However, because both strongly and weakly shocked potassic feldspars exist with either high or low percentage ordering, this variation similarly cannot be ascribed solely or mainly to the processes of shock metamorphism. Potassic feldspars from regional metamorphic terrains occur in differing structural states within a lithologic unit. Barth (1969) reported that a range of triclinicities are exhibited in microclines within migmatites, schists, and gneisses (particularly augen gneisses), and Smithson (1962) concluded that amphibolite facies gneisses (particularly augen gneisses again) are characterized by microcline with a wide range of obliquities (triclinicity).

On the other hand, potassic feldspars at Charlevoix with less-ordered structural states are more common in the most highly shocked samples than among the weakly shocked or unshocked samples. The implication is that shock conditions, largely immediate post-shock temperature, raised the K-feldspars to a state of lower ordering, and subsequent rapid cooling prevented attainment of the pre-shock structural state. Barth (1969) believed disordering of microcline may begin as low as 250°C with transition to orthoclase at approximately 400°C. According to Stöffler (1971a), immediate post-shock temperatures, rather than the instantaneous temperatures produced at the moment of impact, are the major factor influencing many changes observed as shock metamorphic effects. His diagram (see Chapter IV, Fig. IV.3) shows that a post-shock temperature of 250°C is reached in feldspars only at pressures

above approximately 330kb, where instantaneous shock temperatures have reached approximately 630°C in shocked microcline. Thus, if changes of structural state are initiated solely by temperature, and values of 250°C or more are required, samples shocked to greater than 330kb may show changes of ordering. At Charlevoix, samples 92 to 95 are the only ones whose estimated pressures satisfy this condition, and according to the various methods used to determine degree of ordering they consistently exhibit the lowest degree of ordering of any K-feldspars examined.

The effect of shock pressure, exclusive of accompanying residual heat, on common geologic transformations is not well known. Many processes which ordinarily require high temperatures may proceed at considerably lower temperatures under the influence of shock pressure. Thus structural disordering may occur in potassic feldspars at temperatures below the 250°C minimum suggested by Barth (1969), when shocked to a few hundreds of kilobars. As an example, Sclar and Usselman (1970) transformed intermediate microcline to a monoclinic structure at shock pressures of 250kb. Although post-shock temperature attained in this experiment was not reported, it would lie near only 120°C on Stöffler's diagram.

There does, therefore, appear to be some evidence for disordering in the microcline lattice for samples 92 to 95 due to shock conditions associated with shock stress greater than approximately 330kb. An unfortunate sample distribution, however, lessens the possible validity of this observation. Structural state of unshocked or weakly shocked K-feldspar of the charnockitic syenodiorites (in which 92-95 are classed) is based on only one sample (129), because most outcrops lie on Mont des

Éboulements. Thus the nature of the pre-shock structural state has not been really established. In addition, in the charnockitic granites and microcline granites where the unshocked state has been determined on several samples, no examples representing pressures greater than 300kb were found, to determine whether shock-induced disordering occurred. Further sampling, particularly of the charnockitic syenodiorites, may resolve the uncertainty.

Perthitic intergrowth in orthoclase and microcline shocked to approximately 170kb or greater at Charlevoix is morphologically different from the exsolution intergrowth developed in the weakly shocked or unshocked K-feldspars of corresponding structural state and composition. In the latter, narrow film-perthite lamellae parallel to {70$\bar{1}$} are continuous across grains, with a coarser bleb perthite occurring in grain interiors. The lamellae are restricted to grain margins in highly shocked feldspars, coarse albite blebs are not present, and an intricate spindle or string microperthite is developed in the grain centre. A conventional interpretation of these observations is that the two populations, continuous versus discontinuous film perthite, possess different thermal histories. The observation that the two groups correspond to unshocked and highly shocked feldspars respectively, and that this dichotomy applies in all three charnockitic units, indicates that the replacement of {70$\bar{1}$} lamellae by spindle or string microperthite is a feature of shock metamorphism.

The relationship between the film-perthite lamellae and the microperthite gives the impression that the latter is growing at the expense of, and replacing the former. The process immediately envisaged

is one in which post-shock heat from the impact homogenized the albite and orthoclase phases by raising the temperature above the alkali feldspar solvus. The assumed homogenization apparently proceeded outward from the grain interior, but was incomplete on the margins leaving the original film-perthite lamellae. The implication is that if more highly shocked samples were available complete destruction of the lamellae would occur. Extending this hypothesis, subsequent cooling below the solvus resulted in exsolution with a spindle or string-microperthite morphology.

Based on phase relations in the alkali feldspar series, this hypothesis must be considered incorrect. Visual estimates of the amount of perthitic albite in the unshocked grains put the bulk alkali feldspar composition at Or 65±5. At one atmosphere, feldspar of this composition intersects the solvus at approximately 610°±25°C. In other words, homogenization would not occur to any significant extent unless temperatures could be raised above this value. Yoder et al. (1957) demonstrated that as pressure increases, solvus temperatures increase relative to solidus temperatures, particularly near the orthoclase side, so that 610°C represents a minimum value for this composition. Shock temperatures of this magnitude are attained in microcline above approximately 320kb (Stöffler, 1971a), but because they decay instantaneously they would have little influence on sluggish processes like the migration of sodium and potassium atoms. Post-shock temperatures which do endure would not reach 610°C in potassic feldspars at pressures less than 500kb or even 600kb (Stöffler's diagram is incomplete above 420kb), and certainly not at shock levels shown by

the Charlevoix rocks. Therefore heating, homogenization, and exsolution was not the sequence which produced the spindle microperthite.

The solution may lie in the nature of the two types of perthite. Film-perthite lamellae are an example of "continuous" precipitation (Barth, 1969), a process in which only K and Na are relocated in the crystal lattice. Albite nucleates as lamellae along interfaces so that the similar crystal lattices of the Na- and K-feldspars are oriented in parallel. (Perthitic albite lamellae parallel to $\{70\bar{1}\}$ have $\underline{a}^*$ albite parallel $\underline{a}^*$ orthoclase (see Barth, Fig. 1.20, p.36)). "Discontinuous" precipitation occurs along small fractures, at grain boundaries, or around inclusions, and strict parallelism of the two lattices is not necessary. The former is a comparatively slow migration due to symmetry constraints and thus physico-chemical equilibrium may not be attained during growth. Growth rate of perthites by discontinuous precipitation is high and chemical equilibrium is attained. Barth (1969, p.29) states that "...if the feldspars become subjected to external pressure the strain energy will activate the sodium atoms, and exsolution will continue...until practically complete unmixing is attained".

These facts lead to an alternative origin for the perthitic intergrowths in the highly shocked K-feldspars at Charlevoix. During primary (pre-crater) crystallization, exsolution was mainly of a continuous nature, producing film-perthite lamellae and bleb- or patch-perthite in crystallographic continuity. Chemical equilibrium may not have been attained. Strain due to shock pressures then restarted Na diffusion. Distortion of the feldspar lattice, especially in grain

centres, disrupted the parallelism of a* between orthoclase and albite. In some grains this distortion can be detected as extinction position differences between the microperthitic interior and the margins bearing {70$\bar{1}$} lamellae. Sodium atoms from the film-perthite lamellae, blebs and patches, and others in metastable solid solution, found it easier to reprecipitate in a largely discontinuous type of microperthite, nucleating along shock-induced dislocations. Chemical equilibrium may have been reached.

There is, however, little evidence to support this hypothesis, any many features remain unexplained. If complete chemical equilibrium was attained only by the highly shocked feldspars, then their potassic phase should be less sodic than the potassic phase in the unshocked material. The analytical data (Table II.3) do not support this, and in fact the opposite may be true. However, the higher Na values for the highly shocked samples are probably due to difficulty in isolating the K-rich phase in the intimate microperthitic growth. Why do the coarse albite blebs or patches vanish as suddenly as they do? Why does the microperthite form initially in the interior, leaving a relatively uniform rim of lamellae-bearing feldspar?

Whatever the process, shock metamorphism has caused a change in the perthite development, probably accompanied by migration of Na and K atoms. Diffusion of alkalis at unexpectedly low temperatures due to shock metamorphism has been discovered by R.A.F. Grieve (personal communication, 1973). His analyses of maskelynite from Lake Mistastin revealed a higher potassium content than in plagioclase from which it was derived. He believed that homogenization of plagioclase with scattered, minute orthoclase inclusions has occurred by diffusion of alkalis in the

solid state at post-shock temperatures in the range 350° to 450°C.

Shock-induced planar elements of three types, i.e. cleavages, planar deformation features and twins, have been found in Charlevoix and Lac Couture potassic feldspars. Each type has been noted and described in other minerals as a typical shock effect (Stöffler, 1972).

Fracturing parallel to faces along which cleavage is rare or has not been reported occurs in orthoclase shocked to greater than 170kb. The most common orientations are $\{\bar{2}10\}$, $\{120\}$, $\{11\bar{2}\}$, $\{031\}$, $\{011\}$, and $\{101\}$. The first two agree with observations on unshocked rocks (Deer et al., 1963) that partings parallel to possible vicinal faces between (100) and (110) or $(\bar{1}10)$ can occur. The remaining four orientations have no apparent counterparts in conventionally deformed feldspars. Few shock-produced cleavages in feldspars have been reported elsewhere, but in shocked plagioclase from the Ries crater, Engelhardt and Stöffler (1968) described cleavages with unusual orientations but with definite crystallographic control. For a given mineral, shock cleavages initially form at much lower pressures than do planar deformation features, and generally below the Hugoniot elastic limit due to stress relaxation behind the elastic precursor wave (Stöffler, 1972). Observations from the Charlevoix K-feldspars partially support this. Planar deformation features initially occur at approximately 30kb higher than the appearance of the cleavages, but do not become prominent below approximately 250kb. However, the first recognition of shock-induced cleavages at 170kb is considerably higher than expected from a feldspar Hugoniot elastic limit near 100±20kb (Ahrens et al., 1969).

Planar deformation features are similar to those characteristic of quartz and plagioclase shocked in natural and experimental events. Their development at Charlevoix in rocks where coexisting quartz contains abundant planar deformation features supports Dence's (1968) observations that they are not prominent in feldspars below pressures creating type D quartz. Unlike shock features in quartz, which persist to their maximum development as narrow planes, those in orthoclase and microcline assume this character only in the initial 60 to 80kb of their development. Above approximately 270kb most planes, certainly the strongest, are broad, twin-like features. Their extinction position differences, relative regularity of width, and formation along defined crystallographic planes indicate that they are shock-induced examples of polysynthetic mechanical twinning. Crystallographic relationship, or lattice continuity between alternate lamellae, must be shown, to verify this assumption.

Shock-induced mechanical twinning has been described, and in a few cases verified by X-rays, in several minerals (although not feldspars) from lunar and terrestrial impact sites (Stöffler, 1972). Mechanical twinning is a relatively common phenomenon of static deformation for several minerals, particularly chain silicates and high temperature sodic plagioclase. It occurs less frequently in low temperature, highly ordered forms because, in the case of albite, strong bonds have to be broken to allow Al and Si as well as Na and Ca to migrate. Ribbe et al. (1965) believed that mechanical twinning of low albite should not be possible over short periods, but that continued stress may allow the transformation to occur. The same reasoning applies to ordered K-feldspars and no examples of mechanical

twinning of orthoclase or microcline have been recorded.

Shock-induced twinning occurs along planes with the same orientation as the planar deformation features, which may be a clue to the formation of the former. Most authors agree that the typically narrow planar deformation features form by lattice gliding due to shear stresses (Stöffler, 1972). Mechanical twinning occurs where gliding causes the two parts of the lattice to abut according to some twin law (the twin composition plane need not be one of those common in growth twins). Thus the two types of feature seem closely related. It may be that planar deformation features are produced by comparatively weak stress, breaking the bonds linking the alkali atoms to SiO_4 tetrahedra and causing minor slippage. The tectosilicate framework would remain intact and thus no orientation or phase differences would be detected. Greater stress may rupture bonds within the tetrahedra, allowing Si and Al to glide and also causing lattice displacements related by twinning.

The orientation of planar deformation features and shock twins do not agree with normal K-feldspar cleavages and partings, or composition planes of primary twins (Burri, 1962). Two minor exceptions are the weak development of planar features parallel to {010}, the albite twin-composition plane, and $\{70\bar{1}\}$, the Murchisonite parting containing film perthite lamellae.

The orientations of planar features are similar in both orthoclase and microcline in the charnockitic rocks, and these orientations continue throughout the pressure range investigated.

Those from the Lac Couture microclines, however, have different orientations and appear to form at significantly lower pressures than those from Charlevoix. A possible explanation may be due to the relative ordering of the three feldspars. The Charlevoix feldspars, although monoclinic and triclinic, have similar structural states, whereas the shocked maximum microcline from Lac Couture is probably more than 90 per cent ordered.

The twin law for shock-induced twins has not been established. The four instances in which attempts were made to determine the twin law by optics gave data incompatible with either normal, parallel, or complex twins. The shock twins, instead, seem to lie intermediate between the two possible extremes. Burri (1962), in his review of feldspar twinning, makes no mention of twin laws other than these three. However, Smith and Mackenzie (1954, 1959), Mackenzie and Smith (1962) and Smith (1962) noted a "diagonal association" in twinned microcline. It was identified in single crystal b* oscillation photographs in which reflections from these twins lay on a diagonal between reflections from albite- and pericline-twinned units. They did not report whether these twins were visible in thin section nor the orientation of the twin composition plane. Smith and Mackenzie (1954, 1959) believed that the diagonal association could have various positions between the extremes of albite (normal) and pericline (parallel) twins. Marfunin (1962) discovered, by the same technique, a similar association which he called irrational twinning. No clue to the geologic significance or origin of diagonal twins has been proposed, although Smith (1962) suggested they may be caused by strain between albite and pericline twins.

Thus twin laws other than normal, parallel or complex do exist, and at least some shock-induced twinning may obey the diagonal (irrational) association.

A peculiar feature of the shock twins is that lamellae of one set have lower refractive index and are filled with high relief, generally unresolvable material, by comparison with members of the alternate set. In some cases the high relief material is resolvable as minute inclusions forming in trains within narrow, secondary planar features, but in most instances this is not true (Plate II.6b). In a few examples, parts of the high-relief lamellae contain a yellowish, birefringent, microcrystalline aggregate with the appearance of a micaceous alteration product. This description compares closely with those presented for certain deformation features in shock damaged plagioclase. Robertson et al. (1968) found lamellar planes with differing relief and refractive index in andesine from a Canadian impact crater. Engelhardt and Stöffler (1968) reported similar observations for plagioclase from the Ries crater. Taking these modifications one step further, plagioclase is converted to maskelynite with decreased birefringence and refractive index, preferentially along one set of albite twin lamellae (Robertson et al., 1968). Where maskelynite development has not converted the entire grain, subsequent devitrification and/or alteration produces lamellae of microcrystalline material alternating with recognizable feldspar (P.B. Robertson, unpublished data). No satisfactory explanation has been proposed for preferential development along one set of albite twin lamellae.

The high-relief twin lamellae in orthoclase and microcline

may, therefore, represent partial transformation to diaplectic alkali feldspar glass, or a phase in which long-range ordering has been destroyed to some degree. Conversion probably occurred initially along the fine planar features, as it does in quartz and plagioclase (Chao, 1968b) where it has inverted from a high-pressure phase (Stöffler and Hornemann, 1972). (Although no evidence of unusual phases was present in diffraction patterns of the Charlevoix K-feldspars, diminished ordering in the highly shocked feldspars was shown by broad, diffuse peaks). Such a high-pressure phase begins to form within the mixed-phase region of the Hugoniot which may begin below 200kb for feldspars (Ahrens et al., 1969). In experiments, partial conversion of microcline to diaplectic glass occurred at 250kb (Sclar and Usselmann, 1970), and complete transformation of orthoclase was produced at 320kb (Kleeman, 1970) and 360kb (Stöffler and Hornemann, 1972). Thus the pressure range typified by the Charlevoix samples is compatible with such a process and partial conversion to diaplectic glass is likely to have taken place.

Unlike shocked quartz in which certain preferred orientations of planar features characterize successive pressure regions, no such sequence can be constructed for the potassic feldspars. Correlation of shock pressures with shock metamorphic effects in orthoclase and microcline must therefore be based on the combined observation of several types of deformation features.

CHAPTER III

THE EFFECT OF SHOCK METAMORPHISM ON THE COMPOSITIONS OF ALKALI FELDSPARS, CHIEFLY AT BRENT CRATER

III.1 Introduction

Most evidence for shock metamorphism consists of obvious modifications to the structure and/or texture of the shocked rocks and minerals. Such evidence includes fracturing, breccias of several types, and shatter cones (all on an outcrop scale), through planar deformation features, diaplectic glass, and flow textures (observable microscopically), to disordering and conversion to high pressure polymorphs (best verified by X-ray methods). Several of these deformations are uniquely products of shock metamorphism whereas others, although developed by dynamic metamorphism in other geologic environments, are considerably more intense where produced by impact.

In contrast, the ultimate product of shock metamorphism has a commonplace appearance. Immediate post-shock temperatures associated with shock pressures above approximately 1000kb are sufficient, depending on composition, to melt large volumes of the target rocks. The fused material can occur as glassy bombs in unconsolidated ejecta, as glassy or recrystallized masses in mixed fall-back breccias, as dykes of melt with breccia (not pseudotachylite) filling fractures in the crater basement, or as sub-horizontal sheets of igneous rock (Dence, 1971). The first three types are generally glassy and inhomogeneous, and are intimately associated with physical evidence of shock metamorphism, and so their origin is readily confirmed. This ease of identification, however, does not always extend to impact melts, or impactites, of

the fourth occurrence. Impact-melt rocks preserved at the Manicouagan crater are believed to have formed a layer at least 200m thick and 50 to 55km wide, overlying the entire central uplift and extending into the peripheral trough (Dence, 1971). These rocks comprise a lower, fine-grained, nearly massive unit overlain by a coarse-grained, gray igneous rock, which have been mapped as trachyandesite and larvikite respectively (Currie, 1972). The 130m-thick, impact-melt unit on the islands at the West Clearwater Lake crater is, in part, a fine-grained to massive, light red to gray igneous rock, called quartz latite by Bostock (1969). Similarly, the layer of melt rocks at Brent has been described as trachyte of igneous aspect by Currie and Shafiqullah (1967). The melt rocks, then, appear as igneous-textured rocks, of mineralogy consistent with certain igneous rocks, and emplaced in situations not incompatible with an igneous origin. Petrographically, in hand specimen or under the microscope, they cannot be distinguished as the crystallized products of shock fusion. Such a conclusion must therefore be based on their related association with material, particularly xenoliths and xenocrysts, displaying aspects of shock metamorphism.

Dence (1971) compared the analyses of impact melts with analyses of the surrounding country rocks from seven meteorite craters. Summarizing his observations (op. cit. p.5557) he found that "melt rocks...show greater similarity to the composition of adjacent country rocks than to each other. In a number of cases, however, the igneous materials are enriched in magnesia and potash and depleted in silica and soda relative to their respective country rocks". Those who believe that the large "cryptovolcanic"

structures are endogenetic, cite these compositional differences as evidence that the melt rocks are not chemically related to the country rocks but represent a separate event (Currie and Shafiqullah, 1968; Bostock, 1969). Dence (1971) on the other hand, maintains that the differences are minor and can be accounted for by a combination of contamination by meteoritic material, selective melting, difficulty in determining ratio of country-rock types melted, and secondary effects due to circulating vapours and solutions.

If the melting by meteorite impact hypothesis is accepted, the variation of alkalis suggests that an explanation may be found in the behaviour of the alkali feldspars, the predominant source of sodium and potassium in most of the crater country rocks. In order to assess this hypothesis, shocked alkali feldspars from increasing depths beneath the Brent crater were analyzed and compared with those in unshocked country rocks, and with feldspars of the impactite (melt) layer. Brent was chosen because the melt rock, compared with the average country rock, is significantly enriched in K_2O and depleted in Na_2O (Currie and Shafiqullah, 1967) (see Table III.1). In addition, Brent is perhaps the most thoroughly investigated impact crater in Canada.

III.2 Brent Crater

III.2.1 Geology

The Brent crater, Ontario, lies in the Grenville Province of the Canadian Precambrian Shield, approximately 385km west of Montreal (Fig. II.1). Its discovery in 1951, from aerial photographs (Millman et

al., 1960), marked the initial recognition of an ancient, deeply eroded, terrestrial meteorite crater, and led to the systematic investigation of fossil impact structures in many parts of the world. Brent has been extensively studied using geophysics, diamond drilling, isotopic age-dating, and routine mapping and petrographic methods, and the results of most investigations have been summarized by Dence and Guy-Bray (1972).

The present crater is outlined by a remarkably circular depression, 2.9km in diameter by 61m in depth. No evidence remains of a rim raised above the surrounding terrain. The crater is filled by 250m of Middle Ordovician sediments overlying a breccia lens, 610m thick in the centre. The crater was excavated by impact during the Middle Ordovician period, on the eastern side of an antiform in Grenville age (Proterozoic) gneisses (Fig. III.1). The unit underlying most of the crater and forming most of the lithic clasts in the breccia is a quartz-plagioclase-mesoperthite-hornblende gneiss containing traces of garnet and biotite. It is overlain by a quartz-plagioclase-microcline-biotite-garnet gneiss containing traces of hornblende; this unit is intersected by the crater's eastern margin. Pink to gray, quartz-plagioclase-microcline-biotite gneiss containing massive, boudin-like structures of basic garnet amphibolite and garnet-pyroxene coronite, outcrops to the east and southeast of the crater periphery. Granitic and basic garnetiferous gneisses are found further to the east and northeast.

Little evidence of shock metamorphism or indication of the crater structure can be found on the surface, but an extensive drilling programme has yielded abundant information on both aspects. A profile

Fig. III.1

Geology of the Brent crater, Ontario. The crater, outlined by a depression 2.9km in diameter, was excavated on the eastern flank of an antiform in Grenville gneisses. Diagram based on Dence and Guy-Bray (1972, Figure 2). The rock units are:

1. Quartz-plagioclase-mesoperthite-hornblende (-garnet-biotite)-gneiss.
2. Quartz-plagioclase-microcline-biotite-garnet (-hornblende)-gneiss.
3. Quartz-plagioclase-microcline-biotite-gneiss.
4. Interlayered quartz-feldspar and garnet-amphibolite gneiss.
5. Dolostones and limestones.
6. Glacial drift.

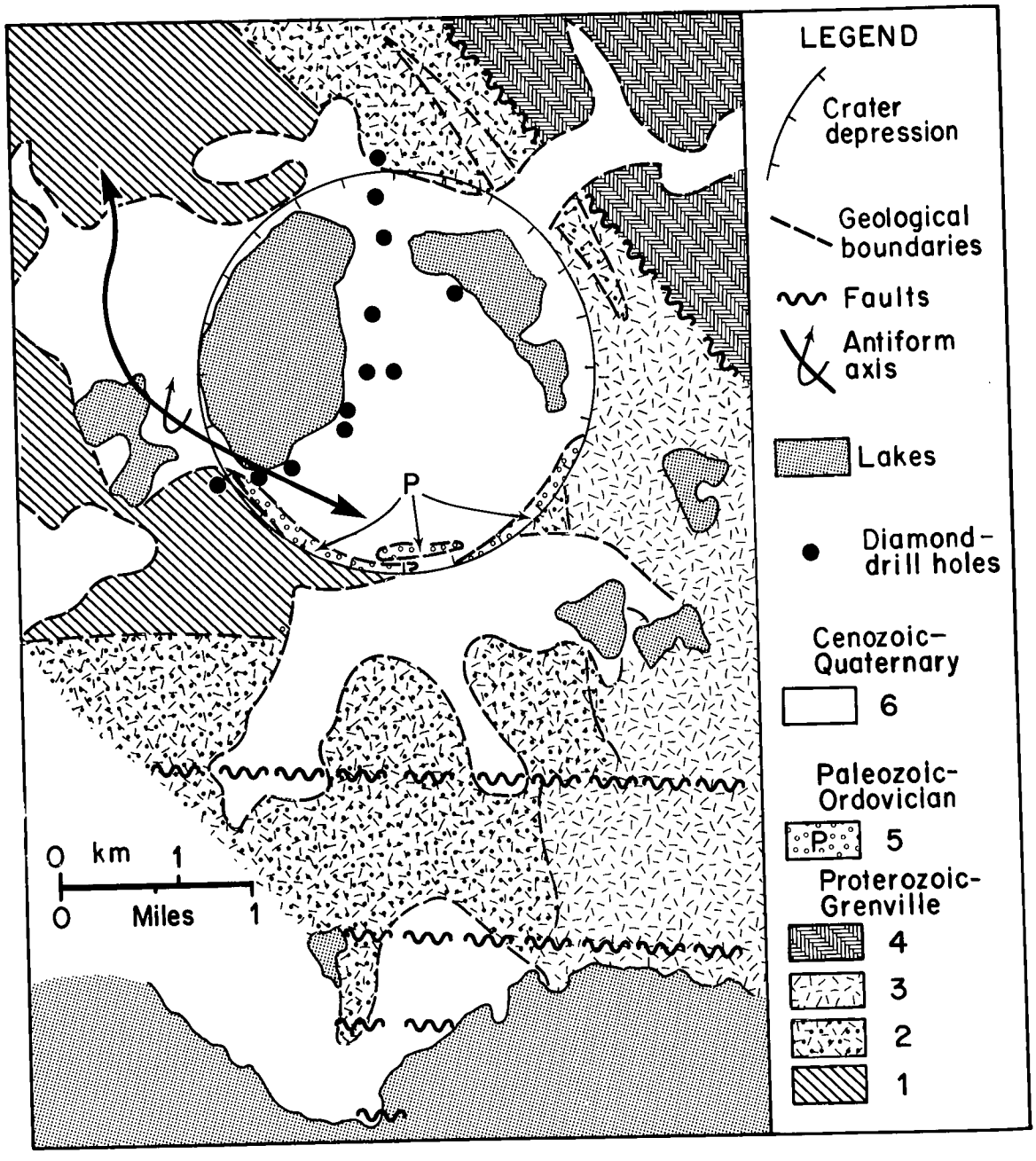
LEGEND
Crater depression
Geological boundaries
Faults
Antiform axis
Lakes
Diamond-drill holes
Cenozoic-Quaternary
6
Paleozoic-Ordovician
P
5
Proterozoic-Grenville
4
3
2
1
P
0 km 1
0 Miles 1

Fig. III.2

Cross-section of the Brent crater compiled from diamond drill hole data. Hole 1-59 penetrated Ordovician sediments, mixed breccias, and impact melt, and terminated in fractured basement gneisses 1064m below the collar. Diagram based on Dence and Guy-Bray (1972, Figure 4).

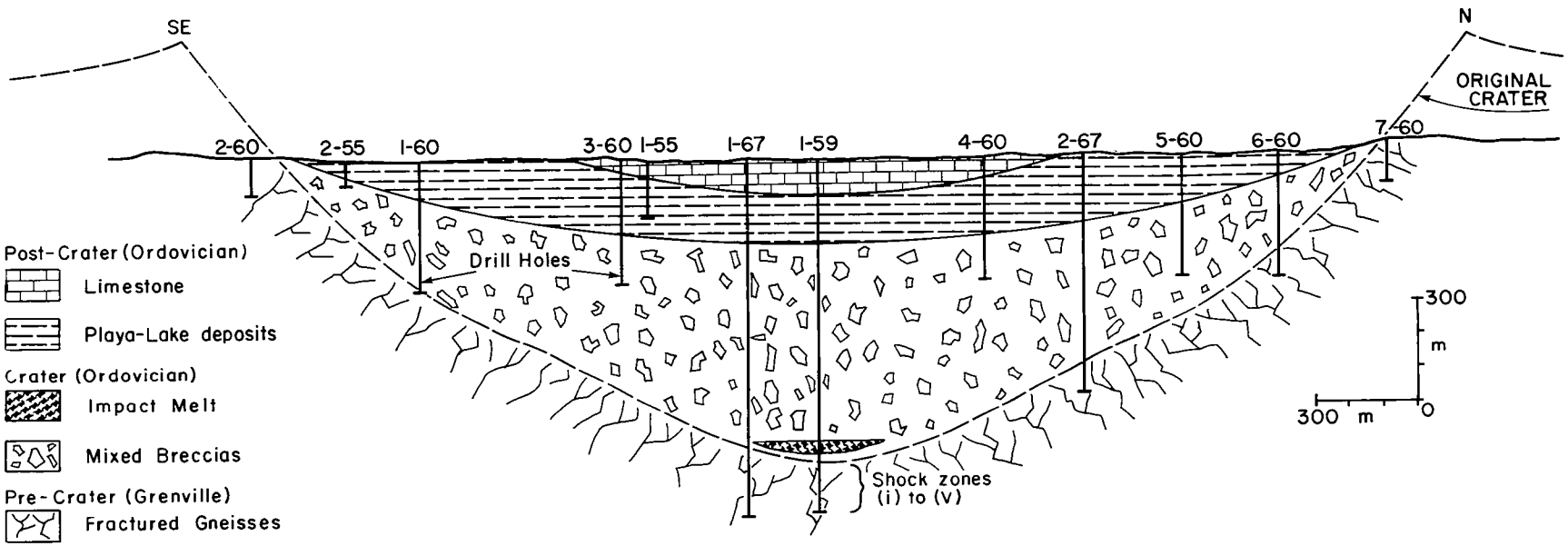
SE
N
ORIGINAL CRATER
2-60
2-55
1-60
3-60
1-55
1-67
1-59
4-60
2-67
5-60
6-60
7-60
Drill Holes
Post-Crater (Ordovician)
Limestone
Playa-Lake deposits
Crater (Ordovician)
Impact Melt
Mixed Breccias
Pre-Crater (Grenville)
Fractured Gneisses
Shock zones (i) to (V)
300
m
0
300 m

of the basin has been constructed from twelve drill holes (Figs. III.1, and III.2) which provided 5,035m of core. Two central holes, 1-59 and 1-67, penetrated sediments, breccias and melt rocks, and extended approximately 210m beneath the crater into unshocked basement gneisses. The sedimentary rocks are dolostones and siltstones from a saline, playa-lake environment, overlain by interlayered limestone and redbeds indicating periods of marine transgression and regression after the crater rim was breached. Breccias contain shock-deformed rock and mineral fragments and melted material, and largely represent material slumped in from the crater walls. The fine-grained melt rock forms a lens approximately 35m thick, comprising inclusion-rich zones at the top and bottom, and a central inclusion-free region. This is underlain by a 10m-thick zone of thermally altered, almost unrecognizable gneiss which grades into country rocks of normal appearance. Basement gneisses are mainly the quartz-plagioclase-mesoperthite-hornblende unit, with shock features detectable in quartz to 33m below the thermal aureole.

III.3 Petrography, Composition, and Genesis of the Igneous Rocks of Brent Crater

The origin of the Brent crater has been hotly debated since its discovery. Formation by meteorite impact has been advocated continually by Dence (1964, 1965, 1968, 1971, 1972) whereas Currie (1965, 1971) and Currie and Shafiqullah (1967) have maintained that it was created by explosive alkaline volcanism. The controversy has centred largely on interpretation of the differences and similarities in composition of the melt layer and the country rocks. The following description of the

impactite is largely from Dence (1968) and Hartung et al. (1971).

The melt layer is approximately 35m thick, having a fairly sharp upper contact with breccia at 823m±0.5m, and grading into an underlying zone of recrystallized gneisses at 858±0.5m. The upper 15 to 20m contain abundant xenoliths up to 1m across, of thermally metamorphosed gneisses recrystallized to a variable extent. Where the gneiss fragments are pinkish or grayish, the matrix has the same general hue. The lower 5 to 10m also contains abundant gneissic xenoliths, some unlike those in the basement rocks underneath. The central 10m is comparatively free of recognizable inclusions and the matrix, coarsest at this level, shows pink and gray parts.

Where the matrix is coarsest (0.5mm) and inclusions are minimal, the melt rock contains a single feldspar which is tabular and euhedral, with strong normal zoning from cores of what Hartung et al. (1971) took to be finely-twinned andesine or oligoclase, through anorthoclase, to rims of almost uniaxial, high sanidine. The cores are actually polysynthetically-twinned anorthoclase, surrounded by an untwinned anorthoclase rim of similar composition, and with only the extreme outer margin being a potassic feldspar, possibly sanidine. Above and below the coarsest section, the untwinned anorthoclase rims are fresh and clear but the cores are cloudy, which Dence (1971) believed was due to replacement of albite by brown potassic feldspar. Smaller grains of clinopyroxene occur in clusters with ilmenomagnetite. Interstitial phases are quartz, brown and green amphiboles, pale green mica, apatite, and considerable secondary chlorite or a brown chloritic mesostasis.

Dence (1971) has not used a descriptive name but Currie believes that the rock is a trachyte, from its mineralogy and texture (Currie and Shafiqullah, 1967).

The composition of the trachyte or impact melt, compared with that of the country rocks, shows some notable differences which have led to the opposing interpretations of the crater's origin. The melt rocks are, in general, more potassic and less sodic than the average country rocks at the surface or beneath the crater (Table III.1). In addition, Currie and Shafiqullah (1967) noted a dominance of MgO over CaO, unusual for such silicic rocks. This, plus apparent potassium fenitization of some of the country rocks, convinced Currie that Brent was a centre of alkaline volcanic activity, particularly as it lies near the Ottawa-Bonnechere graben along which circular Cambro-Ordovician carbonatitic complexes were intruded (Currie and Shafiqullah, 1967; Currie, 1971). Dence (1971), on the other hand, believes that the igneous layer recrystallized from country rocks melted by meteorite impact. He feels that the apparent enrichment of the melt in TiO_2, CaO, and V can be accounted for by incorporation of alnöite, in the amount of 5%, which occurs as dykes in the crater region. Enrichment in Fe and Ni came from the melted meteorite. Potassium enrichment is due largely to replacement of plagioclase (presumably the brown cloudy cores of the zoned feldspar) by potassic feldspar through the action of solutions heated by residual heat in the crater.

In summary, Currie believes that the trachytic rocks were intruded as part of alkaline volcanic activity and were a source of

Table III.1 K_2O and Na_2O content (wt %) of country rocks and igneous rocks from Brent crater.

	Country rocks					Igneous rocks			
	1	2	3	4	5	6	7	8	9
K_2O (average and range)	4.09	4.33 (0.22-5.9)	4.08	4.22 (4.03-4.49)	4.34 (3.85-6.25)	7.60	5.0	8.1	5.78 (4.26-8.05)
Na_2O (" " ")	3.22	3.52 (1.7-4.8)	3.60	n.d.	n.d.	1.86	4.3	2.4	n.d.

1. 9 surface samples (Currie and Shafiqullah, 1967)
2. 22 surface samples (Currie, 1971)
3. 7 basement core samples, hole 1-59 (Currie and Shafiqullah, 1967)
4. 3 basement core samples, below 915m, hole 1-59 (Hartung et al., 1971)
5. 23 basement core samples, below 915m, hole 1-67 (Hamza, 1973)
6. 3 trachytes, hole 1-59 (Currie and Shafiqullah, 1967)
7. coarsest melt phase, hole 1-59 (Dence, 1971)
8. fine-grained melt phase, hole 1-59 (Dence, 1971)
9. 6 melt-zone samples, hole 1-59 (Hartung et al, 1971)

potassium which produced localized potassium fenitization, whereas Dence is of the opinion that the impact melt was a sink for potassium-rich solutions, perhaps connected with the impact event.

III.3.1 Composition of Feldspars Beneath the Brent Crater

In both theories of origin of the igneous rocks at Brent the behaviour of potassium and sodium, during or subsequent to the cratering event, plays a significant role. In one case the igneous rocks are believed to be an alkalic trachyte from which potassium-rich solutions have moved out, fenitizing the country rocks by replacement of sodium with potassium, chiefly in alkali feldspars. In the other case, potassium-rich solutions move into the melt rocks with Na of the alkali feldspars being replaced by K. Where these latter potassium-rich solutions originate has not been made clear, nor the ultimate fate of the sodium which has been released from the feldspars. In any event it seems likely that the feldspars in the country rocks surrounding and beneath the crater would have also been affected by these solutions. In this regard, alkali feldspar and plagioclase in unshocked to moderately shocked gneisses beneath Brent were examined to determine whether compositional changes occur which may help in confirming either of the above hypotheses.

The rocks underlying the crater in hole 1-59 belong to the quartz-plagioclase-mesoperthite-hornblende- (biotite-garnet) gneiss unit outcropping in the western part of the crater (Fig. III.1). In hand specimen they are pinkish, medium- to fine-grained, quartzo-feldspathic

rocks with minor mafic minerals exhibiting generally poor banding. The rocks are dominated by mesoperthitic alkali feldspar (50-60%) in equant, anhedral grains 0.5 to 1mm in diameter, with slightly smaller grains of quartz (20-25%) and well twinned plagioclase (15-20%) (Plate III.1a). Poorly developed mafic bands contain subhedral green hornblende (2-5%) accompanied by minor amounts of biotite, garnet, iron ore, apatite and zircon. The alkali feldspar comprises an orthoclase host with albitic plagioclase in two perthitic intergrowths. One, a film perthite, occurs as narrow (approximately 1μ) lamellae at 4 or 5μ intervals formed probably along the Murchisonite parting (see description of film perthite lamellae at Charlevoix, Chapter III). Blebs of albite, approximately 30 by 60μ and elongate parallel to the film perthite lamellae, make up 40-50% of the central portion of the alkali feldspar, decreasing in abundance towards the margin. The blebs are often connected by small stringers and joined to larger, irregular albitic patches on the grain boundaries. Although weak to moderate grid-twinning occurs in the K-feldspar (Plate III.1b), generally focussed at the ends of the perthite blebs, structural state determinations (three-peak method) show it to be orthoclase with less than maximum monoclinic ordering. This unit is petrographically distinct, particularly according to the mesoperthitic feldspar, from other gneisses in the Brent region, and is readily identified as the sub-crater unit penetrated by drill holes 1-59 and 1-67.

Dence (1968) established six zones of shock metamorphism of the basement gneisses in hole 1-59 (Fig. III.2) based on the relative

Plate III.1

a) Quartz, plagioclase and mesoperthitic alkali feldspar in quartz-plagioclase-mesoperthite-hornblende gneiss, outcropping 1.3km NW of the centre of Brent crater. Crossed polars.

b) Albite blebs and M-twinned potassic feldspar constituting grains of mesoperthite in sample shown in Plate III.1a. Crossed polars.

c) Shock-induced deformation twins trending NE in potassic feldspar. Sample from shock zone (vb), 886.1m, in basement gneisses beneath Brent crater. Crossed polars.

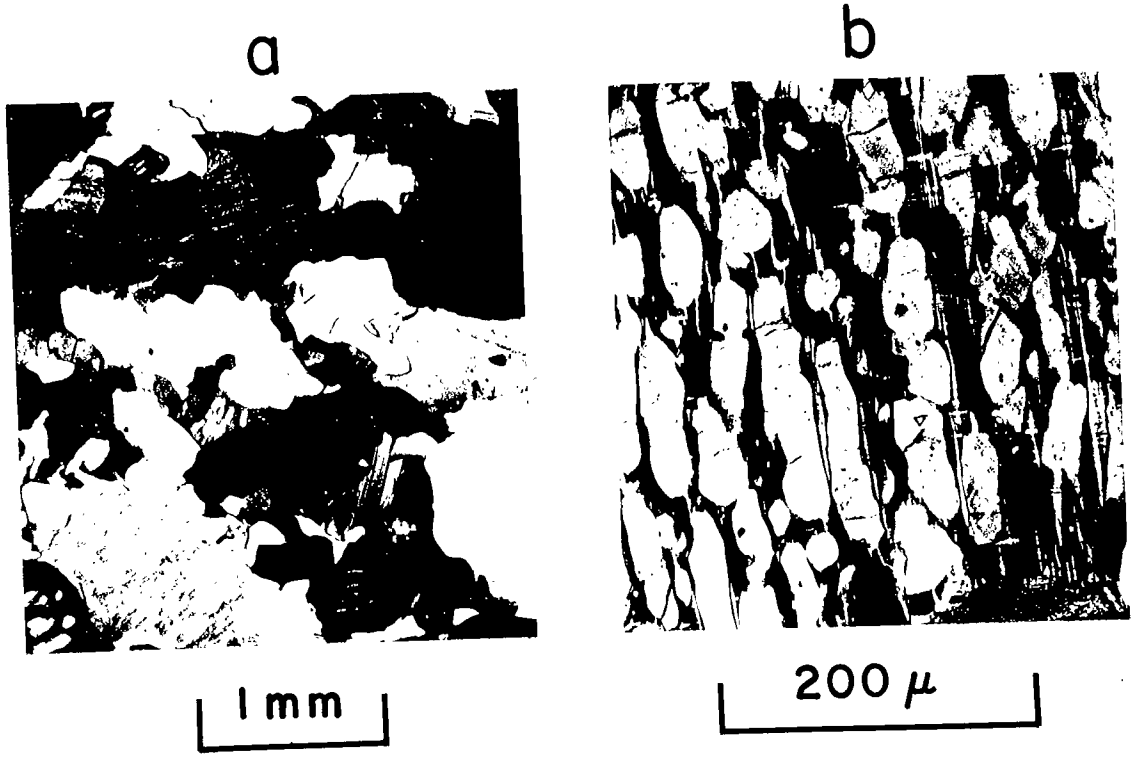
a
b
1 mm
200 μ
c
175 μ

degree of microscopic deformation in the various mineral components. Zone (i), in which grains are fractured, biotite shows kink bands, but planar deformation features are not developed in quartz or feldspar, lies deeper than 930m (3050 ft.). Above this level to 875m (2870 ft.), zones (ii) to (v) are distinguished by increasingly strong development of planar features in quartz (see Chapter II, "Levels of Shock Metamorphism Preserved"). Zone (vi) lies immediately below the melt layer and is characterized by "ductile deformation in the feldspars". Dence (1968) feels that various degrees of shock metamorphism are represented in this upper zone but are not always distinguishable due to the overriding thermal influence of the melt zone.

Most of the basement gneisses are pinkish-orange rocks transected by irregular greenish fractures, both colours deepening with increased shock deformation. The fractures contain brecciated mineral fragments in a fine-grained clastic or recrystallized matrix containing abundant green chlorite. A granular, dusty alteration of the feldspars imparts the pink or orange hues. This alteration is generally confined to one of the feldspar phases, but in some cases it is the K-feldspar, and in others it is plagioclase. Except for the alteration, the mesoperthite and plagioclase grains have a normal, unshocked appearance in zones (i) through (iii). Weak planar features in the K-feldspar plus strong fracturing of the perthitic albite become evident in zone (iv) and prominent in zone (v) rocks (Plate III.1c). Within zone (v) beginning at approximately 886.1m, K-feldspar develops patchy, irregular extinction and reduced birefringence, whereas the

Plate III.2

a) Mesoperthite grain from basement gneisses of shock zone (v), 881.8m, beneath Brent. Lighter coloured albite blebs have normal appearance whereas potassic feldspar has patchy, reduced birefringence, and has probably begun to recrystallize under the influence of thermal metamorphism. Crossed polars.

b) Mesoperthite grain from basement gneiss in shock zone (vi), 879.4m, beneath Brent. Although mesoperthitic texture is still weakly discernible, both albite (medium gray) and orthoclase (lightest gray) have recrystallized and begun to merge. Crossed polars.

a

200 μ

b

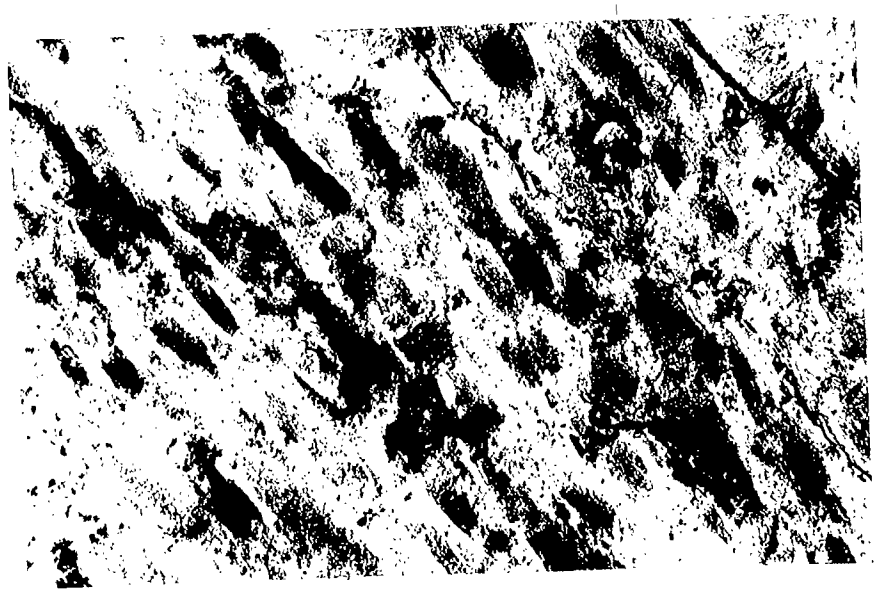

200 μ

perthitic albite retains normal optics. With increasing shock metamorphism (decreasing depth), the potassic feldspar passes gradually into a microcrystalline, recrystallized mosaic (Plate III.2a) with complete recrystallization of this phase at 881.5m. The film perthite lamellae have disappeared. Quartz in these rocks is also recrystallized, and incipient recrystallization of plagioclase grains and perthitic blebs becomes widespread about 1.5m higher. As recrystallization proceeds, the boundary between albite blebs and host K-feldspar becomes diffuse (Plate III.2b) although the two feldspars are still identifiable. With recrystallization the pinkish-orange alteration disappears, leaving a clear K-feldspar but plagioclase has a granular, brownish alteration which imparts a grayish-brown caste to the gneisses of zone (vi). Although recrystallization within zone (vi) is widespread, plagioclase can be identified by remnant twinning, and in rare cases the mesoperthite texture is preserved to a minor degree.

Compositions of feldspar phases in mesoperthite gneisses from beneath the crater were determined by electron microprobe analysis for SiO_2, Al_2O_3, K_2O, Na_2O and CaO (Tables III.2-III.4). In the five unshocked or least shocked samples representing shock zone (i) to weak zone (v) (1006.3, 893.4, 891.5, 889.7, and 887.9m), potassic feldspar, plagioclase in mesoperthite, and separate plagioclase grains each have very narrow compositional ranges both within samples and between samples. The potassic feldspar is orthoclase, Or_{91-96}, in mesoperthitic growth with albite, Ab_{92-98}. Separate grains of albite are Ab_{91-98}. In general, the separate plagioclase grains are very slightly the more

Table III.2 Composition of potassic feldspar (wt %)in basement gneisses beneath the Brent crater (drill hole 1-59)

depth(m)	sample	SiO_2	Al_2O_3	CaO	Na_2O	K_2O	total	Or	Ab	An	Z-group	Y-group	Shock Zone
1006.3	1	64.4	18.8	0.0	0.9	16.4	100.5	92.2	7,8	0.0	15.976	4.178	(i)
	2	64.6	18.7	0.0	0.9	15.8	100.0	91.9	8.1	0.0	16.005	4.058	
	3	65.2	18.7	0.0	1.4	15.1	100.4	88.0	12.0	0.0	16.002	4.027	
	4	64.8	18.7	0.0	0.9	15.8	100.2	91.8	8.2	0.0	16.004	4.047	
893.4	1	63.0	19.8	0.03	0.7	16.2	99.7	94.0	5.8	0.2	16.062	4.085	(iii)
	2	63.8	19.6	0.03	0.5	16.0	99.9	95.0	4.9	0.2	16.072	3.977	
	3	64.8	19.4	0.01	0.6	16.1	95.0	95.0	4.9	0.1	16.059	3.955	
	4	63.6	19.4	0.01	0.6	15.9	99.5	94.5	5.4	0.1	16.067	3.979	
891.5	1	64.0	19.0	0.5	0.7	15.2	99.4	91.7	6.0	2.3	16.034	3.932	(iv)
	2	64.2	18.7	0.3	0.6	15.5	99.3	92.8	5.5	1.7	16.018	3.962	
	3	64.6	18.8	0.2	0.6	15.7	99.9	93.9	5.2	0.9	16.029	3.950	
	4	65.1	19.1	0.1	0.7	15.5	100.5	93.1	6.2	0.7	16.053	3.887	
889.7	1	63.1	19.4	0.1	0.9	15.6	99.1	91.4	8.0	0.6	16.050	4.051	(iv)
	2	63.4	19.4	0.03	0.4	16.1	99.3	96.0	3.9	0.2	16.063	3.998	
	3	62.4	18.3	0.08	0.4	15.8	96.9	95.6	4.0	0.4	16.016	4.032	
	4	61.6	18.4	0.06	0.4	15.9	96.3	96.4	3.3	0.3	16.028	4.039	
887.9	1	63.1	19.1	0.03	0.7	15.6	98.5	93.3	6.6	0.2	16.052	3.998	(va)
	2	63.4	18.7	0.01	0.7	15.5	98.3	93.4	6.5	0.1	16.041	3.966	
	3	65.6	19.2	0.01	0.8	15.4	101.0	92.7	7.3	0.1	16.062	3.869	
	4	65.0	19.0	0.1	0.8	15.3	100.2	92.0	7.5	0.5	16.046	3.903	
886.1	1	65.4	19.4	0.1	1.5	14.0	100.4	85.2	14.1	0.7	16.074	3.833	(vb)
	2	65.1	19.4	0.2	1.6	13.9	100.2	84.1	15.1	0.9	16.071	3.853	
	3	65.3	19.5	0.01	1.6	14.2	100.6	85.6	14.3	0.1	16.086	3.849	
	4	64.0	19.5	0.1	1.2	14.9	99.7	88.7	10.8	0.6	16.066	3.953	
883.6	1	64.9	18.7	0.0	2.1	13.2	98.9	80.9	19.1	0.0	16.058	3.842	(vb)
	2	63.9	18.8	0.04	0.6	13.5	96.8	93.7	6.0	0.2	16.179	3.448	
	3	63.0	18.5	0.06	1.8	13.2	96.5	82.5	17.2	0.3	16.064	3.861	
	4	61.5	19.6	0.0	0.8	15.1	97.0	92.7	7.3	0.0	16.112	3.957	
881.8	1	63.4	19.8	0.4	1.9	13.1	98.6	80.3	17.6	2.1	16.103	3.848	(vc)
	2	64.1	19.9	0.5	2.2	12.6	99.3	77.0	20.2	2.8	16.093	3.828	
	3	64.1	19.2	0.5	1.9	12.9	98.6	79.2	18.1	2.7	16.063	3.836	
	4	64.7	19.6	0.2	1.8	13.6	99.9	82.3	16.8	0.9	16.089	3.847	
880.3	1	65.9	19.5	0.1	3.9	9.3	98.7	60.5	38.7	0.8	16.149	3.559	(vc)
	2	64.9	19.3	0.3	3.9	9.5	97.9	60.9	37.6	1.5	16.111	3.676	
	3	66.2	19.5	0.2	3.2	10.2	99.3	66.8	32.0	1.2	16.142	3.544	
	4	65.8	19.0	0.2	4.0	9.1	98.1	59.5	39.7	0.8	16.128	3.555	
866.3	1	66.1	18.6	0.01	5.7	7.9	98.3	47.6	52.4	0.1	16.035	3.852	(vi)
	2	66.3	19.2	0.07	6.6	7.3	99.4	42.1	57.6	0.3	16.022	3.973	
	3	65.4	18.9	0.03	6.4	7.8	98.5	44.7	55.1	0.1	15.994	4.074	
	4	66.0	18.7	0.01	6.3	8.3	99.3	46.3	53.7	0.1	15.959	4.154	
	5	66.4	18.7	0.06	6.6	7.3	99.0	42.0	57.7	0.3	15.991	4.008	

Table III.3 Composition of plagioclase phase (wt %) in mesoperthites in basement gneisses beneath the Brent crater (drill hole 1-59)

depth(m)	sample	SiO_2	Al_2O_3	CaO	Na_2O	K_2O	total	Or	Ab	An	Z-group	Y-group	Shock Zone
1006.3	1	66.0	22.4	1.4	11.2	0.07	101.0	0.4	93.0	6.6	16.068	4.044	(i)
	2	67.6	22.0	1.5	11.1	0.05	102.2	0.3	92.8	6.9	16.049	3.983	
	3	66.1	22.1	1.4	11.0	0.08	100.6	0.5	92.9	6.7	16.070	3.995	
	4	68.3	21.8	1.7	11.1	0.06	102.9	0.3	92.0	7.7	16.019	3.997	
893.4	1	67.0	22.1	1.2	10.7	0.07	101.0	0.4	93.7	5.9	16.116	3.821	(iii)
	2	68.1	21.5	1.3	10.8	0.06	101.7	0.3	93.6	6.0	16.066	3.858	
	3	67.5	21.8	1.1	10.9	0.06	101.3	0.3	94.3	5.4	16.088	3.877	
	4	68.9	20.8	0.6	10.9	0.07	101.2	0.4	96.8	2.8	16.092	3.745	
891.5	1	65.7	21.3	1.1	11.2	0.2	99.5	1.1	93.8	5.1	16.038	4.077	(iv)
	2	66.4	21.5	1.0	10.9	0.5	100.3	2.6	92.7	4.7	16.067	3.977	
	3	65.7	21.8	1.4	11.0	0.2	100.1	1.2	92.2	6.6	16.048	4.054	
	4	67.3	21.5	0.8	11.6	0.2	101.4	1.2	95.0	3.8	16.039	4.08	
889.7	1	69.1	20.6	0.5	11.3	0.1	101.6	0.7	97.1	2.1	16.049	3.890	(iv)
	2	66.1	20.2	0.5	10.7	0.1	97.6	0.7	97.0	2.3	16.088	3.814	
	3	67.9	19.9	0.7	11.6	0.2	100.3	1.0	96.0	3.0	15.972	4.093	
	4	67.2	20.4	0.7	10.8	0.2	99.3	0.9	95.8	3.3	16.066	3.845	
887.9	1	65.7	20.3	0.3	11.6	0.3	98.2	1.7	97.1	1.3	16.020	4.141	(Va)
	2	64.2	19.8	0.3	11.2	0.4	95.9	2.0	96.4	1.6	16.017	4.128	
	3	68.01	20.5	0.2	12.9	0.3	101.9	1.4	97.9	0.7	15.935	4.407	
	4	68.6	20.9	0.3	11.5	0.3	101.6	1.5	97.2	1.3	16.062	3.941	
883.6	1	65.4	21.6	0.9	10.9	0.6	99.4	3.3	92.4	4.3	16.071	4.052	(Vb)
	2	63.2	19.2	0.3	3.9	10.2	96.8	62.4	36.4	1.3	16.074	3.896	
	3	62.5	20.1	0.4	7.8	3.9	94.7	24.1	73.8	2.2	16.122	3.853	
	4	64.6	19.8	0.4	4.8	8.6	98.2	53.0	44.9	2.1	16.094	3.807	
881.8	1	67.1	20.3	0.8	9.4	1.3	98.9	7.7	88.2	4.1	16.105	3.666	(Vc)
880.3	1	63.8	20.1	0.7	8.4	2.9	95.9	18.0	78.6	3.4	16.107	3.804	(Vc)
	2	63.9	19.0	0.4	4.2	8.1	95.6	54.4	43.1	2.5	16.136	3.558	
	3	64.8	20.0	0.7	4.7	8.2	98.4	51.8	44.6	3.6	16.119	3.687	

Table III.4 Composition of plagioclase (wt %) in basement gneisses beneath the Brent crater (drill hole 1-59)

depth (m)	Sample	SiO_2	Al_2O_3	CaO	Na_2O	K_2O	total	Or	Ab	An	Z-group	Y-group	Shock Zone
1006.3	1	66.6	22.8	1.6	10.8	0.2	102.0	1.0	91.5	7.6	16.097	3.938	(i)
	2	67.0	22.0	1.3	11.3	0.05	101.6	0.3	93.8	6.0	16.051	4.032	
	3	66.2	22.6	1.7	10.7	0.2	101.4	0.9	91.2	8.0	16.093	3.928	
	4	67.0	22.0	1.3	11.8	0.07	102.1	0.4	93.9	5.7	16.012	4.180	
	5	66.7	21.9	1.5	10.9	0.07	101.0	0.4	92.5	7.1	16.056	3.968	
893.4	1	66.7	21.1	1.2	10.4	0.1	99.5	0.6	93.5	6.0	16.084	3.800	(iii)
	2	68.1	21.6	1.3	11.0	0.1	102.1	0.7	93.4	5.9	16.059	3.902	
	3	69.1	20.4	0.3	11.3	0.1	101.2	0.7	97.8	1.5	16.054	3.865	
	4	68.0	20.9	1.2	10.9	0.08	101.0	0.5	94.1	5.5	16.037	3.904	
891.5	1	66.7	22.6	2.2	10.2	0.2	101.9	1.3	88.1	10.7	16.082	3.852	(iv)
	2	64.6	22.1	1.7	10.3	0.2	98.9	1.3	90.5	8.1	16.101	3.908	
	3	67.0	21.9	1.4	11.2	0.2	101.7	1.0	92.4	6.6	16.032	4.067	
	4	66.5	21.2	0.9	10.9	0.1	99.6	0.8	95.0	4.2	16.085	3.896	
889.7	1	68.6	20.4	0.8	10.9	0.1	100.8	0.8	95.5	3.7	16.046	3.838	(iv)
	2	69.3	20.7	0.9	10.9	0.2	102.0	1.1	94.6	4.2	16.046	3.832	
	3	68.1	20.7	1.0	10.8	0.2	100.8	1.4	93.8	4.9	16.046	3.861	
	4	68.7	20.7	0.6	11.1	0.2	101.3	1.1	95.9	3.0	16.057	3.865	
887.9	1	63.3	20.5	0.5	11.7	0.1	96.1	0.7	96.9	2.4	16.007	4.297	(va)
	2	66.1	20.0	0.6	11.6	0.2	98.5	1.0	96.3	2.6	15.983	4.157	
	3	65.7	20.7	0.6	11.5	0.1	98.6	0.7	96.6	2.7	16.036	4.097	
	4	66.4	20.8	0.6	11.4	0.1	99.3	0.4	96.9	2.7	16.051	4.021	
886.1	1	68.7	22.4	0.9	11.2	0.2	103.4	1.1	94.7	4.3	16.110	3.872	(vb)
	2	67.4	22.7	0.8	11.1	0.3	102.3	1.4	94.8	3.8	16.142	3.877	
	3	66.6	22.4	1.0	10.7	0.4	101.1	2.0	93.0	5.0	16.131	3.858	
	4	66.9	21.8	0.9	11.2	0.2	101.0	1.1	94.6	4.3	16.078	3.977	
883.6	1	65.2	20.0	0.4	8.6	3.9	98.1	22.7	75.4	1.9	16.049	3.989	(vb)
	2	65.5	21.7	1.4	10.6	0.5	99.7	2.8	90.6	6.6	16.060	4.004	
	3	64.9	21.3	0.9	10.5	0.6	98.2	3.4	92.4	4.3	16.089	3.955	
881.8	1	67.3	21.3	0.9	10.6	0.9	101.0	5.0	90.9	4.1	16.071	3.923	(vc)
	2	64.8	21.3	0.9	10.7	0.9	98.6	4.9	91.1	4.0	16.066	4.054	
	3	66.8	20.0	0.6	4.8	9.5	101.7	55.2	42.1	2.7	16.050	3.882	
	4	65.7	20.4	0.8	8.8	3.0	98.7	17.4	78.7	3.9	16.062	3.894	
	5	68.4	21.4	1.1	10.3	0.8	102.0	4.8	89.8	5.4	16.075	3.821	
	6	66.3	20.6	0.7	10.5	0.6	98.7	3.7	92.9	3.4	16.069	3.898	
	7	65.8	20.9	0.7	11.2	0.5	99.1	2.9	94.0	3.2	16.031	4.114	
880.3	1	62.5	20.4	1.0	6.7	4.8	95.4	30.3	64.6	5.1	16.136	3.755	(vc)
	2	61.3	20.3	0.4	4.6	7.8	94.4	51.4	46.5	2.1	16.195	3.602	
	3	62.8	19.8	0.5	5.4	6.4	94.9	42.7	54.8	2.6	16.177	3.588	

(cont'd)

Table III.4 (cont'd)

depth (m)	Sample	SiO_2	Al_2O_3	CaO	Na_2O	K_2O	total	Or	Ab	An	Z-group	Y-group	Shock Zone
879.3	1	63.1	20.4	1.3	5.5	4.5	94.8	32.2	60.1	7.8	16.235	3.290	(vc)
	2	63.8	19.8	0.7	7.7	2.9	94.9	19.0	77.2	3.9	16.148	3.602	
	3	63.8	20.8	1.0	5.7	4.3	95.6	30.8	63.1	6.1	16.268	3.240	
	4	63.3	18.4	0.7	5.0	6.1	94.5	42.9	53.3	3.8	16.181	3.434	
878.4	1	66.2	21.0	1.1	10.4	1.0	99.7	5.6	89.1	5.3	16.041	3.989	(vc)
	2	65.8	19.2	2.6	9.9	2.6	100.1	13.0	76.0	11.0	15.755	4.514	
	3	66.4	20.3	0.7	7.9	5.1	100.4	28.8	68.1	3.2	16.032	3.987	
	4	68.1	20.5	1.0	9.8	1.5	100.9	9.0	86.4	4.7	16.054	3.812	
876.0	1	65.6	21.0	2.0	2.8	9.5	100.9	61.5	27.8	10.8	16.132	3.506	(vc)
	2	61.9	18.4	0.3	1.3	19.9	101.8	89.9	9.0	1.1	15.682	5.292	
	3	65.0	19.2	0.5	2.5	12.0	99.2	73.6	23.7	2.7	16.060	3.810	

calcic of the two coexisting albite phases.

In the more highly shocked rocks, from 886.1m to the base of zone (vi), compositional changes in the feldspars are evident and become more pronounced with increasing level of shock metamorphism. A broad compositional range within samples is shown in each phase; the K-feldspar phase becomes progressively more sodic and the plagioclases progressively more potassic. Potassic feldspar at 880.3m, the most highly shocked sample in which original mesoperthite texture is generally discernible, is sodic orthoclase, approximately Or_{60} (Fig. III.3a). Within the same grains, and in samples from 1.5m and 3.3m lower, the pre-alteration albitic phase has compositions ranging from $An_4Ab_{93}Or_3$ to $An_1Ab_{36}Or_{63}$ (Fig. III.3b). Similarly, in these three samples, and in three others in the overlying 4.3m, grains separate from the mesoperthites, with remnant polysynthetic albite twinning, possess compositions spanning the range $An_4Ab_{93}Or_3$ to $An_1Ab_9Or_{90}$ (Fig. III.3c). In general, with diminishing depth, analyses of all three feldspars become poorer as shown by total oxides and deviations from feldspar stoichiometry, particularly in the Y-group cations (Tables III.2-III.4). It is likely that the poor stoichiometry results from poor analyses in some cases, but there are several grains which are poorly stoichiometric in spite of good total oxide values.

Feldspar was analyzed in one sample (866.3m) from zone (vi), approximately 12m below the layer of igneous rocks. This rock consists of a matrix of mainly feldspar laths in a radiating or felted texture (Plate III.3a), with minor interstitial quartz. There is apparently only

Fig. III.3

Compositions, determined by electron-microprobe, of feldspar in fractured gneisses beneath the Brent crater. a) potassic feldspar in mesoperthites; b) sodic feldspar in mesoperthites; c) individual plagioclase grains. Numbers refer to sample depth in metres in drill hole 1-59.

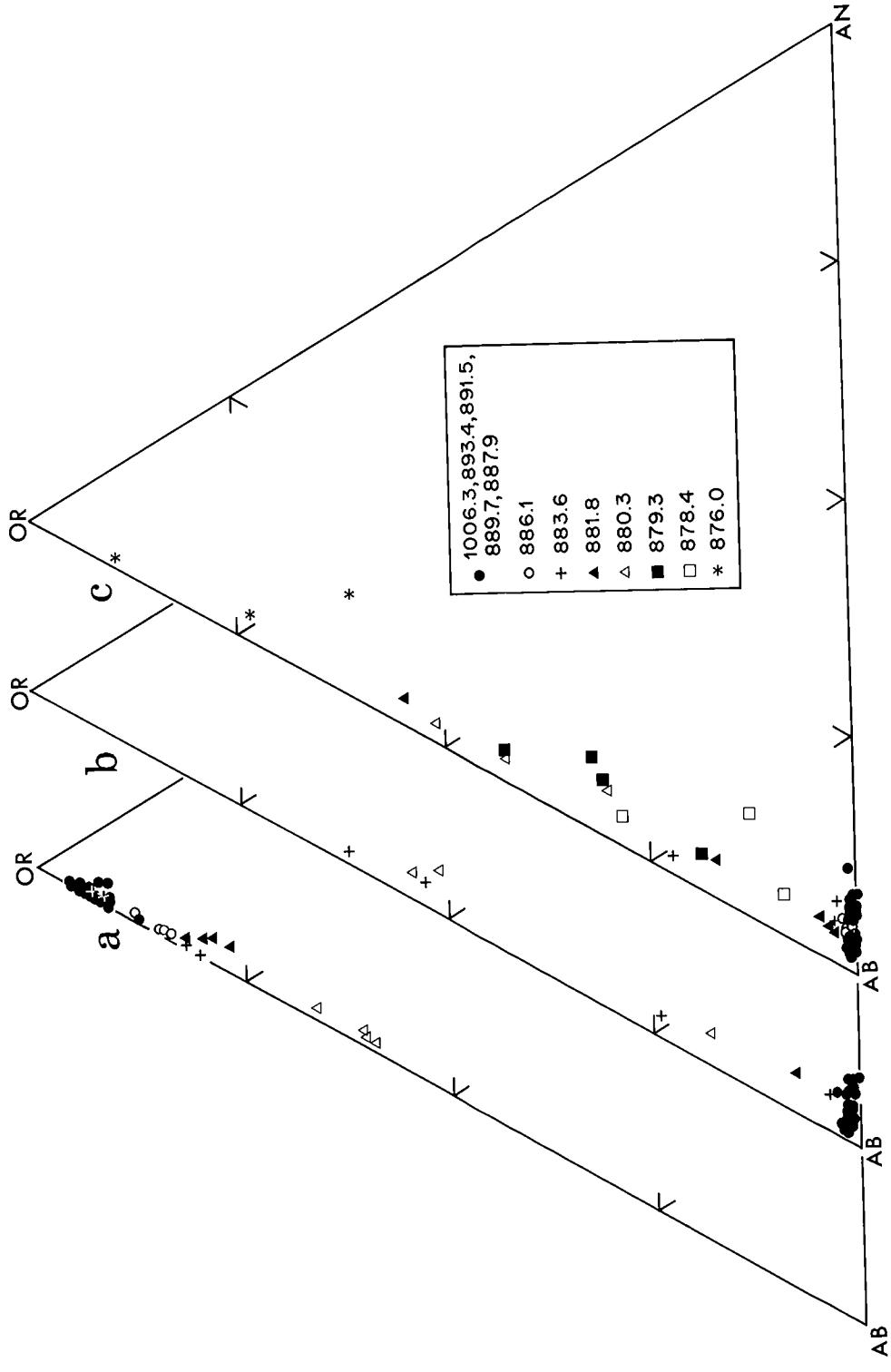
AN
OR
OR
OR
AB
AB
AB
a
b
c
1006.3,893.4,891.5, 889.7,887.9
886.1
883.6
881.8
880.3
879.3
878.4
876.0

Plate III.3

a) Recrystallized matrix of anorthoclase in thermally metamorphosed basement gneiss beneath the Brent crater, shock zone (vi), 866.3m. Crossed polars.

b) Diffuse remnant of thermally metamorphosed, shocked amphibole in sample from 866.3m beneath Brent. High shock pressures have caused thermal decomposition to an oxide and perhaps another amphibole. Subsequent thermal metamorphism has created an aggregate of an opaque, pyroxene, and two unidentified phases. Crossed polars.

a

700 μ

b

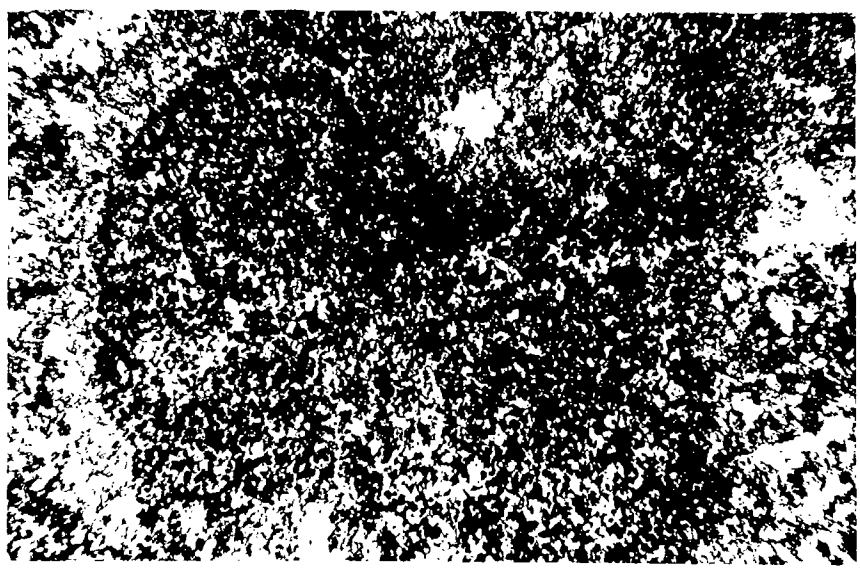

500 μ

one feldspar forming stubby, simply-twinned laths approximately 0.2mm long. Irregular amoeba-like, dark patches (Plate III.3b), 0.5 to 1mm, comprise an aggregate of opaques, a brown sheet silicate, green amphibole (?), and colourless plagioclase (?), each as equant 10-15μ grains. The petrography, and comparison with obvious recrystallized xenoliths in the overlying melt layer, suggest that this rock is a partially melted basement gneiss. Quartz and feldspars were melted at least to the point where a single feldspar recrystallized, and the dark, irregular patches are remnant amphiboles, not melted but thermally broken down into the four-phase aggregate. Analyses show the feldspar to be anorthoclase with a narrow compositional range, Or_{42-48} (Fig. III.4), and good feldspar stoichiometry (Table III.2).

The changes in feldspar chemistry, described above, are detected first in K-feldspar at approximately 886.1m, the same level at which petrographic changes in this feldspar were noted. Similarly the distinct compositional changes in plagioclase at approximately 883.6m correspond to beginnings of albite recrystallization. As recrystallization becomes more complete and widespread, compositional variations are more pronounced.

III.4 Discussion

The compositions of feldspars in gneisses from shock zones (v) and (vi) beneath the melt layer are different from those in weakly shocked or unshocked gneisses at greater depths below the Brent crater. In general, above the 886.1m level the K-feldspar becomes progressively

Fig. III.4

Compositions, determined by electron microprobe, of unmixed anorthoclase rim from feldspars in the melt layer, Brent crater (solid triangles). Compositions lie in shaded area of the smaller, complete feldspar triangle. Recrystallized feldspar in hornfelsed basement gneiss (sample 886.3m) is plotted as open triangles.

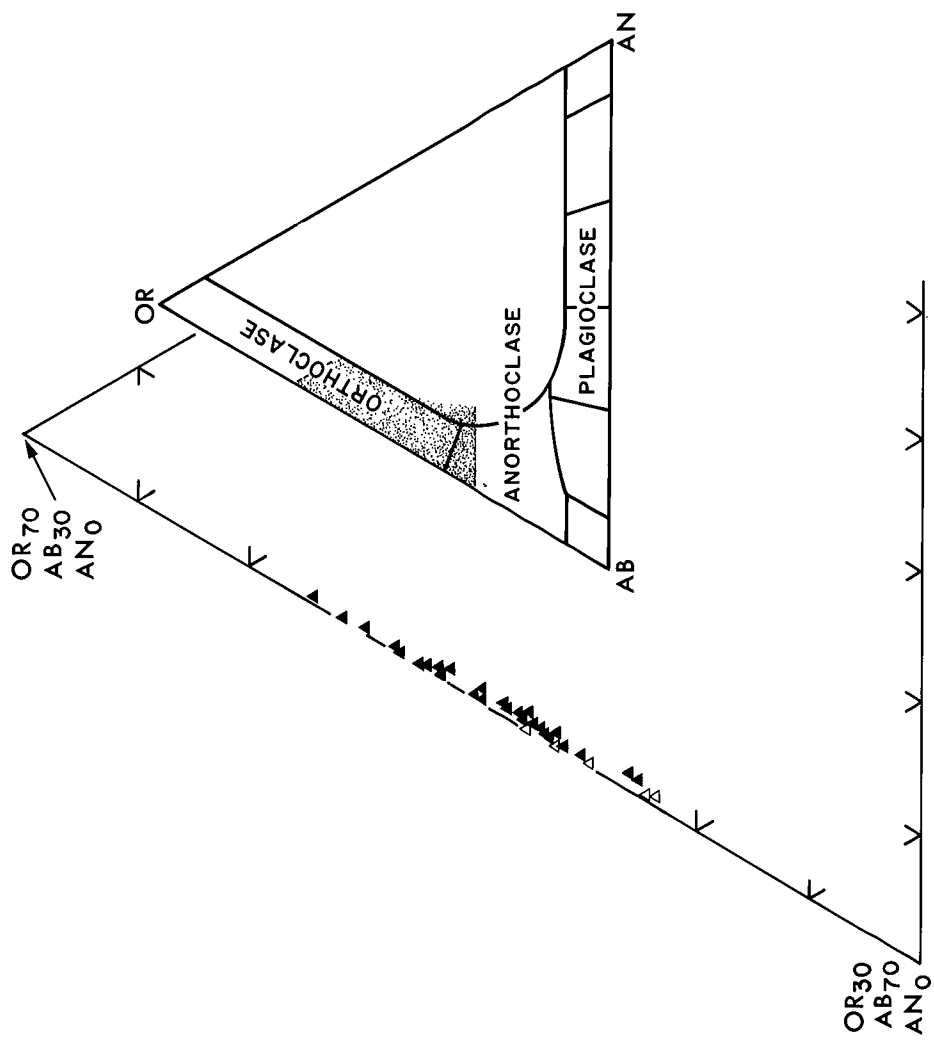
AN
OR
ORTHOCLASE
ANORTHOCLASE
PLAGIOCLASE
AB
OR 70
AB 30
AN 0
OR 30
AB 70
AN 0

more sodic with decreasing depth, and albites in mesoperthite or as separate grains become increasingly more potassic above the 883.6m level. A spread of compositions, which widens with increasing degree of shock metamorphism, is particularly evident in the albites and to a lesser degree in the K-feldspar. However, all three feldspars trend towards a composition of approximately Or_{40-60} (Ab_{60-40}). The initial compositional changes coincide with incipient recrystallization of the feldspars and become more pronounced as the degree of recrystallization progresses. The implication is that as the feldspars recrystallize they tend to homogenize, attempting to achieve equilibrium under metamorphic conditions. In the one instance recorded, sample 866.3m, complete recrystallization has occurred and this has resulted in a single homogeneous feldspar of composition Or_{42-48} (Ab_{58-52}).

The phrase "increasing degree of shock metamorphism" has been used synonymously with "decreasing depth" or "nearness to the melt rocks". Such usage is no doubt valid throughout shock zones (i) to (iv). In these rocks the only visible changes are the formation of planar deformation features in quartz and feldspars. These characteristic features of shock deformation become stronger and more abundant in passing upward through these zones, following the scheme of progressive development outlined by Robertson et al. (1968). Thus, below approximately 887m, elevated shock pressures have been the dominant factor producing the deformation typical of these rocks. According to Dence's (1968) description of the planar features in quartz, shock pressures at the top of zone (iv) may have been approximately 200±25kb.

Zone (v) and particularly zone (vi), however, do not strictly follow the paths of progressive shock metamorphism described in studies of material from other large meteorite craters. Although the development of planar deformation features in quartz and feldspar does increase to levels indicative of moderately high shock pressures (approximately 300kb), the subsequent stages, such as formation of diaplectic glasses, partial melting, and development of planar features in amphibole, cannot be found. The highest recognizable grade of shock metamorphism occurs in some plagioclase grains where one set of albite twin lamellae comprises a microcrystalline growth of perhaps chlorite, interpreted as an alteration product of maskelynite.

Evidence for thermal metamorphism, however, is prominent in the tectosilicates of zone (v), and appears to be the dominant effect in zone (vi) rocks. Thermal effects become stronger as the melt layer is approached, and therefore the rocks of zone (vi) and partly of zone (v) are believed to lie in an aureole of thermal metamorphism surrounding the melt layer. Such an interpretation agrees with Dence's (1968) views, although he didn't extend the thermal aureole into zone (v).

An estimate of temperatures in the thermal aureole can be based on metamorphic assemblages. Some difficulty is encountered in trying to separate the original metamorphic character of the gneisses from the effects of shock metamorphism, subsequent thermal metamorphism, and retrograde effects. At the base of the melt layer, approximately 853m, where obvious xenoliths or fractured basement rocks are more abundant than the matrix of impact melt, an assemblage characteristic

of the pyroxene-hornfels (or K-feldspar-cordierite-hornfels) facies has developed. These rocks comprise a single feldspar, presumably anorthoclase or sodic orthoclase, minor quartz, and aggregates of poorly formed, light green clinopyroxene and opaque minerals. Original opaque minerals and apatite are often present along remnant gneissic bands. Xenoliths of mafic rocks are completely converted to a feldspar-pyroxene assemblage. Although the boundary is indistinct, below the 868m level the pyroxene-hornfels assemblage is replaced by minerals of the hornblende-hornfels facies with poorly formed amphibole and biotite as the mafic minerals, and original feldspars recognizable. This facies persists into the upper limits of zone (v), below which no newly-formed metamorphic minerals are found.

According to Turner (1960, Fig. 8-6) the pyroxene-hornfels facies occurs over the range 575-675°C at shallow depths. He also states that temperatures at contacts of granitic plutons are normally 500 to 550°C. At similarly low pressures the hornblende-hornfels facies occurs over the range 320-575°C. Thus, maximum metamorphic temperatures beneath the melt layer were probably in the neighbourhood of 600-650°C, decreasing to approximately 300-350°C at the base of the detectable thermal aureole. Levels of shock metamorphism at the base of zone (vi) indicate pressures of approximately 350kb, also resulting in post-shock temperatures near 300°C (Stöffler, 1971a, Table 2).

In summary, the changes in feldspar composition in shock zones beneath the Brent crater occur as a result of solid state recrystallization due to thermal metamorphism from the overlying layer of impact melt. These changes are therefore only indirectly

related to shock metamorphism and do not reflect shock behaviour of feldspars subjected to pressures greater than 350kb. The possibility of variation in feldspar chemistry at higher pressures is not ruled out, however, but at Brent the thermal metamorphism has obliterated or obscured the effects of high level shock metamorphism.

Do the compositional adjustments provide data pertinent to theories of the melt rock genesis or its potassium enrichment? There is little direct evidence to support either impact melting or later, unrelated intrusion suggested by Dence and Currie, respectively. However, analyses of feldspar in the melt layer show it to be sodic orthoclase of the same composition as the homogenized feldspar in zone (vi) (Fig. III.4, Table III.5). This may be coincidental, considering the similar bulk compositions of the country rocks and the melt layer, but on the other hand there is a strong compulsion to believe that homogenization of the country rock feldspars, by thermal metamorphism in one case and by shock melting in the other, led to similar recrystallized products. At any rate, the similarity of the two feldspars in no way detracts from the impact melt hypothesis.

Potassium enrichment of the melt relative to the country rocks cannot be correlated with behaviour of alkalis in the feldspars of the shocked gneisses. It was believed at one time that preferential partial melting of potassic feldspars could enrich the melt in potassium. Although there is definite migration of alkalis in the gneisses of zone (vi), the feldspars are not apparently depleted in potassium or enriched in sodium. If Currie's hypothesis is true that alkali

Table III.5 Composition of unmixed feldspars (wt %) in the melt layer, Brent crater (drill hole 1-59)

depth(m)	Sample	SiO_2	Al_2O_3	CaO	Na_2O	K_2O	total	Or	Ab	An	Z-group	Y-group
827.8	1	66.4	19.5	0.1	5.9	8.9		49.6	49.9	0.5	16.005	4.080
	2	65.9	19.0	0.01	5.5	9.5		53.2	46.8	0.1	15.980	4.130
	3	66.1	19.4	0.01	5.4	9.1		52.2	47.7	0.1	16.032	3.988
	4	65.5	18.6	0.01	5.1	9.8		55.9	44.1	0.1	15.984	4.071
	5	65.7	19.2	0.1	6.2	8.7		47.9	51.6	0.5	15.973	4.186
830.0	1	65.8	19.1	0.1	5.5	8.9		51.1	48.3	0.5	16.015	4.009
	2	66.7	19.7	0.2	6.0	8.3		47.5	51.8	0.7	16.032	3.976
	3	66.7	19.2	0.1	5.8	8.4		48.6	50.9	0.5	16.018	3.966
	4	66.3	19.2	0.1	6.6	7.7		43.1	56.2	0.7	15.986	4.104
	5	65.7	18.7	0.1	4.7	9.5		57.1	42.6	0.4	16.029	3.886
840.6	1	63.7	18.6	0.1	5.3	8.7		51.6	48.1	0.3	16.018	4.019
	2	64.2	18.5	0.04	5.3	8.7		51.6	48.2	0.2	16.018	3.980
	3	63.4	18.4	0.04	5.2	9.7		54.9	44.9	0.2	15.959	4.227
	4	63.7	18.7	0.04	5.0	8.9		53.5	46.3	0.2	16.041	3.952
845.2	1	65.8	19.5	0.1	6.4	7.4		42.7	56.7	0.6	16.036	3.983
	2	66.3	19.2	0.1	6.1	8.2		46.7	53.0	0.3	16.005	4.036
	3	66.1	19.2	0.1	5.9	7.9		46.4	53.1	0.5	16.038	3.920
	4	66.1	18.9	0.1	6.4	8.0		45.2	54.5	0.4	15.979	4.100
848.3	1	64.6	18.5	0.04	5.5	8.3		49.5	50.3	0.2	16.024	3.945
	2	64.3	18.7	0.1	5.8	8.0		47.4	52.3	0.3	16.017	4.005
	3	64.6	18.9	0.1	5.6	7.9		47.8	51.8	0.4	16.052	3.887
	4	64.6	18.8	0.03	6.1	7.9		46.1	53.8	0.2	16.015	4.025
853.4	1	66.4	18.6	0.01	5.5	9.2		52.4	47.6	0.1	15.981	4.038
	2	65.2	18.7	0.1	5.7	8.7		49.8	49.9	0.3	15.989	4.082
	3	65.8	18.6	0.1	6.2	8.4		47.0	52.6	0.4	15.958	4.137
	4	66.2	18.9	0.1	6.3	8.4		46.5	53.2	0.3	15.961	4.159
	5	65.0	18.5	0.1	6.1	8.8		48.5	51.1	0.3	15.938	4.246

fenitization of the country rocks has occurred due to metasomatism from the alkalic melt, evidence should be found in the feldspars of zone (vi). Again there is no evidence in these rocks for relative enrichment in sodium or potassium.

The study of feldspar compositions in gneisses beneath Brent therefore have established that chemical adjustments occurred as a necessary consequence of thermal metamorphism, but the data do not provide much evidence in support or rejection of theories of melt rock genesis or potassium enrichment.

The study has, however, provided new insight into a problem briefly mentioned in Chapter II. The structural state of feldspars at Charlevoix was determined, among other ways, from their optic axial angle—composition relationships (Fig. II.5). Sample 94 was not plotted because the wide spread of compositions from this rock make the mean value of little significance. Analysis of fifty grains yielded compositions from Or_{17} to Or_{85}. To determine whether poor or borderline analyses may have been the cause of this spread, only those data were selected for which oxides totalled 100±2% and with Y- and Z-group stoichiometry values of 4.0±0.1 and 16.0±0.1 respectively (based on 32 oxygens). The compositional spread was verified by these ten analyses (Table III.6, Fig. III.5) of feldspars from Or_{23} to Or_{63}. In contrast, for sixteen other samples for which several good analyses were available, a spread of less than 10% Or-content exists in eleven, and in the other five removal of one anomalously low value in each case diminishes the spread to well below 10%. Unshocked, weakly shocked, and highly shocked rocks are included in the sixteen.

Table III.6 Composition of alkali feldspar (wt %) in sample MBP94, Mont des Éboulements, Charlevoix crater.

grain	SiO_2	Al_2O_3	CaO	Na_2O	K_2O	total	Or	Ab	An	Z-group	Y-group
94.30	67.5	20.5	1.0	8.6	4.1	101.7	22.8	72.6	4.7	16.005	4.007
94.50	66.2	20.1	0.1	8.0	5.2	99.6	29.6	70.1	0.3	16.062	3.975
94.2.01	65.3	19.6	0.3	5.8	8.1	99.1	47.0	51.5	1.6	16.038	3.986
94.2.02	66.1	19.4	0.7	6.5	6.9	99.6	39.7	57.2	3.2	16.006	3.970
94.5.02	64.5	18.8	0.4	4.0	10.8	98.5	63.1	35.1	1.8	15.992	4.042
94.7.02	64.8	19.4	2.2	5.3	7.5	99.2	43.2	46.3	10.5	15.929	4.014
94.8.02	65.4	19.6	1.0	5.8	8.1	99.9	45.4	49.7	4.9	15.972	4.082
94.9.01	65.8	19.5	0.5	5.2	9.2	100.2	52.4	45.1	2.4	15.998	4.045
94.9.02	66.9	19.2	0.4	5.1	9.3	100.9	53.5	44.4	2.1	15.997	3.967
94.10.01	66.1	18.7	0.4	4.7	9.5	99.4	55.9	42.1	2.0	15.995	3.943

Fig. III.5

Compositions of alkali feldspars, determined by electron microprobe, within sample MBP 94, Charlevoix crater. The wide range, Or_{23} to Or_{63}, reflects incomplete homogenization under conditions of thermal metamorphism.

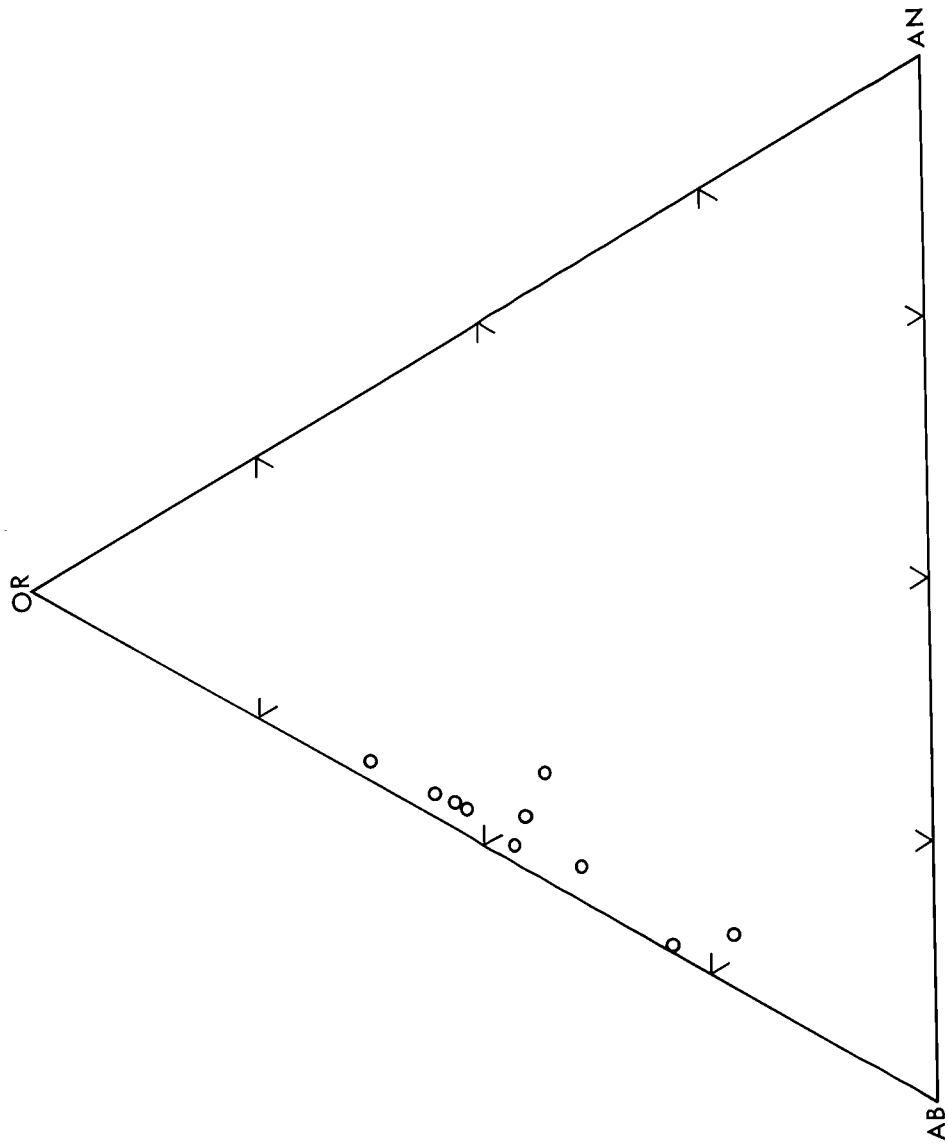
AN
OR
AB

The alkali feldspar of sample 94 is not visibly perthitic, nor does it show any evidence of recrystallization. Plagioclase in this rock, however, is almost completely recrystallized to a microcrystalline mosaic in which sinuous bands or sworls revealed at extinction suggest mobility (Plate II.1b). Remnant albite twinning is commonly visible. These grains are interpreted as having been converted, in large part, to diaplectic glass (maskelynite), and having subsequently recrystallized. The occurrence of maskelynite at most craters is generally as fresh, dense glass or, as described at Brent, glass altered to clay or chlorite minerals. Such textures seem characteristic of relatively rapid cooling, whereas the texture of recrystallized plagioclase at Charlevoix suggests that recrystallization has occurred under at least moderate temperatures maintained for some duration. It is unlikely that post-shock temperatures, estimated at 260°C (Table II.2) were high enough, or retained long enough to be the thermal influence. Another source must be sought.

The studies at Brent suggest that an overlying melt body at Charlevoix, now eroded, could have thermally metamorphosed the underlying shocked rocks. Alkali feldspar, perthitic in unshocked samples, began to homogenize in an attempt to adjust to metamorphic conditions, but complete homogenization was not achieved. Analyses by electron microprobe, although on spots from different grains, actually reveal the inhomogeneity within grains. Two or three outcrops of impact melt, perhaps no more than $50m^3$ in total, occur 8km west of Mont des Éboulements (Rondot, 1971a) and are presumably all that remain of a

blanket of melted rocks like that covering the Manicouagan structure. A considerable thermal aureole must have resulted from such a layer, perhaps 150m thick, initially at a temperature of approximately 600-650°C. It is unlikely that sample 94 could be the only remnant of this aureole, particularly as rocks outcropping within 100m are apparently not thermally metamorphosed. It is more likely that a small concentration of impact melt, perhaps an apophysis filling a fracture in the central uplift, was the cause of localized thermal metamorphism in sample 94. The summit of Mont des Éboulements is heavily wooded and dykes ten of metres in width could go undetected.

The examples from Brent and Charlevoix illustrate that caution must be used in interpreting metamorphic effects in shocked rocks, particularly in the neighbourhood of associated bodies of impact melt.

CHAPTER IV

SHOCK-LOADING EXPERIMENTS ON MICROCLINE

IV.1 Introduction

The preceding chapters have been devoted to a description of the unusual types of deformation found in potassic feldspars from terrestrial impact craters. The observed modifications of physical and chemical properties have been ascribed to the elevated pressures and temperatures produced in the target rocks by the hypervelocity impact of a large meteorite. An attempt has been made to establish a scheme of progressive shock effects with the development of particular deformations in the feldspars indicative of relative levels of shock metamorphism. The pressure range which this scheme encompasses, up to approximately 360kb, was estimated largely by characterizing the deformational effects in coexisting quartz grains, and correlating them with the experimental values of pressure required to produce these quartz deformations (Hörz, 1968). It was hoped to confirm, delimit, and subdivide this range with absolute pressures from a series of shock experiments on potassic feldspars, and thus to directly correlate typical deformation effects produced at known pressures, with similar features observed in naturally-shocked feldspars.

IV.1.1 Equation of State and Recovery Shock Experiments

Shock experiments are generally Equation of State experiments or Recovery experiments, and are based on the pressure-volume-energy relations expressed in the Rankine-Hugoniot conservation equations (Duvall and Fowles, 1963).

$$P_1 - P_0 = \rho_0 (S_1 - p_0) (p_1 - p_0) \quad \text{.....Conservation of momentum}$$

$$\rho_0/\rho_1 = (S_1 - p_1) / (S_1 - p_0) \quad \text{.....Conservation of mass}$$

$$E_1 - E_0 = (P_1+P_0) (V_0-V_1) /2 \quad \text{.....Conservation of energy}$$

These equations express the relationship between initial (subscript 0) and subsequent (subscript 1) density (ρ), specific volume (V), pressure (P), particle velocity (p), shock-wave velocity (S), and internal energy (E) across a single, steady, shock front.

The purpose of an Equation of State, or Hugoniot, experiment (Ahrens and Rosenberg, 1968) is to measure two of the above parameters, usually shock-wave velocity and particle velocity, in order to obtain a series of pressure-volume-energy states which define a Hugoniot curve (or simply a Hugoniot) for the material of interest. From the Hugoniot the material's behaviour under shock stress can be predicted, and discontinuities in compression rates signifying phase changes at particular pressures can be detected (See Appendix D for a discussion of Hugoniots). Hugoniots have been determined experimentally for many metals (Walsh et al., 1955, 1957; Al'Tshuler, 1958; McQueen and Marsh, 1960: Boade, 1966; and others): for a number of rocks (Bass et al., 1963; Ahrens and Gregson, 1964; Dennen, 1965; Bass, 1966; McQueen et al., 1967b; Anderson and Kanamori, 1968; Jones et al., 1969; Petersen et al., 1960): and for several common minerals (Wackerle, 1962; Al'Tshuler, 1965; McQueen et al., 1967a; Anderson and Kanamori, 1968; Ahrens et al., 1969; Stöffler and Arndt, 1969; Ahrens and Gaffney, 1971; Ahrens and Graham, 1972). The arrangement of the sensitive recording devices employed in

an Equation of State experiment does not allow rigid support of the sample at impact, so that the specimen is lost, and post-shock examination is not possible.

Recovery shock experiments are designed to permit recovery of the sample for examination of the shocked state(s). Projectile velocity is the only parameter generally measured (Gibbons and Ahrens, 1971), and pressure is calculated from impedance-matching theory, which requires knowledge of the Hugoniots for the projectile and the target materials (Walsh et al., 1957). The relatively simple design of a Recovery experiment, and the fact that Hugoniot data for many metals and geologic materials are now available, have led to Recovery shock experiments becoming more common (Hörz and Ahrens, 1969; Müller and Hornemann, 1969; Gibbons and Ahrens, 1971; Hornemann and Müller, 1971; Kleeman, 1971; Ahrens and Graham, 1972; Hörz and Quaide, 1973).

IV.1.2 Experimental Deformation of Feldspars

IV.1.2A Static Deformation

Equation of State and Recovery shock experiments, as well as static deformation experiments, have been performed on feldspars with a variety of compositions and structural states. Static, high-pressure, dry quenching experiments have been carried out on alkali feldspars, and on alkali aluminogermanates isostructural with feldspars. Ringwood et al. (1967a) transformed sanidine at 120kb and 900°C to a high density phase with Al and Si in octahedral coordination. The structure of this high-pressure polymorph was correlated with the closely packed hollandite ($Ba_{2-x}Mn_8O_{16}$) structure (Bystrom and Bystrom, 1950), and the dense feldspar

form has been referred to as the $KAlSi_3O_8$-hollandite phase. Kume et al. (1966) produced a high-pressure phase of similar structure from $KAlGe_3O_8$ at 25kb and 980°C. In subsequent experiments with partial substitution of Si for Ge, Kinomura et al. (1971) predicted that hollandite-type $KAlSi_3O_8$ could be formed at approximately 82kb and 900°C. Equivalent hollandite-type structures were formed from $NaAlGe_3O_8$ by Ringwood et al. (1967b) at 25kb and 1000-1100°C, and by Kinomura et al. (1971) at 20kb and 900°C, and from $RbAlGe_3O_8$ at 35kb and 1000-1100°C (Ringwood et al., 1967b). $RbAlSi_3O_8$ glass yielded a different high-pressure phase above 120kb, designated only as "new dense structure Phase A" (Ringwood et al., 1967b).

IV.1.2B Shock Deformation

Hugoniots for several plagioclases have been determined in Equation of State shock experiments by Ahrens and Gregson (1964) (albite, andesine, and labradorite), by McQueen et al. (1967b) (oligoclase and andesine), and by Ahrens et al. (1969) (oligoclase). The Hugoniot Elastic Limit (HEL) for each lies between approximately 50 and 60kb, with partial transformation to a high-pressure phase taking place between this level and 400kb, above which pressure the transformation is complete. It was assumed that the appropriate hollandite-type phase was the one produced. In Recovery experiments, albite was shocked to about 250kb (Sclar and Usselman, 1970), but the recovered material comprised diaplectic glass and residual crystalline feldspar, with no indications of a crystalline high-pressure phase.

Hörz and Quaide (1970) shocked andesine and oligoclase to

pressures of 340kb and 100kb respectively. Debije-Scherrer investigations of the recovered material indicated a progressive breakdown leading to a high-pressure, disordered phase amorphous to X-rays.

Ahrens et al. (1969) partially determined the Hugoniot of single-crystal microcline (Fig. IV.1), whose HEL was delimited between 79 and 85kb. Their data indicated that a large volume decrease took place over the 114 to 296kb range where the products consisted of a mixture of starting material and, as shock pressure increases, greater proportions of a high-pressure polymorph. Release adiabat data were not obtained, nor was any shocked material recovered, so the density or nature of the new phase was not established. They believed, however, that a high proportion of the material had been converted to a hollandite-type structure.

The Hugoniot of single-crystal orthoclase has been determined to 340kb by Ahrens and Liu (1973). The Hugoniot elastic limit lies between 41 and 91kb, the value depending on the final shock pressure achieved. Anomalous compression above 115kb indicates the onset of a shock-induced phase change, and transformation to a polymorph assumed to have the hollandite structure is complete above 300kb.

Three series of Recovery experiments have been carried out on potassic feldspars. Kleeman (1970) achieved shock pressures up to 345kb in powdered orthoclase, producing mixtures of diaplectic glass and normal orthoclase, but he detected no crystalline high-pressure phase. Sclar and Usselman (1970) shock-loaded a particulate sample of intermediate microcline to about 250kb, and within the resulting mixture of diaplectic glass and monoclinic crystalline feldspar were minute grains of a shock-

Fig. IV.1

Partial Hugoniot for single crystal microcline determined by Ahrens et al. (1969, Figure 7).

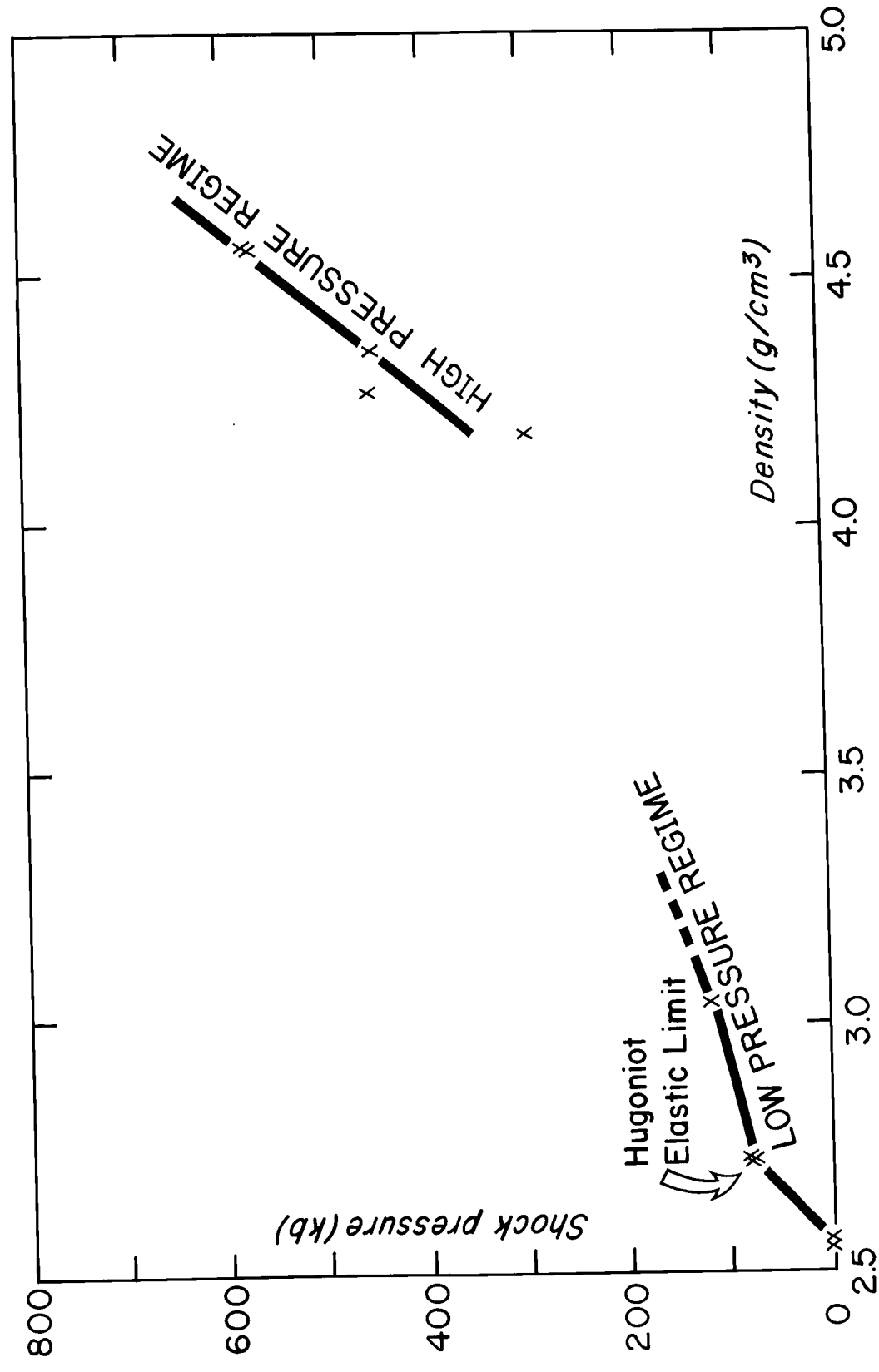
Shock pressure (kb)
Density (g/cm³)
800
600
400
200
0
2.5
3.0
3.5
4.0
4.5
5.0
Hugoniot
Elastic Limit
LOW PRESSURE REGIME
HIGH PRESSURE REGIME

produced high-pressure phase (Table IV.5). They were not able to correlate this phase with Ringwood et al.'s (1967a) hollandite-type K-feldspar but suggested that it might be a transitional, metastable phase formed from the hollandite phase upon removal of the shock load. Stöffler and Hornemann (1972) completely converted adularia ($Or_{90}Ab_{10}$) to diaplectic glass at 360kb, and orthoclase ($Or_{94}Ab_{6}$) to vesicular glass at 575kb.

Therefore, although the existence of at least one high-pressure feldspar polymorph has been determined (the hollandite-type structure) it has not been verified in a shock experiment, but only identified in experiments carried out under slow strain-rate conditions.

Using the data from Equation of State experiments, Ahrens et al. (1969) subdivided feldspar Hugoniots into three sections (Fig. IV.2). Regime I extends to slightly above the Hugoniot elastic limit and covers the region of normal elastic compression without any phase transformation. Regime II represents the nearly horizontal portion of the curve, indicating anomalous compression. This has been referred to as the mixed-phase regime where mixtures of a high-pressure phase and normal feldspar coexist, the proportion of the high-pressure polymorph increasing with pressure. Regime III corresponds to the succeeding portion of the Hugoniot with steepened slope, where the feldspar is completely transformed to the high-pressure phase. Stöffler (1971a) proposed a series of six shock "Stages" by combining these "Regimes" with observations of shock effects in tectosilicates from meteorite craters (Fig. IV.3). His Stages 0 and I correspond closely to Regimes I and II respectively, and Stages II through V are subdivisions of Regime III. The characteristics and approximate

Fig. IV.2

Composite feldspar Hugoniot compiled by Ahrens et al. (1969, Figure 6). Triangles, circles etc. represent data points from various studies. Elastic compression occurs throughout Regime I. Anomalous compression in Regime II (mixed-phase region) is due to partial transformation to high-pressure phase. Regime III is the Hugoniot of the high-pressure polymorph.

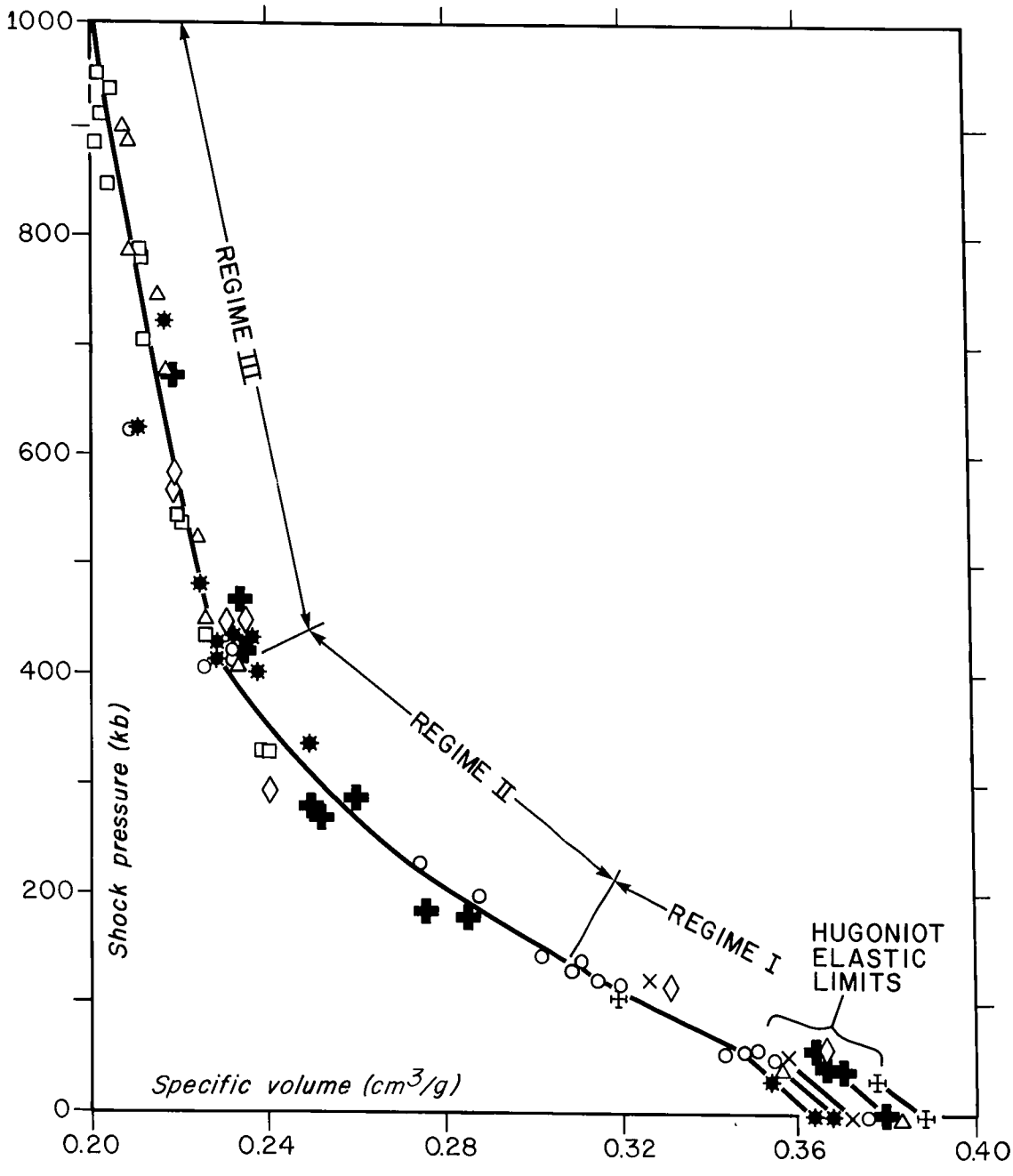
1000
800
600
400
200
0
0.20
0.24
0.28
0.32
0.36
0.40
Shock pressure (kb)
Specific volume (cm³/g)
REGIME III
REGIME II
REGIME I
HUGONIOT
ELASTIC
LIMITS

Fig. IV.3

Shock pressure versus shock temperature (T_H) and post-shock temperature (T_A) for quartz and feldspar. Vertical lines delimit probable pressure ranges for shock metamorphism Stages 0 to IV as defined by Stöffler (1971a, Figure 3).

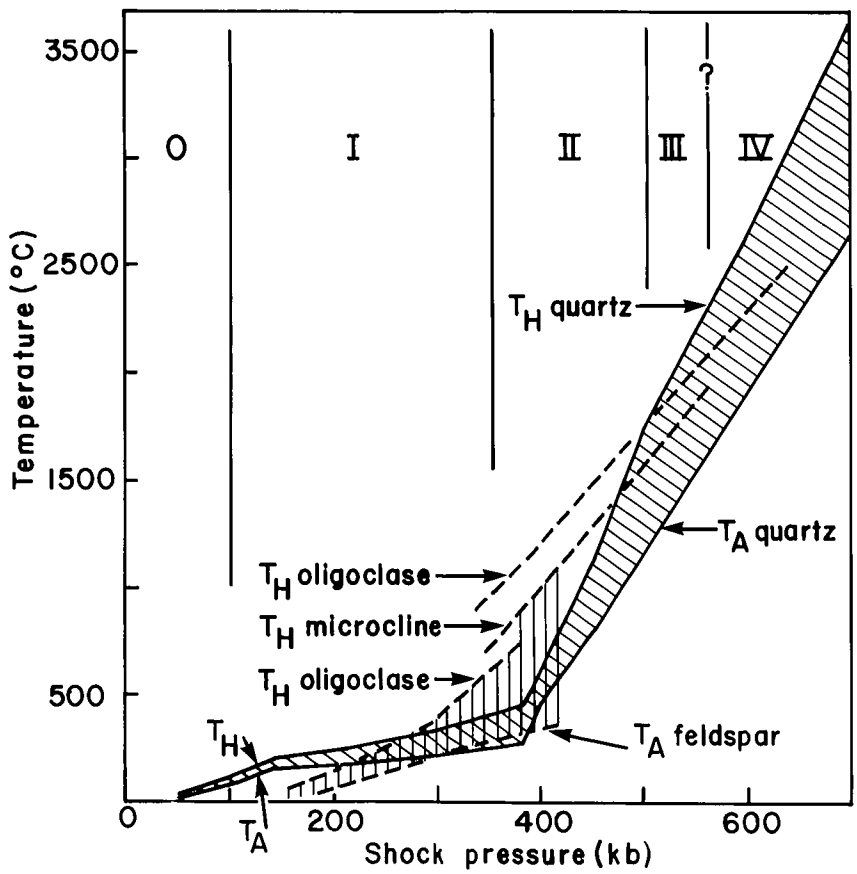
3500
2500
1500
500
Temperature (°C)
0
I
II
III
IV
?
T_H quartz
T_A quartz
T_H oligoclase
T_H microcline
T_H oligoclase
T_H
T_A feldspar
T_A
0
200
400
600
Shock pressure (kb)

Table IV.1 Shock Regimes derived from Hugoniots (Ahrens et al., 1969) and Stages of Shock Metamorphism compiled from observations on naturally shocked tectosilicates (Stöffler, 1971a), applied to microcline.

Shock Regimes		Shock Metamorphism Stages		Recovery experiments on microcline (this study)
Regime	characteristics	Stage	characteristics	
I	Region of Hugoniot up to, or slightly above, the Hugoniot Elastic Limit. Normal elastic compression. Peak pressures 0 to 114kb. Post-shock temperature approx. 180°C.	0	No change in density or other distinct deformation observed on pressure release. Peak pressures 0 to approx. 110kb. Post-shock temperature < 100°C.	37kb 58kb 87kb 96kb 99kb
II	Region of anomalous compression, indicative of partial transformation to high-pressure phase. Peak pressures 114 to 296kb. Post-shock temperature approx. 180° to 500°C.	I	Partial conversion to high-pressure phase with 6-fold Si-O coordination. Recovered phases have post-shock densities which decrease as pressure increases, due to increasing amounts of an amorphous, low density material inverting from the high-pressure phase. Crystals appear partially isotropic. Peak pressures approx. 100 to 360kb. Post-shock temperature approx. 100° to 750°C.	150kb 154kb 167kb 191kb 204kb 250kb 270kb 317kb 320kb
III	Hugoniot steepens and represents the Hugoniot of the high-pressure phase. Peak pressures above 296kb. Post-shock temperature above 500°C.	II	Complete transformation to dense, high-pressure phase which, upon release of pressure, inverts to amorphous, low density diaplectic glass. Peak pressures approx. 360 to 500kb. Post-shock temperature approx. 750° to 1500°C.	417kb
		III	Melting of feldspars	
		IV	Mixed glasses	
		V	Vapourization	

pressure-temperature ranges of each Regime and Stage applied to microcline are summarized in Table IV.1.

IV.2 Recovery Shock Experiments on Microcline

IV.2.1 Procedure

Recovery shock experiments were run on samples of microcline using the facilities of the Seismological Laboratory, California Institute of Technology. A short description of the experimental design (Fig. IV.4) and procedures follows; additional details are presented in Appendix C. Plane-faced projectiles, fired from a 20mm gun, impacted the target after a free-flight of about one metre. The projectile comprises a metal disc (striker plate), usually brass or stainless steel approximately 5mm thick, recessed in the end of a lexan plastic, cylindrical block. The samples were fitted snugly into a well in a stainless steel cylindrical block (the holder), and covered by a thin cap of stainless steel flush with the holder's surface (Fig. IV.5). Samples for this series of experiments were polished, thin discs (0.5mm thick by 6.5mm diameter) cut parallel to the (001) cleavage from a single crystal of perthitic, maximum microcline ($Or_{94}Ab_6$). The unshocked feldspar is described in Appendix C.

The velocity of the projectile was measured by monitoring its passage through two laser beams crossing the flight path. A range of projectile velocities was obtained by varying the explosive powder load, striker plate thickness, and striker plate material (Appendix C, Table C.2). The samples were retrieved by machining the target on a lathe until the surface of the specimen was intersected.

Fig. IV.4

Schematic diagram of shock experiment design (see section IV). Oscilloscope and trigger are in adjacent control room.

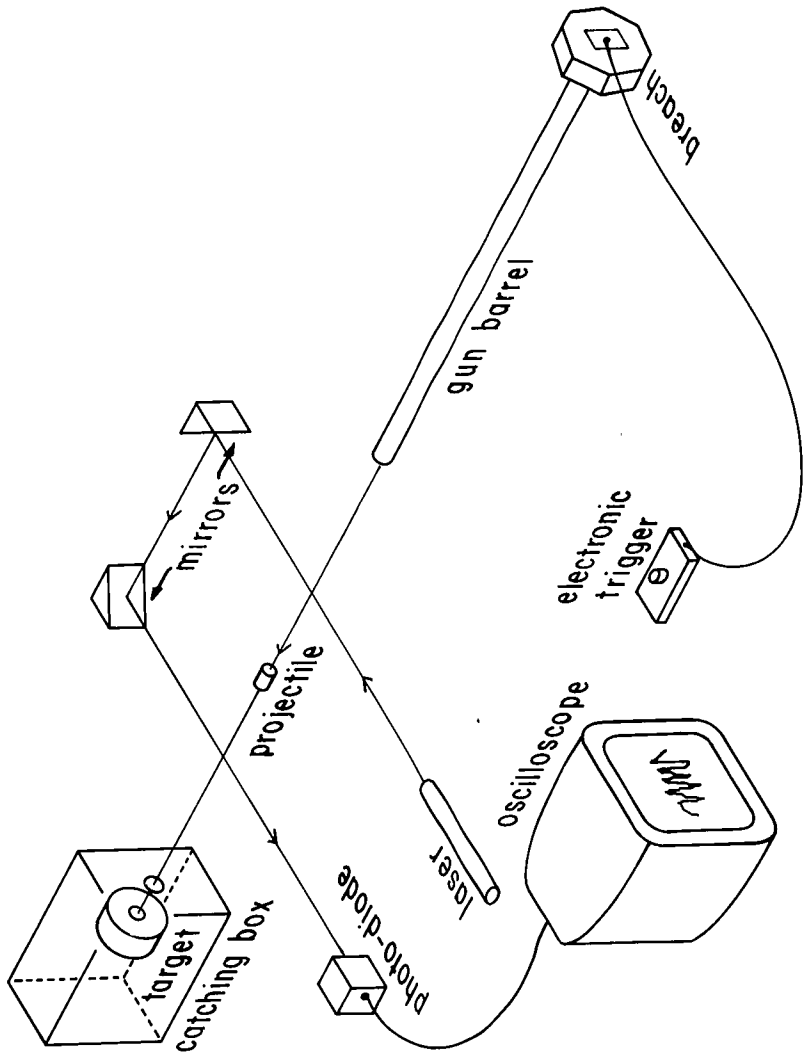
breach
gun barrel
mirrors
electronic trigger
projectile
oscilloscope
laser
photo-diode
target
catching box

Fig. IV.5

Exploded diagram of target and projectile assembly. Microcline disc (sample) is fitted into well in A. A and B are joined and screwed into C, which is recessed in D. The metal striker plate disc is fitted into the lexan projectile. Components A-D are stainless steel.

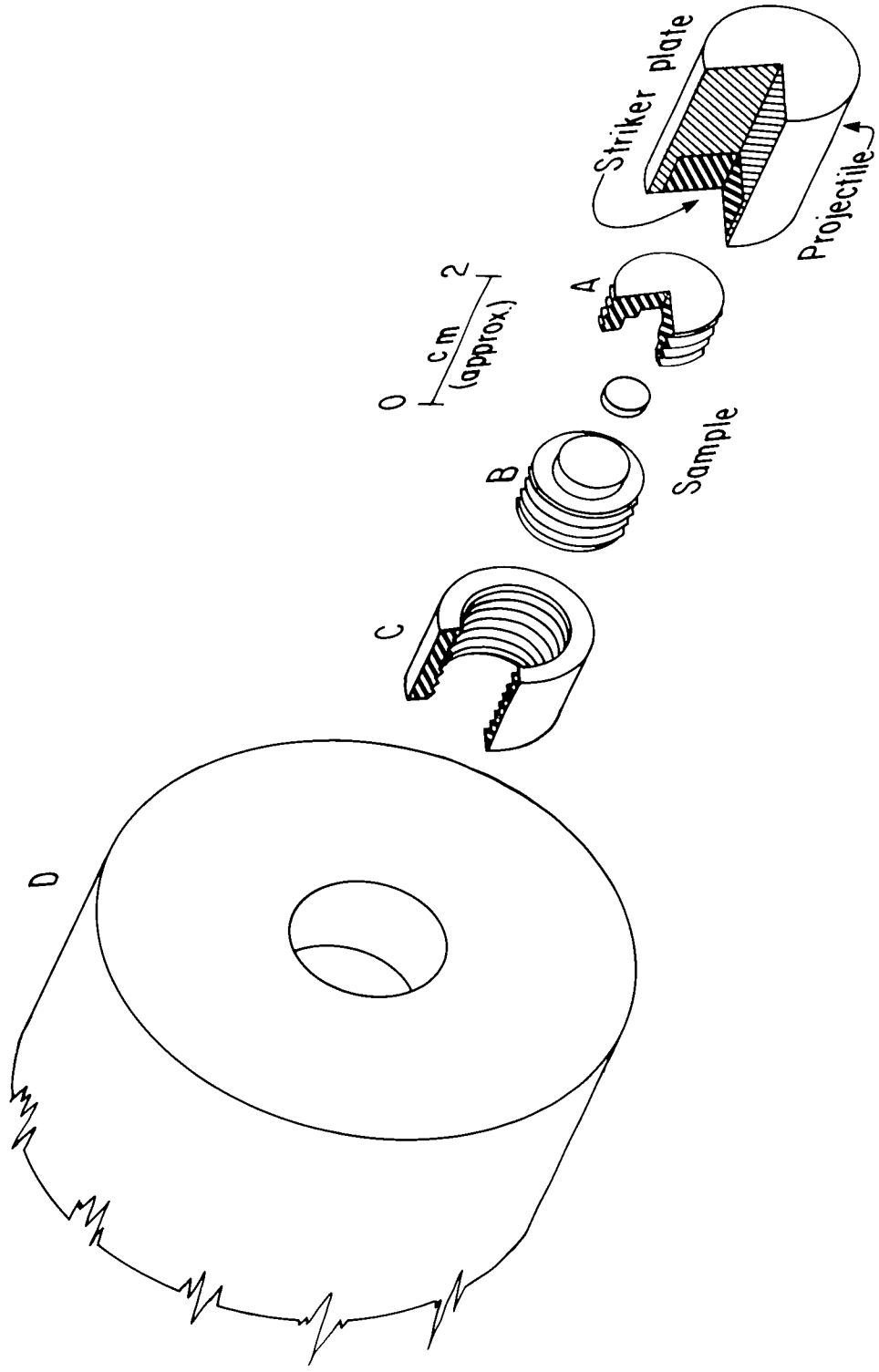
Striker Plate
Projectile
A
0
cm
(approx.)
2
Sample
B
C
D

The peak shock-pressure attained in each shot was determined by a graphical impedance-matching technique (Duvall and Fowles, 1963) using the Hugoniots for the stainless steel target (McQueen et al., 1970), striker plates of brass (Walsh et al., 1957) or Fansteel 77 (Jones et al., 1966), and the measured projectile velocity. The pressure calculated by impedance-matching is the pressure initially produced in the stainless steel cap. Since the feldspar has a lower impedance than the stainless steel, the pressure initially developed in the sample as the shock wave passes from the cap into the feldspar is lower than in the stainless steel. Subsequent reverberations within the samples raise the final pressure attained to that initially produced in the steel cap. The sample discs were of sufficient thinness to allow the peak pressure to be reached in approximately 2μ sec, before attenuation of the shock wave. (A description of a typical graphical impedance-match solution is presented in Appendix D). Temperature was not monitored.

Twenty-three shots were fired, including four blanks for alignment of the gun-target system. Seven of the nineteen loaded shots struck the target off-centre and sheared the samples; they were not recovered. Velocities in the twelve successful shots ranged from 0.552 to 1.850km/sec±1%, and produced pressures between 96kb±3% and 417kb±5% respectively. In addition, F. Hörz provided samples of the same microcline shocked at 37, 58 and 87kb in a similarly designed experiment, so that fifteen samples were available for post-shock examination (Table IV.1).

As a preliminary subdivision, each experiment was assigned to a shock Regime and shock Stage solely on the basis of the calculated

pressure (Table IV.1). If the correlation is valid, the five samples shocked to pressures up to 99kb will exhibit the deformation (or non-deformation in this case) characteristic of Regime I - Stage 0; the seven samples shocked to pressures between 150 and 270kb will reflect the behaviour of samples in Regime II - Stage I; and the feldspar subjected to shock loading of 417kb will show deformation typical of Regime III - Stage II. The transitions from Regime II to III and Stage I to II do not coincide (approximately 296kb and 360kb respectively) and thus the samples shocked to 317kb and 320kb may show deformation characteristics belonging to either Regime II - Stage I or Regime III - Stage II. Observations of shock effects in these two samples may help to correlate the Regimes and Stages in this particular pressure range.

IV.2.2 Post-Shock Examination

IV.2.2A General Observations

The shocked feldspars were tightly compressed in their stainless steel holders and were extracted by scraping out the central part of the disc as a powder or as several large fragments. Material from the outer portion of the discs was also recovered but, because of possible anomalous edge effects, was not examined. The feldspar shocked to 320kb was recovered intact but as a much expanded disc of 8.5mm versus 6.5mm for the unshocked disc.

In contrast to the pale grayish-white of the unshocked microcline the outer surface of the shocked material is medium gray, becoming darker with increasing shock pressure. The darkening is believed to be a light scattering effect caused by the various types

of deformation planes produced.

The density of recovered samples (Table IV.2) was determined by immersing the largest fragment available from each shot (0.5g to 20mg) in a bromoform-acetone solution. The density of the liquid was adjusted by the addition of small amounts of bromoform or acetone until the fragment neither floated nor sank. The density was then calculated by weighing 25ml of the matched solution. The density determined by this procedure of a fragment from an unshocked disc, is 2.552g cm^{-3}, in good agreement with a value of 2.553±0.004g cm^{-3} obtained by the Archimedes method on four hand-specimen size pieces of the feldspar. Although the errors introduced in actual measurement procedures by using this heavy-liquid method can be calculated as ±0.006g cm^{-3}, the inexact "neither floated nor sank" criterion probably results in an error of ±0.01g cm^{-3}.

The density of samples shocked to 154kb or less remains unchanged from that of the unshocked feldspar. At higher pressures, density decreases continuously to 2.396g cm^{-3} for the sample shocked to 417kb (Fig. IV.6). In contrast, all crystalline alkali feldspars have densities greater than 2.551g cm^{-3} and the density of alkali feldspar glasses ranges between 2.375 and 2.391g cm^{-3}, with an extrapolated value of 2.3765g cm^{-3} at $Or_{94}Ab_6$ (Barth, 1969).

IV.2.2B Microscopic Observations

A portion of the grains recovered for each sample, including the unshocked microcline, was prepared as a permanent mount for examination on the universal stage. Part of the remaining sample was crushed to between 80 and 150 mesh for refractive index determinations.

Table IV.2 Bulk density and triclinicity of shocked microcline samples.

sample	bulk density ($g\ cm^{-3}$)	triclinicity $(d_{131}-d_{1\bar{3}1}) \times 12.5$
unshocked	2.553± 0.004	0.94(5)± 0.03
37kb	n.d.	0.90(0)
58kb	n.d.	0.91(6)
87kb	n.d.	0.97(9)
96kb	2.55(1)± 0.01	0.91(5)
99kb	n.d.	0.94(6)
150kb	2.55(0)± 0.01	0.91(3)
154kb	2.55(2)± 0.01	n.d.
167kb	n.d.	0.85(4)
191kb	2.54(3)± 0.01	0.91(6)
204kb	2.53(4)± 0.01	0.97(8)
250kb	2.48(4)± 0.01	0.91(5)
270kb	n.d.	0.85(6)
317kb	2.47(0)± 0.01	no (131)*
320kb	2.45(1)± 0.01	no (131)*
417kb	2.39(6)± 0.01	no (131)*

*-(131) reflections faded beyond resolution

Fig. IV.6

Density versus pressure for microcline shocked in Recovery experiments. Density of feldspar glass of same composition (Or_{94}) is 2.377g cm^{-3}.

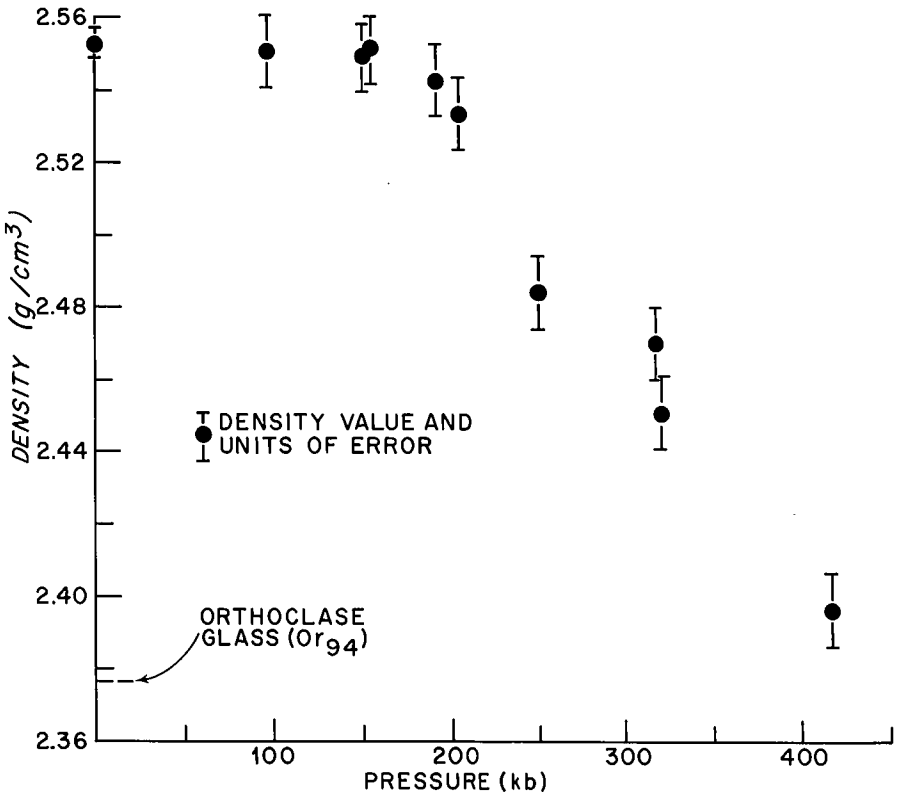
2.56
2.52
2.48
2.44
2.40
2.36
DENSITY (g/cm³)
DENSITY VALUE AND
UNITS OF ERROR
ORTHOCLASE
GLASS (Or94)
100
200
300
400
PRESSURE (kb)

Typically the unshocked microcline grains are equant, usually displaying one moderately good cleavage, have normal even birefringence, and a finely developed grid twinning, commonly visible because the grains lie preferentially on the (001) cleavage. In contrast, moderately to highly shocked feldspar has lower, uneven birefringence, weakly detectable original twinning, poor cleavage, and sets of planar deformations of several types.

Refractive index measurements were made in sodium-vapour light using a standard set of commercial oils, corrected for temperature (Table IV.3). By mixing oils the possible error was reduced to ±0.0002. A range of each refractive index exists between patches within grains. This means that although measurements of the maximum value of n_γ and minimum value of n_α are precise, all other values depend on critical orientation and are thus less easily attainable and less reliable. Generally n_β was not measured in the shocked samples but was calculated from a Mertie chart (Bloss, 1961, p.158) using the measured optic axial angle and n_γ and n_α values.

Refractive indices monotonically decrease over the pressure range investigated (Fig. IV.7) from normal microcline values (n_α=1.5175 ±0.0002, n_γ=1.5249±0.0002) in the unshocked sample to minimum values of n_α=1.4900, n_γ=1.4920 at 417kb. This approaches the 1.4870 value for an alkali feldspar glass of $Or_{94}Ab_6$ composition, interpolated from Barth's (1969) summary data. Beginning at approximately 180kb, a range of about 0.002 exists for each index within grains. Birefringence also decreases over the pressure range from 0.0074 to 0.0020±0.0004, with a variation of approximately 0.004 detectable within grains shocked to pressures

Table IV.3 Optical properties of shock-loaded microcline.

sample	n_α min - max	n_β min - max	n_γ min - max	birefringence min - max	mean $2V_\alpha$	$2V_\alpha$ range (# of grains)
unshocked	1.5175±0.0002	1.5195±0.0002	1.5249±0.0002	0.0074±0.0004	81°±2°	73-85° (10)
37kb	n.d.	n.d.	n.d.	n.d.	81°±2°	76-84° (10)
58kb	n.d.	n.d.	n.d.	n.d.	82°±2°	77-85° (10)
87kb	n.d.	n.d.	n.d.	n.d.	83°±2°	79-88° (10)
96kb	n.d.	n.d.	n.d.	n.d.	83°±2°	81-86° (5)
99kb	1.5170	1.5202*	1.5232	0.0062	84°±2°	75-90° (3)
150kb	1.5160	1.5200*	1.5220	0.0060	86°±2°	80-92° (2)
154kb	n.d.	n.d.	n.d.	n.d.	83°±2°	82.5-83.5° (2)
167kb	1.5158	1.5201*	1.5227	0.0069	81°±2°	(1)
191kb	1.5115-1.5132	-1.5188*	-1.5200	-0.0068	80°±2°	(1)
204kb	1.5085-	1.5105-	1.5113-	.0028-	87°±2°	81-96° (11)
250kb	1.5072-1.5116	-1.5138*	-1.5150	-0.0034	86°±2°	76-101° (8)
270kb	n.d.	n.d.	n.d.	n.d.	87°±2°	82-93.5° (10)
317kb	n.d.	n.d.	n.d.	n.d.	n.d.	n.d.
320kb	1.4980-	1.5003*	-1.5020	-	88°±2°	72-102° (16)
417kb	1.4900-	1.4910-	1.4920-	0.0020-	88°±2°	79-100° (21)

* - Refractive index determined from Mertie chart (Bloss, 1961, p 158); all others by immersion method.

Fig. IV.7

Refractive indices (n_α and n_γ) *versus* pressure for microcline shocked in Recovery experiments. Vertical error bars are asymmetric because maximum n_γ and minimum n_α values were generally measured. Maximum and minimum n_α values were obtained from two samples. Refractive index of feldspar glass of same composition (Or_{94}) is 1.487.

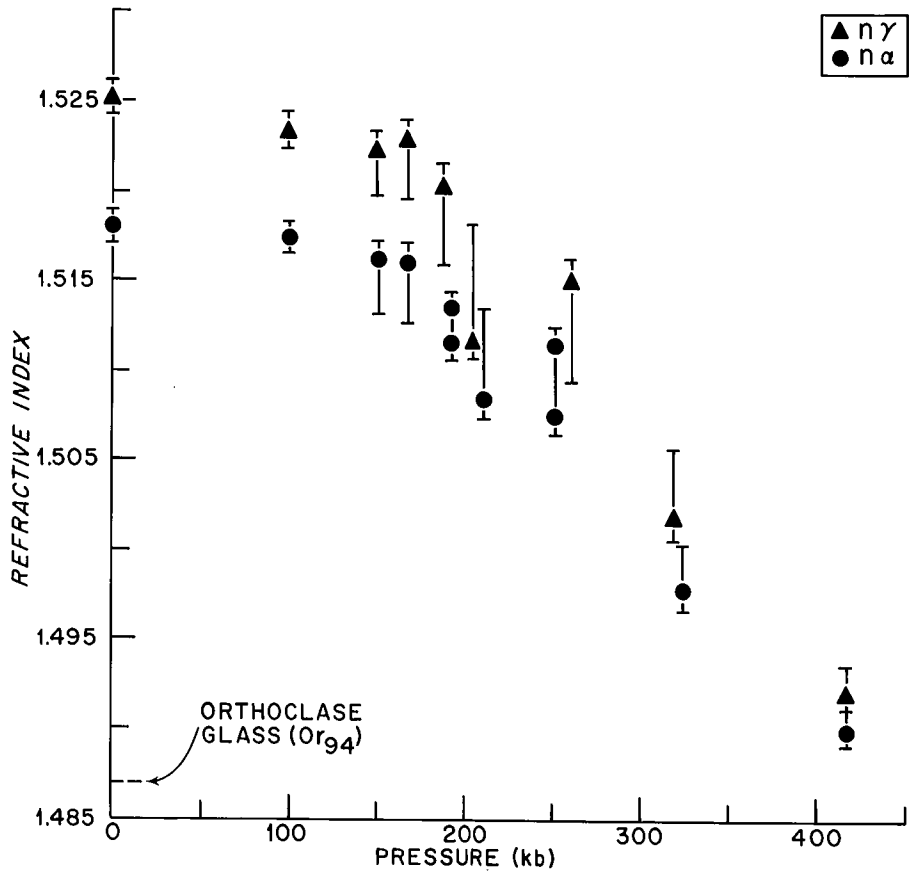
▲ nγ
● nα
1.525
1.515
1.505
1.495
1.485
REFRACTIVE INDEX
ORTHOCLASE
GLASS (Or94)
0
100
200
300
400
PRESSURE (kb)

greater than 180kb. In summary, at pressures above 90kb and below 180kb only a slight decrease in birefringence and refractive index is observed; with successively higher pressures the decrease is more evident, and a mottled appearance is developed due to patches of differing birefringence. Although some of the areas with lowest birefringence appear almost glassy, no completely isotropic regions were seen, as indicated by the refractive index measurements. A visual estimate from the 417kb sample indicates that less than 10% of a grain shows the very low birefringent, almost isotropic character.

Optic axial angle measurements employing standard universal stage techniques were attempted on thirty grains per sample (Table IV.3). The unshocked feldspar has $2V_{\alpha}=81°\pm2°$, which, when combined with its composition ($Or_{94}Ab_{6}$), places it in Tuttle's (1952) microcline-low albite series of alkali feldspars (Fig. II.5). As shock stress rises $2V_{\alpha}$ increases fairly constantly to 88°±2° at 417kb, a value still consistent with the microcline-low albite series. The spread of values measured within samples also increases and several biaxial positive grains were noted, particularly above 200kb. Although the mean 2V values between 96 and 191kb may not be statistically reliable because of few measurements, the lack of grains with suitable orientation in this pressure range is probably significant. Normally microcline fragments tend to lie on the perfect (001) cleavage displaying their characteristic grid twinning. Since the optic plane is also almost parallel to (001) the occurrence of grains oriented so that one or both optic axes are accessible is low. Therefore, only 10 of 30 grains examined in the unshocked and weakly shocked samples provided 2V measurements. The fact

that grains of suitable orientation are even less common in the 96 to 191kb region suggests that a structural control of even greater influence than the usual (001) cleavage causes the shocked grains to prefer a rest position in which the optic plane parallels the microscope stage. However, between 204 and 417kb, grains with usable orientation occur as commonly, or more commonly, than in the unshocked feldspar. The inference is that the orientation control exerted by the basal cleavage in the unshocked feldspar has weakened above 204kb, either because another cleavage has become stronger, or because random fracturing has become more common.

IV.2.2C Shock Deformation Effects

A variety of parallel linear forms, occurring in sets, traverse parts or the whole of both the shocked and the unshocked microcline. They represent the surface traces of structural planes within the grains. In the case of the normal microcline the planes are either twin lamellae or fractures. In the shocked microcline additional sets of unusual planar elements are developed. Thirty grains from each sample were examined on the universal stage to learn the character of these planes. It was necessary to use the "best fit" method (Appendix B) of correlating, with a standard plot, structural data plotted in stereographic projection. This is a common technique where insufficient control is available to permit a unique correlation.

Twinning in the unshocked feldspar is normal and comprises a finely developed combination of polysynthetic albite and pericline lamellae in the familiar grid pattern (M-twins) of microcline. On

the (001) face the pattern is generally uniform, covering the whole grain, with albite (composition plane (010)) and pericline (composition plane (h01)=rhombic section) twin lamellae approximately 3-5μ in width. No other twin laws are evident. Over the range of increasing pressure, twinning becomes slightly weaker in that it is unevenly developed, somewhat less distinct, and lamellae are often slightly bent. The twinning persists in microcline shocked at pressures up to 320kb with both albite and pericline twin lamellae present (Figs. IV.9 and IV.11). In grains shocked to 417kb, however, original twins are rare and usually only the albite twin set is seen. The twins detected in these grains, with composition plane near the rhombic section of the unshocked feldspar (Fig. IV.11), are believed not to be remnant pericline twins (see section IV.2.2C (iv) on symmetry changes).

Two sets of cleavage fractures are developed in the unshocked microcline. Although (001) is more common and cleaner than (010) it is less often measured because grains tend to rest on it parallel to the microscope stage. The cleavages are usually detected as grain edges, but are also visible within grains as tensional fractures across which there has been no significant separation. None of the less common feldspar cleavages or partings (Deer et al., 1963) were observed in the starting material. Both (001) and (010) cleavages occur in the same style in the shocked grains throughout the full pressure range investigated, with the basal form still predominant. Few (001) forms were recorded at 150, 154, 167 and 191kb, suggesting that if this cleavage is present, it is well developed so that the grains have an even stronger preference to lie on it. This is supported by the

observation that 2V measurements are scarce on material shocked between 150 and 191kb because the optic plane, near (001), parallels the microscope stage. Also confirming the 2V data is the renewed abundance of (001) measurements at pressures above 191kb (Figs. IV.8 and IV.11).

Apparently the effect of shock stress on the twin lamellae and cleavages of the original feldspar is to produce a slight to moderate decrease in definition of the M-twins, a possible elimination of the pericline set at pressures above 320kb, and enhancement of the pre-existing basal cleavage between approximately 100 and 200kb.

In addition to those cleavages and twins already described, there are several sets of planar elements visible and measurable in the shocked microcline fragments. Because they are not present in the unshocked material their development must be related to shock stress, and so they are grouped under the heading "shock-induced planar deformations". Three types have been noted: cleavage-like features, twin-like features, and planar deformation features, with gradations between types.

IV.2.2C (i) Cleavage-like features

These are the most common of the shock-induced deformations (Plates IV.1 and IV.2) and are distinguished from the original cleavages largely because they have crystallographic orientations other than (001) and (010). The most common and consistent orientations are near $\{\bar{1}11\}$ and $\{11\bar{1}\}$, one or both occurring in approximately 70% of the grains in the 96 to 167kb sample range, and in 90% of the grains subjected to higher pressures (Table IV.4). Although detailed measurements were

Plate IV.1

a) Shock-induced cleavage in microcline shocked to 87kb. Fracturing along $\{11\bar{1}\}$, the ENE-trending planes, produces weak cleavage faces on upper margin of grain. Common (001) cleavage trends NNE. Plane-polars.

b) Shock-induced cleavage in microcline shocked to 204kb. The NNW-trending fractures parallel to $\{11\bar{1}\}$ are enhanced by interference contrast illumination.

a

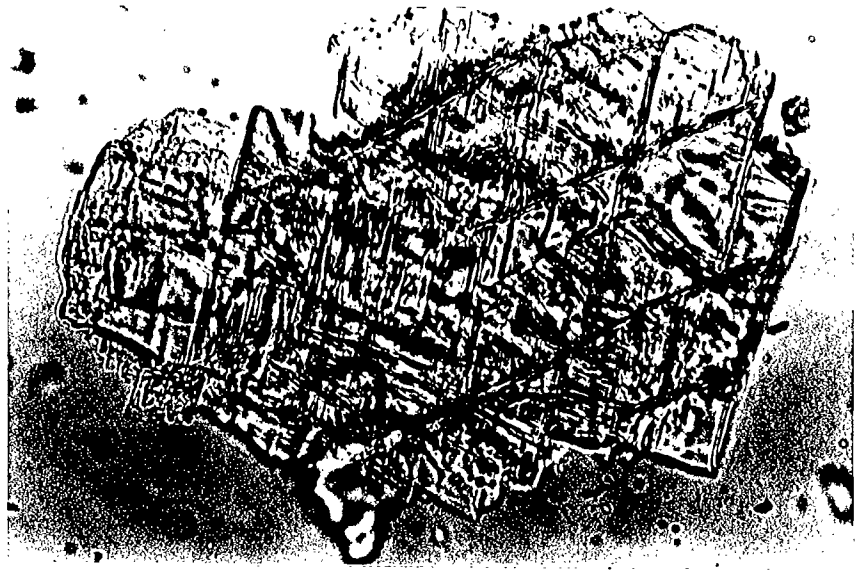

150 μ

b

125 μ

Plate IV.2

a) Extinction bands controlled by shock-induced $\{11\bar{1}\}$ cleavage, trending NNW, in microcline shocked to 250kb. Photographed on universal stage under crossed polars.

b) Extinction bands controlled by shock-induced $\{11\bar{1}\}$ cleavage, trending NE, in microcline shocked to 250kb. Crossed polars.

c) Low refractive-index material (glass?) along shock-induced fractures parallel to $\{11\bar{1}\}$, trending N, in microcline shocked to 167kb. Photographed on universal stage. Plane-polars.

a

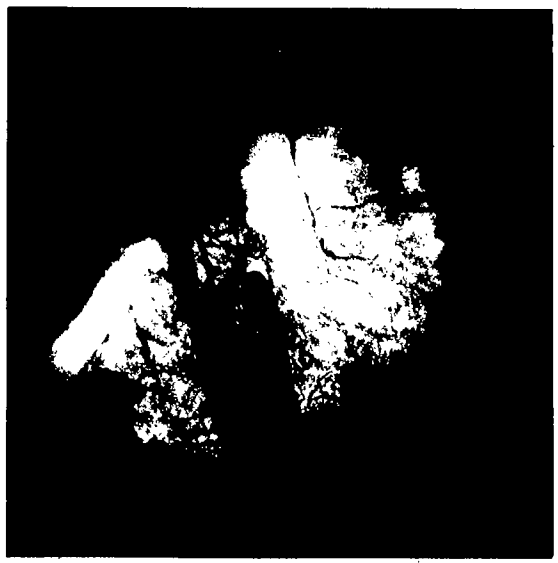

150 μ

b

125 μ

c

150 μ

made only on samples shocked to 96kb or greater, the above orientations have been detected in the 58 and 87kb samples (Plate IV.1a) indicating their initial formation at relatively low shock pressures. Whether both sets or only one orientation appears in a grain is not related to shock level, as approximately one third of the grains with cleavage-like features examined at each pressure contain both sets. Where only one orientation is found it is usually $\{\bar{1}11\}$, although the "best fit" method does not always discriminate between $\{\bar{1}11\}$ and $\{11\bar{1}\}$.

These two cleavage-like features occur as straight fracture planes generally crossing the interior of grains rather than forming faces, however, their cleavage-like nature is shown in Plate IV.1a where a minor grain-edge is produced by parting parallel to the set traversing the interior. The planes are relatively widely spaced, approximately 20 to 25μ apart, with only 3 or 4 per grain extending across the full width. In cases where they are more closely spaced, approximately 15μ, the fractures extend from the margin only a short distance into the fragment. Towards the higher end of the pressure range, where the grains begin to show disruption of optical properties, the shock-induced cleavages roughly separate broad, lamellar domains of differing birefringence. Where the cleavage-like features are relatively closely spaced and the birefringence contrast between regions is distinct, a twin-like character is presented (Plate IV.2), and the distinction from true shock-induced twins (see section IV.2.2C (ii)) is uncertain. Within the lamellar optic domains, birefringence is also somewhat uneven and decreases towards the bounding, shock-induced cleavages. This condition is often enhanced by the occurrence of a

Fig. IV.8

Cleavages (circles) and shock-produced cleavage-like features (triangles) measured by U-stage method in shocked microcline. A) up to 100kb; B) 100 to 180kb; C) 180 to 270kb; D) above 270 kb. Stereogram axes are optic directions X, Y and Z. Measured features are parallel to crystallographic planes of the unshocked microcline lattice, as indicated by stars and Miller indices.

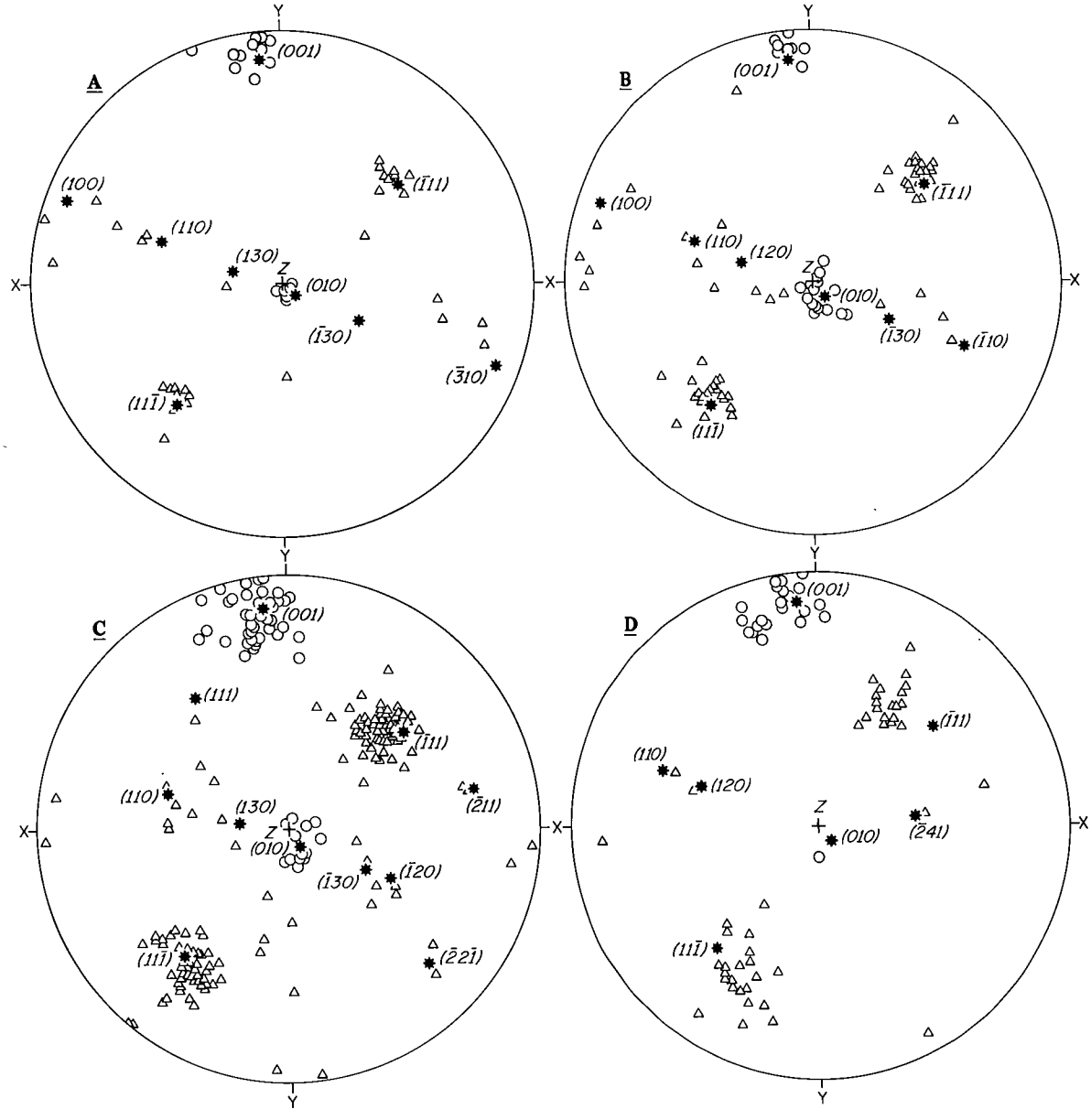
A
(001)
(100)
(110)
(130)
Z
(010)
(1̄30)
(3̄10)
(11̄1̄)
(1̄11)
B
(001)
(100)
(110)
(120)
Z
(010)
(1̄30)
(1̄10)
(11̄1)
(1̄11)
C
(001)
(111)
(110)
(130)
Z
(010)
(1̄30)
(1̄20)
(2̄11)
(11̄1̄)
(2̄2̄1)
(1̄11)
D
(001)
(110)
(120)
Z
(010)
(2̄41)
(11̄1̄)
(1̄11)
X
Y

low-birefringent, almost isotropic material filling some of the $\{\bar{1}11\}$, and $\{11\bar{1}\}$ fracture planes. The refractive index of this material could not be measured except to determine that where it possesses its lowest indices, at 417kb, it is lower than that of the enclosing feldspar.

Although the $\{\bar{1}11\}$ and $\{11\bar{1}\}$ orientations are the most common, accounting for 83% of all shock-induced cleavage-type features, several others have been recorded, almost all at pressures below 200kb. These cleavages do not cluster strongly about one or two definite orientations, but for the most part lie in the [001] zone, generally between (100) and (130), and between $(\bar{1}30)$ and $(\bar{3}10)$. Another group appear as fractures along the rhombic section parallel to the pericline twin composition plane (Fig. IV.8). A few other shock-induced cleavages, particularly those recorded from the 417kb sample, were not assigned Miller indices as they are few and scattered.

In contrast to the $\{\bar{1}11\}$ and $\{11\bar{1}\}$ sets, the [001] zone and rhombic section fractures are similar to the normal (001) and (010) forms in that they generally form cleavage faces, and are imperfect and of short lateral extent in the interior of grains. By comparison, Deer et al. (1963) reported that there is a tendency for parting to develop parallel to possible vicinal faces between (100) and (110) or $(\bar{1}10)$, in the [001] zone, and between (100) and $(\bar{2}10)$, in the zone containing the rhombic section. They reported no evidence for $\{\bar{1}11\}$ or $\{11\bar{1}\}$ forms.

IV.2.2C (ii) Twin-like features

Examples of the second group of shock-induced planar defor-

mations, the twin-like features, are not numerous in the deformed microcline grains except at the highest pressures (Table IV.4). In a true twin pair, one unit appears rotated or reversed, or both, with respect to the other, while some lattice continuity between the two is maintained. The resulting disturbed relationship between the optics of the two members is usually detected by differing extinction positions. In the experimentally shocked microclines, twin-like features occur as sets of indistinct, parallel, narrow lamellae with differing extinction, suggestive of polysynthetic twins (Plate IV.3). The lamellae are generally developed in parts of grains only, in contrast to the original M-twins, although some sets occur over the whole grain. The lamellae are approximately 10μ in width, wider than the albite or pericline twins, although some of the discontinuous sets are narrower. Birefringence is roughly uniform within lamellae, but the distinction between shock-induced, twin-like and cleavage-like features becomes uncertain where birefringence is uneven and lamellae indistinct. Optic parameters could not be measured in the twin lamellae because of their width and generally poor quality, and thus no twin law has been established.

Like the shock-induced cleavages, the twin-like features develop in a few sets with consistent crystallographic orientations (Fig. IV.9). At pressures up to and including 191kb, no unusual twins were detected. Samples shocked to pressures between 204 and 417kb possess twin-like features with apparent composition planes in the [001] zone between {100} and {110}, and fewer between {100} and $\{\bar{1}10\}$. Sets of this orientation are developed in 40% of the grains examined from

Plate IV.3

a) Shock-induced, twin-like planar features trending NW, in microcline shocked to 250kb. Set of planar features trending E shows a less distinct, twin-like character. Although not measured, the orientation of these sets is likely $\{11\bar{1}\}$ and $\{\bar{1}11\}$. Crossed polars

b) Shock-induced, twin-like planar features trending E, in microcline shocked to 417kb. Crossed polars.

c) Shock-induced, twin-like planar features in sets trending NE and NW, in microcline shocked to 417kb. Sets are parallel to $\{11\bar{1}\}$ and $\{\bar{1}11\}$ respectively, and the cleavage faces trending ENE are parallel to (001). Crossed polars.

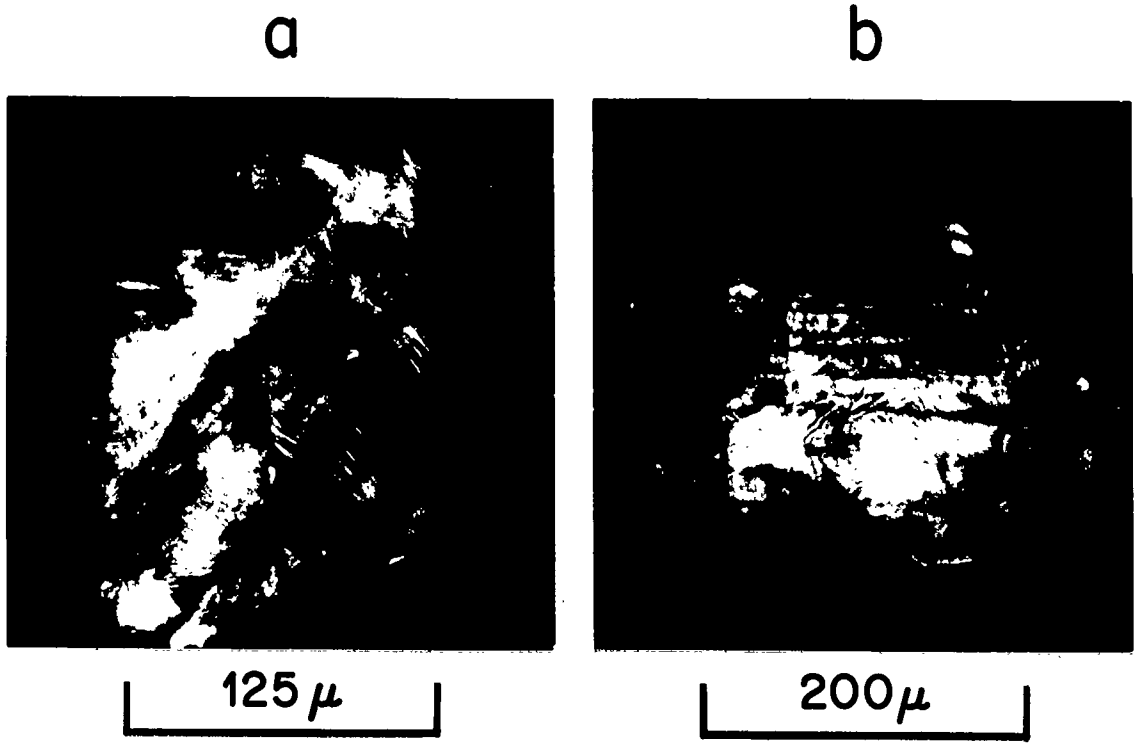
a
b
125 μ
200 μ
c
250 μ

Fig. IV.9

Albite and pericline twins (circles) and shock-produced twin-like features (triangles) measured in shocked microcline. A) 100 to 180kb; B) 180 to 270kb; C) above 270kb. Stereogram axes are optic directions X, Y, and Z. Stars and Miller indices represent crystallographic planes in the unshocked microcline lattice.

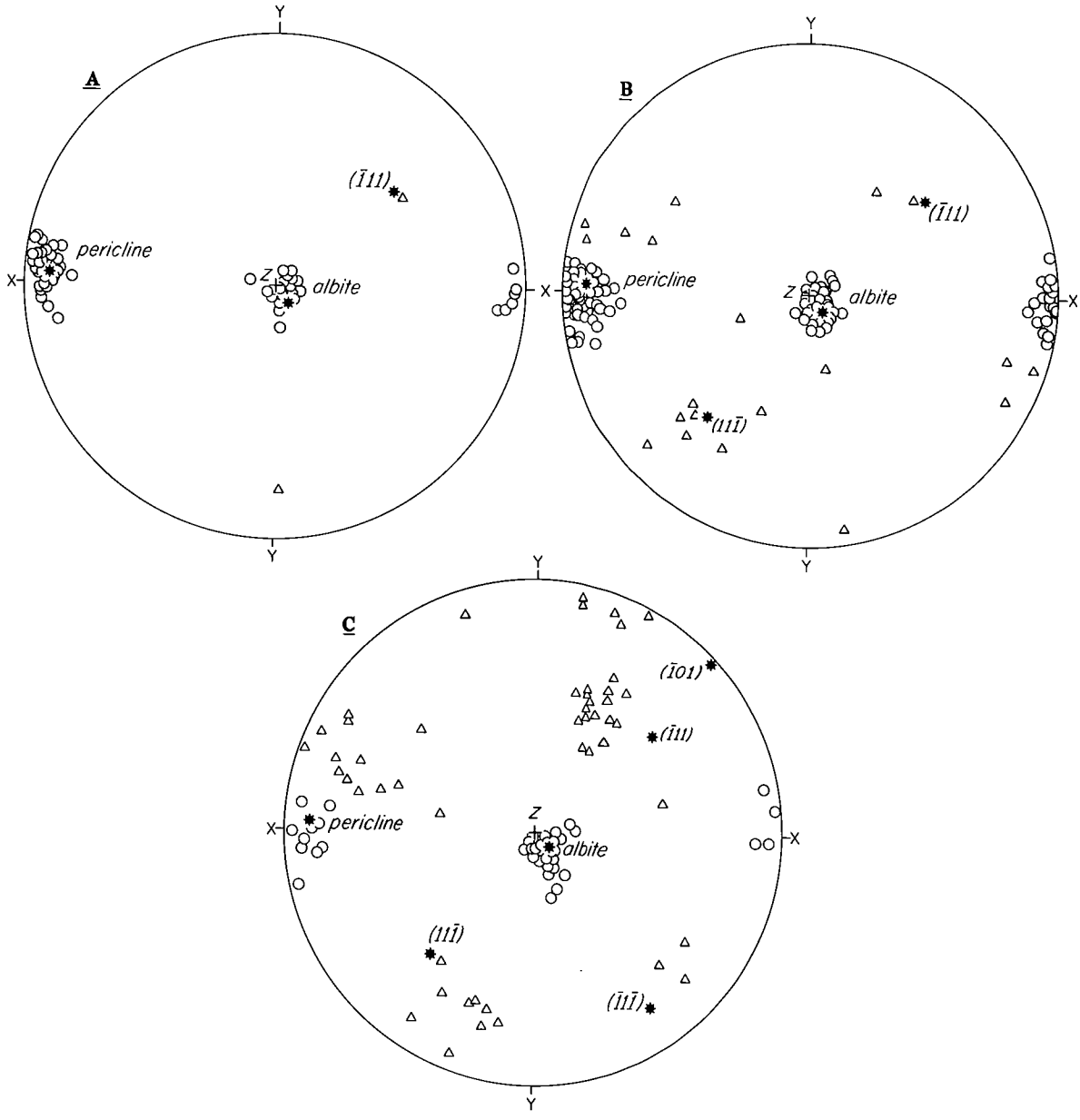
A
Y
X
Z
pericline
albite
(1̄11)
Y
B
Y
X
Z
pericline
albite
(1̄11)
(11 1̄)
Y
C
Y
X
Z
pericline
albite
(1̄01)
(1̄11)
(11 1̄)
(1̄1 1̄)
Y

the 417kb sample.

Commencing also at 204kb are sets of shock twins parallel to $\{\bar{1}11\}$ and $\{11\bar{1}\}$, the two prominent shock-induced cleavage orientations. It is these sets that are difficult to distinguish from the lamellar optic domains bounded by shock-induced fractures. Between 204 and 320kb, most features with these orientations have a greater cleavage-like than twin-like character, but at 417kb the opposite is true. There is no example where both unequivocal cleavage and twins of the same, or almost the same, orientation coexist. However, in some cases the $\{\bar{1}11\}$ set may appear twin-like whereas the $\{11\bar{1}\}$ set is cleavage-like, and vice versa.

The third consistently oriented set of shock-induced twins has an apparent composition plane approximately parallel to $\{\bar{1}01\}$. It is detected only in the 417kb sample where it was measured in 20% of the grains. Although all of the above-mentioned orientations have not been recorded together in one grain, there appears to be no preference for development of any one set in association with any other.

Burri (1962), in his review of feldspar twinning, lists several rare twin laws whose composition planes are similar to those measured in the shocked microcline. For feldspars of triclinic symmetry, Normal twin laws include: prism (110) or $(1\bar{1}0)$, X (100), and Breithaupt $(\bar{1}11)$, of which X-twins are the least rare.

IV.2.2C (iii) Planar deformation features

The remainder of the group of shock-induced planar elements have been designated planar deformation features. Similar features

have been called "planar deformation structures" by Engelhardt and Bertsch (1969) in their description of deformed quartz from the Ries Crater, Germany, and Chao (1967) refers to corresponding features in plagioclase from the same crater as "planar elements". The term "planar deformation features" has been used by Robertson et al. (1968) in describing the same type of deformation produced in naturally shocked quartz and plagioclase from Canadian craters. Engelhardt and Bertsch (1969) believe that planar deformation features are traces of zones of plastic flow accompanying lattice dislocations produced by stresses above the Hugoniot elastic limit. In weakly shocked crystals they are detected as optical discontinuities: at higher pressures by the development of high-pressure phases along the planes, or by the inclusion of numerous minute voids, or gas- or liquid-filled cavities created by annealing.

The planar deformation features in the experimentally shocked microcline are relatively indistinct by comparison with those found in meteorite impact sites. They are generally less than 1μ in width and rarely exceed a length of 50μ, and are difficult to categorize. However, most sets appear to correspond to Engelhardt and Bertsch's "non-decorated planar elements". That is, they appear as narrow planes differing in refractive index and birefringence from the host feldspar (Plates IV.4 and IV.5). A few other sets are apparently visible due to minute inclusions along the planes.

Like the shock-induced cleavages and twins, the planar deformation features in general are formed parallel to a few preferred crystallographic orientations (Fig. IV. 10). They are initially weakly

Plate IV.4

a) Shock-induced planar deformation features in two sets trending NW and NE (weak). Albite and pericline twins form a grid pattern in the upper part of this microcline shocked to 191kb. Crossed polars.

b) Two sets (E and NE) of finely-spaced planar deformation features developed throughout the microcline grain shocked to 270kb. Interference contrast illumination.

a

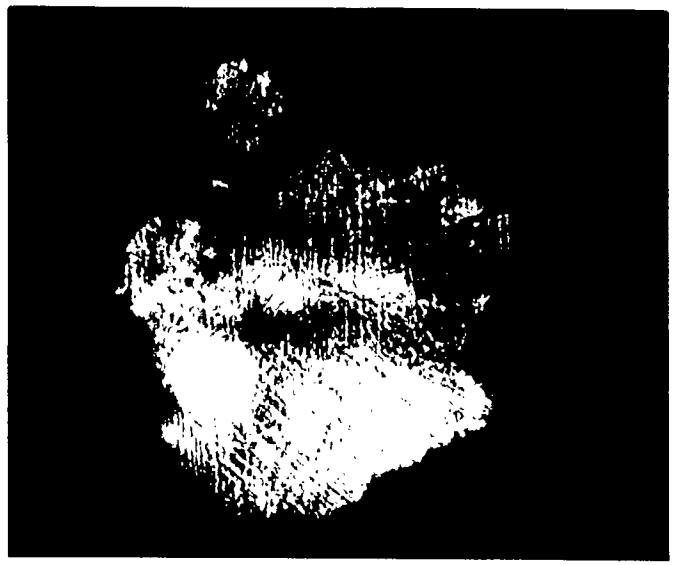

125 μ

b

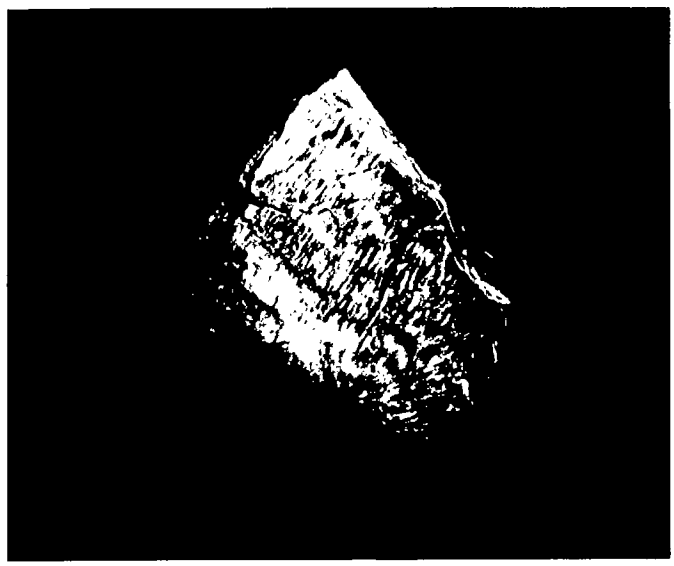

125 μ

EARTH PHYSICS BRANCH
BRANCH ADMINISTRATION
PHOTOGRAPHY SECTION
OTTAWA, ONT., CANADA

NEG. No. 7238.2 DATE 30.4.73
REPRINT ..... DATE .....

Plate IV.5

a) Finely-spaced, non-decorated planar deformation features in microcline shocked to 417kb. Four sets are developed in this grain, two of which (N and NW) are visible on the flat stage. Observation of the planar features has been enhanced by interference contrast illumination and insertion of a λ-plate.

b) Two sets (N and NW) of multiple, non-decorated planar deformation features in microcline shocked to 417kb. Interference contrast illumination.

a

30 μ

b

30 μ

developed in the sample shocked to 150kb (approximately 13% of the grains) which confirms Engelhardt and Bertsch's (1969) observation that planar deformation features are not produced below the HEL. At higher pressures the frequency of these features increases (Table IV.4) to about 60% of the grains at 191, 204, and 250kb; it then drops to 23% at 270kb, and no planar deformation features are present at 320kb. They return in 48% of the grains at 417kb, with as many as five different sets present in one fragment.

The most common orientation is approximately $\{11\bar{1}\}$ accounting for 53% of the planes over the 150 to 270kb range, but at 417kb these sets are rare. It has already been noted that both shock-induced twins and cleavages with this orientation are common, but do not occur together in the same grain. However, many examples of coexisting $\{11\bar{1}\}$ cleavages and planar deformation features have been clearly identified. It can be seen from Figures IV.8c and IV.10b that the two consistently have slightly differing orientations, although both are near $\{11\bar{1}\}$. In contrast to the frequency distribution of the deformation twins and cleavages, where $\{\bar{1}11\}$ is abundant and $\{11\bar{1}\}$ secondary, the approximate $\{\bar{1}11\}$ orientation for planar deformation features is rare and $\{11\bar{1}\}$ predominates (Fig. IV.10).

Three other orientations are of lesser importance in the 150 to 270kb range (Figs. IV.10a,b). They are approximately $\{\bar{1}30\}$, $\{221\}$ and $\{\bar{1}22\}$, each occurring in about 20% of the grains. Unlike the lower pressure samples, planar deformation features at 417kb are scattered, with only about 20% of the fragments exhibiting planes roughly parallel to $\{001\}$, and another 10% with $\{\bar{1}11\}$ or $\{11\bar{1}\}$ orientations (Fig. IV.10c).

Fig. IV.10

Shock-produced planar deformation features (triangles) measured in shocked microcline. A) 100 to 180kb; B) 180 to 270kb; C) above 270kb. Stereogram axes are optic directions X, Y, and Z. Stars and Miller indices represent crystallographic planes in the unshocked microcline lattice.

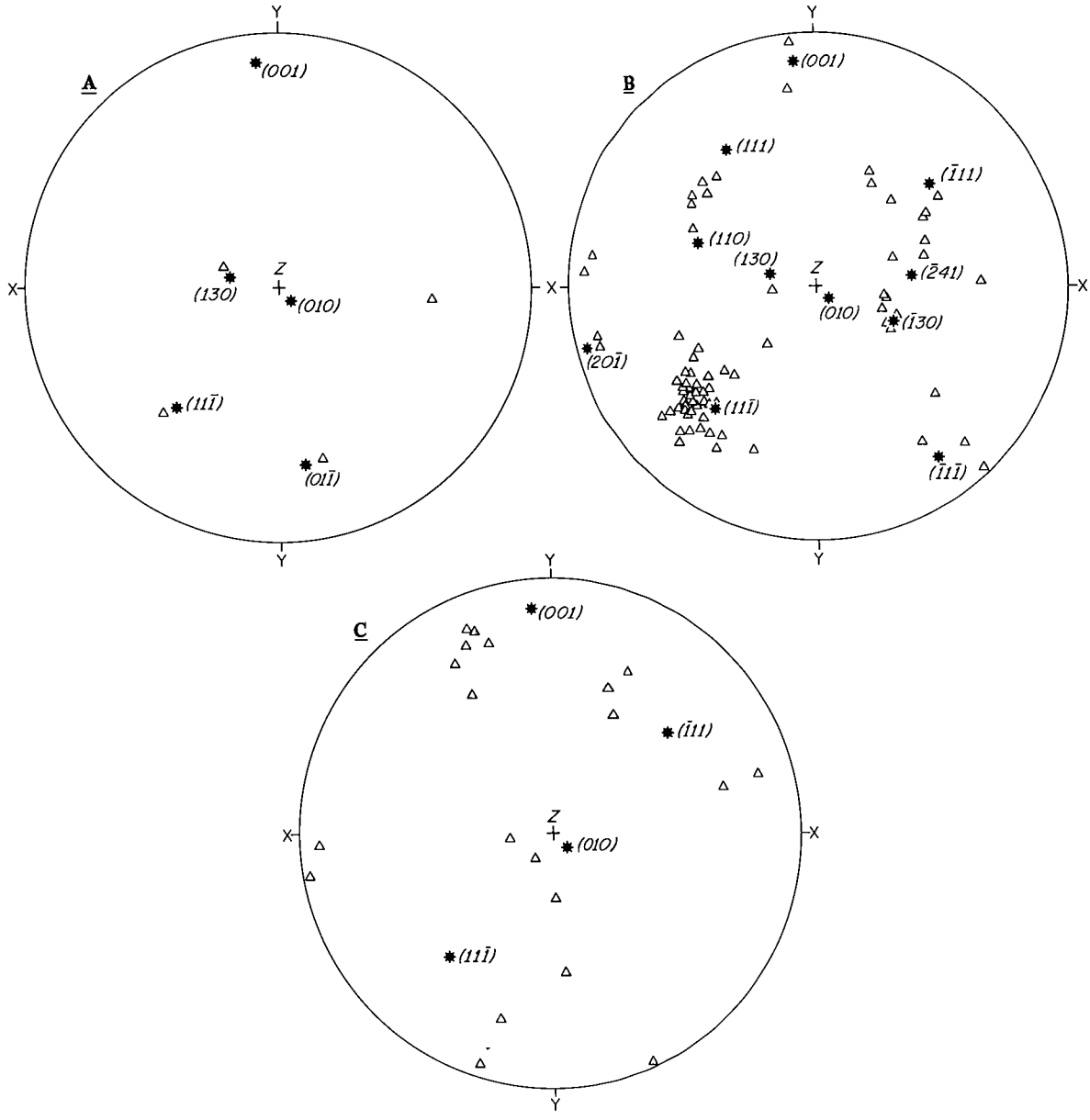
A
(001)
(130)
(010)
(11$\bar{1}$)
(01$\bar{1}$)
B
(001)
(111)
($\bar{1}$11)
(110)
(130)
($\bar{2}$41)
(010)
($\bar{1}$30)
(20$\bar{1}$)
(11$\bar{1}$)
($\bar{1}\bar{1}\bar{1}$)
C
(001)
($\bar{1}$11)
(010)
(11$\bar{1}$)
X
Y
Z

Table IV.4 Development of shock-induced planar deformations in experimentally shocked microcline.

sample	(i) cleavage-like			(ii) twin-like			(iii) planar deformation features			Shock Regime	Shock Stage
	% of grains with planes	average sets per grain with planes	common orient-ations	% of grains with planes	average sets per grain with planes	common orient-ations	% of grains with planes	average sets per grain with planes	common orient-ations		
37kb		not detected			not detected			not detected		I	0
58kb		detected	{$\bar{1}11$},{$11\bar{1}$}		not detected			not detected			
87kb		detected	{$\bar{1}11$},{$11\bar{1}$}		not detected			not detected			
96kb) 99kb)	67	1.5	{$\bar{1}11$},{$11\bar{1}$}, {h10}		not detected			not detected			
150kb) 154kb)	72	1.3	{$\bar{1}11$},{$11\bar{1}$}, {hk0}		not detected		13	1.0	{$11\bar{1}$}	II	I
167kb	72	1.3	{$\bar{1}11$},{$11\bar{1}$}, {hk0}		not detected			not detected			
191kb	96	2.0	{$\bar{1}11$},{$11\bar{1}$}, {hk0}		not detected		52	1.1	{$11\bar{1}$},{$\bar{1}11$}, {$\bar{2}41$}		
204kb	90	1.3	{$\bar{1}11$},{$11\bar{1}$}	30	1.2	{$\bar{1}11$},{$11\bar{1}$}	67	1.5	{$11\bar{1}$},{$\bar{1}11$}, {110}		
250kb	97	1.3	{$\bar{1}11$},{$11\bar{1}$}		cannot be distinguished from other features		60	1.6	{$11\bar{1}$},{$\bar{1}11$}, {$\bar{2}41$},{110}		
270kb	96	1.3	{$\bar{1}11$},{$11\bar{1}$}		"		23	1.2	{$11\bar{1}$}		
317kb) 320kb)	93	1.5	{$\bar{1}11$},{$11\bar{1}$}	27	1.0	{$\bar{1}11$},{$11\bar{1}$}, {201}		not detected		III	II
417kb	68	1.6	{$\bar{1}11$},{$11\bar{1}$}	72	1.3	{$\bar{1}11$},{$11\bar{1}$}, {$\bar{1}01$},{$\bar{1}1\bar{1}$}	48	1.7	{$\bar{1}11$},{$11\bar{1}$}, {001},{010}		

IV.2.2C (iv) Symmetry changes

The "best fit" method used to obtain orientations for planar elements (Appendix B) relies on the three optic directions within grains as standard coordinates. Miller indices were assigned to the various measured planes based on the position of these optic directions in the unshocked microcline lattice. The assumptions made were that the birefringent areas containing planar features retain the original microcline structure, and the positions of optic directions relative to the microcline lattice do not change as shock load increases.

The development of cleavage-like features parallel to $\{\bar{1}11\}$ and $\{11\bar{1}\}$ over virtually the entire pressure range, plus the retention of original pericline twins and the (001) cleavage, provides the opportunity for assessing the validity of these assumptions. Figure IV.11 is a stereogram of the regions of concentration of these four planar elements from samples at roughly 100kb-intervals over the entire pressure range. It is evident that the corresponding areas for each sample are not superimposed but show a distinct counter-clockwise migration with increasing pressure. The angles $Y\Lambda(\bar{1}11)$ and $Y\Lambda(11\bar{1})$ decrease by 13° and 30° respectively, between 96 and 417kb. It might be argued that the crystallographic orientation of the cleavage-like planes varies slightly and systematically from sample to sample, and the angles measured are therefore between Y and different planes, all subparallel to $\{\bar{1}11\}$ and $\{11\bar{1}\}$. However, the similar migrations of the pericline twin composition plane and the (001) cleavage indicates that a continual systematic shift of the optic directions in relation to the feldspar lattice occurs over the pressure range investigated. The

$$\int_{\mathbb{R}^n} \varphi(x)\, dx = \int_{\mathbb{R}^n} \varphi(x)\, dx \qquad (1.1)$$

Fig. IV.11

Composite plot of basal (001) cleavage, pericline twins, and shock-induced planar elements (cleavages, twins, and planar deformation features) parallel to $(\bar{1}11)$ and $(11\bar{1})$ measured in unshocked and shocked microcline. Arrows indicate apparent counter-clockwise migration of lattice with respect to optic directions X, Y, and Z, as pressure increases. Position of twin-like features for 417kb near pericline twins contradicts this rotation, and is thus believed to represent development of shock-induced twins of different orientation.

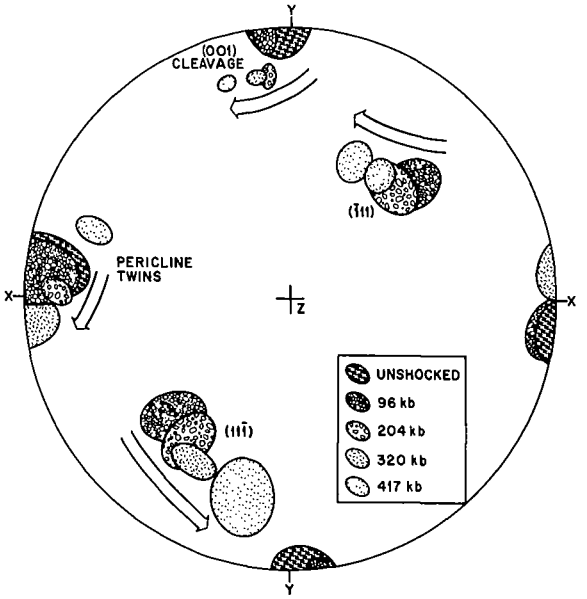
Y
(001)
CLEAVAGE
(1̄11)
PERICLINE
TWINS
X
X
Z
UNSHOCKED
96 kb
204 kb
320 kb
417 kb
(111̄)
Y

counter-clockwise migration is consistent and thus the twin-like features in the 417kb sample which plot near the rhombic section of the unshocked sample cannot be original pericline twins.

Since the $Y\Lambda(11\bar{1})$ angle decreases significantly more than the $Y\Lambda(\bar{1}11)$ angle, the validity of the other assumption may also be questioned. This is confirmed by measurement of the angle $(001)\Lambda(\bar{1}11)$ at the four pressures illustrated as it decreases by approximately 14° in the range 96 to 417kb. This indicates that the crystal structure of the feldspar has been modified continuously, most obviously between 320 and 417kb. The nature of this modification cannot be determined from the little information available in the stereogram. If it is assumed that the structure remains triclinic, then to calculate the six new structural parameters ($\underline{a},\underline{b},\underline{c},\alpha,\beta,\gamma$) would require knowledge of the interplanar angle between six pairs of planes. The decrease in the $(001)\Lambda(\bar{1}11)$ angle could be produced, for example, by a shortening of the $\underline{c}$-axis relative to the $\underline{a}$- and $\underline{b}$-axes, or by an increase in α or β.

IV.2.2D X-ray Examination

X-ray powder diffraction patterns were obtained for each shocked sample and for the unshocked feldspar by using a 114.83mm diameter, Debije-Scherrer camera. A standard series of 2-, 6- and 10-hour exposures was prepared using CuKα radiation. Several of the highly shocked samples received longer exposures in attempts to improve weak patterns, and various samples were subjected to extended periods (up to 98 hrs) of Cr or Co radiation in the hopes of achieving finer resolution of the crowded feldspar pattern.

The unshocked feldspar has an x-ray pattern typical of maximum microcline, with a few reflections due to albite in perthitic intergrowth (Plate IV.6, Figure IV.12). A high degree of Si-Al ordering in the unshocked microcline is shown by triclinicity values of 0.91 and 0.94±0.03 (Table IV.2), determined from Debije-Scherrer patterns and diffractometer traces respectively. Parameters for the microcline unit cell (Table C.1, Appendix C) were determined from measurement and indexing of the Debije-Scherrer patterns, and use of a revised version of Evans et al.'s (1963) least squares unit-cell refinement program. The highly potassic composition and maximum symmetry are confined by plotting a vs b, α^* vs γ^*, and $2\theta CuK\alpha_1$ (060) vs $2\theta CuK\alpha_1$ ($\bar{2}04$), and comparing with standard plots (Wright and Stewart, 1968; Wright, 1968) which allow graphical determinations of structural state.

Three main regions within the pressure range can be distinguished from examination of the Debije-Scherrer patterns of the shocked samples and comparison with that for the normal feldspar mixture. The five samples shocked to below 100kb produce patterns identical in character and intensity to the unshocked material, indicating that no permanent structural changes have taken place. Within the pressure range represented by samples shocked to 150 to 270kb, the patterns exhibit a gradual modification which can be described as the combined result of four changes. (1) The intensity of the microcline reflections shows a continuous decrease so that at 270kb, virtually all the original weak reflections, particularly those of the back-reflection region, have faded to obscurity and others are much reduced. The fact that reflections such as ($\bar{1}\bar{1}1$), ($1\bar{1}1$) and (131) disappear whereas ($\bar{1}11$), (111) and ($1\bar{3}1$) remain cannot be attributed to a

Plate IV.6

Debije-Scherrer patterns of experimentally shocked microcline and perthitic albite. Top, unshocked feldspar. Middle, shocked at 191kb. Microcline lines, particularly back reflections (right) are weakened. Initial appearance of reflection from high-pressure phase with d=5.16°A. Bottom, shocked at 413kb. Pattern largely that of high pressure phase (cf. Fig. IV.12). Exposed to CuK_{α} radiation for 10 hours.

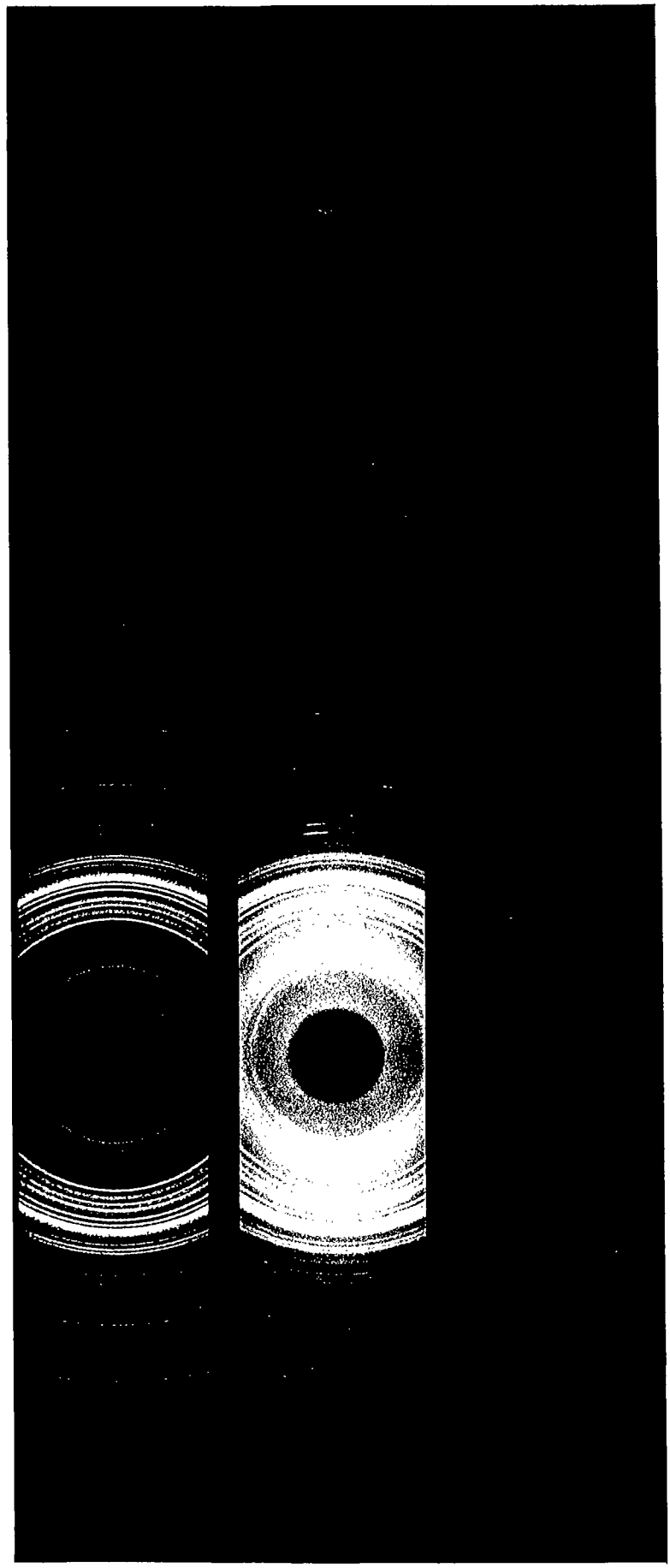

shift to monoclinic or higher symmetry. Triclinicity calculations (Table IV.2) reveal that the two sets of reflections do not show a tendency to approach and merge, but rather the former set disappear simply because they are originally weak reflections. (2) The albite reflections not masked by microcline lines, such as $(\bar{2}01)$ and (002), increase in intensity by comparison with their intensity relative to the microcline lines in the unshocked sample. In addition, some of the microcline lines also exhibit this relatively stronger character, in contrast to the general fading of the microcline pattern. However, in all cases these reflections coincide with strong to moderate albite lines, such as (001), (111), $(\bar{1}30)$, $(1\bar{3}1)$, $(\bar{2}\bar{4}1)$ and $(\bar{2}41)$, and it is the strengthening of these albite reflections which is actually apparent. Thus the microcline structure experiences a breakdown of long-range ordering, which encompasses a successively greater proportion of the sample as pressure increases. The albite structure appears unaffected, or very little affected, and so represents an increasingly higher proportion of the crystalline part of the sample. (3) A weak reflection from planes of d=5.16Å spacing is first detected at 191kb, and increases in intensity as the shock stress rises. Since such a reflection is not part of the original microcline or albite pattern, and because it becomes stronger with increasing pressure, it is interpreted as an indication of the development of a high-pressure phase. (4) A slight but distinct strengthening of a reflection from planes with d=2.07Å is noticed in the 270kb sample. Although this line coincides with weak reflections for both albite and microcline, it appears to exhibit an anomalous increase compared with other feldspar lines of corresponding original intensity. It is thus

also interpreted as belonging to a high-pressure phase. Therefore, in the 270kb sample the Debije-Scherrer pattern consists of a moderately weakened microcline signature, and a comparatively stronger set of albite reflections, plus two reflections from an unknown, presumed high-pressure phase.

A marked change in the pattern occurs between the 270 and 317kb samples. In the 317kb sample, the microcline reflections have weakened considerably and most of the albite lines have also faded to a great extent. However, several lines, originally indexed in the albite or microcline structures, still appear as strong as for lower pressure samples. The two new reflections at 5.16Å and 2.07Å have become stronger. For the 417kb sample the overall pattern is virtually identical to that obtained 100kb lower except that the fading, undoubted microcline and albite lines have practically disappeared, and several new, very weak and dubious reflections have appeared. Thus the Debije-Scherrer pattern for the most highly shocked sample of the experiments comprises 21 resolvable lines in contrast to well over 80 from the original material (Figure IV.12). Five of the weaker lines are remnants of the original strong microcline ($(\bar{2}01)$, $(\bar{1}\bar{1}2)$, (060) and $(\bar{2}04)$) and albite ($(\bar{2}01)$) reflections which have not faded to obscurity. Three others (d=5.16, 4.72 and 2.07Å) are distinct, new reflections readily detected in all patterns prepared from the 417kb sample. Four additional new lines (d=8.89, 5.93, 5.57 and 4.92Å) are extremely weak and not consistently observed. The remaining nine reflections, which are generally the strongest lines of the pattern, agree closely with original microcline and albite reflections. However, because they retain a high

Fig. IV.12

Schematic, partial Debije-Scherrer pattern of front reflections from unshocked perthitic microcline (right), compared to those from microcline shocked to greater than 300kb (left). Shocked pattern comprises five original feldspar reflections, twelve reflections from high-pressure phase, and four weak reflections observed in some patterns only.

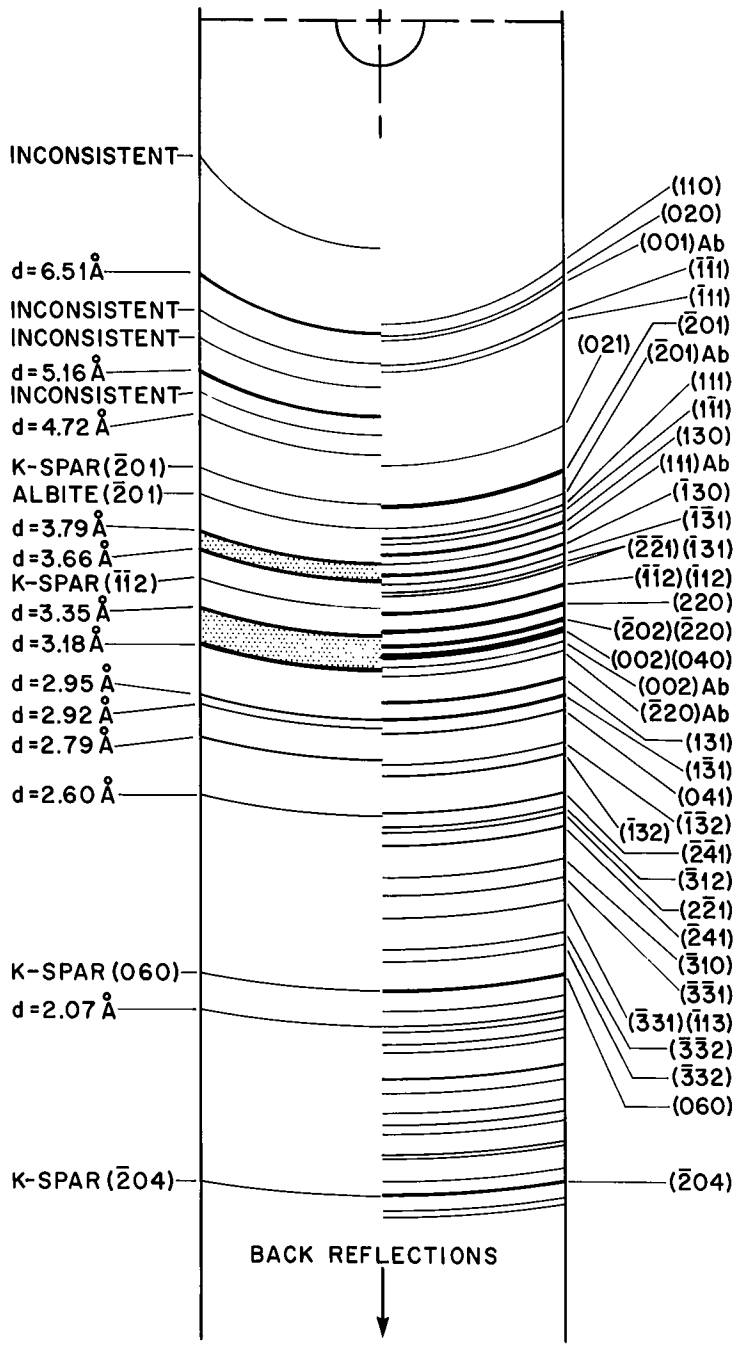
INCONSISTENT
d=6.51Å
INCONSISTENT
INCONSISTENT
d=5.16Å
INCONSISTENT
d=4.72Å
K-SPAR(2̄01)
ALBITE(2̄01)
d=3.79Å
d=3.66Å
K-SPAR(1̄1̄2)
d=3.35Å
d=3.18Å
d=2.95Å
d=2.92Å
d=2.79Å
d=2.60Å
K-SPAR(060)
d=2.07Å
K-SPAR(2̄04)
(110)
(020)
(001)Ab
(1̄1̄1)
(1̄11)
(2̄01)
(021)
(2̄01)Ab
(111)
(11̄1)
(130)
(111)Ab
(1̄30)
(1̄31)
(2̄2̄1)(131)
(1̄1̄2)(1̄12)
(220)
(2̄02)(2̄20)
(002)(040)
(002)Ab
(2̄20)Ab
(131)
(1̄31)
(041)
(1̄32)(1̄3̄2)
(2̄41)
(3̄12)
(22̄1)
(241)
(3̄10)
(3̄3̄1)
(3̄31)(1̄13)
(3̄3̄2)
(3̄32)
(060)
(2̄04)
BACK REFLECTIONS

intensity by comparison with their fading, originally strong neighbours, and show slight differences in spacing from the original feldspar planes, they are interpreted as belonging to a high-pressure phase (or phases). The resulting twelve strong reflections and four uncertain lines representing onr or more high-pressure phases are listed in Table IV.5 and depicted in a schematic Debije-Scherrer pattern in Figure IV.12.

Identification of the new phase or phases present in the 320 and 417kb samples is unfortunately difficult and inconclusive. One of the main problems is assumed to be due to the presence of two separate phases, microcline and albite, in the original material. Because the Hugoniots for these two minerals are almost identical (Ahrens et al., 1969) as a consequence of their similar chemistry and structure, there is a high probability that high-pressure polymorphs for both phases have been formed, and the resulting Debije-Scherrer pattern may be due to a mixture of the two.

The unknown pattern was compared with patterns for the predicted feldspar high-pressure polymorphs, patterns of possible products of feldspar breakdown, possible reflections due to contamination from the stainless-steel sample holder, and mixtures of two or more of these likely phases. The Debije-Scherrer pattern for the highly shocked feldspar does not coincide with: (a) the potassium-hollandite structure (Ringwood et al., 1967a), (b) jadeite plus quartz, coesite or stishovite, the high pressure breakdown products of albite (Kennedy, 1961), (c) $NaAlSiO_4$ (calcium ferrite structure) plus quartz, coesite or stishovite, the predicted high-pressure breakdown products of jadeite (Reid et al., 1967), (d) austenite (18-8 steel) (no high-pressure phase of 304 stainless

Table IV.5 Interplanar spacing for reflections from tectosilicate high-pressure phases.

Microcline* (320 & 417kb)		Sclar and Usselman** (250kb)		$KAlSi_3O_8$*** (hollandite structure)		Jadeite****		Stishovite****	
dÅ	I	dÅ	I	dÅ	I	dÅ	I	dÅ	I
6.487-6.525	M								
				6.635	15				
5.164-5.158	M								
4.708-4.720	VW			4.692	15				
						4.347	15		
						4.281	24		
3.789-3.792	M								
3.652-3.666	M								
3.347-3.360	M								
				3.314	18				
3.174-3.182	S								
				2.965	81				
2.956	W							2.955	100
2.920	VW					2.917	100		
						2.827	72		
2.784-2.789	W								
		2.74	S						
2.603-2.608	VW								
						2.488	47		
						2.414	30		
				2.291	22				
								2.247	25
						2.158	17		
						2.151	17		
				2.096	12				
2.076-2.084	VW								
						2.066	19		
				2.059	54				
		2.01	M						
								1.979	39
		1.96	M			1.966	18		
								1.869	12
				1.839	10				
		1.76	VW	1.749	22				
				1.563	12	1.570	15		
								1.530	42
				1.469	21			1.478	15
				1.291	17				
								1.235	13
		0.865	VW						
		0.838	W						

* - This study ** - Personal communication, 1972 *** - Ringwood et al., 1967 **** - Borg and Smith, 1969

steel is predicted from its Hugoniot (McQueen et al., 1970), (e) the reflections from a phase (unidentified) produced by Sclar and Usselman (1970 and personal communication) in recovery shock experiments on intermediate microcline, (f) leucite plus silica, low pressure-low temperature breakdown products of K-feldspar.

The weak reflections at d=2.956Å and 2.92Å, however do agree with the strongest lines in the potassium-hollandite (d_{310}= 2.965Å), jadeite ($d_{\bar{2}21}$=2.917Å) and stishovite (d_{110}=2.955Å) patterns, although none of the less intense reflections of these minerals can be detected. In other words, jadeite, stishovite, or potassium-hollandite may exist in small quantity in the shock product mixture, but the major phase or phases cannot be correlated with known high-pressure polymorphs produced or predicted as the result of shock metamorphism of alkali feldspars.

Attempts were made to assign Miller indices to the reflections on the basis of cubic, tetragonal, and orthorhombic symmetry but without success. Similar systematic trial solutions requiring monoclinic and triclinic symmetry were not attempted because of the difficulties involved in varying four and six parameters respectively. The possibility of high symmetry cannot be ruled out, however, as more than one phase may be present, and the resulting intermixing of the patterns would tend to confuse straightforward indexing procedures.

IV.2.2E Electron Microprobe Analysis

A small portion, approximately 2mm square, of the sample recovered from the 417kb experiment was analyzed using an electron

Table IV.6 Composition of shocked and unshocked alkali feldspar from electron microprobe analyses (wt %).

	Unshocked Feldspar*		Feldspar Shocked to 417kb**
	Potassic Phase	Sodic Phase	Bulk
SiO_2	63.70	67.93	64.64
Al_2O_3	18.65	18.38	17.78
K_2O	16.25	0.09	16.19
Na_2O	0.74	11.73	0.54
CaO	0.01	0.21	0.01
Total	99.35	98.34	99.16

* - analysis by P.B.Robertson, University of Durham

** - analysis by A.G.Plant, Geological Survey of Canada

Plate IV.7

a & b) Electron microprobe, x-ray scanning photographs showing distribution of potassium (light areas) in microcline shocked to 417kb. Grid squares are approximately 12μ square.

c) X-ray scanning photograph of Na-distribution (lighter regions) over same area as IV.7b, showing that the shocked microcline comprises small, irregular, Na-rich regions in a potassium-rich host. (Na regions seen as dark patches in a) and b)).

a

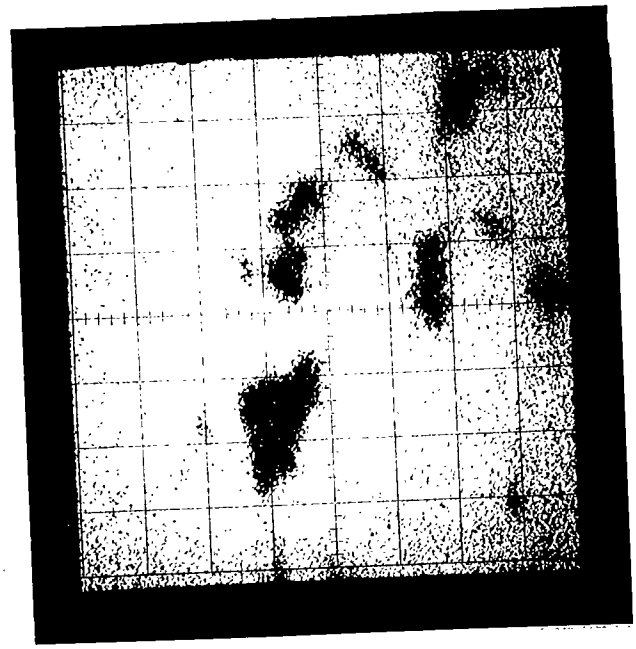

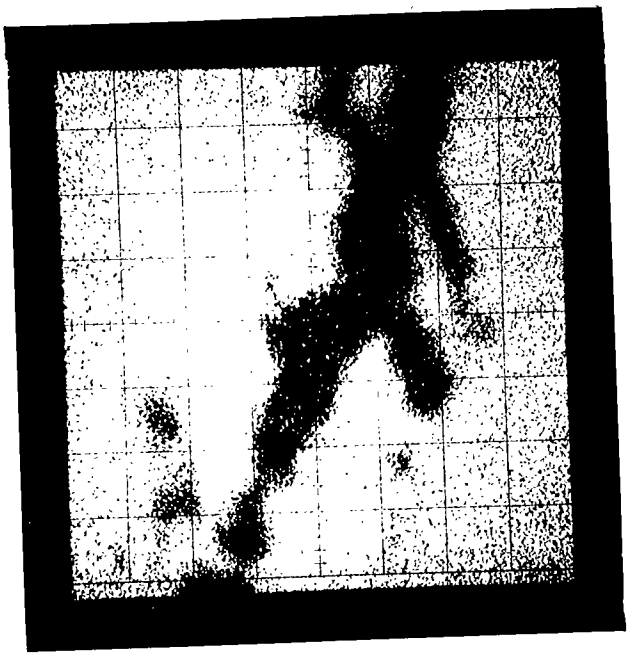

b

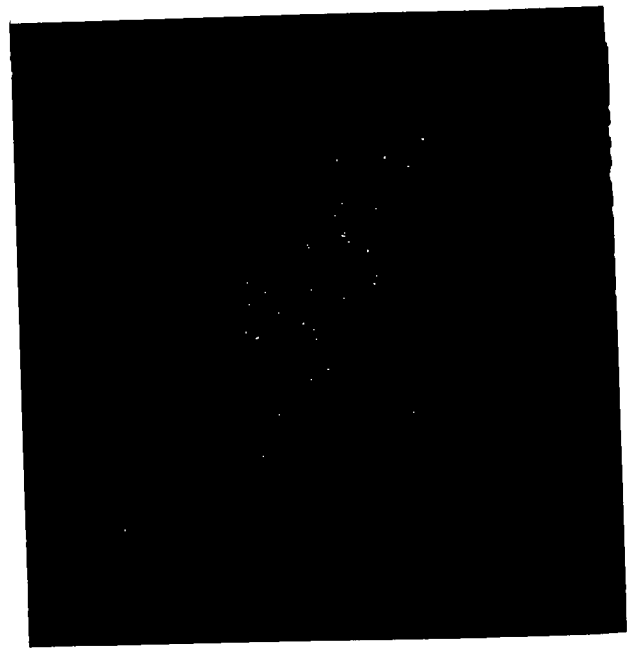

c

microprobe. The grain was mounted with the (001) cleavage perpendicular to the electron beam.

Generally, the loss of alkalis from crystalline feldspars during microprobe analysis can be minimized by using a defocussed beam. A rapid decrease, however, of x-ray intensity for Na and K from the shocked feldspar under the defocussed beam was encountered; such behaviour is more typical of alkali feldspar glasses. To further counteract alkali loss the sample was continuously translated under the defocussed beam and the bulk composition was obtained (Table IV.6).

The bulk composition of the shocked feldspar and of the potassic phase of the unshocked material are in good agreement. The shocked feldspar was analyzed on a polished grain so that phase differences, such as remnant perthitic blebs or stringers of albite, were not visible optically. The low Na_2O value detected indicates that albite-rich areas were not encountered as the sample was translated under the beam. Na-rich areas were, however, detected elsewhere in the grain but were too small for analysis using the defocussed beam and moving specimen technique. X-ray scanning photographs of potassium (Plates IV.7a,b) and sodium (Plate IV.7c) distribution reveal the small size and irregular nature of some of these presumably albite-rich areas.

IV.3 Discussion and Summary

The behaviour of the alkali feldspar, largely microcline, in the shock-loading experiments generally coincides with that predicted or observed in related experiments, and with observations on naturally

shocked tectosilicates. In particular, the pre-assignment of samples to the three Shock Regimes and Shock Stages solely on the basis of peak pressures has been validated by observation of the characteristic deformations in samples within each particular group. The shock effects produced in microcline in this series of experiments are summarized, therefore, using the Regime-Stage subdivisions.

IV.3.1 Regime - Stage Subdivisions of Shock Effects

Regime I - Stage 0. Peak pressures of 37, 58, 87, 96 and 99kb.

Within experimental error the density does not change from the 2.553g cm^{-3} value of the unshocked perthitic microcline.

Refractive indices show a slight decrease (approximately 0.001) at 99kb from the values of the unshocked microcline. Birefringence also decreases slightly but is uniform within the shocked material. Optic axial angle ($2V_{\alpha}$) increases slightly from 81° to 84°.

The original cleavages parallel to (001) and (010) retain the same relative prominence as in the unshocked feldspar. Cleavage-like features parallel to $\{\bar{1}11\}$ and $\{11\bar{1}\}$ are first developed in the sample shocked to 58kb. They differ from the pre-shock cleavages in that they traverse the interior of grains but seldom form cleavage faces or edges.

The original M-twins retain their strong development over this pressure range.

The intensity and spacing of reflections in Debije-Scherrer patterns remain the same as those of the unshocked feldspar.

The deformation, or lack of it, in Regime I-Stage 0 indicates

that no reconstructive transformation has occurred in the microcline. Although the maximum pressure in this group of samples (99kb) is above the Hugoniot elastic limit determined for microcline (79-85kb), Ahrens et al. (1969) believed that no anomalous compression occurs below 114kb. The development of cleavage-like features parallel to $\{\bar{1}11\}$ and $\{11\bar{1}\}$ does appear to be a characteristic of shock. Although tensional fractures are produced at normal geologic strain rates, $\{\bar{1}11\}$ and $\{11\bar{1}\}$ orientations for such cleavages have not been reported.

Regime II - Stage I. Peak pressures of 150, 154, 167, 191, 204, 250 and 270kb.

The microscopic and x-ray observations indicate that this pressure range can be divided into a lower Regime II-Stage I between approximately 100kb and 175kb, and an upper Regime II-StageI from 175kb to approximately 300kb.

Within lower Regime II-Stage I, slight and gradual decreases occur in density, refractive indices, and birefringence of the shocked feldspar. Insufficient optic-axial angle measurements were available to determine whether a corresponding gradual change of this optical parameter has continued. An apparent enhanced development of the (001) cleavage over this region would cause the optic axial plane to lie preferentially nearly parallel to the microscope stage and it would thus be inaccessible for 2V measurements.

Shock-induced cleavages parallel to $\{\bar{1}11\}$ and $\{11\bar{1}\}$ now occur in approximately 70% of the grains. In addition, cleavage-like features parallel to the [001] zone and the rhombic section are evident within

lower Regime II-Stage I.

Planar deformation features, generally also parallel to $\{\bar{1}11\}$ and $\{11\bar{1}\}$, show an initial weak development over this range, appearing in 13% of the grains from the sample shocked to 150kb. Original albite-pericline M-twins persist and no other twins or twin-like features were detected. As pressure increases, Debije-Scherrer patterns of the shocked feldspar show a gradual decrease in intensity of the microcline reflections, particularly in the back-reflection region. Reflections from the perthitic albite phase are apparently less affected and thus appear relatively strengthened in relation to the weakening microcline lines.

For the most part, the deformations which characterize upper Regime II-Stage I (175-300kb) are those initiated in the 100-175kb region, but to a more pronounced degree. A sharper decrease occurs in density and refractive indices, with a relatively greater drop in $n\gamma$ causing a corresponding diminution in birefringence. Patchy birefringence within grains exists due to non-uniform decreases in the refractive indices. Sufficient grains are available with the optic plane accessible to indicate a continuing, modest increase in $2V\alpha$, reaching 87° in the sample shocked to 270kb.

It is possible that the reduced tendency for grains to rest on the (001) cleavage indicates poorer development along this plane. Shock-induced cleavage-like planes parallel to $\{\bar{1}11\}$ and $\{11\bar{1}\}$ are abundant, detected in over 90% of the grains at each shock pressure. The cleavage-like features parallel to (hk0) and the rhombic section are only rarely encountered.

Planar deformation features parallel to {$\bar{1}11$} and {$11\bar{1}$} are commonly developed, reaching a maximum occurrence in 67% of the sample shocked to 204kb, and diminishing at higher pressures.

Twin-like, shock-induced planar features are first detected in samples from upper Regime II-Stage I. It is often difficult to distinguish between the twin-like type of deformation and planar deformation features. This may be responsible for the apparent decrease in development of the latter type above 204kb.

Breakdown of the feldspar structure, as evidenced by decreasing intensity of the Debije-Scherrer patterns, continues. The pattern produced by the sample shocked to 270kb comprises a moderately weakened microcline signature with no back reflections, and a comparatively stronger (but weaker in absolute terms) set of albite reflections. In addition, two non-feldspar reflections at d=5.16Å and d=2.07Å are first detected at 191kb and 270kb respectively.

The shock effects described for Regime II - Stage I result from four consecutive processes: distortion of the microcline structure, breakdown of the microcline structure, formation of a high-pressure phase, and inversion from the unstable, high-pressure phase.

Distortion of the microcline structure causes dislocation and lattice gliding to produce planar deformation features. The more common orientations of these planes are not those along which normal cleavage or twinning occurs, suggesting that shock compression has deformed the original structure creating new planes of weakness. The initial development of planar deformation features at 150kb agrees with the observations of Müller and Hornemann (personal communication in

Stöffler, 1972) on experimentally shocked plagioclase.

Shock compression begins to destroy the long-range ordering of the microcline by creating domains with a range of sizes, each of which retains the ordered structure. Disorientation of adjacent domains results in decreased intensity of x-ray reflections from particular planes. Planes of small d-spacing are most sensitive to even slight disorientation, and thus the back-reflections in the Debije-Scherrer patterns fade and disappear more rapidly than those reflections of low 2θ. The continuous intensity decrease in Debije-Scherrer patterns for samples subjected to pressures greater than approximately 100kb is due to breakdown of the microcline structure into successively smaller domains as pressure increases. Hörz and Quaide (1973) calculated that for plagioclase, back reflections begin to fade for domains in the range 10^{-6} to 2×10^{-5}cm in diameter; back reflections disappear for domains between 5×10^{-7} to 10^{-6}cm; and plagioclase is amorphous to x-rays for domains smaller than 5×10^{-7}cm.

Increased shock compression transforms the minute domains to a high-pressure phase with six-fold coordination of silicon and oxygen (Stöffler and Hornemann, 1972). The initial transformation may occur along the planar deformation features (Stöffler, 1971a). With increasing pressure, a greater proportion of the sample is transformed and in the present case, forms a percentage sufficient for x-ray detection in the 191kb sample.

Following the passage of the shock wave, the unstable, high-pressure phase inverts in part to an amorphous, low density, dia-

plectic glass. The reduction in bulk density, refractive indices, and birefringence for Regime II - Stage I samples is due to the coexistence of original feldspar, high-pressure phase, and diaplectic glass, with the latter forming a larger proportion as pressure increases.

Regime III - Stage II. Peak pressures of 317, 320 and 417kb.

The density of the shocked feldspar continues its monotonic decrease to a value of 2.396±0.01g cm^{-3} for the sample subjected to 417kb. This value lies well below those of normal crystalline feldspars, but lies above 2.377g cm^{-3} for a thermally melted feldspar glass of Or_{94} Ab_6 composition.

Refractive indices and birefringence steadily decrease as peak shock-pressure increases. The values for $n\alpha$ (1.490), $n\gamma$ (1.492) in the nearly isotropic areas of the most highly shocked sample, are higher than the values for potassic feldspar glass (n=1.487). Optic axial angle measurements were obtained from between 50% and 68% of the grains examined from samples in this pressure range, compared with 33% in the unshocked and weakly shocked material. The slight increase in $2V\alpha$ continues, reaching a maximum average value of 88°.

The trend toward increased development of shock-induced planar elements also continues. The $\{\bar{1}11\}$ and $\{11\bar{1}\}$ cleavage-like planes maintain their dominance and the few other orientations present are not as convincingly grouped.

Planar deformation features generally with these Miller indices are less common than in the Regime II - Stage I samples. They appear to give away to a higher proportion of twin-like features of the same

common orientations. In addition, twin-like planar elements parallel to $\{\bar{1}01\}$ are developed only in grains shocked to Regime III - Stage II levels. Many of the $\{\bar{1}11\}$ and $\{11\bar{1}\}$ planar elements, particularly the cleavage-like fractures, contain a low refractive index, almost isotropic phase which may be diaplectic glass.

The main definitive characteristic of Regime III - Stage II samples is their internal structure revealed in Debije-Scherrer patterns. Whereas the patterns from the less highly-shocked material show a continuous, gradual decrease in intensity of the feldspar reflections, the modifications are minimal above 300kb, when a stabilized, largely non-feldspar pattern is produced. The reflections, about 21 in total (in contrast to well over 80 from the unshocked feldspar), are weak. Several are original microcline or albite reflections. Others, often the strongest, are apparently related to feldspar lines but are modified in intensity and position. Reflections from planes with d=5.16, 4.72, and 2.07Å are new, non-feldspar lines. As yet, the pattern produced by these highly shocked feldspars, with or without the half-dozen original microcline and albite reflections, cannot be correlated with any identified phase or combination of phases.

Electron microprobe analysis shows that the composition of the shocked feldspar and the microcline phase of the unshocked feldspar are in good agreement. Sodium-rich areas detected by x-ray scanning for Na and K indicate that more than one phase exists in the most highly shocked sample, and that complete homogenization has not occurred.

IV.3.2 Comparison with Observations of Others on Shocked Feldspars

Regime III of a tectosilicate Hugoniot has been considered by Ahrens et al. (1969) as the Hugoniot of the high-pressure phase; in this region (above approximately 300kb) the entire starting material has been converted to a dense polymorph. In nature, Stage II (above approximately 360kb for tectosilicates) is typified by complete transformation to diaplectic glass which has inverted from a high-pressure polymorph (Stöffler, 1971a). Debije-Scherrer patterns for the 317, 320 and 417kb samples described here, conform partly to both these observations, with microcline reflections virtually disappearing and an unidentified, crystalline phase forming a constant fraction of the highly disordered material. The development of planar features in this anisotropic phase has two possible explanations. The planes may be tensional features produced in the new phase upon pressure release, or they may have originated as dislocations in the microcline lattice which were then preserved in the structurally-related, high-pressure phase. The presence of glass along the planes, and the constant orientation of the cleavage-like, twin-like, and planar deformation features in both weakly shocked microcline and the high-pressure phase suggest the latter explanation.

The lower limit of Stage III is set where peak pressures are accompanied by post-shock temperatures exceeding the melting point of tectosilicates. Stöffler (1971a) suggests that the softening temperature of synthetic feldspar glass, 850-900°C, may be an appropriate threshold value. Although temperature was not determined in the current experiments, Ahrens et al. (1969) calculated that post-shock temperatures reached 600-

668°C in oligoclase shocked to 417kb in a similar experiment. The shocked microcline described here shows no evidence of melting. Therefore, Stage III or higher deformation of microcline was not produced in these shock experiments.

IV.3.3 High-Pressure Phase

Certain properties of the shock-product assemblages in these experiments are significantly different from those predicted or observed in related experiments and in natural shock-metamorphic suites.

Ahrens et al. (1969) and Ahrens and Liu (1973) concluded from Equation of State experiments that at shock pressures greater than approximately 300kb, microcline and orthoclase are completely converted to the high-pressure form with hollandite structure. They believed that this dense polymorph inverts almost entirely to a diaplectic glass upon pressure release. This was supported by Kleeman's (1971) experiments in which at least 95 per cent of the assemblage produced by shock-loading orthoclase to 320, 322, and 345kb consisted of diaplectic, alkali feldspar glass. Similarly, adularia (Stöffler and Hornemann, 1972) and labradorite (Müller and Hornemann, 1967) were completely converted to appropriate diaplectic phases at shock pressures of 360kb and 330kb respectively. In addition, natural diaplectic feldspar glasses are well known from impact sites (see section I.1.2C) but contain no evidence for the hollandite-type, crystalline polymorph.

The present set of experiments partially concurs with these observations and hypotheses; the microcline structure has been virtually destroyed in the 317, 320 and 417kb samples, and a nearly isotropic phase

is present. Refractive indices of the near-isotropic areas range from a maximum of 1.502 at 320kb to a minimum of 1.490 at 417kb, and thus lie within the span of R.I. values (approximately 1.488 to 1.508) determined by Stöffler and Hornemann (1972) for natural and experimental diaplectic K-feldspar. In contrast to the earlier work, however, the present assemblage is not entirely diaplectic glass; in fact, approximately 90 per cent of each of these samples is weakly birefringent. Debije-Scherrer patterns indicate the presence of a weakly developed crystalline phase, but not the hollandite-type feldspar. The apparent inconsistency, of a large amount of anisotropic material producing a weak x-ray pattern, may be the result of only limited long-range ordering in the crystalline structure.

Three possible explanations for the results of these experiments and the differences from other related studies are: (1) A crystalline, high-pressure phase other than the hollandite-type structure was created directly from the alkali feldspar, and a small amount has inverted to diaplectic or near-diaplectic forms. (2) The feldspar was completely converted to the hollandite-type phase which inverted to diaplectic glass, and a lower density, crystalline phase has nucleated from most of the glass. (3) Peak pressures, produced a high-pressure phase (hollandite-type?) along planar elements and it has inverted to diaplectic glass. Gradual disordering of the bulk of the feldspar by the shock process has directly produced a highly-disordered, low density crystalline phase closely related in structure to the original feldspar.

Arguments opposed to the first possibility are: a high-pressure

phase created directly from the shock-wave would have a high density, inconsistent with the measured values; a high-pressure compact, highly-ordered phase would produce a strong x-ray pattern, particularly as crystalline material constitutes at least 90% of the products; it is more likely that a high-pressure phase would be preserved along deformation planes, rather than selective inversion to diaplectic glass along these features. The second possible explanation may be considered analogous to the high-pressure transformation of quartz where coesite is believed to nucleate from diaplectic glass which has inverted from the unstable polymorph, stishovite. Considering the present experiments, although the shocked microcline was not quenched, cooling was rapid by comparison with the natural shock environments where elevated post-shock temperatures have persisted allowing the growth of coesite. It is unlikely, therefore, that a feldspar equivalent of coesite could have formed during rapid cooling. Also, if such a phase did nucleate from diaplectic glass then planar elements containing fresh diaplectic glass would not be preserved.

The third explanation is the most plausible. The entire grain was not converted to a high-pressure phase with subsequent inversion to a diaplectic form. The only true diaplectic glass occurs along planar elements where conversion to high-pressure phases begins. Planar deformations which would probably disappear, or not even be produced in the high-pressure phase, exist at all but the lowest shock levels, and with the same orientations. Original twinning is weakly preserved in even the most highly shocked microclines. The decrease in density, refractive index and intensity of x-ray reflections with increasing pressure indicates

a gradual, progressive disordering of the microcline structure, virtually complete above 300kb, to a high-pressure form. This phase is designated as a high-pressure product due to its formation in the shock experiments, although it is not a dense, compact microcline polymorph. It may be possible to duplicate it under other physical conditions which induce disordering. Why this disordered phase has been produced in contrast to the formation of diaplectic feldspar glasses at the same pressures in similar experiments, is not understood.

CHAPTER V

CONCLUSIONS

Potassic feldspars subjected to strong shock pressures by the impact of a large meteorite or in laboratory experiments, exhibit several types of deformation of which some may be considered characteristic of shock metamorphism. The object of the present investigation, namely to describe the various styles of deformation and to delimit their conditions of formation throughout the entire range of pressures and temperatures produced in an impact event, has largely been realized. The three craters sampled, Charlevoix, Lac Couture and Brent, provided a reasonably complete suite of unshocked to moderately highly shocked material. Peak pressures attained in these natural samples were estimated at a maximum of 360±40kb. Material representative of higher shock levels is believed to have been eroded and lost, as at Charlevoix, or to have experienced subsequent thermal metamorphism which obscured most shock effects, as at Brent. The experimentally shocked material, however, permitted examination of potassic feldspars shocked to a maximum pressure of 417kb. Thus the scheme of progressive shock metamorphism compiled for potassic feldspars is applicable more precisely in the low to moderately high shock levels. Observations from the literature, describing more highly deformed feldspar, can be appended to the scheme. Not surprisingly, the development of deformation is similar in microcline and orthoclase but, on the other hand, differences exist between microclines shocked in natural and experimental events.

Shock deformation of alkali feldspars results in changes in (i) physical appearance (fracturing, planar deformation features, twinning,

colour), (ii) crystal structure (degree of ordering, phase changes, density), (iii) optical properties (refractive index, birefringence, optic angle) and (iv) compositional rearrangements (perthitic intergrowths). The appearance or evidence of each modification has been described in earlier chapters, and in the following paragraphs their formation is related to particular sets of conditions and an explanation of their development is attempted.

V.1 Changes in Outward Physical Appearance, Visible either in Hand Specimen or Microscopically

V.1.1 Fracturing

Shock-induced fracturing in feldspars is of three types: random, along common cleavage planes, and parallel to faces rarely or never reported as planar fracture surfaces. Irregular or random fracturing, without apparent crystallographic control, is weakly developed at low shock pressures. Quartz, in contrast, shows strong random fracturing below 100kb (Robertson et al., 1968). The comparatively weak development in feldspar is probably a result of strain release preferentially along lattice planes of weakness, resulting in the commonly found cleavages. Such planes are less well-defined in the quartz lattice, resulting in fewer cleavages and a greater degree of random fracturing. The most common feldspar cleavages, (001) and (010), are developed over the pressure range investigated with the possibility, determined from the shock experiments, that the basal form may be more prominent in the 150 to 200kb portion. Cleavages or partings with uncommon or unusual orientations are first developed between 150 and

170kb, and can be found up through the most highly shocked feldspars. The first of these lie in the [001] zone between (100) and (130), possibly (120), and between ($\bar{1}30$) and ($\bar{3}10$), probably ($\bar{2}10$). Cleavages in this zone are rare but are known in unshocked feldspars. At higher pressures, above perhaps 300kb, cleavages are formed in the [111] zone along ($11\bar{2}$), (031), ($01\bar{1}$), and (101). As far as is known, such planes have not been reported as feldspar cleavages elsewhere. Their production by strong shock pressures has two possible explanations. Stresses may have reached the threshold needed to break bonds along planes of only moderate weakness in the existing feldspar structure. On the other hand, rearrangement of the feldspar lattice under compression may have created new planes of weakness; fracturing occurred which, upon stress relaxation and restoration of the feldspar structure, can be given indices in the unshocked lattice.

Prominent shock-induced fractures along {$11\bar{1}$} and {$\bar{1}11$} in experimentally deformed microcline are an apparent anomaly. They are strongly developed even in their initial occurrence at <60kb, much lower than the first appearance of the other rare cleavages, and are prominent to the highest pressures, but yet were not recorded in the naturally shocked feldspars. It might be argued that these planes are a function of orientation of the material with respect to the stress, as the one-dimensional shock waves are always normal to (001). Deformation along particular planes is undoubtedly more readily produced by certain favourable stress directions, as has been demonstrated in shock experiments on quartz (Hörz, 1968; Müller and Défourneaux, 1968). However, if this were the sole criterion for formation of {$11\bar{1}$} and {$\bar{1}11$} cleavages, at least

some grains at Charlevoix should, by chance, have been oriented favourably for their development. A second possible argument might be that the $\{11\bar{1}\}$ and $\{\bar{1}11\}$ planes have been misidentified or misplotted, and that actually they have Miller indices corresponding to features measured at Charlevoix or Lac Couture. This doubt is allayed when it is considered that there is agreement between the experimentally and naturally shocked material on the indices of the other shock-induced cleavages. Also, the $\{11\bar{1}\}$ planes lie approximately 65° from (010) in the experimental material, whereas at Charlevoix the prominent groupings for which they may have been mistaken lie approximately 37° from (010), a plane readily identified. These experimentally shock-induced planes, moreover, have a slightly different character than the [001] cleavages, as outlined in Chapter IV. It seems probable that the nature, orientation and initial development, at surprisingly low pressures, of the $\{11\bar{1}\}$ and $\{\bar{1}11\}$ fracture planes are a function of the particular set of experimental conditions, and that the significance of an absence or existence of such planes in naturally shocked potassic feldspars cannot be evaluated until additional experimental data are available.

V.1.2 Planar Deformation Features

Planar deformation features of the general type described extensively from shock metamorphosed quartz and plagioclase are produced by high strain-rate deformation of potassic feldspar. They are first detected as a weak development between 150 and 200kb, and become stronger and prominent up to approximately 300kb. There are generally two or three sets developed per grain, with a maximum of six sets recorded.

Like the planar features in quartz they conform to certain preferred crystallographic planes but, in contrast to the development in quartz where particular orientations are recorded only above defined stress levels and thus serve as an estimate of shock pressures, no sets or combination of sets seem characteristic of particular levels of shock metamorphism in K-feldspar.

Typically, shocked feldspar grains exhibit two prominent sets of planar features with orientations more or less symmetric about the b-axis. In addition, weaker or secondary sets generally form within 5-10° of the prominent features with the result that most planar features cluster about two primary orientations. Other strong and weak sets with different indices may also be present. Within each suite of feldspars, i.e. Charlevoix orthoclases and microclines, Lac Couture microclines, and experimentally deformed microclines, there is consistency in orientation of the common, best developed sets of planar features. However, between suites this is not strictly the case. At Charlevoix, the two prominent groupings in shocked orthoclase are near $\{24\bar{1}\}$ and $\{\bar{2}41\}$, lying approximately 35° symmetrically about {010}, whereas the principal concentration in microcline is near $\{13\bar{1}\}$, also approximately 30° from {010} but displaced 15° from $\{24\bar{1}\}$. Similarly the two groupings in maximum microcline from Lac Couture lie roughly 40° symmetrically opposed to {010}, but near $\{\bar{1}30\}$ and between {130} to {120}. This actually corresponds to the second most prominent development in the Charlevoix microclines. The pattern is repeated in the experimentally shocked microclines with the dominant planar features parallel to $\{11\bar{1}\}$ and $\{\bar{1}11\}$, approximately 60° on either side of {010}. The orientation

of planar deformation features recorded in the four suites, listed in decreasing order of abundance for each suite are:

Orthoclase (Charlevoix)	- {24$\bar{1}$} and {$\bar{2}$41}
	- [001] zone near {110} and {010}
	- [$\bar{1}\bar{1}$0] zone near {$\bar{1}$10} and {$\bar{1}$11}
	- [$\bar{1}$1$\bar{2}$] and [$\bar{3}$1$\bar{2}$] zones
	- {70$\bar{1}$} (Murchisonite parting)
Intermediate microcline	- {13$\bar{1}$}
(Charlevoix)	- [001] zone near {110}, {120}, {120} & {010
	- [131] zone
Maximum microcline	- {120} and {130}
(Lac Couture)	- {$\bar{1}$30}, {110} and {210}, {11$\bar{1}$} and {22$\bar{1}$}
	- [110] zone between {$\bar{1}$10} and {00$\bar{1}$}
Maximum microcline	- {11$\bar{1}$} and {$\bar{1}$11}
(shock experiments)	- {$\bar{1}$30}, {221} and {$\bar{1}$22}
	- {001}

The nature of planar deformation features has not been completely resolved but several authors have speculated on their conditions and processes of formation. The general concensus is that they are produced by crystal gliding due to yielding at final shock states above the Hugoniot elastic limit (Stöffler, 1972), along glide planes which contain the shortest Bravais vectors (greatest point density) (Engelhardt and Bertsch, 1968). It is likely that translation gliding under high strain-rate deformation of the potassic feldspar lattice creates planar deformation features in this mineral. The observations that the most prominent planes developed in the four suites are different in orientation

is probably due to slight changes in the feldspar structure as a result of increased ordering from orthoclase to maximum microcline. Also it was noted, in connection with abnormal shock-induced fracturing, that experimental conditions do not fully replicate those in natural impact events.

V.1.3 Deformation Twinning

In potassic feldspars subjected to final shock states above approximately 300kb, such as in Charlevoix orthoclases and intermediate microclines, and above 150-200kb in the two groups of maximum microclines, shock-induced twins are developed. Although no confirmation from single crystal X-ray patterns is available, they are considered to be twins on the basis of optics. The orientation of the apparent twin-composition planes of the broadest, best developed twins is the same as that of the prominent planar deformation features created at lower shock pressures. Narrower, weaker twin lamellae, similarly correspond in orientation to less prominent planar deformation features. Normal, narrow planar features of other orientations coexist in grains with deformation twins. Generally, alternate lamellae of the shock-induced twins contain narrow planar deformation features or other, finer sets of deformation twins. The intervening lamellae commonly appear to be without either type of planar deformation. In a frequently observed pattern, using Charlevoix orthoclase as an example (although the equivalent pattern is repeated to a lesser degree in the other suites), $\{24\bar{1}\}$ deformation twins contain subordinate features near $\{\bar{2}41\}$, and $\{\bar{2}41\}$ lamellae of the same grain bear narrow $\{24\bar{1}\}$ planar features. The following are orientations

of shock-induced twins recorded in the three suites where they were measured:

Orthoclase (Charlevoix)	- $\{24\bar{1}\}$, $\{\bar{2}41\}$ and $\{110\}$
Maximum Microcline (Lac Couture)	- $\{120\}$, $\{130\}$, $\{\bar{1}30\}$, $\{010\}$ and $\{\bar{1}1\bar{1}\}$
Maximum Microcline (shock experiments)	- $\{\bar{1}11\}$, $\{11\bar{1}\}$, [001] zone between $\{100\}$ and $\{110\}$ and between $\{100\}$ and $\{\bar{1}10\}$, and $\{\bar{1}01\}$.

It has not been established whether conventional twin laws (normal, parallel or complex) are obeyed although the few optical data suggest that a "diagonal" twin law may be in effect in at least some instances. Shock metamorphism does not enhance pre-shock growth twins.

The deformation twins are believed to result from glide twinning produced by yielding at final shock states above the Hugoniot elastic limit. Their similar orientation to planar deformation features and the hypothesis that gliding is responsible for both, suggests that the creation of shock-induced twinning represents a higher shock-level form of planar deformation. The constraints may very well be the following. The energy provided by dynamic stress at low shock levels is sufficient to move atoms out of their normal, low free-energy site over a low energy barrier into a continuation site. Thus a dislocation is produced but the crystal lattice is continuous. More intense shock stress provides energy sufficient for atoms to surmount higher inter-site boundaries and drop into sites which result in a twin configuration.

It is evident from the ubiquitous development of shock twins at pressures as low as 155kb and 204kb in the maximum microclines from Lac Couture and the shock experiments, respectively, in contrast to their

occurrence only above 300kb in the Charlevoix potassic feldspars, that peak pressure is not the sole factor influencing their formation. The similar intermediate degree of order of the Charlevoix orthoclase and intermediate microcline compared with the highly ordered maximum microclines suggests that structural state may be an important variable in the formation of shock-induced glide twinning. In a highly ordered structure even a slight deviation may be detectable, whereas in the disordered lattice, where several sites may 'look' roughly equivalent, large displacements may be necessary before the dislocation becomes evident.

V.1.4 Colour Changes

A gradual colour darkening of potassic feldspar occurs with increasing level of shock metamorphism, as described for the experimentally deformed microclines. It is believed that this is a light-scattering effect due to an increasing abundance of planar deformation features and planar fractures in the shocked material. This assumption agrees with Peredery's (1972) observations that the darkening of shocked quartz at Sudbury can be correlated with an increasing development of planar deformation features.

V.2 Crystal Structure Changes

Plastic deformation above the Hugoniot elastic limit produces structural changes in the alkali feldspar lattice ranging from disordering to creation of high-pressure polymorphs. Evidence for these changes is detected primarily through X-ray examination of the shocked material.

V.2.1 Disordering

Evidence for shock-induced disordering of alkali feldspar, from this study and from others involving high strain rates, is inconclusive. Barth (1969), after reviewing the results of several heating experiments pertaining to feldspar ordering, concluded that the triclinic $\rightleftharpoons$ monoclinic transition temperature is variable and depends upon whether it is heating or cooling that is involved, the rate of temperature change (particularly within various temperature ranges) and the initial structural state. It is possible that disordering may begin as low as 250°C in the most highly ordered microcline structures and that the transformation to orthoclase may occur around 400°C. Correlation of these conditions with shock deformation indicates that enduring post-shock temperatures of this magnitude in potassic feldspar, accompany shock pressures of 330kb (250°C) and >400kb (400°C) (Stöffler, 1971a). These values imply that a decrease in ordering of maximum microcline could be detected above 330kb, that further disordering in intermediate microcline (such as at Charlevoix) would not begin below possibly 300kb, and that further disordering in monoclinic K-feldspar (Charlevoix orthoclases) would require 450kb or higher, assuming that shock stress does not affect the transformation temperatures proposed. Stöffler (1971a) believes that Shock Stage II, recognized by complete transformation of tectosilicates to diaplectic glass, begins at approximately 360kb. It is likely, therefore, that at pressures where significant disordering might be expected to occur, alkali feldspar will be converted directly to a high pressure polymorph and invert to diaplectic glass, so that shock-induced structural state changes will not occur. Support for this assumption is found in the

experimentally shocked maximum microcline in which no variation in structural state was detected up to 417kb. The possible disordering reported in some orthoclase samples at Charlevoix may be real, but is more likely a sampling effect.

V.2.2 Phase Transformations, Disordering and Diaplectic Glass

Under high pressure the feldspar lattice is unstable and is converted to a more stable configuration. Such transformation commences at approximately 115kb, about 43kb and 33kb above the Hugoniot elastic limits of orthoclase and microcline, respectively. With increasing pressure a greater proportion of the sample is converted to the high pressure polymorph until complete transformation is achieved at approximately 300kb (Ahrens et al., 1969; Ahrens and Liu, 1973). The high-pressure phase, although not recovered from shock experiments nor identified in nature, is believed to be the dense hollandite-type structure with Al and Si in octahedral co-ordination, such as produced from sanidine in static experiments. Virtually nothing is known of the stability field of the hollandite-type polymorph, unlike that of the high-pressure quartz polymorph, stishovite. Neither it nor an equivalent plagioclase polymorph have been found in highly shocked crater debris. It is therefore assumed to be very unstable in post-shock environments and, in the manner generally postulated for maskelynite formation, inverts to a more disordered, metastable phase.

The nature of the disordered crystalline phase recovered from the current experiments has not yet been established. It is not the hollandite-type K-feldspar nor the phase produced by Sclar and Usselman

(1970), nor any known modification of potassic feldspar. Its comparatively low density and weak X-ray pattern indicate that it is not a dense, compact high-pressure phase such as predicted from the K-feldspar Hugoniots (Ahrens et al., 1969; Ahrens and Liu, 1973). Its properties suggest that it is probably a poorly ordered, high-pressure modification of K-feldspar possibly a form transitional between microcline and the hollandite-type structure, mixed with a nearly isotropic, diaplectic microcline phase. The absence of a shock-produced, dense feldspar polymorph, such as the hollandite-type phase believed to have been produced at equivalent pressures, is not understood.

Stöffler and Hornemann (1972) have shown that diaplectic glass formed in Stage I from a given feldspar, may exist with a range of structural states. There is little direct observational evidence from the current study to suggest a widespread occurrence of diaplectic potassic feldspar glass over this pressure range. Engelhardt and Bertsch (1968) and Chao (1967), among others, believe that initial transformation to the high pressure tectosilicate polymorphs takes place along planar deformation features due to added shear stress. Inversion to diaplectic glass creates an optical discontinuity along the planes resulting from differences in relief and refractive index between the glass and original material. In the finest of planar features the glassy phase is not resolvable but is visible in broader features. It is assumed that the same process operates in alkali feldspars and that planar deformation features in orthoclase and microcline from Charlevoix, Lac Couture and the Recovery experiments, first visible in the range in which transformation to a high-pressure phase proceeds (>100kb) are detectable because of a diaplectic alkali feldspar glass along the plane.

There is little doubt that the high relief, low refractive index, glassy material filling $\{11\bar{1}\}$ and $\{\bar{1}11\}$ fractures in the experimentally deformed microcline, is diaplectic glass. Similarly, alternate lamellae of shock deformation twins with high relief and low refractive index are believed to be a slightly altered diaplectic glass. This latter development preferentially within one set of lamellae duplicates the formation of maskelynite initially along one set of albite twin lamellae (Robertson et al., 1968). No explanation for this pattern has been given.

V.2.3 Density Changes

The compression of geologic materials at high shock stresses results in increased density. The hollandite-type potassic feldspar polymorph has a density of 3.84g cm^{-3} compared with approximately 2.55g cm^{-3} for the normal feldspar. The products recovered from the shock experiments, which comprise diaplectic feldspar glass and the unidentified crystalline polymorph, show a gradual bulk density decrease as pressure increases above 154kb (corresponding to initial development of the high-pressure phase), from 2.55g cm^{-3} to 2.396g cm^{-3} at 417kb. This decrease is due in part to progressively greater portions of the sample having been converted to low density, disordered phases, but also to the fact that diaplectic phases exist in a sequence of structural states whose refractive index and density decrease with increasing pressure and temperature (Stöffler and Hornemann, 1972).

V.3 Changes in Optical Properties

Shock deformation changes in refractive index, birefringence

and optic angle of potassic feldspar are related to formation of disordered, high-pressure phases and diaplectic glass.

V.3.1 Refractive Index Changes

Refractive index gradually decreases from normal values in unshocked potassic feldspars, through intermediate values as disordering in the crystalline material proceeds, to $n\alpha$=1.4900 and $n\gamma$=1.4920 in the least birefringent areas in the sample (Or_{94}) shocked to 417kb. Fused glass of this composition, by comparison, has an R.I. of 1.487. Stöffler and Hornemann (1972) discovered that, unlike quartz and plagioclase, diaplectic K-feldspar glass has a slightly lower R.I. than the fused feldspar glass. On this basis, the lowest ordered diaplectic glass possible from the Or_{94} starting material in the shock experiments should have an R.I. value <1.487. The fact that the values at 417kb are higher, and that a slight birefringence remains indicates that the ultimate diaplectic glass was not achieved. The refractive index of the visibly crystalline material in these samples was not measured but is assumed to be close to that of the weakly birefringent areas because no relief contrast is detectable. The decrease in R.I. correlates with reduced density over the pressure range investigated.

Refractive index changes noted in the naturally deformed material consist of a relative reduction in the glassy, high relief portions of planar deformation features or twins, assumed to be a stage of diaplectic glass development.

V.3.2 Birefringence Changes

Birefringence gradually diminishes from normal values in unshocked potassic feldspars, through intermediate values as disordering in the crystalline material proceeds, to a minimum of 0.002 in the least birefringent portions of the microcline shocked to 417kb. The decrease correlates with disordering and development of diaplectic glass. Although all refractive indices decrease, a proportionally greater lowering of $n\gamma$ creates the lessened birefringence. This could be due to greater expansion of the structure in the Z-optic direction, or approximately [010].

V.3.3 Optic Axial Angle Changes

A slight gradual increase in optic angle from $2V\alpha=81°$ in unshocked material to 88° at 417kb, occurs in experimentally shocked microcline. The higher values are interpreted as the optic axial angle of the crystalline disordered phase. This biaxial phase must therefore have either orthorhombic, monoclinic, or triclinic symmetry.

V.4 Chemical Changes

Changes in the bulk composition of the shocked feldspars have not been observed in weakly to moderately highly shock metamorphosed material, and are not believed to occur at shock levels where post-shock temperatures do not exceed melting temperatures. At lower shock levels, migration of sodium and potassium atoms within the alkali feldspar structure may take place in adjustment to the shock environment. At shock pressures above 170kb, or perhaps less, where post-shock temperatures

Table V.1 Summary of observations on shock-metamorphosed potassic feldspar

Pressure	0kb — 100kb — 200kb — 300kb — 400kb
Charlevoix orthoclase and intermediate microcline	breakdown of film perthite lamellae to spindle micro-perthite bleb perthite disappears no distinctive shock deformation material eroded - no examples found shock cleavages ($\bar{2}10$)(120) ..... plus (11$\bar{2}$)(031) (01$\bar{1}$)(101) planar features 1 set ..... 1-2 sets ..... 2-4 sets. (24$\bar{1}$)($\bar{2}$41)(110)(010)($\bar{1}$10)($\bar{1}$11)(70$\bar{1}$) in orthoclase (13$\bar{1}$)(110)(120)($\bar{1}$20)(010) in microcline deformation twins ($24\bar{1}$)($\bar{2}41$) - incipient diaplectic phase
Lac Couture maximum microcline	not examined strong planar deformation features and broad deformation twins (120)(130)($\bar{1}$30)(110)(210)(11$\bar{1}$)(22$\bar{1}$) incipient diaplectic phase not examined
Experimentally shocked maximum microcline	shock cleavages (11$\bar{1}$)($\bar{1}$11) plus (hk0) forms ..... (11$\bar{1}$)($\bar{1}$11) contain diaplectic glass at highest pressures planar features (11$\bar{1}$)($\bar{1}$11)($\bar{1}$30)(221)($\bar{1}$22) ..... (001) weak strong weak n_α decreases gradually then sharply from 1.517 ..... to 1.516 .... 1.512 ..... 1.507 ..... 1.498 ..... 1.490 birefringence reduced from 0.007 ..... to 0.003 ..... to 0.002 density decreases continuously from 2.55g cm^{-3} ..... to 2.48 ..... 2.45 ..... 2.40 intensity of X-ray reflections weakens, back reflections disappear as disordering proceeds high-pressure phase appears, becomes dominant crystalline phase

lie below the alkali feldspar solvus, shock stress can initiate renewed migration in 'discontinuous' perthite textures in which chemical equilibrium was not originally attained, resulting in a new, microperthitic texture. At higher pressures, probably in the neighbourhood of 450kb, where alkali feldspar is completely converted to diaplectic glass, homogenization may take place by migration of sodium and potassium in the solid state. This is speculation as there are no reported instances, but the equivalent process does occur in homogenization of maskelynite.

V.5 Experimental vs. Natural Shock Deformation

Throughout the preceeding paragraphs the observations made on naturally and experimentally shock-loaded potassic feldspars have been compared and contrasted. In several instances the two have differed either in the form, magnitude, orientation, or pressure range in which a particular type of deformation was perceived. Granted, some of the discrepancies may arise from the use of maximum microcline in the experiments, whereas the majority of natural examples were initially less ordered feldspars. However, the most common inconsistency concerns the pressure range, particularly the lower limit, at which a characteristic deformation, for example unusual shock-induced cleavage, is produced. Certainly, the method of estimating peak shock-pressures in the samples from meteorite craters by using the associated development of planar features in quartz must, in at least some cases (sample MBP-100) lead to a somewhat erroneous estimate. It is unlikely, however, that a consistent error of more than ten per cent has been made.

The differences between experimental and natural shock

conditions have been alluded to as the possible cause of these observational inconsistencies. The experiments in this study constitute a special case of shock metamorphism probably not often duplicated in natural impact situations. The microcline discs were single crystals of considerably greater width than thickness which, for the purposes of calculating shock stress, made them essentially one-dimensional. When a shock-wave of uniform lateral extent moves through the thickness of the disc, rarefaction or compressional waves, depending on the impedance of the surrounding medium, are produced at the boundaries. Interference takes place between rear-surface reflections and boundary reflections moving into the grain centre, creating potentially destructive stress concentrations along the plane of intersection. In Equation of State experiments to determine Hugoniots, only the initial encounter of the shock-wave with rear surface is recorded. In thin samples this shock-wave reaches the free surface before edge rarefactions are transmitted to the centre, so that the material's behaviour due to the passage of a single, plane wave front is determined. In Recovery experiments where observations are not made until the shock process, including resulting interference stress concentrations, has been completed, an attempt is made to reproduce Hugoniot data by sampling only the centre of the mineral where edge effects are assumed to be minimal.

The target rocks in a meteorite impact event are polycrystalline, either monomineralic or polymineralic, with a multitude of irregular interfaces in a small volume. On the macro scale, impact creates a stress which passes radially outward into the country rocks as a single, uniform, shock-wave front of constant velocity. This simplistic picture breaks down on the microscopic scale. Heterogeneity of the rock

mass in terms of physical properties, such as different impedance and grain shapes, and the presence of voids, results in wave interferences capable of generating highly localized stress concentrations. Rinehart (1968) described several interface configurations likely to cause intense deformation. A common example occurs in the corners of grains where reflected rarefactions or compressional waves interfere along a plane, producing intensified tensional or compressional deformation. Robertson et al. (1968) noted that planar deformation features in Type A quartz tend to develop first and more intensively in corners of grains. The suggestion drawn from these complications is that for comparison with experimentally produced shock phenomena, the shock metamorphism level of natural materials should be characterized by deformation developed in grain interiors.

Closer agreement between the two conditions could be attained by shock experiments on polycrystalline, monomineralic aggregates or rock sections. Kleeman (1971) and Sclar and Usselman (1972) used powdered feldspars in their experiments with results, described in Chapter IV, notably different from those obtained from shock loading of single-crystal microcline.

The consistent orientation of the microcline lattice in relation to the stress direction must also create a bias in the development of various types of deformation, particularly orientation of planar elements. It has already been noted that certain orientations of planar deformation features in quartz are preferentially formed from a given stress direction. It seems likely that in feldspar, a mineral considerably further from structural isotropism than quartz, directional

stress will have a significant influence on the orientation of planar deformations. Ahrens and Liu (1973) make the point that the orthoclase Hugoniot they determined was along (010), implying that in any other plane it might be significantly different.

V.6 Loose Ends

In most intriguing studies, for each question answered or problem solved there are two more proposed, and the investigation of shock metamorphism of potassic feldspars has been no exception. Although the general pattern of deformation has been established, with supporting details interspersed, there remain a number of whys?, why nots? and what ifs? to be resolved. Following is a list of some of these puzzles, not necessarily in order of fascination, with possible lines of investigation for their solution.

1. Is the hollandite-type alkali feldspar polymorph really produced by shock stress, either in experiments or by meteorite impact, and if so, under what conditions can it survive? Is the unidentified, disordered phase an intermediate stage leading to formation of the hollandite feldspar phase? What is its structural nature? Is it a single phase or a mixture of potassic and sodic high-pressure phases? Does its formation, or that of some other polymorph, depend on stress direction?

It is possible that many of these queries could be answered by further shock experiments. Target materials could again be single crystals, but of a homogeneous, synthesized orthoclase, cut parallel to various directions. Experiments need only be performed at pressures predicted to produce high-pressure polymorphs, approximately 380-480kb,

with recovery of quenched and unquenched products from duplicate shocks.

The search for high-pressure polymorphs in crater debris must be centered on diaplectic alkali feldspar glass. So far, no suitable material has been recovered from Canadian impact sites, but the Ries crater may be a productive hunting ground.

2. What influence does stress direction have on the orientation and onset of planar features? Does degree of ordering in the pre-stressed feldspar lattice play a significant role? Again, Recovery shock experiments should provide some answers. Target materials should be single crystals cut in a few standard orientations from preferably homogeneous, synthesized K-feldspar available with a range of structural states. Shock stresses should span the 40kb to 300kb range at appropriate intervals.

3. Are the so-called shock deformation twins truly lattice twins, and what laws, if any, do they obey? Single-crystal oscillation X-ray photographs on grains with coarse twinning, plucked from the Lac Couture breccias, would readily resolve this uncertainty.

4. The cause of the apparent potassium enrichment of the Brent impact melt is still unknown, and for that matter the controversy regarding the genesis of the melt continues unabated. Hopefully, a program now underway involving extensive petrographic examination of the melt rocks, particularly the feldspars, plus chemical analyses of the melt layer and country rocks by electron microprobe and more classical methods, will shed light on the problem.

It is clear that even with the considerable advances over the past dozen years in the description and understanding of shock metamorphism, many commonly encountered phenomena remain incompletely

characterized and explained. In the next decade, a more thorough comprehension of shock metamorphism processes will undoubtedly be gleaned from concentrated studies of lunar, and perhaps even Martian samples, complemented by the continuing investigations at terrestrial meteorite impact sites.

APPENDIX A

Table A.1 Unit cell parameters of potassic feldspars in the charnockitic rocks of Charlevoix

	Sample	a(Å)	b(Å)	c (Å)	α	β	γ
		±0.005	±0.005	±0.005		±5'	
Charnockitic Granites	8	8.586	12.981	7.203	90°	116°3'	90°
	11	8.580	12.982	7.194	90°	116°2'	90°
	25	8.567	12.974	7.203	90°	116°2'	90°
	51	8.542	12.970	7.187	90°	116°2'	90°
	52	8.579	12.980	7.199	90°	116°3'	90°
	67	8.578	12.989	7.201	90°	116°2'	90°
	74	8.560	12.969	7.198	90°	115°59'	90°
	77	8.580	12.980	7.200	90°	116°2'	90°
	84	8.581	12.993	7.196	90°	116°3'	90°
	104	8.569	12.986	7.200	90°	116°2'	90°
	106	8.578	12.998	7.195	90°	116°4'	90°
	130	8.577	12.973	7.194	90°	115°59'	90°
Charnockitic Microcline Granites	35*	8.583	12.966	7.205	90°	116°1'	90°
	64*	8.524	12.954	7.207	90°	115°58'	90°
	97*	8.553	12.963	7.207	90°	115°57'	90°
	121	8.567	12.983	7.205	89°51'±5'	115°57'	90°18'±5'
	133*	8.570	12.964	7.202	90°	116°0'	90°
	139*	8.579	12.965	7.211	90°	116°3'	90°
Charnockitic Syenodiorites	91	8.567	12.963	7.197	90°	115°59'	90°
	92	8.530	13.004	7.189	90°	116°0'	90°
	93	8.527	12.980	7.189	90°	116°4'	90°
	94	8.534	12.978	7.181	90°	116°2'	90°
	100	8.570	12.983	7.200	90°	116°5'	90°
	129	8.567	12.984	7.199	90°	116°1'	90°

* Microclines with low triclinicity were indexed more easily in the monocline system.

APPENDIX B

"BEST FIT" METHOD

The "best fit" technique for correlating measured data, plotted in stereographic projection, with a standard stereographic plot, is used where insufficient control is available to allow a unique correlation. The technique was employed in this study to determine orientations of shock-produced planes both in the naturally- and experimentally deformed feldspars.

To establish the coordinates of any point in space its relation to three non-coplanar fixed points must be known. Miller indices of a plane in a crystal lattice can be thus determined from its angular relationship with three other planes (or their poles). In petrographic investigations (in contrast to X-ray methods), these known planes can be cleavages or partings, twin-composition planes, or planes of perthitic intergrowth.

In the alkali feldspars from Charlevoix, three commonly visible planes are {001} and {010} cleavages, and $\{70\bar{1}\}$, the Murchisonite parting containing film perthite lamellae. Unfortunately {001} is not always developed and {010} is even more rare. In addition, the large interplanar angles between each pair of planes prevents access to all three on the universal stage except in rare, fortuitous grain orientations. Standard reference planes in Charlevoix, Lac Couture, and experimentally shocked microclines are {001} and {010} cleavages, the albite twin-composition plane {010}, and the pericline twin composition plane (the rhombic section). Although all these

planes are commonly developed, again the large interplanar angles exclude their usefulness for all but a few grains. Therefore, the occurrence and accessibility of three known crystallographic planes in one grain is rare.

The problem is partially solved by substituting optic directions for crystallographic planes. Two optic directions are always measurable and the third is located at 90° to these. Although optics are not rigidly controlled by the crystal structure they remain fixed in feldspars of equivalent composition and structural state. The ambiguity of relying solely on optics, however, is illustrated in Fig. B.1. Each stereogram is plotted about the Z-optic direction with the X-direction N-S. For crystals of low symmetry, such as feldspars, in which no optic directions are parallel to symmetry axes, four equivalent stereograms can be plotted. The schematic poles in Fig. B.1 are the same forms in each case.

It is readily seen that each stereogram can be equilibrated with any other by a simple 180° rotation about the appropriate axis. However, without any additional information there is no way of telling whether the two planes plotted in the upper left stereogram are the same as those in, say, the lower right stereogram, or whether they are entirely different planes.

In most grains, at least one identifiable reference plane can be measured. The $\{70\bar{1}\}$ parting plots near the open circles of Fig. B.1, and the {001} and {010} cleavages near the Y- and Z-optic directions respectively. A standard stereographic projection was prepared for the alkali feldspars, centred on the Z-optic direction

Fig. B.1

Stereograms with optic directions as reference axes. Because the positive and negative optic directions cannot be distinguished without crystallographic data all four stereograms centered on Z are possible. The two poles plotted are the same in each case but are rotated about an optic direction through 180°.

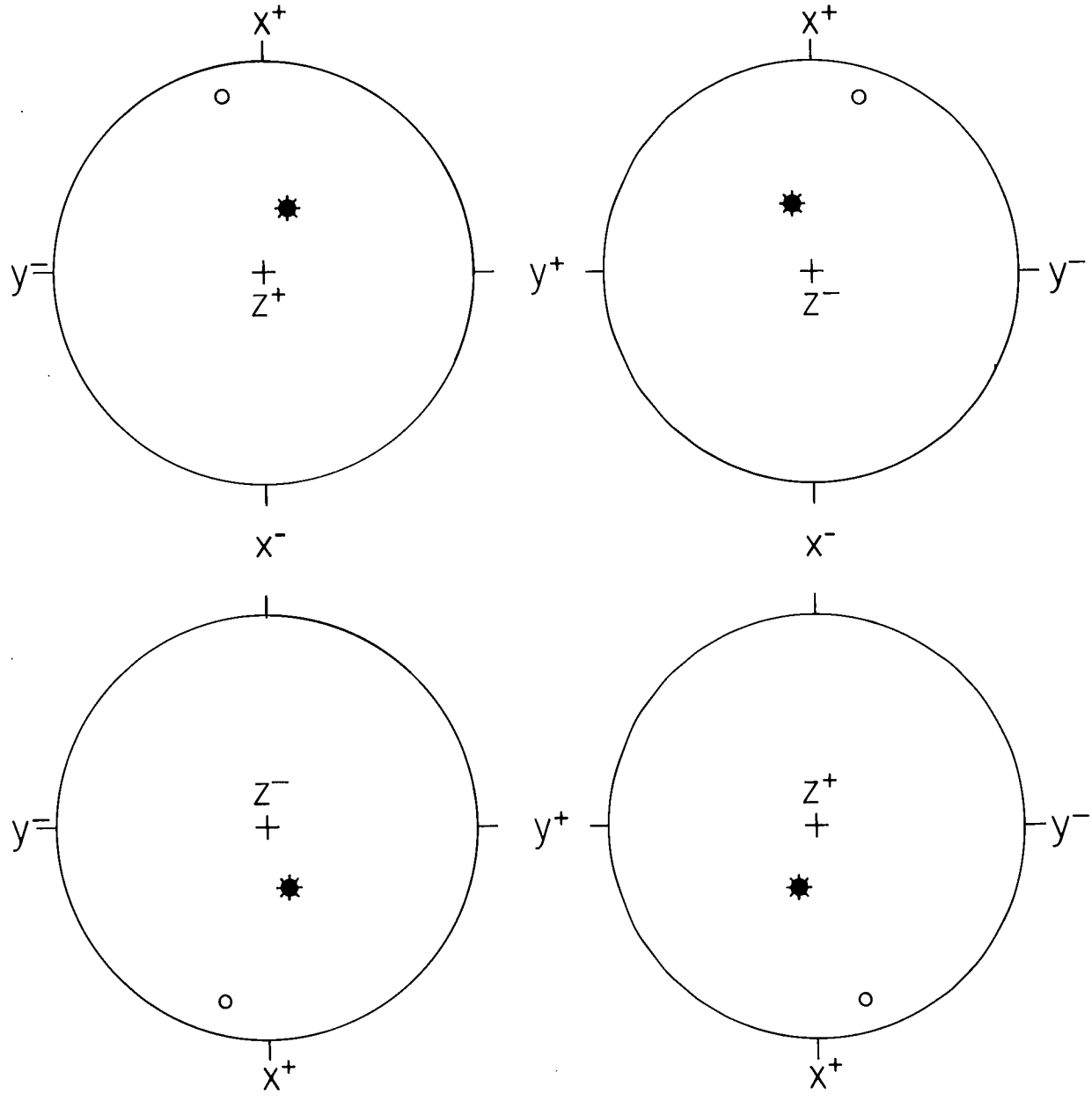
X+
y=
Z+
X-
X+
y+
Z−
y−
X-
Z−
y=
X+
X+
Z+
y+
y−
X+

with the X-direction N-S; positions of various reference planes were also plotted. For each feldspar grain studied, a stereogram with the same axes was plotted, incorporating all planes measured in that grain. All points were rotated graphically through 180° about the optic directions to generate the four equivalent stereograms. Beginning with grains having three measured reference points, followed by those with two, and then only one, each of the four stereograms was superimposed on the standard plot. The one selected was that with reference points coinciding with those of the standard, and positions of the shock-induced planes in that orientation were plotted on the standard stereogram. Between approximately 20 and 40% of the grains in each sample have no measurable reference planes. For these grains, each of the four stereograms was superimposed on the composite diagram and the one selected was that with shock-induced planar elements coinciding with those obtained from grains with better control. This is, of course, the ideal case. In some instances none of the four equivalent stereograms coincided to an acceptable degree with the composite plot. In others, two orientations both agreed reasonably well with the composite diagram. In such circumstances an arbitrary decision was made to select the "correct" one or, in some cases, the data were not used. The resulting stereographic plots (Figs. II.10 to II.12, II.14, IV.8 to IV.10) therefore were compiled from data of which approximately 60 to 80% have some crystallographic control, another 10 to 30% are based entirely on the "best fit" correlation, and the remainder, approximately 10%, are of uncertain value.

APPENDIX C

RECOVERY SHOCK EXPERIMENTS

C.1 Experimental Design

The Recovery shock experiments were carried out using the facilities of the Seismological Laboratory, California Institute of Technology, and were supported in part by NASA grant NGL 05-002-105. Each experiment consisted of impacting the target with a plane-faced projectile fired from a gun, and measuring the projectile velocity during the short free-flight. The arrangement of the experimental firing range is shown in Fig. IV.1, and a description of the components follows.

Gun

Two guns were used, each with rifled steel barrel and attached breach assembly.

	"Short" gun	"Long" gun
length	123cm	303cm
inner diameter	20.6mm	19.6mm
outer diameter	66.8mm	50.0mm
shell	Weatherby 460 Magnum	special manufacture
primer	generally Federal 215	
powder	generally Dupont IMR (improved military rifle powder) 422	
shell capacity	approx. 6.5gm	approx. 20gm

Table C.1 Properties of alkali feldspar used in recovery shock experiments.

	Composition (wt %)		
	bulk*	microcline**	albite**
SiO_2	64.60	63.70	67.93
Al_2O_3	19.62	18.65	18.38
K_2O	13.71	16.25	0.09
Na_2O	1.96	0.74	11.73
CaO	nil	0.01	0.21
Total	99.98	99.34	98.33
Or		93.86	0.53
Ab		6.10	98.44
An		0.05	1.04

Optics		Structure	
$2V_\alpha$	$81^\circ \pm 1^\circ$	a	8.581±0.005Å
n_α	1.5175±0.0005	b	12.970±0.005Å
n_β	1.5195±0.0005	c	7.224±0.005Å
n_γ	1.5249±0.0005	α	$90^\circ 43' \pm 5'$
		β	$115^\circ 59' \pm 5'$
		γ	$87^\circ 39' \pm 5'$
		triclinicity	0.94(5)±0.05
		density	2.553±0.004 g cm^{-3}

*Wet chemical analysis (Spence, 1932, p. 101)

**Electron microprobe analyses, this study.

Table C.2 Shock experiment variables

shot number	striker plate material	striker plate thickness	explosive powder load	velocity	pressure
1 *	brass	5mm	6.6g	0.974km/sec ±1%	191kb±3-5%
2 *	"	"	5.8g	0.529 "	99"
3 *	"	"	5.9g	0.858 "	167"
4 *	"	"	5.0g	0.783 "	150"
5	stainless steel	"	10.0g	1.031 "	218" ***
6 **	brass	"	16.9g	1.639 "	356" ***
7	fan steel	"	13.5g	1.301 "	356" ***
8 **	fan steel	"	18.0g	1.506 "	428" ***
9 **	brass	"	8.0g	1.124 "	227" ***
10 **	"	"	12.7g	1.489 "	316" ***
11	"	"	13.0g	1.485 "	317"
12	"	"	13.5g	1.489 "	320"
13 **	"	"	10.0g	1.301 "	270"
14	"	"	8.5g	1.213 "	250"
15	"	"	7.0g	1.017 "	204"
16	"	"	17.0g	1.850 "	417"
17	"	9mm	6.5g	0.820 "	160" ***
18	"	"	5.0g	0.803 "	154"
19	"	"	4.0g	0.522 "	96"

* = small gun (see text), all others large gun

** = gun barrel evacuated

*** = sample not recovered

Projectile (Fig. IV.2)

projectile	lexan	lexan
projectile diameter	20.3mm	19.3mm
striker plate	leaded brass, Fansteel 77, or 304 stainless steel	
striker plate diameter	15.9mm	15.2mm
striker plate thickness	5mm and 9mm	

Target (Fig. IV.2)

Samples used in the Recovery shock experiments were from a perthitic microcline, pale greenish or grayish white, obtained from the Back (Wallingford) Mine, Papineau County, Quebec, where it occurs in a very coarse-grained pegmatite (Spence, 1932; Papezik, 1961). Twinned albite, in a veined perthitic intergrowth with M-twinned microcline, accounts for approximately 10 per cent of the alkali feldspar. Properties of the bulk feldspar and component phases are presented in Table C.1. Discs of the feldspar, 0.5mm thick by 6.5mm diameter, were sections of a core taken from a single crystal, with the core axis normal to the (001) cleavage. They were ground to the required thickness, polished, and then snugly fitted into section A of the holder. Parts A and B were joined and screwed into C, which in turn was pressed into D and the surface was faced off on a lathe. The assembly was mounted in a metal box to catch the target after impact.

Velocity Monitoring (Fig. IV.1)

A laser beam reflected by angled mirrors crossed the 110cm free-flight path at two points, 201.5mm apart. The reflected beam was

received by a photo-diode whose output was scanned by a dual-beam oscilloscope together with time pulses from a calibrated oscillator. The double intersection of the beam by the projectile was photographically recorded (Plate C.1a) and the velocity calculated.

C.2 Experimental Procedure

(1) The gun barrel was aligned by passing a laser beam through it from the breach end and adjusting the barrel clamps so that the beam exited from the centre of the muzzle.

(2) The assembled target was mounted on its carrier in the catching box and a small flat mirror was attached to its face. The gun-target system was aligned, and the target face made perpendicular to the projectile path by adjusting the carrier until the laser beam was reflected from the target back down the centre of the barrel. The mirror was removed.

(3) The projectile was prepared by pressing the striker plate into the recess in the lexan cylindrical block. A shell was fitted with a primer and filled with a weighed amount of explosive powder calculated to produce the desired velocity. The projectile and shell were loaded into the breach.

(4) In some cases the barrel was pumped down to a rough vacuum (Table C.2).

(5) The gun was fired electronically from the adjoining control room where a Polaroid photograph of the oscilloscope trace was produced.

(6) The target was retrieved and allowed to cool. Rarely did the target assembly remain intact, but in a perfect shot, parts A, B and C

Plate C.1

a) Oscilloscope record of projectile velocity. Small dots were generated by oscillator at 0.01 sec intervals. The two peaks separated by 0.135 sec are the photo-diode record of passage of the projectile through laser beams 201.5mm apart. Velocity in this case was calculated at 1.489km/sec.

b) Target (part D) recovered after impact of 417kb. Cavity is twice as deep and wide as original. Note resemblance to large scale meteorite craters with 'ejecta' ray pattern, raised rim, radial and circumferal fractures.

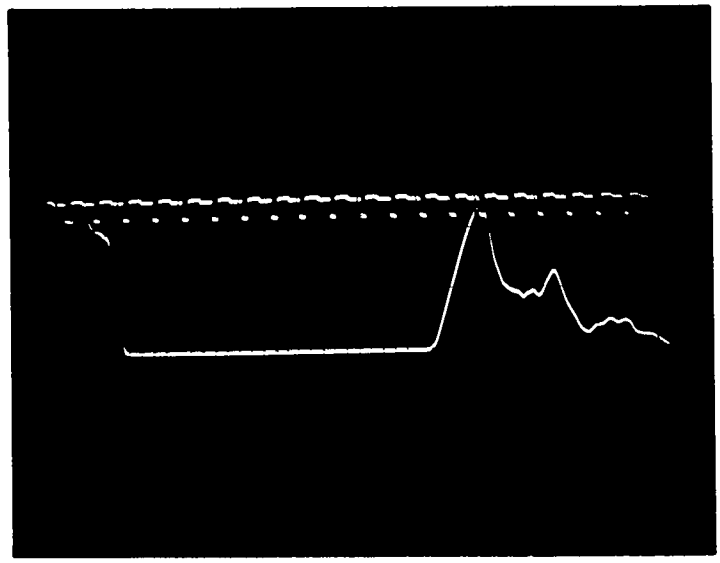

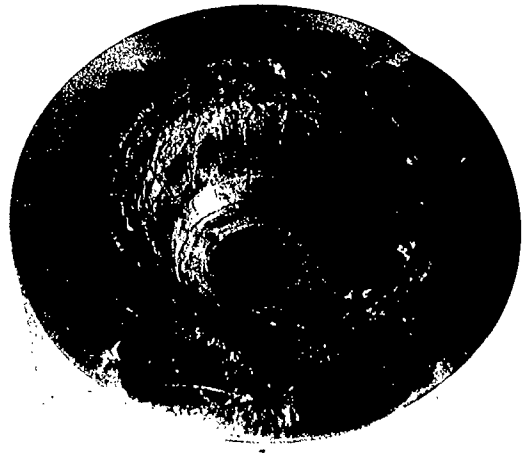

popped out as a unit leaving an impact crater in part D (Plate C.1b). The recovered part of the target containing the sample was placed in a lathe and the rear surface of part B was turned off until the sample was exposed.

(7) The projectile velocity was calculated from the oscilloscope record as in the sample calculation below based on Plate C.1a.

velocity = distance/time = 201.5mm/135.3x10^{-3}sec =1.489km/sec

APPENDIX D

HUGONIOT EQUATION OF STATE

D.1 Propagation of Shock Waves and Equation of State

The Recovery shock experiments described in Chapter IV rely on Equation of State theory. The following discussion of various aspects of this theory is based on several comprehensive reviews of the subject (Walsh et al., 1957; Duvall and Fowles, 1963; Ahrens and Gregson, 1968; McQueen et al., 1970).

When a one-dimensional shock-wave is driven into a sample, a normal stress is generated at the interface and this disturbance propagates into the specimen. The Rankine-Hugoniot equations for the conservation of mass (1), momentum (2), and energy (3) across a single, steady shock front.

$$\rho_0 / \rho_1 = (S_1 - p_1) / (S_1 - p_0) \ldots\ldots\ldots (1)$$

$$P_1 - P_0 = \rho_0 (S_1 - p_0) (p_1 - p_0) \ldots\ldots\ldots (2)$$

$$E_1 - E_0 = (P_1 + P_0) (V_0 - V_1) /2 \ldots\ldots\ldots (3)$$

relate the density (ρ), specific volume (V), internal energy (E), pressure (P), shock-wave velocity (S), and particle velocity (p) of the material in the initial state (subscript 0), and behind the shock front (subscript 1). If the material is initially in its standard rest state, the equations reduce to:

$$\rho_0 / \rho_1 = (S_1 - p_1) /S_1 \ldots\ldots\ldots\ldots\ldots (4)$$

$$P_1 = \rho_0 (S_1) (p_1) \ldots\ldots\ldots\ldots\ldots (5)$$

$$E_1 - E_0 = P_1 (V_0 - V_1) /2 \ldots\ldots\ldots\ldots (6)$$

The measurement by experiment of any pair of the variables in equations (1) to (6), coupled with the known initial parameters, completely defines the state of the shocked material. Shock-wave velocity (S) and particle velocity (p) are the variables usually measured in Equation of State experiments. A Hugoniot curve, or simply a Hugoniot, is the graphical representation of the Equation of State, and in produced by plotting the relationship between any pair of variables determined from a series of experiments. Examples of the most commonly plotted Hugoniots are shown in Fig. D.1.

The simple shock behaviour of most metals is illustrated by the Hugoniot in Fig. D.1c. A single, steady shock front passes through the material creating elastic, one-dimensional, continuous compression, but no internal rearrangement takes place over the pressure range investigated. Geologic materials, however, generally behave in a different manner as shown in the schematic Hugoniot of Fig. D.2. For shock states lying between A and B, produced by pressures less than P_B, a single, elastic shock front passes through the sample, and one-dimensional compression results. P_B is the Hugoniot Elastic Limit and is the maximum normal stress which will not induce internal rearrangement. The discontinuity in the curve at B indicates that a structural change occurs for shock pressure greater than P_B. States lying between B and D, for example C, are the result of a double-shock process. The material is raised initially to the state B by the passage of an elastic shock front, and a following deformational shock-wave further raises the state to C. States between D and E are produced by the passage of only a deformational

Fig. D.1

Typical equation of state curves, or Hugoniots, relating stress, particle velocity, shock-wave velocity, and compression. See equations (1) to (6), page 291.

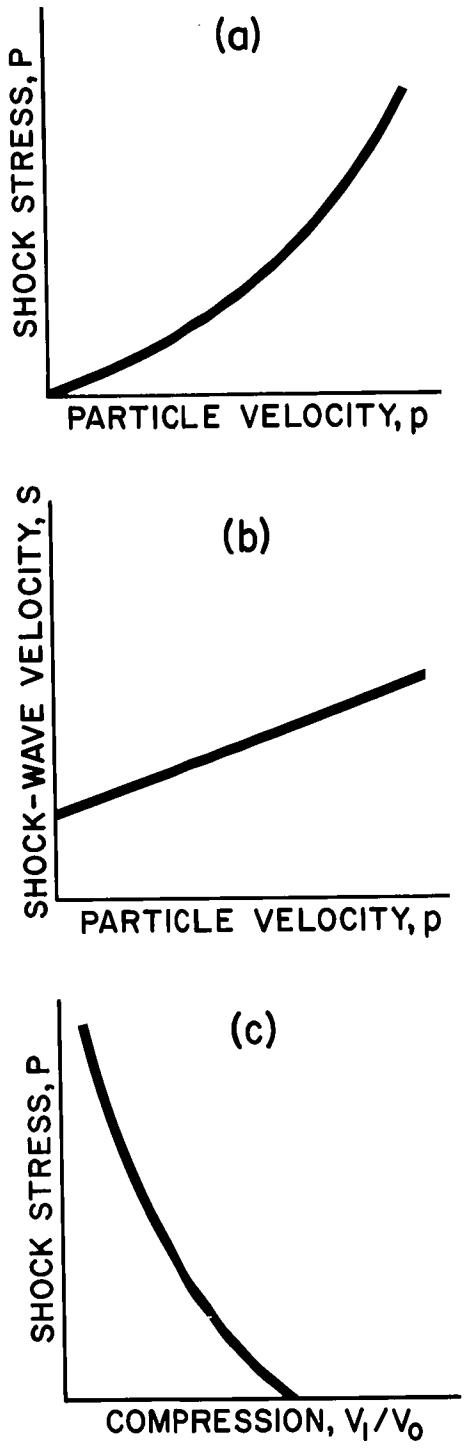
(a)
SHOCK STRESS, P
PARTICLE VELOCITY, p
(b)
SHOCK-WAVE VELOCITY, S
PARTICLE VELOCITY, p
(c)
SHOCK STRESS, P
COMPRESSION, V_1/V_0

Fig. D.2

Pressure-compression Hugoniot typical of some geologic materials. Dense, high pressure phase(s) created above Hugoniot elastic limit (HEL) reverts along release adiabats to compressed state.
See text, page 297.

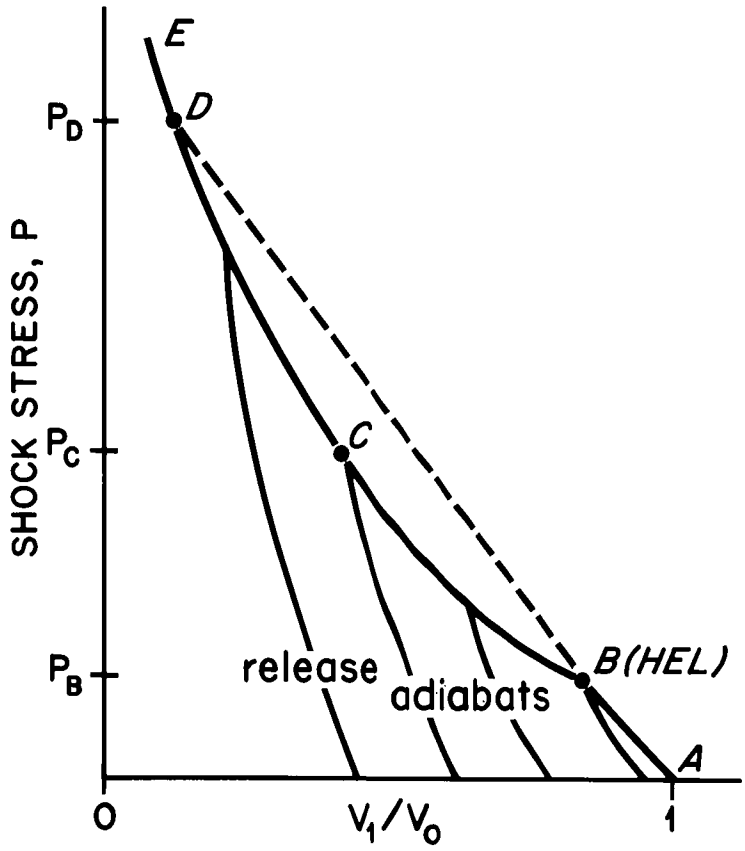
E
D
P_D
C
P_C
P_B
B(HEL)
A
release
adiabats
SHOCK STRESS, P
0
V_1/V_0
1

shock front.

A Hugoniot curve shows plots of the locus of states through which a material passes if subjected to continually increasing shock stresses. Release adiabat curves, on the other hand, define the succession of states through which the shocked material passes if allowed to return to zero pressure (Fig. D.2). The shocked samples return to their original zero-pressure state, A, only for very weak elastic shocks, but on release from pressures above the Hugoniot elastic limit the zero-pressure state remains in a compressed form, although generally not the state achieved at peak shock pressure. Release adiabat curves are determined from measurements of particle velocity in the release states, using an experimental technique similar to that for Hugoniot determinations. Ahrens and Rosenberg (1968) have found close agreement between densities calculated from release adiabats, and those determined on material recovered in shock experiments.

D.2 Impedance Matching

Impedance matching is a technique originated by Walsh et al. (1957) for determining points on an unknown Hugoniot by measuring shock-wave velocity in the specimen, and free-surface velocity in a standard material whose Hugoniot is known. In the experiment, the sample whose Hugoniot is to be determined is mounted on the rear surface of the standard of known Hugoniot (Fig. D.3a), and a shock wave is generated at the front surface of the standard. The shock-wave (P_1) moves through the standard to the interface with the specimen, at which point a shock-wave (P_2) moves into the specimen, matched by a disturbance reflected into the standard. If

Fig. D.3

a) Propagation of shock waves in Equation of State experiment for determining points on Hugoniot by impedance matching. See text, page 297.

b) Propagation of shock waves in experiment to determine pressure in specimen of known Hugoniot. See text, page 300.

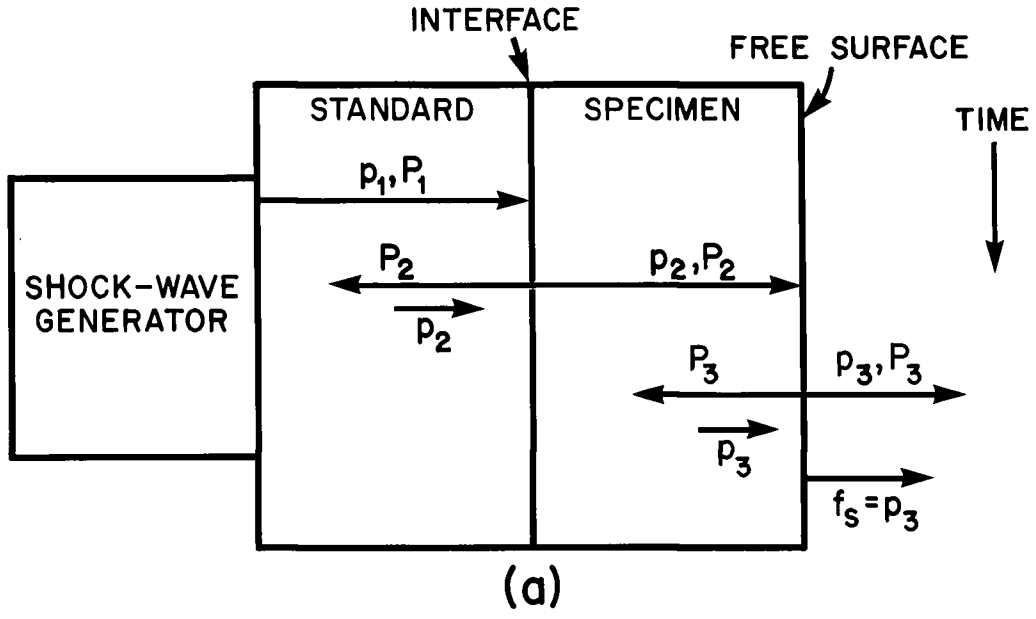
INTERFACE
FREE SURFACE
STANDARD
SPECIMEN
TIME
SHOCK-WAVE GENERATOR
p_1, P_1
P_2
p_2, P_2
p_2
P_3
p_3, P_3
p_3
$f_s = p_3$

(a)

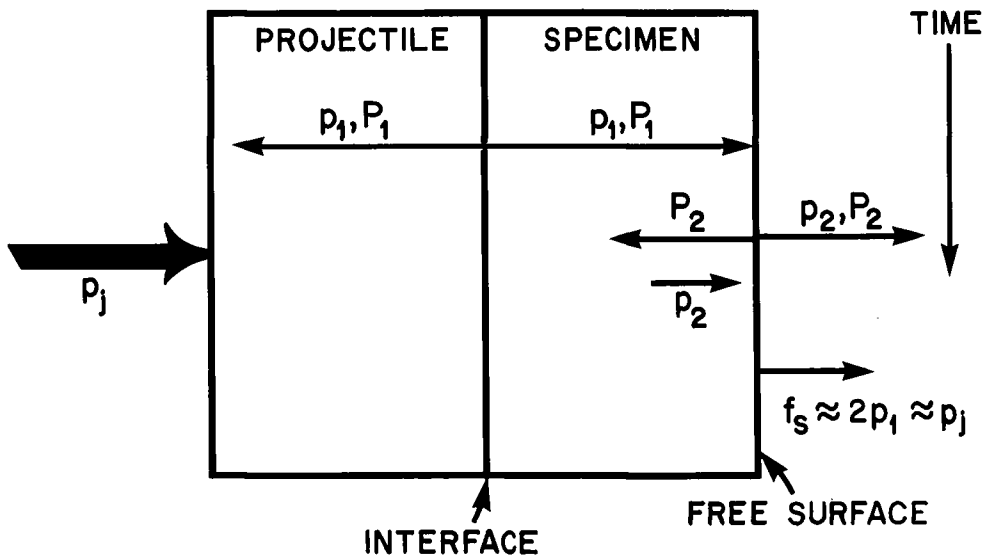
PROJECTILE
SPECIMEN
TIME
p_1, P_1
p_1, P_1
P_2
p_2, P_2
p_j
p_2
$f_s \approx 2p_1 \approx p_j$
FREE SURFACE
INTERFACE

(b)

the specimen has a higher impedance than the standard (impedance is directly proportional to density), the reflected disturbance will be a shock-wave which raises the pressure in the standard above the P_1 level. However, particle velocity in the standard will be reduced due to the interference of the right- and left-going particle motions. In contrast, if the specimen has a lower impedance than the standard, the reflected disturbance will be a rarefaction wave which lowers the pressure in the standard to a level below P_1. The rarefaction wave, however, provides a particle velocity component to the right, which increases the original particle velocity (p_1). The boundary conditions of the experiment require the pressure and particle velocity to be constant across an interface so that P_2 left = P_2 right, and p_2 left = p_2 right. Thus, pressure in the specimen will equal pressure in the standard and will be either greater or smaller (or the same) than P_1, depending on the relative impedance of the two materials.

When the shock front (P_2) reaches the rear surface of the specimen the same conditions apply. The air has a lower impedance than the specimen and so a rarefaction wave (P_3) moves back into the specimen and an equal, weak shock-wave advances through the air. The velocity with which the target moves off in relation to its surroundings, the free-surface velocity (f_s), is the resulting particle velocity in the specimen (p_3) which is p_2 plus the component p_r due to the rarefaction wave. That is; $f_s = p_2 + p_r = p_3$. For a solid-air interface, $p_r \sim p_2$, so that $f_s \sim 2p_2$.

A variation of the standard-specimen arrangement is shown in Fig. D.3b where a projectile of velocity p_j impacts the specimen and shock disturbances (P_1) move out from the interface. If the projectile

and specimen have similar impedance, for example two metals, the initial projectile velocity is approximately equally partitioned into resulting particle velocities (p_1) in the specimen and projectile. As before, at the free surface $f_s \sim 2p_1$ projectile velocity (p_j).

As was stated earlier, pressure and particle velocity must be constant across an interface, so that it is therefore convenient to work in the pressure-particle velocity plane (Fig. D.4a). The Hugoniot originating at P_0, p_0 is the locus of all pressure-particle velocity states attained by a right-going shock-wave in the standard (Fig. D.3a). When the shock-wave meets the interface with the specimen, a left-going disturbance reflects into the standard, and the locus of P-p states which can be reached by a reflected disturbance is given by the curve of negative slope in Fig. D.4a. This curve nicely approximates the mirror image of the Hugoniot for the standard reflected about the resulting particle velocity (p_2 in Fig. D.4a) which makes the P=0 intercept, $2p_2 \sim f_s$. Equation (5) is the equation of a straight line from the origin in the P-p plane with slope $\rho_0 S_1$ (impedance) for a particular shock-wave velocity S_1. The shock state achieved in the specimen must lie on the reflected Hugoniot of the standard, and on the straight line from the origin, and the intersection of these two defines a point, P_x-p_x, on the Hugoniot of the specimen. If the impedance of the specimen is lower than that of the standard, the lower line of Fig. D.4a applies, and the point P_y-p_y on the Hugoniot indicates the decrease in pressure across the interface. A series of experiments at different pressures produces other points to define the Hugoniot of the specimen.

This technique of impedance matching to determine the Hugoniot of a specimen by measurement of free-surface velocity and shock-wave velocity

Fig. D.4

a) Graphical calculation of point on unknown Hugoniot using impedance matching and experiment illustrated in Fig. D.3a. See text, page 301.

b) Graphical calculation of pressure in specimen of known Hugoniot using impedance matching and experiment illustrated in Fig. D.3b. See text, page 301.

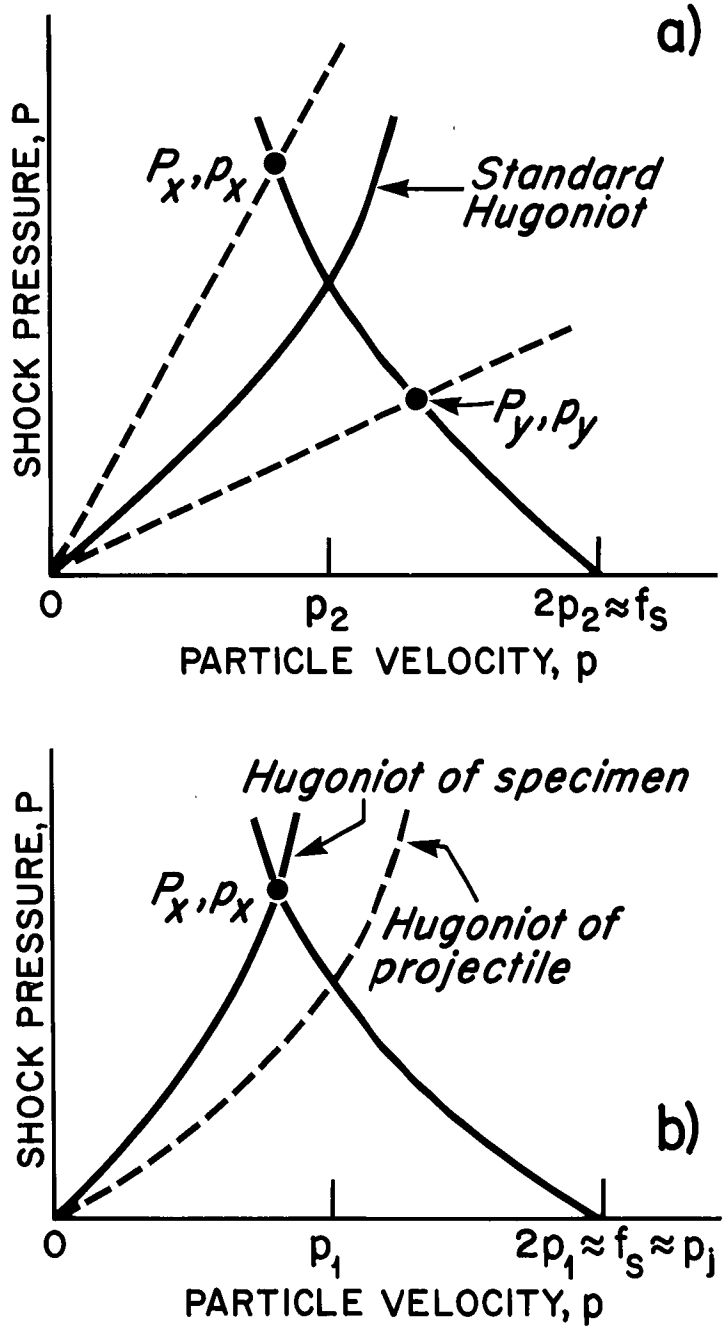
a)
SHOCK PRESSURE, P
P_x, p_x
Standard Hugoniot
P_y, p_y
0
p_2
$2p_2 \approx f_s$
PARTICLE VELOCITY, p
b)
SHOCK PRESSURE, P
Hugoniot of specimen
P_x, p_x
Hugoniot of projectile
0
p_1
$2p_1 \approx f_s \approx p_j$
PARTICLE VELOCITY, p

has since been modified to permit determination of the pressure in a sample of known Hugoniot by measuring only free-surface velocity. The graphical procedure is illustrated in Fig. D.4b for the experiment in Fig. D.3b. The Hugoniot of the standard (projectile) is reflected about the particle velocity, p_1. This is an unmeasured quantity but the intercept of the reflected curve on the P = 0 axis is $2p_1 \sim f_s \sim$ projectile velocity, which is measured. The intersection of the reflected projectile Hugoniot with the Hugoniot of the specimen (P_x-p_x) is the pressure-particle velocity state developed in the specimen. In the case illustrated, impedance of the specimen is higher than the projectile so that pressure has increased at the interface.

A further modification of impedance-matching theory permits calculation of pressure in a specimen whose Hugoniot is unknown by enclosing the specimen in a material of higher impedance and known Hugoniot (Fig. D.5a). As before, a shock wave (P_1) propagates into the standard when struck by the projectile. The value of P_1 can be determined from the Hugoniots of projectile and standard, plus the projectile velocity using the technique illustrated in Fig. D.4b. At the interface A-A_1 the disturbances P_2 are set up, but because the impedance of the sample is lower than that of the standard, then $P_2 < P_1$. However, at the interface B-B_1 the shock wave again meets the higher impedance standard so that the disturbance $P_3 > P_2$. P_3 reflects back through the sample to A-A_1, where it again meets a higher impedance, so that $P_4 > P_3 > P_2$. The pressure in the sample will continue to increase by successive reverberations until it equals P_1, the calculated pressure attained in the standard. The main constraint is that the sample be thin enough to allow P_1 to be reached before

Fig. D.5

a) Shock-wave propagation in recovery experiment to determine pressure in sample of unknown Hugoniot by impedance matching. See text, page 304.

b) Graphical calculation of pressure in sample of unknown Hugoniot. using impedance matching and experiment illustrated in Fig. D.5a. Example shown is shot 16, projectile velocity 1.850km/sec. See text, page 307.

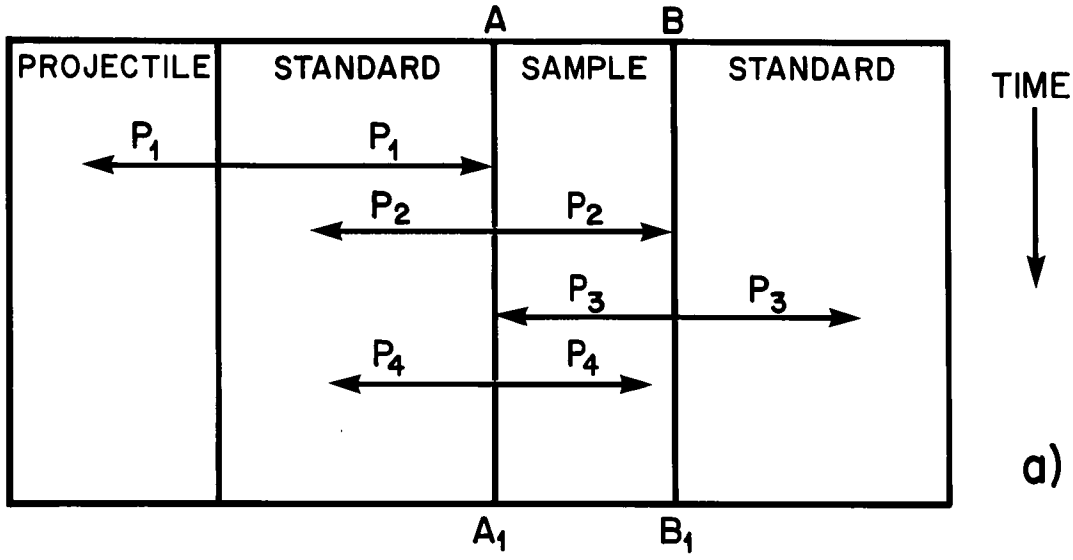
A
B
PROJECTILE
STANDARD
SAMPLE
STANDARD
TIME
P1
P1
P2
P2
P3
P3
P4
P4
A1
B1
a)

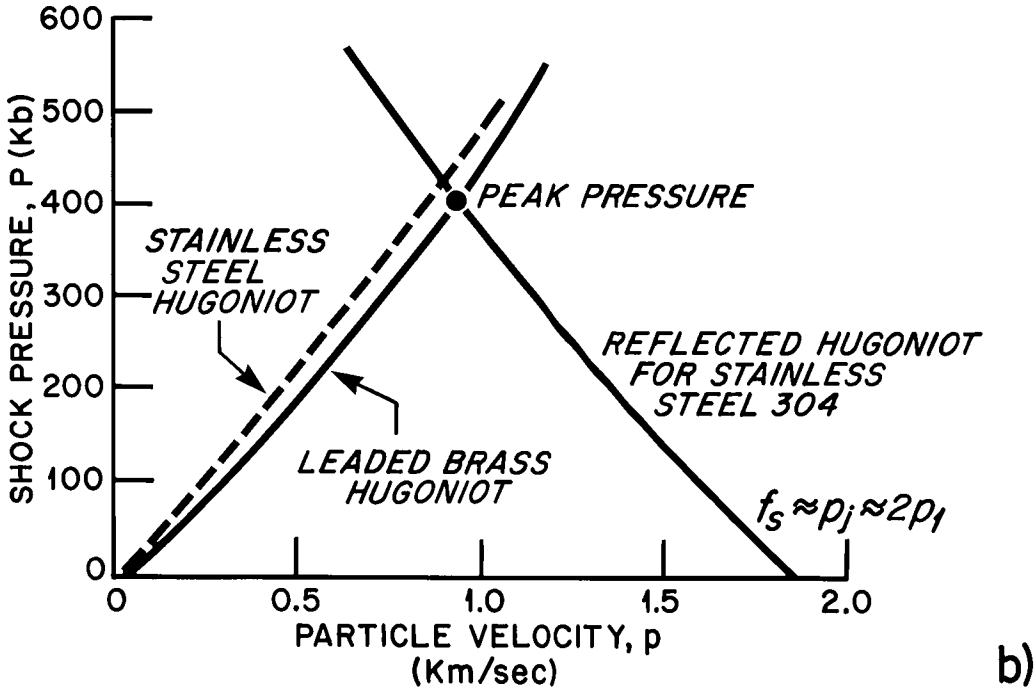
600
500
400
300
200
100
0
SHOCK PRESSURE, P (Kb)
PEAK PRESSURE
STAINLESS STEEL HUGONIOT
REFLECTED HUGONIOT FOR STAINLESS STEEL 304
LEADED BRASS HUGONIOT
$f_s \approx p_j \approx 2p_1$
0
0.5
1.0
1.5
2.0
PARTICLE VELOCITY, p (Km/sec)
b)

the shock wave attenuates. Gibbons and Ahrens (1971) calculated that approximately 0.3μsec was required for peak pressure to be reached in a 0.15mm thick sample shocked to approximately 300kb, and that the shock wave would attenuate in about 2μsec using a 5mm-thick striker plate.

The above technique for calculation of pressure was used in this series of Recovery experiments with microcline as the sample, stainless steel as the standard, and leaded brass commonly being the striker plate of the projectile. A typical calculation is presented below and illustrated in Fig. D.5b.

Shot # 16

Striker plate ---------- leaded brass (Cu 65%, Zn 33%, Pb 2%)

Standard ---------- 304 stainless steel (Fe-Cr-Ni)

Sample ---------- microcline

Measured projectile velocity ----- 1.850km/sec ± 1%

The maximum pressure attained in the stainless steel is calculated as 417kb. Based on Gibbons and Ahrens' calculations (ibid), peak pressure in the 0.5mm thick microcline disc should be reached in less than the 2μsec available before attenuation of the shock wave. The uncertainty in the standard Hugoniots, plus a ± 1% accuracy in projectile velocity measurements, results in an error of ± 3-5% for the calculated pressure.

REFERENCES

Aitken, F.K., 1970, An x-ray powder diffraction study of potassium feldspar from six possible meteorite impact sites, Ph.D. thesis, Pennsylvania State Univ., University Park, Pa., 152pp.

Aitken, F.K., and Gold, D.P., 1968, The structural state of potash feldspar: a possible criterion for meteorite impact?, in *Shock Metamorphism of Natural Materials*, French, B.M. and Short, N.M. editors, Mono Book Corp., Baltimore, 519-530.

Ahrens, T.J., and Gregson, V.G., Jr., 1964, Shock compression of crustal rocks: data for quartz, calcite, and plagioclase rocks, *J. Geophys. Res.*, 69, no. 22, 4839-4873.

Ahrens, T.J., and Rosenberg, J.T., 1968, Shock metamorphism experiments on quartz and plagioclase, in *Shock Metamorphism of Natural Materials*, French, B.M. and Short, N.M. editors, Mono Book Corp., Baltimore, 59-81.

Ahrens, T.J., Petersen, C.F., and Rosenberg, J.T., 1969, Shock compression of feldspars, *J. Geophys. Res.*, 74, no. 10, 2727-2746.

Ahrens, T.J., and Gaffney, E.S., 1971, Dynamic compression of enstatite, *J. Geophys. Res.*, 76, no. 23, 5504-5513.

Ahrens, T.J., and Graham, E.K., 1972, A shock-induced phase change in iron-silicate garnet, *Earth Planet. Sci. Lett.*, 14, 87-90.

Ahrens, T.J., and Liu, Hsi-Ping, 1973, A shock-induced phase change in orthoclase, *J. Geophys. Res.*, 78, no. 8, 1274-1278.

Al'Tshuler, L.V., Krupnikov, K.K., Ledenev, B.N., Zhuchiklin, V.I., and Brazhnik, M.I., 1958, Dynamic compressibility and equation of state of iron under high pressure, *J. Expmtl. Theoret. Phys. (U.S.S.R.)*, no. 4, 874-885.

Al'Tshuler, L.V., Trunin, R.F., and Simakov, G.V., 1965, Shock-wave compression of periclase and quartz and the composition of the Earth's lower mantle, Izv. Acad. Sci. U.S.S.R., *Phys. Solid Earth*, 10, 657-660.

Anderson, D.L., and Kanamori, H., 1968, Shock-wave equations of state for rocks and minerals, *J. Geophys. Res.*, 73, no. 20, 6477-6502.

Barth, T.F.W., 1969, *Feldspars*, John Wiley and Sons Inc., New York, 261pp.

Bass, R.C., 1966, Additional Hugoniot data for geologic materials, Sandia Corp. Albuquerque, *SC-RR-66-548*, 29pp.

Bass, R.C., Hawk, H.L., and Chabai, A.J., 1963, Hugoniot data for some geologic materials, Sandia Corp. Albuquerque, *SC4903(RR)*, 19pp.

Beals, C.S., Dence, M.R., and Cohen, A.J., 1967, Evidence for the impact origin of Lac Couture, *Pub. Dom. Obs. Canada*, 31, no. 10, 409-426.

Bloss, F.D., 1961, *An Introduction to the Methods of Optical Crystallography*, Holt, Rinehart and Winston, New York, 294pp.

Boade, R.R., 1966, Shock loading of porous tungsten, Sandia Corp. Albuquerque, *TID-4500 Physics*, 1-21.

Borg, I.Y., 1970, Mechanical <101> twinning in shocked sphene, *Am. Min.*, 55, 1876-1888.

Bostock, H.H., 1969, The Clearwater complex, New Quebec, *Geol. Surv. Canada Bull.*, no. 178, 63pp.

Bunch, T.E., 1968, Some characteristics of selected minerals from craters, in *Shock Metamorphism of Natural Materials*, French, B.M., and Short, N.M. editors, Mono Book Corp., Baltimore, 413-432.

Bunch, T.E., and Cohen, A.J., 1964, Shock deformation of quartz from two meteorite craters, *Bull. Geol. Soc. Am.*, 75, 1263-1266.

Bunch, T.E., Cohen, A.J., and Dence, M.R., 1967, Natural terrestrial maskelynite, *Am. Min.*, 52, 244-253.

Burri, C., 1962, A survey of feldspar twinning, *Norsk Geologisk Tidsskrift*, 42, 193-206.

Byström, A., and Byström, A.M., 1951, The crystal structure of hollandite, the related manganese oxide minerals, and α-MnO_2, *Acta Cryst.*, 3, 146-154.

Carter, N.L., 1971, Static deformation of silica and silicates, *J. Geophys. Res.*, 76, no. 23, 5514-5540.

Chao, E.C.T., 1967a, Shock effects in certain rock-forming minerals, *Science*, 156, no. 3772, 192-202.

Chao, E.C.T., 1967b, Impact metamorphism, in *Researches in Geochemistry*, 2, Abelson, P.H. editor, John Wiley and Sons Inc., New York, 204-233.

Chao, E.C.T., 1968, Pressure and temperature histories of impact metamorphosed rocks - Based on petrographic observations, *Neues Jahrbuch für Mineralogie Abhandlungen*, 108, no. 3, 209-246.

Chao, E.C.T., James, Odette B., Minkin, Jean A., Boreman, Judith A., Jackson, E.D., and Raleigh, C.B., 1970, Petrology of unshocked crystalline rocks and evidence of impact metamorphism in Apollo 11 returned lunar sample, in *Proc. of the Apollo 11 Lunar Science Conference*, 1, Levinson, A.A. editor, Pergamon Press, New York, 287-314.

Cummings, D., 1968, Shock deformation of biotite around a nuclear explosion, in *Shock Metamorphism of Natural Materials*, French, B.M., and Short, N.M. editors, Mono Book Corp., Baltimore, 211-217.

Currie, K.L., 1965, Analogues of lunar craters on the Canadian Shield, *Annals New York Acad. Sci.*, 123, art. 2, 915-940.

Currie, K.L., 1971, A study of potash fenitization around the Brent crater, Ontario, - a Paleozoic alkaline complex, *Can. J. Earth Sci.*, 8, no. 5, 481-497.

Currie, K.L., 1972, Geology and petrology of the Manicouagan resurgent caldera, Quebec, *Bull. Geol. Surv. Canada*, no. 198, 153pp.

Currie, K.L., and Shafiqullah, M., 1967, Carbonatite and alkaline igneous rocks in the Brent crater, Ontario, *Nature*, 215, 725-726.

Currie, K.L., and Shafiqullah, M., 1968, Geochemistry of some large Canadian craters, *Nature*, 218, 457-459.

Deer, W.A., Howie, R.A., and Zussman, J., 1963, *Rock-Forming Minerals, vol. 4, Framework Silicates*, John Wiley and Sons Inc., New York, 435pp.

Dence, M.R., 1964, A comparative structural and petrographic study of probable Canadian meteorite craters, *Meteoritics*, 2, 249-270.

Dence, M.R., 1965, The extraterrestrial origin of Canadian craters, *Annals. New York Acad. Sci.*, 123, art. 2, 941-969.

Dence, M.R., 1968, Shock zoning at Canadian craters: petrography and structural implications, in *Shock Metamorphism of Natural Materials*, French, B.M., and Short, N.M. editors, Mono Book Corp., Baltimore, 169-184.

Dence, M.R., 1971, Impact melts, *J. Geophys. Res.*, 76, no. 23, 5552-5565.

Dence, M.R., 1972, The nature and significance of terrestrial impact structures, *Proc. 24th Int. Geol. Congress*, Montreal, section 15, 77-89.

Dence, M.R., and Guy-Bray, J.V., 1972, Some astroblemes, craters, and cryptovolcanic structures in Ontario and Quebec, *Guidebook, Field Excursion A65, 24th Int. Geol. Congress*, Montreal, 61pp.

Dence, M.R., Robertson, P.B., and Wirthlin, R.L., 1973, Coesite from the Lake Wanapitei crater, Ontario, *Earth Planet. Sci. Lett.*, in press.

Dennen, R.S., 1965, Synthesis of rock Hugoniots, IIT Research Institute, Chicago, *AD 474687*, 143pp.

Deribas, A.A., Dobretsov, N.L., Kudinov, V.M., and Zyuzin, N.I., 1966, Shock compression of SiO_2 powders, *Dokl. Akad. Nauk, SSSR*, 168, 127-130.

Duvall, G.E., and Fowles, G.R., 1963, Shock waves, in *High Pressure Physics and Chemistry*, 2, Bradley, R.S. editor, Academic Press, New York, 209-291.

Dworak, U., 1969, Stosswellenmetamorphose des Anorthosits vom Manicouagan Krater, Québec, Canada, *Contr. Min. and Pet.*, 24, 306-347.

El Goresy, A., and Donnay, G., 1968, A new allotropic form of carbon from the Ries Crater, *Science*, 161, 363-364.

Engelhardt, W. von, and Stöffler, D., 1968, Stages of shock metamorphism in crystalline rocks of the Ries Basin, Germany, in *Shock Metamorphism of Natural Materials*, French, B.M., and Short, N.M. editors, Mono Book Corp., Baltimore, 159-168.

Engelhardt, W. von, and Bertsch, W., 1969, Shock induced planar deformation structures in quartz from the Ries Crater, Germany, *Contr. Min. and Pet.*, 20, 203-234.

Engelhardt, W. von, Stöffler, D., and Schneider, W., 1969, Petrologische Untersuchungen im Ries, *Geologica Bavarica*, 61, 229-295.

Engelhardt, W. von, Arndt, J., Müller, W.F., and Stöffler, D., 1970, Shock metamorphism of lunar rocks and origin of the regolith at the Apollo 11 landing site, in *Proc. of the Apollo 11 Lunar Science Conference*, 1, Levinson, A.A. editor, Pergamon Press, New York, 363-384.

Ernst, W.G., Seki, Y., Onuki, H., and Gilbert, M.C., 1970, Comparative study of low-grade metamorphism in the California Coast Ranges and the outer metamorphic belt of Japan, *Geol. Soc. Am. Mem. 124*, 276pp.

Evans, H.T., Jr., Appleman, D.E., and Handwerker, D.S., 1963, The least squares refinement of crystal unit cells with powder diffraction data by an automatic computer indexing method (abstr.), *Program, Am. Cryst. Assoc.*, Annual Meeting, Cambridge, 42-43.

Frondel, C., and Marvin, U.B., 1967, Lonsdaleite, a hexagonal polymorph of diamond, *Nature*, 214, 587-589.

Gibbons, R.V., 1973, Experimentally induced shock effects in plagioclase and pyroxene (abstr.), *Trans. Am. Geophys. Union*, 54, no. 4, 351.

Gibbons, R.V., and Ahrens, T.J., 1971, Shock metamorphism of silicate glasses, *J. Geophys. Res.*, 76, no. 23, 5489-5498.

Green, H.W., 1972, Metastable growth of coesite in highly strained quartz, *J. Geophys. Res.*, 77, no. 14, 2478-2482.

Hamza, V.M., 1973, Vertical distribution of radioactive heat production in the Grenville geological province and the sedimentary sections overlying it, Ph.D. thesis, Univ. of Western Ontario, London, 268pp.

Hartung, J.B., Dence, M.R., and Adams, J.A.S., 1971, Potassium-argon dating of shock-metamorphosed rocks from the Brent impact crater, Ontario, Canada, *J. Geophys. Res.*, 76, no. 23, 5437-5448.

Holland, T.H., 1900, Charnockite series, a group of Archaean hypersthene rocks in peninsular India, *Mem. Geol. Surv. India*, 28, 119-249.

Hornemann, U., and Müller, W.F., 1971, Shock-induced deformation twins in clinopyroxene, *Neues Jahrbuch für Mineralogie*, H. 6, 247-256.

Hörz, F., 1968, Statistical measurements of deformation structures and refractive indices in experimentally shock loaded quartz, in *Shock Metamorphism of Natural Materials*, French, B.M., and Short, N.M. editors, Mono Book Corp., Baltimore, 243-253.

Hörz, F., 1969, Structural and mineralogical evaluation of an experimentally produced impact crater in granite, *Contr. Min. and Pet.*, 21, 365-377.

Hörz, F., and Ahrens, T.J., 1969, Deformation of experimentally shocked biotite, *Am. J. Sci.*, 267, 1213-1229.

Hörz, F., and Quaide, W.L., 1973, Debye-Scherrer investigations of experimentally shocked silicates, *The Moon*, 6, 45-82.

Howie, R.A., 1955, The geochemistry of the charnockite series of Madras, India, *Trans. Roy. Soc. Edinburgh*, 62, part 3, 725-768.

James, Odette B., 1969, Jadeite: shock-induced formation from oligoclase, Ries Crater, Germany, *Science*, 165, no. 3897, 1005-1008.

Jones, A.H., Isbell, W.M., and Maiden, C.J., 1966, Measurement of the very-high-pressure properties of materials using a light gas gun, *J. Appl. Phys.*, 37, no. 9, 3493-3499.

Jones, A.H., Isbell, W.M., Shipman, F.H., Perkins, R.D., Green, S.J., and Maiden, C.J., 1969, Material property measurements for selected materials, *Proc. AIAA Hypervelocity Impact Conference*, Cincinnati, 296-328.

Kennedy, G.C., 1961, Phase relations of some rocks and minerals at high temperatures and high pressures, *Adv. in Geophys.*, 7, Lundsberg, H.E., and Van Mieghem, J. editors, Academic Press, New York, 303-322.

Kieffer, Susan W., 1971, Shock metamorphism of the Coconino Sandstone at Meteor Crater, Arizona, *J. Geophys. Res.*, 76, no. 23, 5449-5473.

Kinomura, N., Ueda, S., Shimada, M., Kume, S., and Koizumi, M., 1971, High-pressure transformation of germanate feldspar, *Min. Soc. Japan Spec. Paper I*, 67-69, in Proc. Int. Min. Assoc. - Int. Assoc. Genesis of Ore Deposits, Tokyo-Kyoto, 1970.

Kleeman, J.D., 1971, Formation of diaplectic glass by experimental shock loading of orthoclase, *J. Geophys. Res.*, 76, no. 23, 5499-5503.

Kume, S., Matsumoto, T., and Koizumi, M., 1966, Dense form of germanate orthoclase ($KAlGe_3O_8$), *J. Geophys. Res.*, 71, no. 20, 4999-5000.

Kurat, G., and Richter, W., 1968, Ein alkalifeldspat-Glas im Impaktit von Köfels/Tirol, *Naturwiss.*, 55, no. 10, 490.

Kurat, G., and Richter, W., 1972, Impaktite von Köfels, Tirol, *Tschermaks Min. Petr. Mitt.*, 17, 23-45.

Laves, F., 1950, The lattice and twinning of microcline and other potash feldspars, *J. Geol.*, 58, 548-571.

Mackenzie, W.S., and Smith, J.V., 1962, Single crystal x-ray studies of crypto- and micro-perthites, *Norsk Geologisk Tidsskrift*, 42, 72-103.

Marfunin, A.S., 1962, *The Feldspars, Phase Relations, Optical Properties, and Geological Distribution*, transl. by Kolodny, J., 1966, IPST Press, Jerusalem, 317pp.

Masaitis, V.L., Futergendler, S.I., and Gnevushev, M.A., 1972, Alamazy v impaktitakh Popigaiskogo meteoritnogo kratera, *Zapiski Vsesoyuznogo Mineralogicheskogo Obshchestva*, Part CI, issue 1, 108-112.

McQueen, R.G., and Marsh, S.P., 1960, Equation of state for nineteen metallic elements from shock wave measurements to two megabars, *J. Appl. Phys.*, 31, no. 7, 1253-1269.

McQueen, R.G., Jamieson, J.C., and Marsh, S.P., 1967a, Shock-wave compression and x-ray studies of titanium dioxide, *Science*, 155, no. 3768, 1401-1404.

McQueen, R.G., Marsh, S.P., and Fritz, J.N., 1967b, Hugoniot equation of state of twelve rocks, *J. Geophys. Res.*, 72, no. 20, 4999-5036.

McQueen, R.G., Marsh, S.P., Taylor, J.W., Fritz, J.N., and Carter, W.J., 1970, The equation of state of solids from shock wave studies, in *High-Velocity Impact Phenomena*, Kinshaw, R. editor, Academic Press, New York, 293-417.

Millman, P.M., 1971, The space scase of Earth, *Nature*, 232, 161-164.

Minkin, Jean A., and Chao, E.C.T., 1971, Single crystal x-ray investigation of deformation in terrestrial and lunar ilmenite, in *Proc. of the Second Lunar Science Conference*, 1, Levinson, A.A. editor, M.I.T. Press, Cambridge, Mass., 237-246.

Müller, W.F., and Défourneaux, M., 1968, Deformationsstrukturen in Quarz als Indikator für Stosswellen: Eine experimentelle Untersuchung an Quarz-Einkristallen, *Zeitschrift für Geophysik*, 34, 483-504.

Müller, W.F., and Hornemann, U., 1969, Shock-induced planar deformation structures in experimentally shock-loaded olivines and in olivines from chondritic meteorites, *Earth and Planet. Sci. Lett.*, 7, 251-264.

Papezik, V.S., 1961, Rapport préliminaire sur la region de Glen Almond, cantons de Derry et de Buckingham, comté de Papineau, *province de Québec Ministère des Richesses Naturelles, Rapport préliminaire 444*, 11pp.

Parras, Kauko, 1958, On the charnockites in the light of a highly metamorphic rock complex in Southwestern Finland, *Bull. de la Commission Geologique de Finlande*, 181, 137pp.

Peredery, W.V., 1972, The origin of rocks at the base of the Onaping formation, Sudbury, Ontario, Ph.D. thesis, University of Toronto, 366pp.

Petersen, C.F., Murri, W.J., and Cowperthwaite, M., 1970, Hugoniot and release-adiabat measurements for selected geologic materials, *J. Geophys. Res.*, 75, no. 11, 2063-2072.

Reid, A.F., Wadsley, A.D., and Ringwood, A.E., 1967, High pressure $NaAlGeO_4$, a calcium ferrite isotype and model structure for silicates at depth in the earth's mantle, *Acta Cryst.*, 23, 736-739.

Ribbe, P.H., Smith, J.V., and Stewart, D.B., 1965, *Short course on feldspars, A.G.I. Committee on Education*, Lawrence, Kansas.

Rice, M.H., McQueen, R.G., and Walsh, J.M., 1958, Compression of solids by strong shock waves, in *Solid State Physics*, 6, Seitz, F., and Turnbull, D. editors, Academic Press, New York, 1-63.

Rinehart, J.S., 1968, Intensive destructive stresses resulting from stress wave interactions, in *Shock Metamorphism of Natural Materials*, French, B.M., and Short, N.M. editors, Mono Book Corp., Baltimore, 31-42.

Ringwood, A.E., Reid, A.F., and Wadsley, A.D., 1967a, High-pressure $KAlSi_3O_8$, an aluminosilicate with sixfold coordination, *Acta Cryst.*, 23, 1093-1095.

Ringwood, A.E., Reid, A.F., and Wadsley, A.D., 1967b, High-pressure transformation of alkali aluminosilicates and aluminogermanates, *Earth and Planet. Sci. Lett.*, 3, 38-40.

Robertson, P.B., 1965, Petrography of the bedrock and breccia erratics in the region of Lac Couture, Quebec, M. Sc. thesis, Pennsylvania State Univ., University Park, Pa., 112pp.

Robertson, P.B., 1967, The Malbaie structure, Quebec - an ancient meteorite impact site (abstr.), *30th Ann. Meeting, Meteoritical Society*, Ames Res. Center, Calif.

Robertson, P.B., 1968, La Malbaie structure, Quebec - a Palaeozoic meteorite impact site, *Meteoritics*, 4, no. 2, 89-112.

Robertson, P.B., Dence, M.R., and Vos, M.A., 1968, Deformation in rock-forming minerals from Canadian craters, in *Shock Metamorphism of Natural Materials*, French, B.M., and Short, N.M. editors, Mono Book Corp., Baltimore, 433-452.

Robertson, P.B., and Grieve, R.A.F., 1973, Impact structures in Canada, *Priroda*, in press.

Rondot, J., 1966, Geology of La Malbaie area, Charlevoix county, *Prelim. Rept. No. 544, Ministère des Richesses Naturelles*, Québec, 18pp.

Rondot, J., 1967, Geology of L'Anse Saint-Jean area, Chicoutimi and Charlevoix counties, *Prelim. Rept. No. 556, Ministère des Richesses Naturelles*, Québec, 13pp.

Rondot, J., 1968, Nouvel impact météoritique fossile? La structure semicirculaire de Charlevoix, *Can. J. Earth Sci.*, 5, no. 5, 1305-1317.

Rondot, J., 1969, Geology of the Rivière Malbaie area, *Prelim. Rept. No. 576, Ministère des Richesses Naturelles*, Québec, 30pp.

Rondot, J., 1970, La structure de Charlevoix comparée à d'autres impacts météoritiques, *Can. J. Earth Sci.*, 7, no. 5, 1194-1202.

Rondot, J., 1971a, Impactite of the Charlevoix structure, Quebec, Canada, *J. Geophys. Res.*, 76, no. 23, 5414-5423.

Rondot, J., 1971b, Geology of the Rivière du Gouffre region, Charlevoix county, *Prelim. Rept. No. 605, Ministère des Richesses Naturelles*, Québec,

Schairer, J.F., and Bowen, N.L., 1955, The system K_2O-Al_2O_3-SiO_2, *Am. J. Sci.*, 253, 681-746.

Sclar, C.B., 1971, Shock-induced features of Apollo 12 microbreccias, in *Proc. of the Second Lunar Science Conference*, 1, Levinson, A.A. editor, M.I.T. press, Cambridge, Mass., 817-832.

Sclar, C.B., and Usselman, T.M., 1970, Experimentally induced shock effects in some rock-forming minerals (abstr.), *Meteoritics*, 5, no. 4, 222-223.

Shoemaker, E.M., 1963, Impact mechanics at Meteor Crater, Arizona, in *The Solar System, vol. IV, The Moon, Meteorites and Comets*,

Middlehurst, B.M., and Kuiper, G.P. editors, The University of Chicago Press, Chicago, 301-336.

Short, N.M., 1966a, Effects of shock pressures from a nuclear explosion on mechanical and optical properties of granodiorite, *J. Geophys. Res.*, 71, no. 4, 1195-1215.

Short, N.M., 1966b, Shock processes in geology, *J. Geol. Education*, 14, no. 4, 149-166.

Short, N.M., 1968, Nuclear-explosion-induced microdeformation of rocks: an aid to the recognition of meteorite impact structures, in *Shock Metamorphism of Natural Materials*, French, B.M., and Short, N.M. editors, Mono Book Corp., Baltimore, 185-210.

Smith, J.V., 1962, Genetic aspects of twinning in feldspars, *Norsk Geologisk Tidsskrift*, 42, 244-263.

Smith, J.V., and Mackenzie, W.S., 1954, Further complexities in the lamellae structure of alkali feldspars, *Acta Cryst.*, 7, part. 4, 380.

Smith, J.V., and Mackenzie, W.S., 1959, The alkali feldspars V. The nature of orthoclase and microcline perthites and observations concerning the polymorphism of potassium feldspar, *Am. Min.*, 44, 1169-1186.

Smithson, S.B., 1962, Symmetry relations in alkali feldspars of some amphibolite facies rocks from the Southern Norwegian Precambrian, *Norsk Geologisk Tidsskrift*, 42, 586-599.

Spence, H.S., 1932, Feldspar, *Canada Dept. Mines Branch Pub. No. 731*, 145pp.

Stöffler, D., 1966, Zones of impact metamorphism in the crystalline rocks of the Nördlinger Ries crater, *Contr. Min. and Pet.*, 12, 15-24.

Stöffler, D., 1967, Deformation und Umwandlung von Plagioklas durch Stosswellen in den Gesteinen des Nördlinger Ries, *Contr. Min. and Pet.*, 16, 51-83.

Stöffler, D., 1970, Shock deformation of sillimanite from the Ries Crater, Germany, *Earth and Planet. Sci. Lett.*, 10, 115-120.

Stöffler, D., 1971a, Progressive metamorphism of shocked and brecciated crystalline rocks at impact craters, *J. Geophys. Res.*, 76, no. 23, 5541-5551.

Stöffler, D., 1971b, Coesite and stishovite in shocked crystalline rocks, *J. Geophys. Res.*, 76, no. 23, 5474-5488.

Stöffler, D., 1972, Deformation and transformation of rock-forming minerals by natural and experimental shock processes: I. Behaviour of minerals under shock compression, *Fortschritte der Mineralogie*, 49, 50-113.

Stöffler, D., and Arndt, J., 1969, Coesit und Stishovit Hochstdruck-modifikationen des Siliciumdioxids, *Naturwiss.*, 56, 100-109.

Stöffler, D., and Hornemann, U., 1972, Quartz and feldspar glasses produced by natural and experimental shock, *Meteoritics*, 7, no. 3, 371-394.

Turner, F.J., 1968, *Metamorphic Petrology*, McGraw-Hill Book Co., New York, 403pp.

Tuttle, O.F., 1952, Optical studies on alkali feldspars, *Am. J. Sci., Bowen vol.*, 553-567.

Tuttle, O.F., Gold, D.P., Robertson, P.B., Aitken, F.K., Wyllie, P.J., and Vand, V., 1965, Study of structural and mineralogical significance of meteorite impact sites, including mineral paragenesis, high pressure polymorphs, microfractures and quartz lamellae, *2nd Ann. Rept. to NASA, Jan. 1964-Dec. 1964, grant NSG-473.*

Wackerle, J., 1962, Shock-wave compression of quartz, *J. Appl. Phys.*, 33, no. 4, 922-937.

Walsh, J.M., and Christian, R.H., 1955, Equation of state of metals from shock wave measurements, *Phys. Review*, 97, no. 6, 1544-1556.

Walsh, J.M., Rice, M.H., McQueen, R.G., and Yarger, F.L., 1957, Shock-wave compression of twenty-seven metals. Equation of state of metals, *Phys. Review*, 108, no. 2, 196-216.

Wilson, A.F., 1950, Some unusual alkali feldspars in the Central Australian charnockitic rocks, *Min. Mag.*, 29, 215-224.

Wolfe, S.H., and Hörz, F., 1970, Shock-effects in scapolite, *Am. Min.*, 55, 1313-1328.

Wright, T.L., 1968, X-ray and optical study of alkali feldspar: II. An x-ray method for determining the composition and structural state from measurement of 2θ values for three reflections, *Am. Min.*, 53, 88-104.

Wright, T.L., and Stewart, D.B., 1968, X-ray and optical study of alkali feldspar: I. Determination of composition and structural state from refined unit-cell parameters and 2V, *Am. Min.*, 53, 38-87.

Yoder, H.S., Stewart, D.B., and Smith, J.R., 1957, Ternary feldspars, *Ann. Rept. Geophys. Lab., Carnegie Inst., Washington, Yearbook*, 56, 206.